The Dissertation Committee for Irnela Bajrovic Certifies that this is the approved version of the following Dissertation:

Development and Characterization of Thermostable Thin Films as a Novel Vaccine Dosage Form

Committee:

Maria A. Croyle, Supervisor

Hugh D. Smyth

Debadyuti Ghosh

Jennifer A. Maynard

Charles R. Middaugh

For my parents Džemal and Rahima, and my sister, Minela

without whom none of this would have been possible.

Acknowledgements

I joined Dr. Maria Cryole's lab in 2014 as an undergraduate student hoping to gain some research experience and learn about vaccine delivery. Little did I know that one semester would turn into six years and two degrees that have forever changed my life for the better. First and foremost, I would like to thank Dr. Croyle for giving me the guidance and support to learn and grow as a scientist. I will treasure the time we spent together and everything I learned from her. I would also like to thank my committee members Dr. Hugh Smyth, Dr. Debadyuti Ghosh, Dr. Jennifer Maynard, and Dr. Charles Middaugh for their guidance, support, and encouragement. Special thanks to Stephen Schafer who served as great sounding board and brainstorm partner. To past and present Croyle lab members Dr. Kristina Jonsson-Schmunk, Trang Doan, and Matthew Le, I also say thank you. Your advice and support contributed to the completion of the projects in this document and I am grateful for the friendships we have built.

I would also like to thank my family for always encouraging me and reminding me that I am capable of anything I set my mind to. My wonderful parents, Rahima and Džemal, have sacrificed so much to give my sister and I a better life. I hope to honor their sacrifice with this document and a steadfast devotion to science. To my sister Minela, who taught me confidence and ambition, I am eternally indebted. She is my forever role model and I hope to make her proud. And to the friends that are like family, Lauren Cardenas, Zainab Shahid, Shehnaz Haqqani, Saad Dawoodi, Melissa Soto, and Ahlam Qerqez a special thanks for reminding me of the strength I have within. And finally, I would like to thank Karen Stewart, for opening up her home to me while I was preparing this document and providing me with a comfortable and quiet space to focus on my work. I will never forget her generosity.

Abstract

Development and Characterization of Thermostable Thin Films as a Novel Vaccine Dosage Form

Irnela Bajrovic, PhD

The University of Texas at Austin, 2020

Supervisor: Maria A. Croyle

Thermostabilization of vaccines can significantly simplify vaccine storage and distribution processes, eliminating the need for cold-chain maintenance, and resulting in global access to life-saving vaccines. Despite this benefit, all approved vaccines for use by the Food and Drug Administration must be refrigerated for long term storage in order to guarantee potency. The first study described in this thesis demonstrated that formulation of live adenovirus in the novel thin film matrix protects the virus from degradation at 4°C and 20°C for a minimum of three months, as well as 14 days at 37°C and 5 days at 40°C. The film matrix protected virus through 16 freeze-thaw cycles as well. As formulations prepared with surfactant outperformed those without it, the second study was designed to characterize and evaluate the intermolecular interactions between the surfactant and adenovirus capsids. in order to better understand the surfactants contribution to stability. The data suggested that surfactant stabilizes adenovirus by preventing aggregation of capsids via electrostatic and hydrophobic interactions. Additionally, the other formulation components in our multi-component preparation mitigates the interactions between adenovirus and the surfactant without interfering with stability. Lastly, the principles of surfactant stabilization were applied to the identification of alternative excipients for stabilization

of a virus with different properties from adenovirus, H1N1 influenza. The third study evaluated the ability of the thin film platform to induce an immune response and the impact of a natural adjuvants on the cytokine response and bioavailability of the vaccine dose. A preliminary screen demonstrated that vaccination with the thin film platform resulted in a stronger humoral response following mucosal vaccination than with traditional intramuscular vaccination. Additionally, the optimized formulation improved bioavailability of the viral dose across human buccal explants. Further characterization of the immune response also revealed that sublingual routes induced a strong TH_1 polarized immune response which resulted in greater protective efficacy than intramuscular immunization. Taken together, these studies identified a novel thin film platform capable of stabilizing adenovirus at ambient temperatures, provide key insights into viral stabilization in the novel thin film platform, and illustrate the utility of the thin film as mucosal vaccine dosage form.

Development and Characterization of Thermostable Thin Films as a Novel Vaccine Dosage Form

by

Irnela Bajrovic

Dissertation
Presented to the Faculty of the Graduate School of
The University of Texas at Austin
In Partial Fulfillment
of the Requirements
for the Degree of

Doctor of Philosophy

The University of Texas at Austin
December 2020

Table of Contents

List of Tables

List of Figures

Chapter 1: Breaking the Cold Chain for Viral Vaccines: A Move Toward Needle Free Delivery

The earliest form of vaccination was known as variolation, where material collected from smallpox lesions of infected patients was given to naïve people with the intended goal of inducing protective immunity against smallpox (1). Edward Jenner, who believed an agent virulent for animals would be less pathogenic but remain immunogenic in humans, built upon this idea by using an animal pox virus to vaccinate humans against smallpox resulting in mild infections and protection (Figure 1.1)(2). However, it was Louis Pasteur's accidental success in inoculating the chickens with cultures of fowl cholera left in the lab unattended during a holiday, presumed to be no longer viable, that solidified the concept of attenuation. When the chickens did not develop cholera, he challenged them with a live, fresh strain of the organism. They remained healthy and did not get sick, leading to Pasteur's realization that weakened strains of viruses could immunize against disease (1, 3).

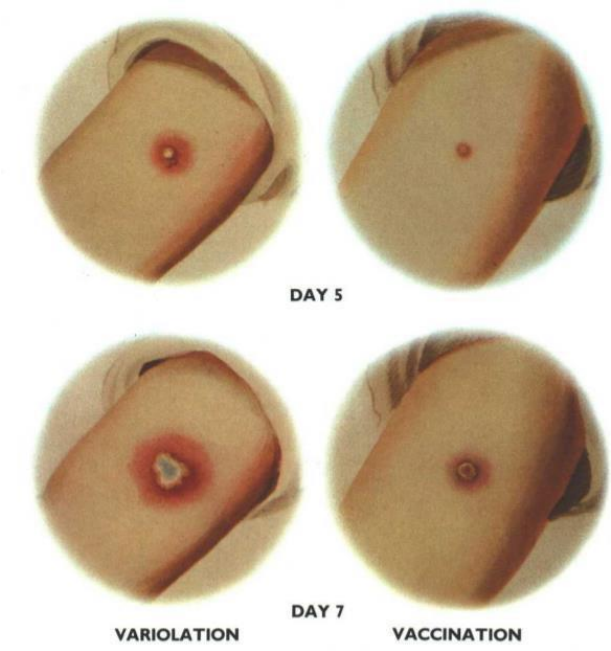

Figure 1.1: Variolation and Vaccination. Colored drawing by George Kirtland, made in 1801, showing the appearance of smallpox lesions at various times after variolation and vaccination, depicting the lessened severity following vaccination. Figure from ref 2.

Live-attenuated vaccines [LAV], which contain a weakened version of a living microbe, mimic natural infections by eliciting strong cellular and antibody responses resulting in long

term immunity without causing full blown disease (4). Live attenuated viral vaccines currently on the market protect against adenovirus, measles, mumps, rubella, polio, vaccinia, varicella zoster, yellow fever, rotavirus, and influenza infection. Commercially available live attenuated bacterial vaccines protect against *M. tuberculosis*, *V. cholerae*, and rickettsia, which cause typhus (5, 6). In very rare cases, attenuated pathogens can revert to their original form and cause disease. This initially happened with the oral polio vaccine (7-9). As a result, the World Health Organization (WHO) recommends use of a very limited number of vaccines produced by attenuation. These include BCG, Oral Polio, Measles, Rotavirus, and Yellow Fever vaccines (10-14). Even though vaccines are critically important for patients with compromised immune systems, such as those with HIV, rheumatoid arthritis, organ transplants or undergoing chemotherapy, use of live or live attenuated vaccines is limited due to the heightened risk of adverse side effects or vaccine-related disease (15, 16).

Inactivated vaccines provide a safe alternative to LAV vaccines. Processes utilized to produce these vaccines kill or inactivate the disease-causing microbe by treating them with chemicals, heat, or radiation (17, 18). Currently available viral-based inactivated vaccines protect against polio, influenza, Japanese encephalitis, hepatitis A, and rabies infection (19-23). Inactivated bacterial-based vaccines protect against *B. pertussis*, *V. cholerae*, *S. typhi*, and *Y. pestis* infections (24-27). While the risk of adverse events and development of vaccine - associated disease are greatly reduced by these vaccines, they stimulate a much weaker immune response than LAV vaccines and require at least one additional boosting dose or more to maintain long lasting immunity (28). This is a significant drawback in rural regions where access to health care is challenging.

Subunit vaccines, consisting of a purified part or parts of the pathogen that elicits a protective immune response instead of the entire organism, represent an even safer alternative to inactivated vaccines. These vaccines are divided into four main categories: protein-based, polysaccharide-based, protein/polysaccharide conjugates, and toxoids. Protein-based subunit vaccines are derived from a protein isolated from the pathogen, which is known to be processed and presented as an antigen to the immune system to stimulate an effective immune response (29). These highly purified products are produced through the use of recombinant DNA technology which significantly contributes to the cost of a vaccine (30). Currently approved examples of anti-viral protein-based recombinant vaccines protect against hepatitis B (HBsAg), human papillomavirus (L1), influenza (HA), and zoster (gE) infections. Bacterial recombinant vaccines (and the protein they contain) protect against *salmonella* Typhi (Vi polysaccharide) and anthrax (PA). Since proteins are highly susceptible to degradation by changes in pH, hydrolysis or proteolytic enzymes *in vivo*, they can stimulate the production of antibodies that only partially or weakly bind to the native pathogen. For this reason, protein-based subunit vaccines are not very immunogenic and when given alone can result in partial or short-term immunity (30, 31). Inclusion of adjuvants and the addition of multiple boosting doses to the immunization regimen are required for these vaccines (32).

Polysaccharide subunit vaccines consist of purified sugars that form the protective capsule of certain bacteria and aim to stimulate the immune system to weaken this protective shield around the pathogen and prevent it from attaching to target cells. Soon after their development it was realized that polysaccharides could not induce T cell-mediated immune responses because T cell receptors only recognize protein molecules (33). Administration of polysaccharides alone could directly stimulate B cells to produce IgM antibodies but, without the

activation of helper T cells, only small amounts of neutralizing IgG antibodies were produced, and memory B cell production was absent. To address this notable deficiency, additional protein was introduced into these vaccines through covalent attachment of diptheria or tetanus toxoids to the polysaccharides. These proteins, which consist of an inactivated toxin secreted by bacteria, reconstitute the helper T cell response and support long-term protective immunity. Thus, conjugate vaccines prevent bacterial infections more efficiently than plain polysaccharide vaccines (34, 35). Current examples of approved bacterial based polysaccharide conjugate vaccines provide protection against *Haemophilus* influenzae type b pneumococcus, and meningococcus infections (36, 37). It is also important to note that bacterial toxoids alone comprise some vaccine products (6). However, these require the use of an adjuvant to elicit a well-rounded, protective immune response and often require repeat boosting doses (38, 39). For example, the Tdap vaccine, which protects adolescents and adults from contracting tetanus, diphtheria, and pertussis; requires a booster dose every ten years. Other currently approved bacterial-based toxoid vaccines protect against *staphylococcus* infection. While all subunit vaccines have excellent safety profiles, the process to identify the appropriate combination of antigenic components and adjuvants in order to elicit strong, long-lasting immunity is complex, extremely time-consuming and significantly contributes to the overall cost of the vaccine (40).

More than half of the commercially available vaccines in the United States are dedicated to inducing protective immunity to viruses (Appendix Table 1 and 2) (41, 42). These fall in two categories: those capable of inducing strong long-lasting immunity with limited utility in specific patient populations due to adverse effects and those regarded as safe, but which require additional adjuvants and multiple doses. With over 70% of all emerging diseases of viral origin, Acquired Immunodeficiency Syndrome (AIDS), Avian Influenza, Severe Acute Respiratory

Syndrome (SARS), Middle East Respiratory Syndrome (MERS), Ebola Virus Disease, and COVID-19, virus infections are high priority global public health concerns (43, 44). Thus, development of novel technologies that effectively stabilize and deliver viral antigens for long term immunity is highly dependent on a thorough understanding of the physical properties of viruses and their requirements for stabilization in a variety of different environments.

1.1 Physical Properties of Viruses

Viruses were first discovered after the development of the Chamberland-Pasteur porcelain filter, which could remove all visible bacteria (as determined via microscopy) from any liquid sample. In 1892, Dmitri Ivanowski showed that this disease could be transferred from plant to plant via liquid extract from an infected plant even after the Chamberland-Pasteur filter had removed all the viable bacteria from the filtrate (45). In 1901, it was proven that the infectious agents in the filtrate were not submicroscopic bacteria, but were smaller disease-causing particles with the first known human virus discovered by the US physician Walter Reed who reported it as the agent responsible for causing yellow fever (46). While the true origin of viruses is often a subject of debate, there is consensus that viruses do not have a single common ancestor and that they evolved from genetic material that can be supported from a variety of free living cells (47).

The size of animal viruses is highly variable with individual particles having average diameters of 20 -300 nm. Development of the electron microscope in the 1930s allowed scientists to view viruses for the first time (48). Thus, viruses were initially classified by shared morphology (49). Virus capsid proteins generally assemble around the virus genome in three

distinct shapes: icosahedrons, filaments, and head-tail. Parvoviridae and Picornaviridae are the smallest known viruses and exhibit icosahedral shapes of 20 nm in diameter (50). Filamentous viruses include the Paramyxoviridae, Orthomyxoviridae, Coronaviridae, and Rhabdoviridae families with an average diameter of 150 to 300 nm, 80 to 120 nm, 125 nm, and 100 to 400 nm respectively (51-53). Head and tail viruses, like tobacco mosaic virus, infect bacteria and have an average length of 300 nm (54). The shape of a specific virus can vary based upon features of the host cell that supports its replication. For example, smallpox virus particles have diameters between 250 to 400 nm and are either brick or oval-brick shaped because they are wrapped by the endoplasmic reticulum of the host cell (55). The Mimivirus, with a genome of roughly 1.1 million base pairs of DNA and an icosahedral capsid with a diameter of 520 nm is the largest known virus. A thick layer of fibrils extending from the capsid increases the overall hydrodynamic diameter of each particle to 680 nm, illustrating that additional structural features of a virus also contribute to its size (56, 57).

Later, viruses were classified further by the type of nucleic acid they contained, DNA or RNA, and whether their nucleic acid was single- or double-stranded. The genome of double-stranded DNA viruses must first enter the host nucleus before they initiate the replication process (Figure 1.2A). Promoter elements within the virus genome take over cellular machinery to induce cell division and ensure that each daughter cell contains a copy of the virus and associated growth promoting proteins. Single stranded DNA viruses only contain expression elements for capsid proteins and a DNA replication enzyme. However, since the only template for transcription in living mammalian cells is for double-stranded DNA, single-stranded viruses must first convert their genome into dsDNA by using the cell's DNA polymerase (Figure 1.2B)(58, 59). RNA viruses replicate in the host cell's cytoplasm since they do not rely on host

replication polymerases to the same degree as DNA viruses. Single-stranded RNA (ssRNA) viruses are further divided into positive-sense and negative-sense categories. Viral proteins are directly translated from positive-sense genomes, while negative-sense genomes include an RNA-dependent RNA polymerase which must first produce a complementary mRNA strand that can then be translated into viral proteins (Figure 1.2C) (60, 61). Examples of positive-sense ssRNA viruses include SARS and MERS coronaviruses. Negative-sense ssRNA viruses include Rabies and Marburg viruses. Double-stranded RNA viruses transcribe a complementary mRNA strand which is then translated into viral protein (Figure 1.2D) (62).

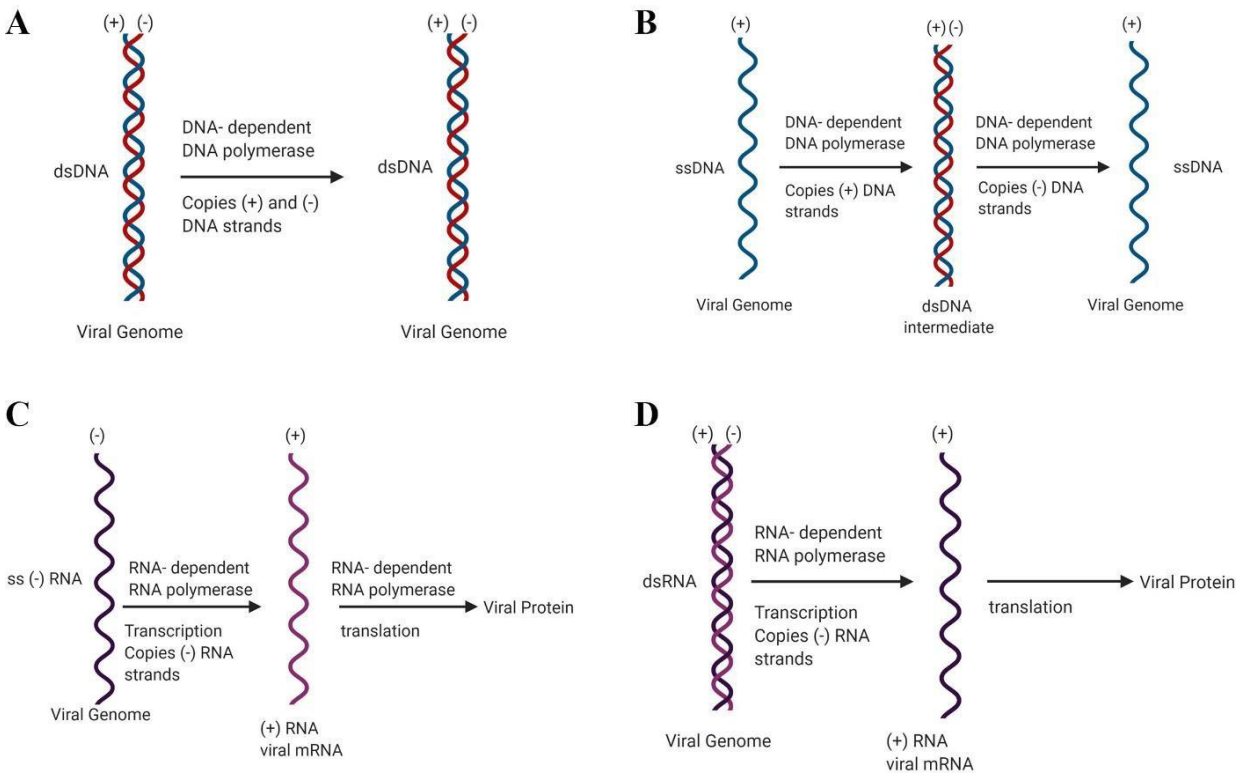

Figure 1.2: Viral Replication.
To replicate the dsDNA viral genome DNA-dependent DNA polymerase enzymes copy the (+) and (-) strands of the genome to produce dsDNA (**A**). To replicate the ssDNA viral genome DNA-dependent DNA polymerase enzymes copy the (+) DNA strand of the genome producing a dsDNA intermediate. Then DNA-dependent DNA polymerase enzymes copy the (-) DNA strand into (+) ssDNA viral genome (**B**). To translate viral proteins the (-) ssRNA viral genome RNA-dependent RNA polymerase enzymes transcribes the (-) RNA strand of the genome producing a (+) RNA, or mRNA which can then be translated into viral protein (**C**). To translate viral proteins the dsRNA viral genome's RNA-dependent RNA polymerase enzymes transcribes the (-) RNA strand of the genome producing a (+) RNA, or mRNA which can then be translated into viral protein (**D**). Figure created with BioRender.com.

While nucleic acid content drives viral replication and gene expression, capsid proteins play a key role in packaging, protecting the virus genome from the environment, and mediating cell entry. These functions are achieved through binding distinct cellular receptors and/or charge dependent interactions. Adenovirus 5 enters cells when its fiber protein binds coxsackievirus adenovirus receptor (CAR) and the RGD (Arg-Gly-Asp) motifs on its penton base interact with cellular integrins. Meanwhile, adenovirus 37 binds negatively charged sialic acid receptors to

enter cells via the positively charged fiber-knob (63, 64). Viruses that are released from the host cell, by a process called budding, are surrounded by a lipid envelope (Figure 1.3)(65). This "cloak" often helps the virus avoid the host's immune system, however, if the next cell the virus infects is genetically distinct from the host cell, the innate immune response may be triggered (66). Viral envelopes contain a combination of negatively charged phospholipids, neutral lipids and glycoproteins. The glycoproteins, responsible for binding to cell surface receptors mediate viral entry and contribute to the overall surface charge of the virus particle. For example, the positively charged hemagglutinin glycoprotein of the influenza virus mediates cell entry through direct interaction with negatively charged sialic acid receptors (67). Exposure of virus particles to environmental (extreme temperature, light, moisture) and chemical (pH, organic solvents, surfactants) stressors may not fully disrupt the particle but instead shift the overall structure to expose additional charged regions on the particle surface. This facilitates particle interactions leading to aggregation and eventual inactivation of the virus (68). It can also foster particle to surface interactions, leading to inactivation or loss of active virus in a pharmaceutical product (69).

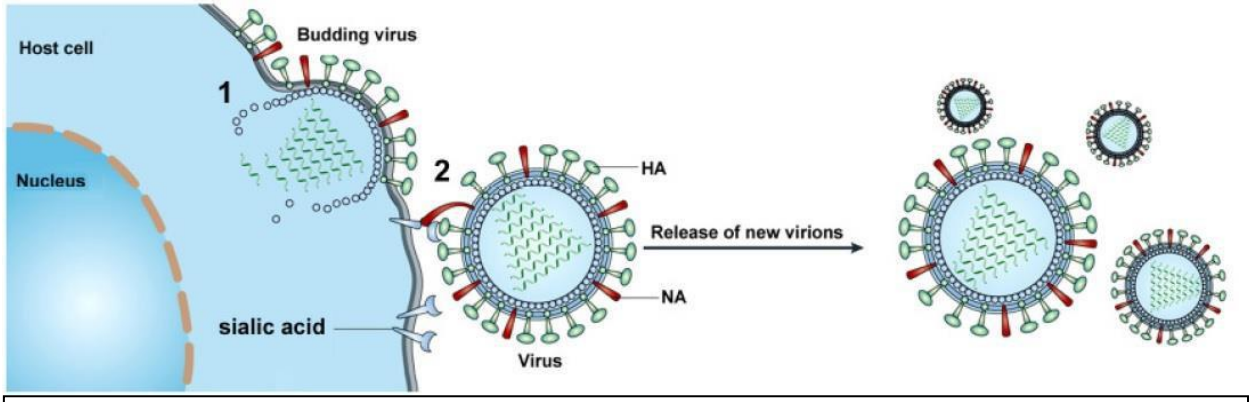

Figure 1.3: Influenza Virus Assembly and Budding.
As the viral particle assembles in the plasma membrane of the host cell, the membrane begins to bend and eventually the virus buds out of the cell [1]. This is followed by complete release of the virion as the glycoprotein neuraminidase (NA) cleaves sialic acid resides from the virion and host cell [2]. Figure adapted from ref 65.

1.2 Chemical and Environmental Stressors which Impact Virus Stability

Temperature, relative humidity, and light represent the primary environmental stressors which significantly impact the structure and stability of virus particles. It is well established that all viruses are heat sensitive, however, resistance to heat varies. Infectious titer assays confirmed that enveloped H1N1 influenza virus was inactivated after only 5 minutes of exposure to 70°C, while naked adenovirus type 5 required 20 minutes of exposure to 70°C (70, 71). Adeno-associated virus 8 (AAV8) capsids are amongst the most heat stable. Capsid disassembly only occurred after exposure to 80°C for 20 minutes (72). Without the addition of a cryoprotectant, viruses also experience cold denaturation in varying degrees. At low temperatures, hydrogen bonds are weakened and aggregation results in viral inactivation. Adenovirus 5 and Influenza A experienced a two-log reduction in infectious titer after only being thawed once from -70°C to room temperature (73). However, measles virus is capable of withstanding 5 freeze-thaw cycles (74). When comparing results from various stability studies it is essential to ascertain the relative humidity (RH) at which the experiments were performed, as the salt and protein concentration of air droplets has been reported to impact viral transmission (75). Specifically, enveloped viruses survived best in aerosols at low relative humidity, while non-enveloped viruses were more stable at high relative humidities (75). This trend can be linked to the seasonal cycle of viruses, as RH is typically low in the winter and high in the summer. As RH gradually increased from 20% to 80%, transmission efficiency of enveloped H1N1 influenza, a common infection in winter months, incrementally decreased (76). A similar trend has been observed with the Severe Acute Respiratory Syndrome Coronavirus 2 (SARS-CoV-2) pandemic wherein transmission rates in Wuhan decreased as RH increased from 60% to 100% (77). Conversely, non-enveloped

poliovirus transmission, a common infection in summer months, increased as RH increased (75). Therefore, various environmental factors impact stability of viruses in varying degrees and must be tightly controlled in order to prevent viral inactivation.

Solar ultraviolet (78) radiation acts as a natural virucide in the environment by chemically modifying viral DNA and RNA. Previous studies have established that dsDNA and dsRNA viruses are generally more resistant to UV inactivation than viruses with single stranded genomes (79). Adenovirus (dsDNA) has been reported as the most UV resistant virus, while Rabies virus (ssRNA) is one of the most susceptible to viral degradation (80). UV germicidal irradiation (UVI) follows an identical trend, wherein double stranded viral genomes required 2 to 3 times higher UV doses for viral inactivation (81). UVI results in the formation of pyrimidine dimers in the DNA sequence of microorganisms which interferes with DNA duplications and leads to the destruction of nucleic acids, effectively inactivating viruses. It has been primarily used to sterilize surfaces and prevent transmission of disease via fomites. For example, during the SARS-CoV-2 pandemic, studies have confirmed that UVI can be used to disinfect N95 masks and respirators for health care workers, due to the national shortage of personal protective equipment (82, 83).

Chemical stressors have also been used to limit the spread of viruses. In general, enveloped viruses exhibit a higher sensitivity to chemical stressors than their non-enveloped counterparts. Poliovirus and human enterovirus are amongst the most resistant viruses to organic solvent mitigated viral inactivation, while SARS coronavirus, MERS coronavirus, ebolavirus, and influenza A virus can be inactivated in less than 30 seconds of exposure to ethanol-based

solutions (84). A common detergent used for viral inactivation, Triton X-100, solubilizes the lipid membrane of viral envelopes and prevents the virus from infecting cells. After 1 minute of exposure to 75% Triton X-100 (v/v), enveloped H1N1 influenza virus did not have a detectable infectious titer (70). Detergents are not effective at inactivating naked capsids, like adenovirus, as the bulky nonpolar head cannot penetrate water-soluble proteins (85). Environmental pH, on the other hand, has a profound effect on both enveloped and non-enveloped viruses. This is most likely because particles must be pH responsive for efficient release of the virus genome in the endosome during replication (Figure 1.4)(86). Preparations of pH 6-8 have successfully stabilized adenovirus type 5 particles at ambient temperature (87, 88). When pH falls below 5, the adenovirus capsid disassembles, preventing the virus from entering cells.

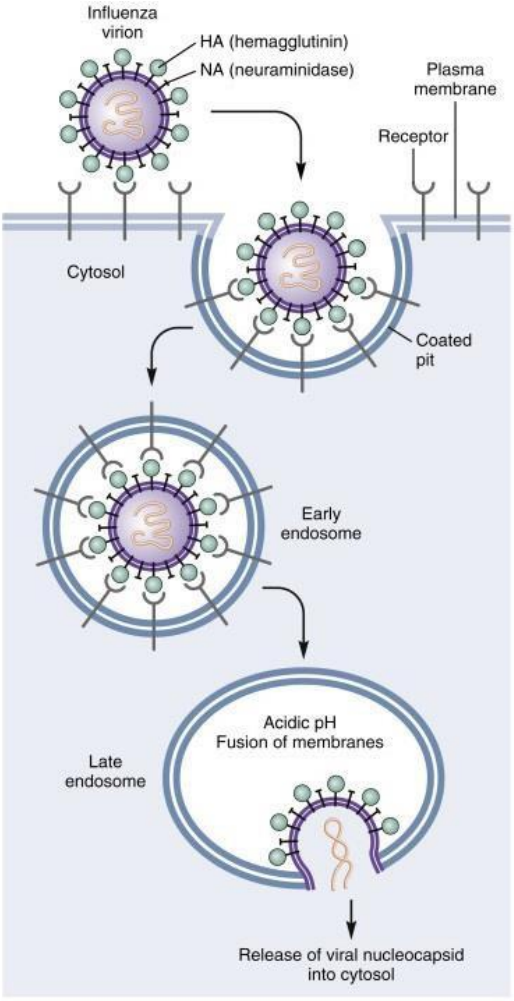

Figure 1.4: Influenza Virus Cell Entry. The virus attaches to the cells and is internalized by endocytosis. The acidic pH of the endosome (pH <5.5) leads to fusion of viral and vacuolar membranes and a release of the viral nucleocapsid into the cytosol. Figure from ref 86.

Influenza viruses exhibit an identical pH stability profile, with inactivation of hemagglutinin in acidic environments, which prevents cell entry (89, 90). During vaccine preparation, integrity of virus particles and conformational structure of antigenic proteins must be maintained. Understanding how particle size, shape, nucleic acid content, capsid proteins and the lipoprotein

envelope contribute to the physical properties of viruses is key in the development of stability profiles for virus-based products.

1.3 Principles of Formulation Design

The primary goal of any vaccine formulation is to protect and preserve the microbe or purified antigen's functional three-dimensional shape from physical and chemical pathways of degradation brought on by the environmental and chemical stressors covered in section 1.2. Figure 1.5 provides an overview of physical and chemical degradation pathways that can impact the functionality of proteins (91). Physical degradation pathways, such as denaturation and aggregation, result in the disruption of the secondary, tertiary, and quaternary structures of antigen proteins (91). Denaturation describes the process of protein unfolding. While some proteins easily recover their natural state when they do not the process is irreversible and detrimental to stability (92). Aggregation is a result of incorrectly folded proteins reversibly or irreversibly associating to form large clusters, which can impact protein function (93). These processes are typically brought on by extreme solvent pH and ionic strength, temperature, and denaturing chemicals (91).

Chemical inactivation pathways, such as oxidation, deamidation, hydrolysis, and racemization/βelimination, result in the disruption of the primary structure of antigen proteins wherein covalent modification of the protein occur through bond formation or cleavage. Cysteine and methionine are the two most susceptible amino acids to oxidation, wherein aldehyde and ketone residues form on side chains, due to exposure to peroxides, light, metals, and ionizing radiation (94, 95). Deamidation is typically brought on by extreme changes in pH, during which asparaginyl and glutaminyl residues are hydrolyzed and form free carboxylic acid groups on side

chains, converting them to aspartic acid and glutamic acid (91, 96, 97). Extreme pH can also result in hydrolysis, commonly aspartic acid-proline peptide bond hydrolysis, wherein interactions with water molecules result in peptide fragmentation and impact protein functionality (91). Racemization and β-elimination both start with the removal of a proton from the α-carbon of an amino acid. In racemization the proton recombines with the carbon anion to reform the original amino acid in either a d or l format. During β-elimination the proton can be rearranged, resulting in the formation of a double bond between the α and β carbons. These reactions are also brought on by extreme temperatures and pH and can play a significant role in viral aggregation. Formulation of viral proteins and viruses, which consist of a complex combination of several capsid proteins, for vaccine delivery is integral to successful immunization. To that goal, various excipients and vaccine dosage forms have been identified to maintain viral protein stability and immunogenicity during storage and distribution of vaccine products.

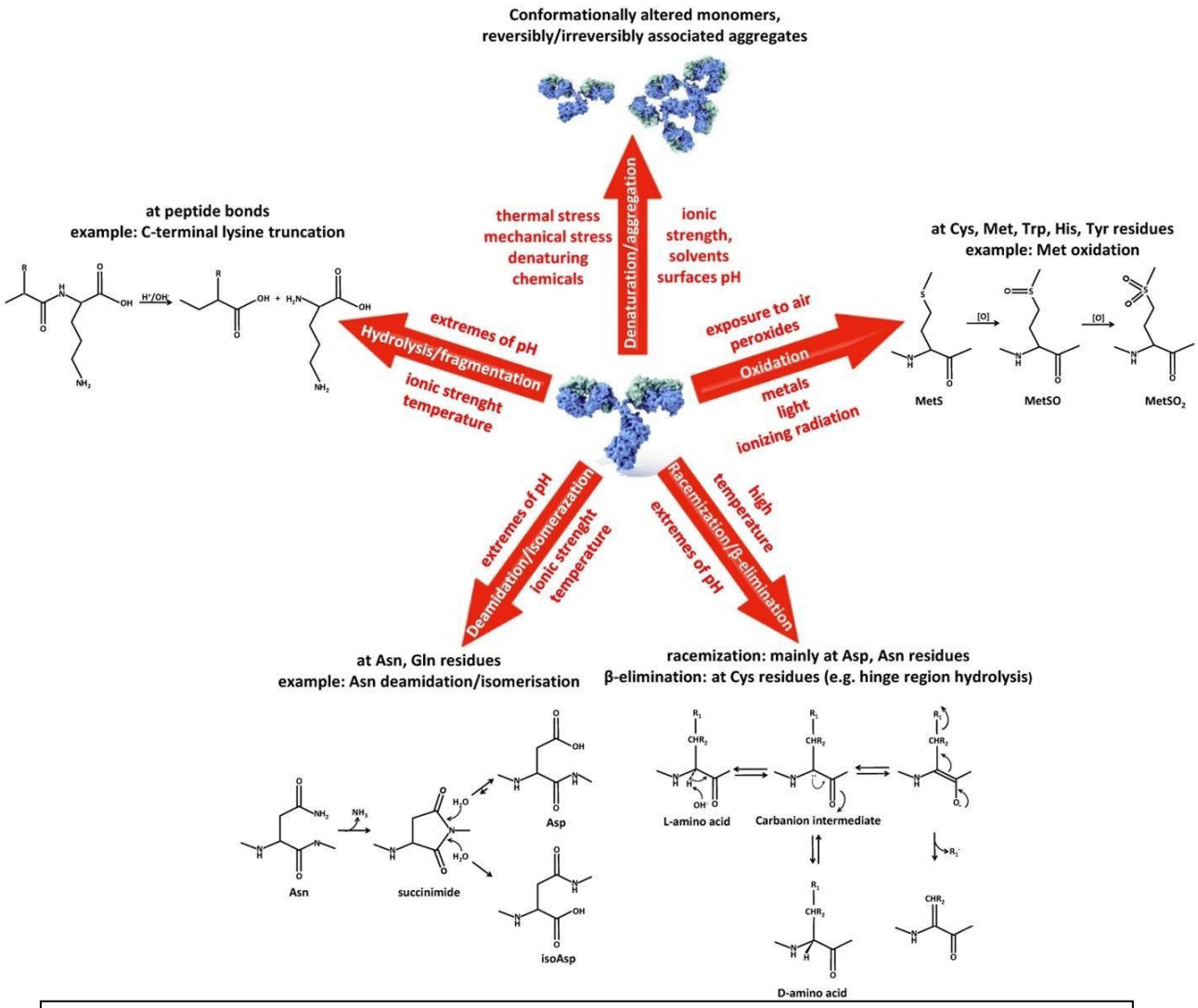

Figure 1.5: Chemical and Physical Pathways to Degradation.
Figure from ref 91.

1.4 Liquid Formulations for Viral Stabilization

Established standards by the World Health Organization (WHO), the Food and Drug Administration (FDA), and other governmental agencies require for any vaccine under development to remain stable during storage at a minimum of 2-8°C (98). As of September 23, 2020, 63 of the 89 vaccines approved for use by the Food and Drug Administration are formulated as liquid solutions for storage at 2-8°C with reported expiration dates ranging from

16 weeks (Flublock) to 3 years (Vaqta, RabAvert, Havrix, etc.) (6, 41). The stability of liquid formulations is maintained through the use of excipients which fall into several different categories: osmolytes, polymers, proteins, surfactants, and arginine (Table 1.1).

Table 1.1: Excipients Used in Liquid Formulations

Excipient	Contribution	Examples
Osmolytes	Pull water away from protein, prevent surface binding, line up at air-water interface (99-103)	Sorbitol, mannitol, sodium phosphate, sodium citrate, sucrose, trehalose, putrescine, spermidine, glycine, proline, glutamine, histidine
Polymers/Proteins	Stabilize via electrostatic interactions, prevent oxidation and deamidation, molecular crowing to prevent protein denaturation (99, 104-107)	Dextran, gelatin, enoxaparin, phytic acid, carboxymethyl cellulose, bovine serum albumin, cyclodextrins, polyethyleneimine (PEI), polyethylene glycol (PEG)
Surfactants	Prevent aggregation, adsorption to surfaces, line up at air-water interface, form micelles and seal protein in protective bubble above CMC (99, 108-110)	Polysorbate 80, polysorbate 20, Pluronic F-68
Arginine	Reduce viscosity, prevent aggregation, increase solubility (99, 111-113)	*note: Arginine is a unique amino acid that does not behave as an osmolyte

Understanding the contribution that each type of excipient offers a liquid formulation will allow the pharmaceutical scientist to efficiently develop effective and stable vaccine products. Solution pH and ionic strength play key roles in maintaining the integrity of virus particles and proteins (87, 114-116) while minimizing their interaction with various surfaces (117, 118) and each other (68). Thus, osmolytes, which include polyols, sugars, amines, salting out salts and amino acids, stabilize the native structure of proteins in order to prevent loss of vaccine potency due to pH-mediated unfolding of virus capsids and subunit proteins, aggregation, and adherence to container closure surfaces (119). Conversely, surfactants, proteins, polymers, and arginine are

used to suppress protein degradation pathways but have a minimal impact on protein folding (120).

Surfactants prevent aggregation that arises from heating and agitation of viral formulations through a variety of mechanisms. Above the critical micelle concentration surfactants form micelles which can trap the virus particle or protein inside or can fill the spaces between the particles to prevent aggregation (121, 122). Surfactants can also be used to minimize exposure of viruses and virus proteins to the air-water interface and prevent adsorption to surfaces by exploiting their hydrophobic and hydrophilic regions (123-125). The value of surfactants can be illustrated by the fact that about a third of approved liquid vaccine formulations (23 of 63) contain the surfactant polysorbate 80 (Appendix Table 1 and 2)(41, 126). Other amphiphilic excipients, like proteins and polymers, prevent surface adsorption of biomolecules through competitive binding at the surface interface as well (127). Furthermore, charged polymers are efficient at preventing aggregation via electrostatic interactions with the viral particle or protein and force the molecules into their native confirmation by molecular crowding (120, 128-132). Additionally, hydrogen bonding of polymers prevents metal ion catalyzed oxidation and deamidation (133, 134).

Reagents like sugars, polyols, and amino acids, or osmolytes, at concentrations of 0.1 to 1 M are often included in liquid vaccine formulations to support virus capsid integrity and prevent hydrolysis of virus capsid proteins during storage. These kosmotropic solutes are repelled from the surface of the virus particle or protein in a vaccine, since the concentration of the stabilizing molecule is lower at the protein: solvent interface than it is in the bulk solution. According to solution thermodynamics, this concentration difference locks in virus capsid and protein subunit structures as degradation and unfolding of proteins would increase the overall surface area of the virus particle and protein, significantly restricting the molecular motion/entropy of the stabilizer and creating an environment that is thermodynamically and energetically unfavorable. Thus, the vaccine remains in its native conformation as in this system it remains in its lowest energy state (Figure 1.6)(120, 135-137). It is important to note that the amino acid arginine does not interact with viral proteins through this mechanism. Instead arginine is very efficient at preventing viral aggregation by slowing protein-protein association interactions, with a minimal impact on protein folding (138). While these excipients at certain concentrations can stabilize virus and protein based vaccines for

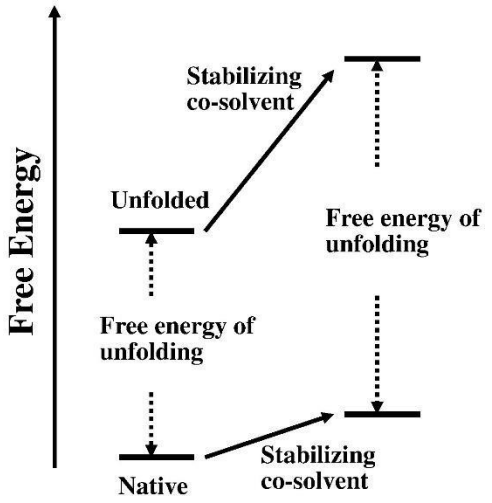

Figure 1.6: Thermodynamics of Protein Unfolding.
Since osmolytes are excluded from the protein surface, this is believed to be a thermodynamically unfavorable interaction which increases the free energy of the native state of the protein. As unfolded proteins have a greater surface area, it is hypothesized that the increase in free energy is even greater as there are more points of contact between the osmolytes and the unfolded protein. This results in a large energy difference between the native and unfolded protein state, meaning that more energy is required for proteins to unfold in the presence of osmolytes. Figure adapted from ref 120.

significant periods of time as a refrigerated liquid product, many liquid vaccine preparations are freeze-sensitive, as they cannot prevent disruption of the native three-dimensional shape of the virus/antigen by ice during freezing.

Accidental freezing of liquid vaccine products occurs through improper storage of vaccines (139), mechanical system malfunctions in storage units (140-142) and deviations from cold chain during global transport (143). Formulations that partially prevent ice crystal formation during freezing will fracture the virus particle/antigen during freezing and expose small regions that serve as points of nucleation for aggregate formation after melt (68, 144). While these aggregates may remain soluble and undetectable to the naked eye, they can significantly reduce the potency of the vaccine product. The presence of some adjuvants like alum also contribute to the sensitivity of a vaccine product to freezing. When aluminum oxide is frozen, it loses its colloidal structure and is fractured into crystalline parts which can cause severe adverse reactions such as aseptic abscesses at the injection site (53). The damage induced by freezing is irreversible and a field test, the "shake test", has been designed as a screening tool during immunization campaigns to prevent accidental administration of ineffective vaccines. Control vials of intentionally frozen vaccines and a vial from the shipment is shaken and then observed over time. If the aluminum adjuvant has been physically altered, the vaccine appears clear instead of opaque (Figure 1.7)(145).

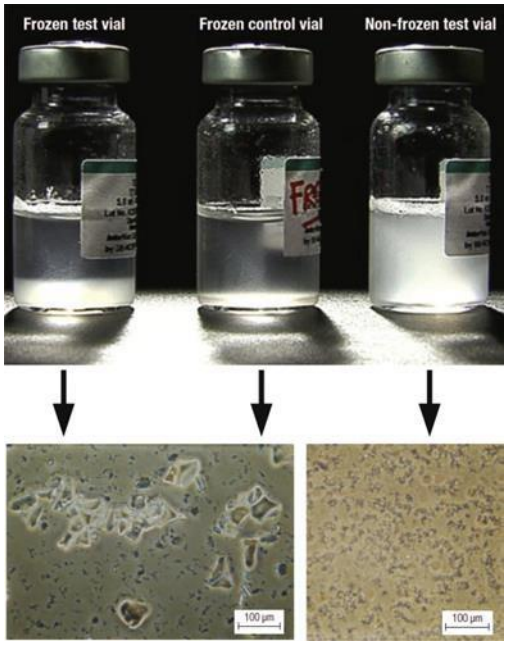

Figure 1.7: Shake Test. Visual assessment and optical microscopy to detect freeze damage to an aluminum adjuvanted vaccine after a "shake test" followed by settling for 90 s. Figure from ref 145.

In the absence of alum based adjuvants, increasing the concentration of small molecules like salts, sugars, and polyols to greater than 1M concentrations in a liquid vaccine product can significantly reduce loss of vaccine potency during a single freeze-thaw cycle by minimizing ice crystallization (120, 146, 147). However, these preparations are hypertonic and can cause significant pain upon injection. In some cases, they also demonstrate poor stability profiles for extended periods of time at 2-8°C due to their ability to effectively pull water away from the surface of the virus/antigen, facilitating aggregation and precipitation of vaccine over time (148). In an effort to generate vaccine products with limited cold chain requirements that could survive environmental stressors such as freezing and extreme heat, a significant effort has been put forth to stabilize virus and protein subunit vaccines in the solid state.

1.5 Solid Formulations for Vaccine Stabilization

Effective stabilization of live-attenuated viral vaccines requires long term maintenance of virus capsid integrity and preservation of internal genetic material during long term storage. This can be achieved best through formulation as a dry powdered product (98). For more than 50 years freeze-drying has been utilized to stabilize live microbes in the dry state for a variety of applications (149-151). This process, also referred to as lyophilization, has been accepted as the method of choice for stabilizing small molecule drugs, biologics and vaccines in dry powder formats by the pharmaceutical industry and regulatory agencies (98, 137, 152-156). Twenty of the current eighty-nine approved vaccines are available as lyophilized preparations (6, 41, 42).

Many of the excipients in Table 1.1, such as surfactants, osmolytes, and amino acids, are also employed in lyophilized preparations. However, Table 1.2 provides a summary of the unique contributions that these excipients make to dry formulations.

Table 1.2: Excipients Used in Lyophilization

Excipient	Contribution	Examples
Sugars/Polyols	Protein stabilizer, bulking agent, tonicity modifier (120, 137)	Sucrose, trehalose, lactose, maltose, sorbitol, mannitol
Polymers	suppressing protein aggregation, improve solubility upon reconstitution (157-159)	Dextran, CMC, polyethylene glycol (PEG), hydroxypropyl β-cyclodextrin (HPβCD)
Surfactants	Prevent aggregation (160-162)	Polysorbate 80, polysorbate 20
Amino Acids	Protein stabilizer (137, 163-165)	Histidine, Arginine, Leucine

Some of the primary components of a lyophilized product are sugars, polymers or other polyols at concentrations that allow them to effectively replace the water surrounding the virus or antigen to maintain three-dimensional structure (Figure 1.8) and minimize ice crystallization during the freezing step of the process (166). Freezing is generally performed at a fast (1°C/min) rate to a temperature that is below the glass transition temperature (Tg') of the formulation (167). At this temperature, the formulation generates an amorphous, glassy matrix in which hydroxyl groups of formulation excipients can form the highest

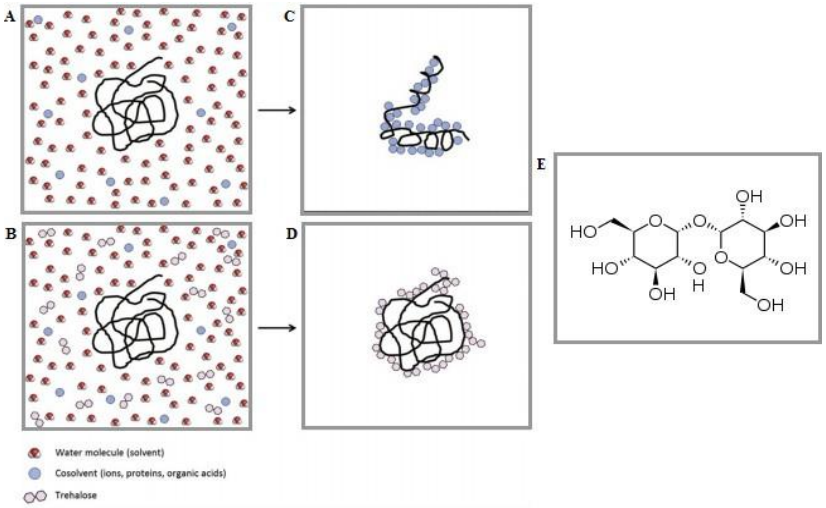

Figure 1.8: Water Replacement Theory.
A hydrated protein is surrounded by water and cosolvents (**A**). A hydrated protein is in a solution containing water, cosolvents, and trehalose (**B**). Dehydration of the protein results in unfolding (**C**). During dehydration compatible solutes, like trehalose, replace water molecules by forming hydrogen bonds with the protein, and preserving its conformation (**D**). Trehalose structure (**E**). Figure from ref 166.

number of hydrogen bonds with the vaccine candidate (166, 168). Water is initially removed during the primary drying stage through sublimation. During this process, loss of vaccine potency can be observed due to concentration of buffer and salts with a corresponding loss in product pH, however, incorporation of appropriate concentrations and/or blends of sugars, polymers or other polyols mitigates this effect (98). The primary drying stage is complete when the product temperature will stop increasing without manual input, indicating that bulk water has been effectively removed from the formulation (169). Removal of any excess water trapped within the solid matrix is achieved during secondary drying (170, 171). This process involves slowly raising the temperature (0.1°C/min to 0.3°C/min) to room temperature until the target moisture content is achieved. Effective formulation development plans include physical and biological characterization of the vaccine candidate during each phase of the lyophilization process and subsequent modification of formulation and process conditions to ensure minimal loss of original vaccine potency in the initial dried product.

Although the final product is a dried powder, a specific amount of water must remain in a virus-based vaccine product for optimal stability (172, 173). The optimal amount of residual moisture in a product usually falls within a very narrow range of 1-3% (170). Excessive moisture present in the dried product will facilitate proteolytic degradation of virus capsids and antigens over time. Excessive desiccation will result in collapsed virus capsids and physically damaged antigens capable of inducting semi-protective immune responses resulting in vaccine failure and possibly severe adverse reactions.

Specific diluents are often provided with a lyophilized vaccine product for reconstitution prior to administration. Although sterile water is often used in reconstituting many vaccines (Imovax, MMRII, ProQuad, RabAvert, Varivax, Zostavax), other diluents contain salts, amino

acids, or buffers to adjust tonicity of the product (YF-VAX, Hiberix) (174). Diluents can also contain low concentrations of surfactants (polysorbate 80) to prevent aggregation that might occur upon rehydration of vaccine contents and to minimize loss of vaccine due to adsorption to the vial surface and preservatives (thiomersal) to maintain sterility after reconstitution (174, 175). It is important to realize that the diluents selected for use with specific vaccines contribute little to the overall stability profile of the vaccine as the majority of vaccines, such as Zostavax, YF-Vax, Varivax, and ProQuad, currently utilized in immunization protocols must be discarded if not administered within 1 hour after they have been reconstituted (175).

While freeze-drying of vaccines was initially adopted in an effort to minimize reliance on the cold chain during global distribution, none of the products currently in use can be stored at ambient temperatures for significant periods of time (Appendix Table 1 and 2)(6, 41). Six of the 20 currently approved vaccines still require storage at temperatures of -15°C or less (ProQuad, MMRII, ACAM 2000, Varivax, Zostavax, Vaxchora) while the remaining 14 products are to be stored at 2-8°C (176). Despite this, a freeze-dried influenza vaccine with favorable stability at 4, 25 and 37°C for 40 months has recently been described as part of the National Strategy for Pandemic Influenza preparedness in the United States (177), suggesting that improvements in the understanding of physical characteristics of viruses, excipient selection and the lyophilization process will result in more thermostable vaccines in the future. However, the cost and complexity of the freeze-drying process and associated issues with dry powder vaccines such as strict requirements for reconstitution, proper dilution, and administration, makes it a somewhat impractical form of vaccine stabilization.

1.6 Spray-Drying

Spray-drying technology has been utilized since the early 1940s in the pharmaceutical industry for the generation of stable dry powder formulations of small molecule therapeutics and some biological drugs (78, 178, 179). A dry powder is produced in a single-step process that involves atomization of a formulated drug solution in a hot, dry environment where temperatures can range from 60 to 220°C, rapid removal of solvent, and collection of dry drug particles (Figure 1.9) (178). Excipient selection for therapeutic proteins follows the same principles as those outlined for lyophilization, with the main driver being the ability of an excipient to replace water surrounding the protein allowing it to maintain its three-dimensional shape during drying. As with freeze-drying spray drying consists of a two-step process. In the first drying phase, the rate of drying is constant until a state of equilibrium is attained between the droplet and dry air. As the moisture content declines and saturation conditions can no longer be maintained, the secondary drying phase begins. As moisture is continually lost, the droplet becomes concentrated and a solid outer shell forms around the droplet. Additional solvent is pulled through the solid layer. While the heating and evaporation of water from atomized droplets can affect the virus particles and other antigens by altering secondary structure through changes in pH and precipitation of active ingredients, the self-cooling effect of droplets

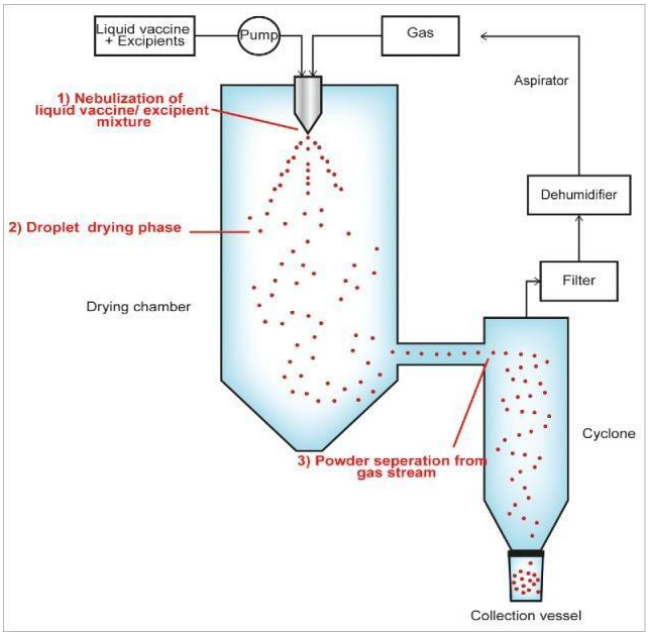

Figure 1.9: Overview of the spray drying process.
Figure from ref 178.

during evaporation prevents temperature increase on the droplet surface above the wet bulb temperature (180). Spray drying processes have been further adapted to address the thermal sensitivities of vaccines. This is done through the use of the lowest inlet air temperature that allows for drying, inclusion of co-current spraying flow patterns so that the driest particles interact with the low temperature regions within the dryer and the wettest particles interact with the highest air temperatures, and minimal drying times ranging from 0.2 to 30 seconds per droplet depending upon the capacity of the spray drier and airflow rate (178).

There are many advantages to utilizing spray drying technology to stabilize vaccines. Unlike lyophilization, spray drying does not expose the product to the stress associated with freezing and removal of water under vacuum conditions. The one step drying process is less time consuming and requires significantly less energy and operating costs than standard freeze-drying protocols. The resultant dispersed fine powder also does not require reconstitution for delivery to mucosal routes of administration (80-83). Notably, Wang et al. successfully immunized rabbits after storing an anthrax dry powder vaccine for 2 years at room temperature via the intranasal route (181). Spray-drying also has various advantages over the liquid stabilization approach for vaccines. Preservatives can complex buffering systems needed for stability in the liquid state and can be eliminated from many spray dry powder formulations without compromising the physical stability of the vaccine product at ambient and elevated temperatures which is highly advantageous for distribution and use in remote developing countries (179, 182). A few studies have demonstrated superior long-term stability of dry powder vaccines. Kanojia et al. spray dried a H1N1 inactivated virus which retained antigenic stability after 3 months of storage at 60°C (183). Ohatke et al. successfully stabilized a live attenuated measles vaccine for 8 weeks at 37°C (184).

However, there are various draw backs to spray-drying as well. Shear stress during atomization and elevated temperatures during drying along with the formation of large air-water interfaces during droplet formation can lead to antigen instability and denaturation (185). An alternative technique, spray freeze drying where liquid formulations are immediately atomized into a cryogenic medium instead of a heated gaseous medium (78) has been developed to minimize exposure of a vaccine product to elevated temperature. Influenza, diphtheria, tetanus, hepatitis B, anthrax, and plague vaccines have been successfully stabilized by this technique (181, 186-189). Carbon dioxide-assisted nebulization with bubble drying (CAN-BD®) can also minimize exposure to extreme temperature during drying. This process involves the mixing and dissolution of carbon dioxide within an aqueous vaccine formulation at a pressure of 8-10 MPa and temperature of 30-50°C (190). The mixture is then released as a spray through a nozzle and rapidly dried by heated nitrogen gas, at 25 to 65°C. Live attenuated measles and hepatitis B surface antigen vaccines have been developed using the CAN-BD technique (191-193). However, these particles are still subject to atomization and therefore reduced antigen function and immunogenicity. Furthermore, to achieve a low residual moisture content in the final product, a secondary drying step is sometimes required and results in increased drying time and energy expenditures, negating one of the key advantages of spray-drying technology in comparison to lyophilization.

1.7 Film Formation for Vaccine Stabilization

The United States Food and Drug Administration (US FDA) defines “film” in three different ways with respect to pharmaceutical drug products (194): a) a thin layer or coating, b) a

drug delivery system that releases drug over an extended period in such a way to maintain constant drug levels in the blood or target tissue (extended release film) and c) a thin layer or coating which is susceptible to dissolution when in contact with liquid (orodispersible film) (195). A number of registered and commercialized small molecule pharmaceutical drug products formulated in platforms that fall within these definitions as thin film dosage forms and several mucosal oral films containing biologic drugs have entered clinical testing within the last 2-3 years (196, 197). Thus, it is clear that oral dissolvable films are a highly promising and emerging dosage form.

Many of the principles involved in stabilization of biologicals during lyophilization can also apply to stabilization of vaccines in a thin film. However, several additional types of excipients are necessary to confer physical properties that define the film dosage form. Table 1.3 provides a brief explanation of common types of excipients utilized in thin film dosage forms, the role each excipient class plays in film formation and a few examples currently utilized in FDA approved products.

Table 1.3: Types of Excipients Evaluated in Thin Film Formulations

Excipient	Contribution	Examples
Polymer	Film forming agent, mucoadhesive (196, 198)	Hydroxy propyl methyl cellulose (HPMC), methyl cellulose, pullulan, sodium alginate, polyacrylate and polymethacrylate derivatives, and chitosan
Sugars	protein stabilizer (120, 199-201)	Sucrose, glucose, fructose, maltose, arabinose, trehalose
Surfactants and Bile Salts	Improve absorption, stabilize proteins, suppress aggregation (120, 196, 198-201)	Sodium glycocholate, palmitoyl dimethyl amino propane sulfonate, pluronic F-68, polysorbate 20 and 80, PEG-3350
Fatty Acids	Permeation enhancer (196, 202)	Pluronic® f-127, oleic acid, eicosapentaenoic acid, docosahexaenoic acid, palmitic acid
Plasticizers/Polyols	Flexibility/resistance (203, 204)	Glycerin, polyethylene glycol, propylene glycol, glycerol, maltitol, sorbitol

Polymers are the most important excipient in film formulation since they are used as the film-forming material and act as mucoadhesive (196, 205). The mechanism of mucoadhesion is currently unclear but it is believed that five theories- wetting theory, diffusion theory, electrostatic theory, adsorption theory, and fracture theory- each contribute in complimentary ways. Table 1.4 briefly summarizes each theory.

Table 1.4: Defining the mechanisms of polymer mucoadhesion[1]

Wetting	Diffusion	Electrostatic	Adsorption	Fracture
Polymer binds to imperfections on surface of mucosal layer by producing adhesive anchors via contact angle and thermo-dynamics	Adhesion occurs once polymeric chains reach 0.2-0.5µm of depth in mucosal layer, into glycoprotein mucin chains	Electrons establish an electrical double layer due to electron transfer from polymer and mucosal surface	Surface forces act on each other's chemical structures after initial contact	Describes the force required to separate two adhering surfaces, in order to quantify adhesion limitations

[1] This information was adapted from Refs (196, 205)

As with lyophilized products, sugars play a pivotal role in film preparations at a concentration that suspends the vaccine in an amorphous matrix during drying. Surfactants, when included in a formulation above the critical micelle concentration (CMC), can trap the vaccine candidate within micelles to minimize protein surface denaturation (206). Ionic surfactants can also interact with the surface charge of vaccine components to form a large network of individual particles dispersed throughout the film matrix (207)(Chapter 3). Surfactants also promote distribution of vaccine across physiological barriers like the cheek, as is evidenced by a decrease in transepithelial electrical resistance (TEER) measurement when added to in vitro models of the oral mucosa (208). Bile salts, which act as physiological surfactants, can improve absorption by increasing the solubility of hydrophobic drugs or increasing the fluidity of the apical and basolateral membrane (209, 210). Fatty acids are also employed in film formulations in order to improve permeability across the epithelial barrier by resulting in calcium ion influx which activates potassium channels and increases channel opening (196, 201, 211).

While surfactants and sugars work together to stabilize proteins, plasticizers contribute to the mechanical properties of films, like tensile strength and maximum elongation (203, 204). When biomolecules are dehydrated without plasticizers, proteins change conformation which results in denaturation and loss of activity. It is hypothesized that the hydrophobicity index of polyols, which are a type of plasticizer, is inversely correlated with net stabilization effect of biological molecules, which results in these mechanical changes and prevents protein denaturation (212). Once the formulation components have been identified, film layers can be prepared by several different techniques which include: solvent casting, hot melt extrusion, and thermal inject printing. Table 1.5 provides a brief explanation of each technique.

Table 1.5: Summary of Standard Film Forming Techniques

	Solvent Casting	Hot Melt Extrusion	Thermal Inkjet Printing
Description	soluble polymer is dissolved in a volatile solvent to result in the formation of a homogenous solution including the vaccine and other excipients; the solvent is removed via evaporation, pressurization, and heating (213)	Transforms distinct materials into a homogenous mixture by melting, mixing, and forcing through a die (214)	Substrate matrix for printing and drug loaded liquid phase, followed by deposition in a solid matrix via printing (215)
Advantages	Not heat sensitive, well defined, one step procedure	Highly reproducible, uniform dose forms, well defined	Small volumes can be deposited (pL), mass production friendly, uniform
Disadvantages	Direct contact between virus and solvent which affect viral activity, potential decrease in homogeneity, potential aggregation	Heating required, high shear stress, recrystallization during storage	Not well defined, heat pulse required for ejection

Since viruses are heat sensitive, solvent casting is the most appropriate film formation technique for viral based vaccine products. However, since solvent casting typically employs organic solvents, it could adversely affect viral activity. These hurdles have recently been addressed by the use of water-based solvents and the use of a proper combination of the excipients reviewed previously. Taking this approach, Leung et al. stabilized Herpes Simplex Virus type 2 and Influenza A virus for 12 weeks at 23°C in a film matrix containing the polymer pullulan and trehalose (216). Stinson et al. successfully vaccinated Wistar rats using an inactivated Polio vaccine stabilized in silk fibroin films, which were reconstituted and injected, was stored at 45°C for two weeks (217). Adenovirus was stabilized in thin films containing hydroxypropyl methyl cellulose, sorbitol, and a novel amphiphilic surfactant at 20°C and 4°C for three months and through 16 freeze-thaw cycles (207)(Chapter 2). This same dosage form

induced a strong humoral immune response to influenza following sublingual administration to mice (Chapter 4). Other studies have evaluated the effect of film stability when layered onto microneedles, for buccal and dermal administration of vaccines. Mistilis et al. found that films composed of sodium carboxy methyl cellulose, arginine, and heptagluconate, dried on microneedles, successfully stabilized influenza for 4 months at 60°C and was able to effectively immunize mice after one year of storage at 25°C (218). Kim et al found that films, containing carboxymethylcellulose, lutrol, and trehalose coated on microneedles maintained 65% of Hemagglutinin activity for 24 hours at 4°C and protected 100% of mice from lethal challenge with influenza (219). Vaccine formulation in films has resulted in not only a unique platform for stabilization, but also a novel platform for delivery. The following sections will evaluate current standards for vaccine delivery and novel approaches to inducing protective immunity both locally and systemically.

1.8 General Overview: Immune Response to Virus Based Vaccines

Pain and inflammation at the site of injection are the most commonly reported side effects of injectable vaccines (220, 221). Cytokines and chemokines released during the inflammatory response increase vascular permeability to enhance recruitment of dendritic cells, macrophages, monocytes, and neutrophils from the circulation to the injection site (Figure 1.10)(222, 223). Various components of the vaccine drive the type of immune response that results after injection. Inactivated virus particles or antigens are taken up by cells, processed and presented by major histocompatibility complex (MHC) class I molecules on the cell surface, ultimately resulting in a pathogen specific cytotoxic CD8+ T cell response (224).

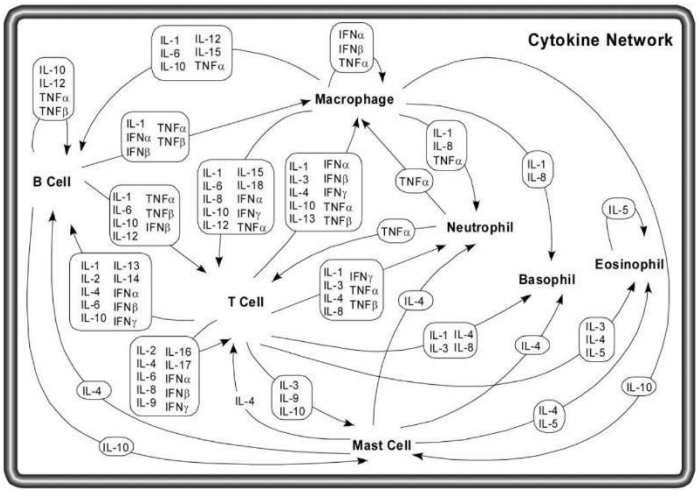

Figure 1.10: Schematic drawing depicting immune cell activation via cytokine response. Figure from 223.

Live, attenuated and recombinant virus based vaccines (for example Zabdeno® (Ad26.ZEBOV), an adenovirus 26 vector expressing the Ebola Zaire glycoprotein in infected cells) also facilitate processing and presentation of antigens made by infected cells by MHC class II molecules on the cell surface, ultimately resulting in activation of pathogen specific helper CD4+ T cells in addition to a cytotoxic CD8+ T cell response (225, 226). In response to cytokines released by antigen presenting cells, CD4+ T cells can differentiate into Th1 helper cells to strengthen the cytotoxic T cell response (IL-12, IFN-γ) or Th2 cells to support B-cell proliferation and differentiation into plasma cells for an antigen-specific antibody mediated response (IL-4, IL-2) (227). Regardless of route of administration, antigen-specific CD8+ T cells and plasma cells are generally detectable in the circulation 10-14 days after immunization (Figure 1.11)(228). Antibody levels generally peak approximately 4 weeks after immunization (229). Maintenance of proper structure of the antigen in a vaccine formulation can significantly impact the strength and the breadth of the antibody response (230-232). Responses to improperly processed antigens or those in which proper confirmation was compromised can result in partially protective immune response or as seen with dengue vaccines, antibody mediated enhancement of infection (233). One a vaccine is cleared, remaining T cells differentiate into memory T cells. Central memory T cells, located in lymphoid organs and bone marrow, have a high proliferative

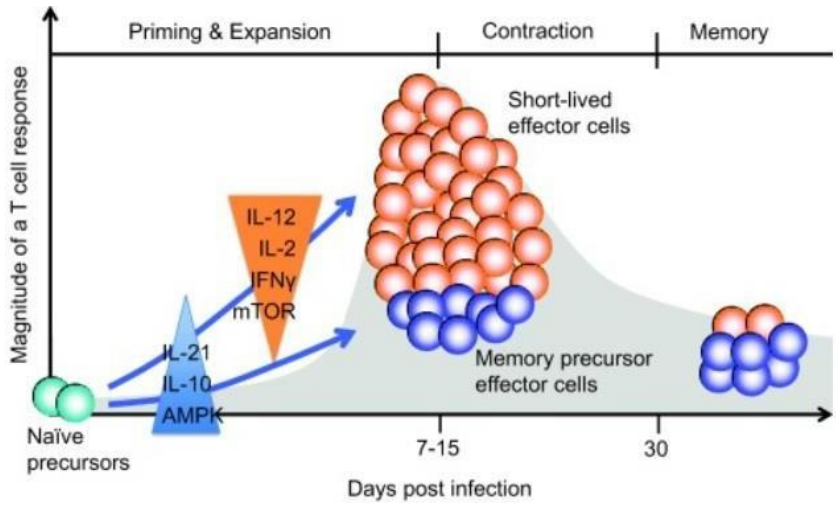

Figure 1.11: T cell Proliferation Timeline.
Following infection, antigen-specific T cells are activated and divide into short-lived effector cells or memory precursor cells based on the cytokines present. After peak responses, effector T cells mostly die while memory cells develop into long-lived memory cells. Figure from ref 228.

potential, whereas effector memory T cells in peripheral tissues remain in a preactivated form that enables them to immediately recognize pathogens (122). Resident memory cells remain in specific organs providing local immunity, often in the intestine, lungs, and skin. The degree to which these cells are produced in response to a vaccine significantly depends upon the manner in which it is given.

1.9 Administration of Vaccines: The Injectables

Of the 89 vaccines approved for use by the FDA 83 of them are available as injectable products (Appendix Table 1 and 2)(6, 41). Injectable vaccines are given by the intramuscular (IM), subcutaneous (SC) and intradermal (ID) routes (Figure 1.12) (234). The route of vaccine administration greatly affects vaccine efficacy in inducing immune response. Intramuscular injections are absorbed faster than subcutaneous injections because muscle tissue has a greater blood supply and it can also hold a larger fluid volume (235). This larger volume can also facilitate dispersal of common adjuvants which can cause severe erythema, contact hypersensitivity, granulomas, and nodules within the subcutaneous space (236, 237). Vaccines developed for IM and SC administration must be administered by highly trained staff due to requirements for proper needle selection and placement to maximize efficacy and minimize adverse effects (134-136). The length of needles utilized for a given vaccine also needs to be modified according to age as muscle density changes over time to ensure the vaccine reaches the intended target (137). Conventional sites for intramuscular injection include the deltoid muscle of the arm, vastus lateralis muscle of the thigh, and ventrogluteal muscle of the hip. de Lalla et al. found that subjects given an HBV vaccine by IM injection in deltoid muscles experienced the highest rates of seroconversion in comparison to those given the vaccine by IM injection in the gluteal muscle. This was attributed to the lack of bioavailability as the needle was not capable of reaching the gluteal muscle efficiently and

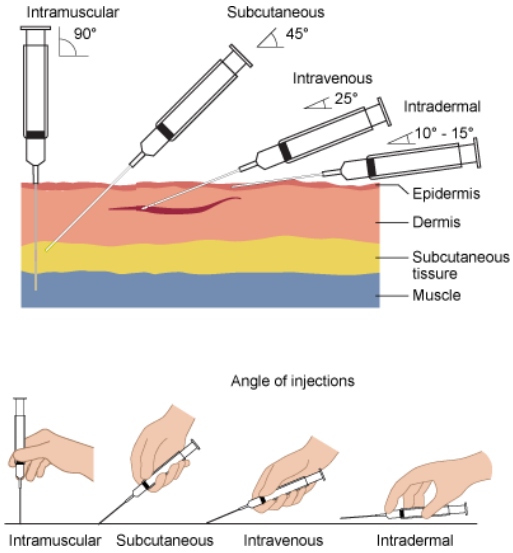

Figure 1.12: Parenteral Injection administration.
Figure from ref 234.

unilaterally across patients of different age and gender (238, 239). Other studies have demonstrated that the thigh is also a better location than gluteal muscles for pertussis and the DTap vaccines (240). Subcutaneous injections are most often administered in the abdomen around the umbilicus, back or side of the upper arm, and front of the thigh. Vaccination by the subcutaneous route has generally been used for live attenuated vaccines, however the immune response is generally comparable to intramuscular routes of vaccination (241). This has been demonstrated for Hepatitis A, measles-mumps-rubella, diphtheria-tetanus, and meningococcal vaccines (242-244). To date, intramuscular administration of vaccines is considered to be the gold standard treatment. Currently 65 of the 89 approved vaccines in the United States are given by IM injection only, while only 9 are given by the SC route only (Vaccine Appendix Table 1 and 2)(6, 41).

One of the more significant limitations of IM administration of vaccines is the fact that muscle tissue contains a very low density of antigen presenting cells, requiring large doses of vaccine and the use of adjuvants to increase dendritic cell recruitment to the site of injection (245). The epidermis and dermis layer of the skin, however, is rich in dendritic cells (dermis), Langerhan cells (epidermis), T lymphocytes, natural killer cells, macrophages, and mast cells with direct access to draining lymph nodes (Figure 1.13) (246, 247). For this reason, administration of vaccines by the intradermal (ID) route has resulted in significantly

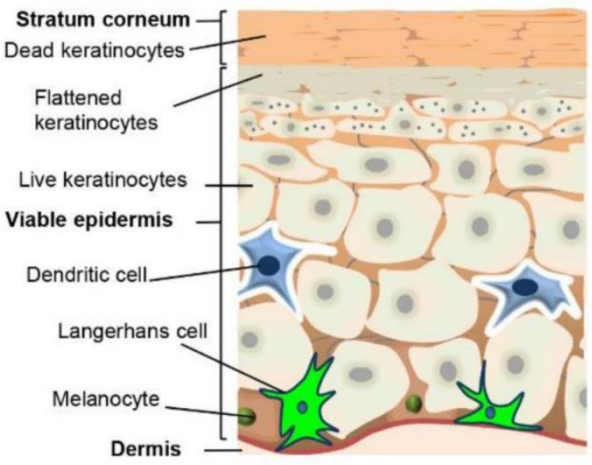

Figure 1.13: Intradermal Anatomy and Location of Local Antigen Presenting Cells.
Figure from ref 247.

stronger immune responses than that observed with the same vaccine given by the IM route in a dose sparing manner (248). One of the major challenges associated with ID immunization, correct placement of commercially available needles within the epidermal space, has been addressed through devices designed specifically for this purpose. To date, only one of the currently licensed vaccines is given by the ID route: the Bacille Calmette Guérin (BCG) vaccine for tuberculosis (6, 41)(Appendix Table 1 and 2).

Gene guns, traditionally used to introduce DNA into plants, have also been used for administration of genetic vaccines to the skin (Figure 1.14)(249). Initial work involved pushing DNA coated gold particles deep into the intradermal layer through the use of high-pressure gas emitted from the barrel of the gun (250). Vaccines administered with a gene gun have been poorly protective against diseases that require T helper 1 (Th1) type immunity and are less effective in these cases than the same vaccine given by the canonical IM injection (251). Addition of molecular adjuvants to a vaccine formulation in specific ratios can overcome this effect in some cases, however, exact mechanisms that dictate the Th2 bias of vaccines delivered by gene gun are a subject of continuing investigation (252-254). For this reason, clinical trials of DNA based vaccine have replaced the

Figure 1.14: A Gene Gun. Gold nanoparticles are coated with the genetic vaccine and loaded onto a membrane. A compressed gas, such as helium, is used as the force that moved the filter down the barrel of the gun, which then pushes the membrane to a barrier. Once the membrane strikes the barrier, the force of the momentum will dislodge the nanoparticles form the membrane and they will travel beyond the barrel to interact with the target (cells, tissues, etc.). Figure from ref 249.

gene gun with devices that deliver material to the intradermal space via adaptive electroporation (255). Instead of forcing particles coated with vaccine into the skin, this process introduces short bursts of electrical current under the skin surface that creates transient increases in cell membrane permeability, thus enhancing DNA uptake by at least 500 fold in a less painful manner, leading to a more robust immune response (256).

Microneedles can be fabricated in a patch format consisting of arrays of microscopic needles ranging from 25-2000 μm in height to ensure that vaccine can reach the depth of the skin's capillary system, without damaging the nerves located in the dermis layer in a relatively pain-free manner (257, 258). Microneedle technology is highly adaptable to a variety of vaccines as needles have been constructed from stainless steel, biodegradable polymers, and silicon in arrays of tens to hundreds of individual projections. Antigens can be formulated and dried onto metal microneedles, encapsulated within polymer derived needles, or delivered through hollow microneedles. Several studies have shown that microneedle technology is capable of inducing protective systemic and mucosal immune responses. Pattani et al. immunized mice through the ID route with the HIVgh140 antigen formulated in mucoadhesive copolymer Gantrez® AN-139, PBS, and polysorbate 80 microneedles. Sixty-eight days after the initial ID dose, mice that received three booster doses via the intranasal route (on days 14, 28, and 42) produced an antigen specific IgG response systemically and high levels of IgA in vaginal washes (259). In another study, microneedles coated with recombinant trimeric soluble hemagglutinin induced a stronger response in ID immunized mice than that observed by IM injection. These mice were also protected from lethal Influenza challenge and had greater levels of IgA in serum and vaginal washes (260).

As discussed in section 1.7, microneedles have also been proven to stabilize virus-based vaccines (261-263). In order to achieve a stable form, excipients are optimized to maintain vaccine activity during manufacturing and storage. For example, trehalose and methylcellulose have been used to stabilize hemagglutinin in microneedles (219, 264). Another study found that arginine and heptagluconate was the ideal combination of excipients for the successful stabilization of a trivalent subunit influenza vaccine at extreme and ambient temperatures (218). Despite this promising data, microneedles are currently not utilized in the clinic due to a few limitations. Mechanical failure of silicon microneedles fracturing and polymer-based microneedles buckling during insertion results in ineffective vaccine dose delivery and is undesirable in clinical applications (265). While metal microneedles eliminate problems associated with mechanical failure, they contribute to the production of sharp bio-hazardous tip wastes. Current research is focused understanding the mechanical behavior of microneedles against skin in order to improve design methodologies and overcome this barrier to successful delivery.

1.10 Intranasal Vaccine Delivery

The nasal mucosa is one of the most promising alternative immunization routes since it is often the site from which many infections start and also the site from which both systemic and local immune responses can be initiated. Immune inductive sites, often referred to as nose-associated lymphoid tissue (NALT), are found on the ventral surface of the nasal cavity near or within the nasopharyngeal duct (Figure 1.15A) (247). Following nasal vaccination, soluble antigens can penetrate epithelial cells lining this region and directly interact with antigen

presenting cells that populate the mucosal space (Figure 1.15B) (266, 267). Particulate antigens,

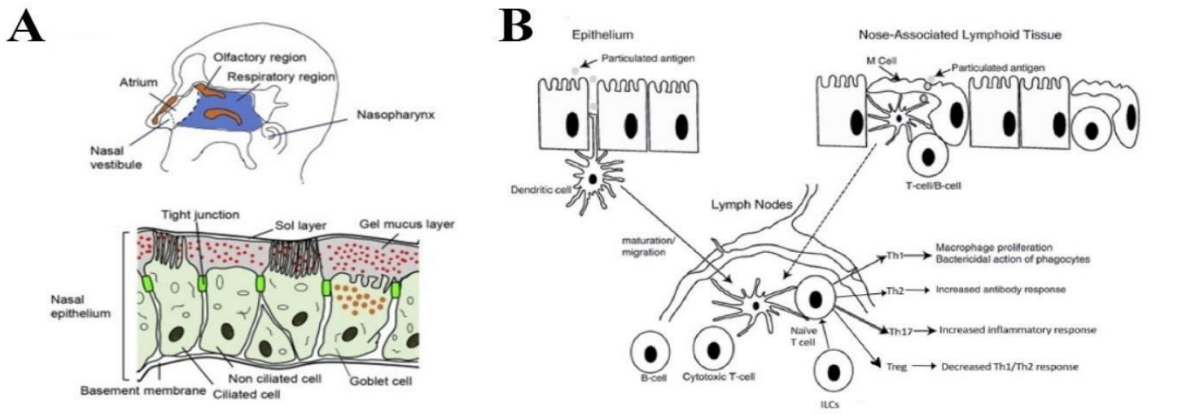

Figure 1.15: Aspects of Intranasal Vaccine Delivery.
Nasal Cavity (A). Figure from ref 247.Representative pathways by which antigens stimulate local and systemic immune responses after intranasal immunization (B). Figure from ref 267.

too large to cross the epithelium, can be taken up by microfold (M) cells, which transport antigens across the mucous membrane to underlying lymphoid cells (268). In both instances, antigen presenting cells activate both T and B cells some of which remain in the mucosal space, primed for the next infection while a fraction of the population travels through the lymphatic system to induce immunity in other mucosal sites and systemic lymphoid organs (140, 142).

The nasal cavity also offers a route by which vaccines can be given in a needle free manner, effectively reducing the cost of immunization campaigns by allowing self-administration. The initial popularity of FluMist (US), FluMist Qudravalent (US) and Nasovac (India) influenza vaccines over injectable products for children illustrates the attractiveness of this route of immunization with regard to patient compliance (269, 270). The intranasal route also allows for administration of liquid and dry vaccines so vaccine stabilization techniques can be more versatile (271). Some of the disadvantages associated with administration of intranasal vaccines include size-restricted permeation across epithelial barriers and mucociliary clearance

of antigen before it is properly processed. This latter issue can be overcome by the addition of mucoadhesives to vaccine formulation to increase contact with and residence time within the nasal cavity. CriticalSorb™, a novel absorption enhancer based on Solutol®, is a highly effective nasal delivery system for macromolecules which could be utilized for intranasal vaccination (153). The μco™ System, a proprietary powder formulation mucoadhesive carrier technology with an accompanying easy-to-use device (Fit-lizer™) to deliver its powder drugs into the nasal cavity in a highly reproducible fashion (272), elicited significantly higher anti-influenza IgA antibodies in the nasal wash in non-human primates than the same preparation given by IM injection or as a liquid nasal spray (267). Chitosan, a sugar obtained from the hard outer skeleton of shellfish and which plays a role in wet-resistant adhesion of mussels in nature (273), can form a strong adhesion layer on mucosal surfaces and open tight junctions in mucosal membranes and increase antigen penetration (146-148). Although ChiSys®, a chitosan-based formulation has been shown to evoke robust immune responses against a variety of antigens, including diphtheria, seasonal influenza, avian influenza, anthrax, and Norwalk virus (274), it has not yet been included in any marketed nasal formulations despite holding monographs in the US and EU Pharmacopeias (275). Additional concerns about the impact of pre-existing immunity to certain viruses on the efficacy of nasal vaccines (276, 277) and the absence of safe mucosal adjuvants (278-280) have motivated investigation into alternative needle free methods for vaccine delivery.

1.11 Oral Vaccine Delivery

Administration of vaccines by the oral route offers similar advantages as intranasal immunization such as needle free administration and the ability to induce both systemic and mucosal immune responses. As in the nasal mucosa, the intestine is peppered with immune inductive sites, known as Peyer's patches, located in regular intervals in the duodenum, jejunum, and ileum and collectively are called the gut-associated lymphoid tissue (GALT) (Figure 1.16A)(247, 281-283). If an antigen can successfully pass through the acidic and enzyme-rich conditions in the stomach to the intestine, it is often trapped in a viscous layer of mucus, produced by goblet cells which physically trap and neutralize pathogens. Antigens can, however, be taken up by M cells, specialized epithelial cells with underdeveloped microvilli that do not harbor the tight junction properties of other enterocytes which restrict absorption of nutrients and electrolytes through transcellular and paracellular pathways (284, 285). These cells, found within the follicle associated epithelium (FAE) of Peyer's patches, are located in areas with a limited number of goblet cells and little or no mucus. They act as a direct entryway for vaccine antigens, bacteria, and viruses, as they offer transport in a lysosome-

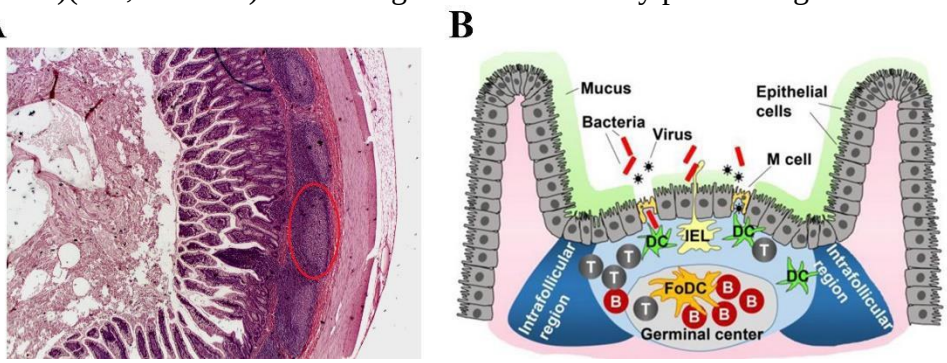

Figure 1.16: Aspects of Oral Vaccine Delivery.
A histology section from the ileum depicting a Peyer's Patch (circled in red). (**A**). Peyer's patch schematic displaying M cells and the different immune cell populations (**B**). T: T cells, B: B cells, DC: dendritic cells, IEL: intraepithelial lymphocyte, FoDC: follicular dendritic cell, IFR: intra-follicular region. Panel A: Wikimedia Commons accessed 25 September 2020; available at: https://commons.wikimedia.org/wiki/File:Peyer%27s_patch_(improved_color).jpg. Panel B: ref 247.

independent manner and present them intact to dendritic cells and intraepithelial lymphocytes to activate antigen-specific B and T cell mediated immune responses (Figure 1.16B)(285). Even though the average adult has about 30,000 individual lymph nodes distributed along the gastrointestinal tract (282), each node contains a limited number of cells and their composition is influenced by the intestinal microbiota and diet, posing an even greater challenge to development of oral vaccines for use in global populations (286-288).

Formulations for oral vaccine products must contain excipients to protect antigens and viruses from acid and enzymatic degradation in the gastrointestinal tract. The adenovirus 4 and 7 oral vaccine made by Teva Pharmaceuticals consists of 2 enteric coated tablets designed to pass intact through the stomach and release the live virus in the intestine (289). This product must be stored at 2-8 °C with desiccant. Vivotif ®, a product containing live attenuated *Salmonella typhi*, is formulated as an enteric coated capsule that is not stable at ambient temperatures (290). One round of immunization requires a capsule be taken approximately 1 hour before a meal with cold water (temperature should not exceed body temperature, e.g., 37 °C) on alternate days for one week (e.g., days 1, 3, 5 and 7). This series should be repeated every 5 years under conditions of repeated or continued exposure to typhoid fever (291). Vaccines formulated as liquid products, for oral delivery, include excipients like alginate, polyvinyl alcohol, hyaluronan and cellulose to increase the viscosity and increase mucosal adhesion in the gut (292). RotaTeq^{TM} consists of a liquid formulation of 5 live rotaviruses that is given dropwise in the inner cheek (293). The vaccination series consists of 3 doses, the first starting at 6 to 12 weeks of age and subsequent doses administered at 4- to 10-week intervals. It is stored and transported at 2-8°C and should be administered as soon as possible upon removal from refrigeration (294). Rotarix® consists of lyophilized live, attenuated human rotavirus which must be reconstituted in a prefilled oral

applicator just prior to administration (295). In contrast to RotaTeq^{TM}, it only requires a two-dose regimen and is stable in the reconstituted form for 24 hours at 20 °C. It must be discarded as biohazardous waste if not used within 24 hours after reconstitution. Given that vaccines currently available for oral administration require refrigeration and multiple dose regimens, a significant amount of work has been put forth to stabilize viruses and associated antigens in polymeric microparticles, nanoparticles, or liposomes to increase the amount delivered to Peyer's patches and minimize multiple dose regimens (296-298). Advances in plant engineering has sparked a global initiative to produce edible vaccines in plants like rice, lettuce, maize, alfalfa, algae and carrots (299). In these products, genes encoding the antigens of the disease-causing agent can be produced by the plant or within a seed and consumed without losing its immunogenic property (300). Virus like particles produced in plants are currently being evaluated in the clinic as influenza vaccine candidates, however these are injectable products and not for oral use (301). Limitations of this approach for oral immunization include the time required for plants to grow with respect to production time of current vaccines, the amount of plant bulk material that may be required to achieve reproducibility of antigen delivered and immune response induced after oral administration and acceptance by the global population (302).

1.11.1 Administration of Vaccines: Sublingual and Buccal Delivery

Administration of vaccines by the buccal and sublingual route offer advantages over traditional oral delivery of vaccines as they can effectively allow antigen to be processed by local antigen presenting cells while bypassing exposure to acidic pH and digestive enzymes in the gastrointestinal tract (303, 304). The sublingual mucosa consists of the ventral surface of the tongue and the floor of the mouth under the tongue (Figure 1.17A). It consists of a non-

keratinized, stratified squamous epithelium 100–200 μm thick with direct access to the systemic circulation via the lingual vein (305). The buccal mucosa is broadly described as the non-keratinized, stratified squamous epithelium lining various parts of the cheeks, gums, upper and lower lips that is 500 - 800 μm thick (Figure 1.17A). Vaccines that successfully traverse the buccal mucosa access the systemic circulation through the internal jugular vein (306). Antigens delivered by both routes also can directly access the lymphatic system through submandibular lymph nodes scattered along the jugular vein as was observed in early studies with small molecule drugs (307). The sublingual and buccal mucosa both contain specialized resident antigen presenting cells, Langerhans cells (LCs, Figure 1.17B), which serve as the "sentinels" of the mucosa, altering the immune system not only to pathogen entry but also of tolerance to self-antigen and commensal microbes (308). They work in concert with resident myeloid dendritic cells (mDCs,Figure 1.17B) to process antigen within 30-60 minutes after administration (304, 309) and recruit additional dendritic cells to the site of immunization. Within 24 hours, mDCs migrate to draining lymph nodes where they interact with naïve CD4 and CD8 T cells to stimulate production of antigen specific CD4 and CD8 T cells which then migrate to distant sites (Figure 1.17B)(304). Thus, administration of vaccines by the buccal and sublingual epithelial routes have been shown to induce both systemic and mucosal immune responses in a broad range of tissues, including the upper and lower respiratory tract, small intestine and reproductive tract (310).

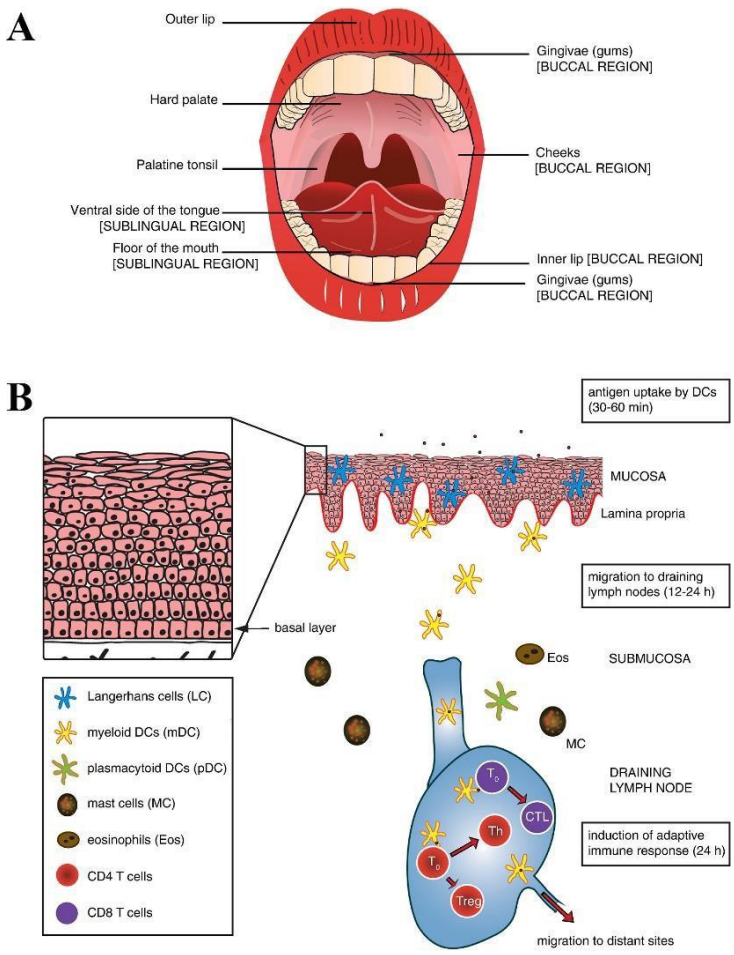

Figure 1.17: Buccal and Sublingual Anatomy and Immunology.
The anatomy of the oral cavity with the sublingual and buccal regions indicated (**A**). Immune response generated following sublingual or buccal vaccination (**B**). Following vaccine delivery, Langerhans cells (LC) and myeloid dendritic cells (mDCs) capture the antigen. DCs, carrying the antigen, migrate to draining lymph nodes where they activate CD4 and CD8 T cell differentiation and induce the adaptive immune response. Figure from ref 304.

Due to the thickness of the buccal mucosa, initial efforts on the development of oromucosal vaccines focused on sublingual region. Salivary composition, pH, and flow rate vary depending on diet and age and can significantly degrade antigens in preparations for sublingual administration before Langerhans cells and dendritic cells can process them (304, 311, 312). Dose dilution is also a significant concern due to a higher salivary flow rate than what is observed in the buccal mucosa (311, 313). Thus, formulation strategies for vaccines given by the

sublingual route should contain surfactants (pluronic f68, polysorbate 20 and 80), sugars (trehalose, sucrose), and polyols (sorbitol, mannitol) to protect antigens from degradation (120). The inclusion of mucoadhesive polymers like hydroxy propyl methyl cellulose (HPMC), methyl cellulose, pullulan, sodium alginate, and chitosan can also minimize dilution and clearance of antigen form the sublingual area (196, 198, 312).

Vaccines have been specifically formulated for successful sublingual immunization using liposomes, thermoresponsive gels, and mucoadhesive tablets as delivery devices, to name a few (304). Oberoi et al. designed PEG modified liposomes with methylglycol chitosan and administered them to mice with HA. This resulted in the induction of a strong Hemagglutinin Inhibition titer in serum and antigen specific IgA in tracheal and vaginal washes (314). White et al prepared thermoresponsive gels, which are liquid at room temperature but turn to a gel after contact with the warmer oral mucosa, using carbopol, hydroxy propyl methylcellulose, and Pluronic® F127. Following sublingual administration of the thermoresponsive gels containing an inactivated polio vaccine, antigen specific IgG was detected in serum and IgA was detected in saliva and fecal matter of mice (315). Mucoadhesive tablets containing carbopol, lactose, and microcrystalline cellulose were prepared with ovalbumin and successfully induced antigen specific IgG in serum and IgA in the small of mice, following sublingual administration (316). However, to date the majority of pre-clinical studies evaluating vaccines delivered by the sublingual route have involved administration of unformulated vaccine under the tongue. Song et al. administered unformulated mouse-adapted influenza sublingually and successfully induced virus-specific IgG in the serum, secretory IgA in nasal wash, and protective immunity from intranasal virus challenge (317). Choi et al. sublingually immunized mice and guinea pigs using an unformulated adenovirus-based vaccine which resulted in protection against lethal Ebola

challenge (309). An unformulated replication-defective adenovirus (rAd) encoding the globular head region of Hemagglutinin (HA) from mouse-adapted influenza was used to immunize mice sublingually against influenza and resulted in significant levels of antigen specific IgA and IgG in bronchoalveolar lavage (BAL) fluid and complete protection from influneza challenge (318). Adjuvants have also been included with subunit vaccines administered by the sublingual route to boost the associated immune response (304, 319, 320). Sublingual administration of an unformulated HIV subunit vaccine, adjuvanted with cholera toxin, induced antigen specific IgG and IgA in serum as well as antigen specific IgG in vaginal wash. Sublingual immunization in the absence of cholera toxin, however, failed to induce an antigen specific antibody response in serum or in vaginal wash (321). The majority of phase I clinical trials that have explored sublingual vaccine delivery have simply administered an injectable vaccine formulation as a droplet to the sublingual cavity and evaluated immunogenic effects (322). While one study performed by Nitto Denko Corporation in 2017 used a proprietary mucoadhesive tablet, NSV0001, for immunization against seasonal influenza the results have not been published (323). Although it is clear that sublingual administration of vaccine has shown great promise in pre-clinical models, use of liquid formulations increases the chance that a portion of a given dose was possibly swallowed. Translation of regimens to larger animal models and humans has been difficult due to difficulties with dose scaling and identifying doses that induce immunity instead of immune tolerance (324, 325).

Within the last 10 to 20 years, the buccal mucosa has begun to be an attractive target for vaccine delivery. While formulations of vaccines must still offer protection to the antigen from degradation in saliva, a bigger concern is increasing distribution across the thick epithelial layer. Thus, a variety of devices have been developed to improve permeability across the buccal

membrane. The 3-dimensional (3D) printed MucoJet is a capsule-sized 0.6 inch cylinder with a 0.3 inch bulb on the end that consists of two compartments: one filled with water and the other, a dry chemical propellant composed of citric acid and baking soda separated by a thin membrane. When the bulb is held against the inside of the cheek, the pressure breaks the membrane, mixing the water with the acid and soda, which generates enough pressure to push on a piston in the cylinder, which pushes a small reservoir of the vaccine out the other end through a small nozzle with enough force to penetrate the buccal tissue (Figure 1.18)(326). Rabbits immunized using the MucoJet system had three orders of magnitude higher IgG and IgA ovalbumin-specific antibody titers in serum and buccal tissue, than rabbits receiving dropper administration of unformulated ovalbumin to the buccal region (326). Microneedles have also been

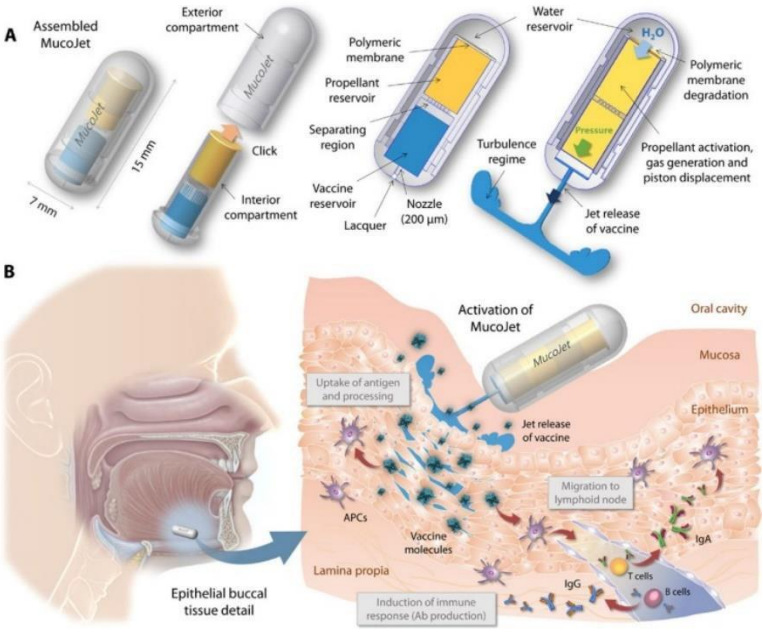

Figure 1.18: A schematic depicting the MucoJet 3D-printed vaccination device.
The interior compartment includes a propellant and vaccine reservoir which is separated by a porous membrane and a moving piston. Prior to administration, the water reservoir of the exterior compartment is filled with water and the interior compartment is placed in the exterior compartment. When this happens, the polymeric sealing membrane is dissolved and water from the exterior compartment comes into contact with the chemical propellant in the propellant reservoir. A chemical reaction takes places which results in the generation of carbon dioxide and increasing pressure, subsequently forcing the piston toward the vaccine reservoir, and ejecting a high-pressure liquid jet of vaccine (**A**). Graphic portraying administration of MucoJet and subsequent drug release, which penetrates the buccal mucosal layer and exposes the vaccine to antigen presenting cells (B). Figure from ref 326.

used as a device to delivery buccal vaccines due to their ability to adhere to buccal mucosa and result in an increased residence time along with physical penetration of the mucosa (Figure 1.19). McNeilly et al. used 110 μm -long silicon sputter-coated conical microprojection arrays, which are a type of microneedle array that is typically smaller and higher density, coated with Fluvax® to buccally immunize mice. A hemagglutinin inhibition assay determined that only arrays placed on the buccal mucosa and ear using a clip applicator, were able to induce protective levels of immunity (327). Zhen et al. developed liposome-loaded microneedles made of mannose-PEG1000-cholesterol conjugate (MPC), soy phosphatidylcholine (SPC), stearylamine (SA), monophosphoryl lipid A (LA), sucrose, bovine serum albumin (BSA), and Polyvinylpyrrolidone K-30 (PVPk30) for oral mucosal vaccination and evaluated the response to BSA adjuvanted with alum in mice. This resulted in a strong systemic and mucosal immune response in comparison to conventional intradermal administration (328). These microneedle arrays were then used develop an oral mucosal vaccine against hepatitis B virus which elicited a stronger mucosal response than intradermal and subcutaneous routes (329). Mucoadhesive films have also been used to overcome the permeability barrier of the buccal membrane. Films containing live, attenuated H1N1 influenza virus and given by the buccal route generated a significantly stronger antibody-mediated immune response than films given by the sublingual route or unformulated vaccine given by intramuscular injection (207). Masek et al developed a multilayer nanofiber based

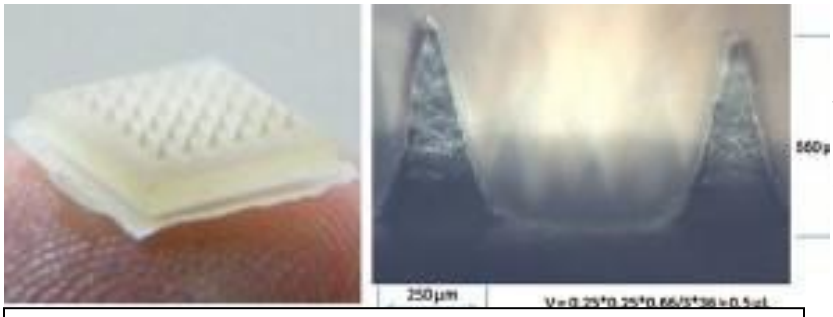

Figure 1.19: Microneedle Array and amplified image depicting measured dimensions.
Figure from ref 329.

mucoadhesive film, containing carbopol, hydroxypropyl methyl cellulose and Eudragit®, which successfully delivered PLGA-PEG nanoparticles, as a model antigen, to the buccal mucosa *ex vivo* (330). There are currently no buccal vaccine candidates in clinical trials in the United States.

Immunization averts an estimated 2.5 million child deaths a year but, despite this success, 24 million children in developing countries, almost 20% of all children born annually, do not get all immunizations scheduled for their first year of life (176). While the reasons for this are varied, the unmet demand for current vaccines coupled with the increasing threat of pandemic influenza, bioterrorist attacks and public health campaigns for global eradication of vaccine-preventable diseases make the need for minimally invasive delivery methods urgent. Advances in reverse vaccinology and proteomics have accelerated discovery and production of potent vaccine candidates with the potential for eradication and elimination of a variety of maladies including cancer, gingivitis, and microbial infection. Despite the significant improvement in technology to develop these vaccines, they remain largely given by the injectable route and cannot deviate from refrigerated conditions for significant periods of time which poses a significant barrier for access to these life-saving treatments in regions where they are needed the most.

Here we have shown that the theoretical principles involved in creating liquid vaccine formulations differ slightly from those for solid formulations and that vaccines formulated in a solid platform are more thermostable than those in liquid formulations. However, they require use of expensive equipment and facilities to support freeze-drying and hot melt extrusion and must be further manipulated by medical personnel prior to administration. Between September 2012 - June 2015, the Institute for Safe Medication Practices received 1,256 confidential reports

of vaccine error through their Vaccine Errors Reporting Program (VREP). Errors varied from administration of vaccine to the wrong-age patient, incorrect vaccine administration, extra dose, underdose, incorrect dosing intervals, expired vaccines, and incorrect route of administration (27). This illustrates the need for accelerated development of thermostable vaccines that can be easy to administer and which provide protective immunity in a single dose. Successful completion of this task would result in fewer vaccine preventable deaths world-wide.

1.12 Objectives

The objective of this research project is to characterize and develop a thermostable mucosal based vaccine platform that is easily adaptable to a variety of vaccine candidates. Recent work from our laboratory identified a formulation that significantly enhanced potency of a recombinant adenovirus-based Ebola vaccine when given by the intranasal route (331). When it was administered as a single dose to non-human primates, it offered full protection from a lethal dose of Ebola for an extended period of time (Figure 1.20) (331, 332). We have also shown that when the same vaccine was given as an unformulated solution by the sublingual route to mice, generated an immune response that was superior to the same vaccine given orally and could also afford protection against a lethal dose of mouse-adapted Ebola (Figure 1.21)(309). These studies motivated us to develop the following hypothesis in the current project: Incorporation of live virus-based vaccines in this formulation will significantly improve thermostability at ambient and elevated temperatures after exposure in the liquid state and in a dried film matrix. A secondary hypothesis was that the use of a novel zwitterionic surfactant will be the component in a multi-component formulation responsible for improved thermostability

and in vivo performance. These hypotheses will be tested by successful completion of the following aims:

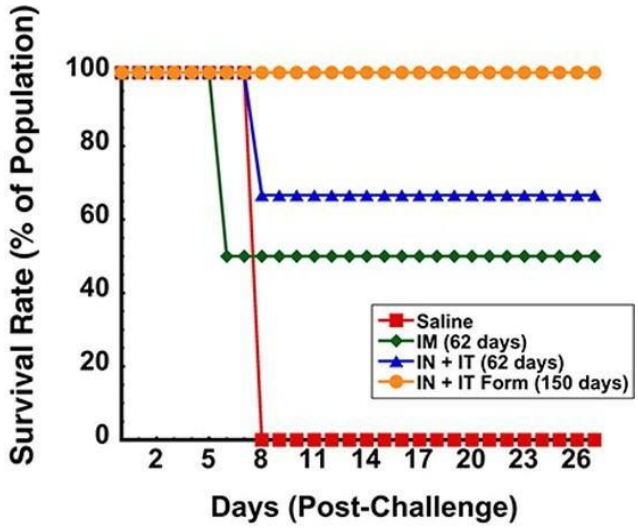

Figure 1.20 A Single Dose of Formulated Recombinant Adenovirus-Based Ebola Vaccine Induces Protective Immunity 150 days After Intranasal Immunization.

Cynomolgus macaques were challenged with a lethal dose of 1.21 x 10^3 $TCID_{50}$/mL Ebola virus (strain Kikwit) by intramuscular injection 62 days after immunization with 1.4 x 10^9 infectious virus particles of recombinant adenovirus expressing Ebola Zaire glycoprotein by intramuscular (IM) and intranasal/intratracheal (IN/IT) routes. Macaques immunized by the IN/IT route with formulated recombinant adenovirus expressing Ebola Zaire glycoprotein (10 mg/mL poly(maleic anhydride-*alt*-1-octadecene) substituted with 3-(dimethylamino)propylamine in phosphate buffered saline) at the same dose as IM and IN/IT were challenged with a lethal dose of 1.21 x 10^3 $TCID_{50}$/mL Ebola virus (strain Kikwit) by intramuscular injection 150 days after immunization, indicated as IN/IT Form. Red lines/squares: saline controls. Blue lines/triangles: IN/IT immunization. Green lines/diamonds: IM immunization. Orange lines/circles: IN/IT formulation immunization. Figure from ref (332).

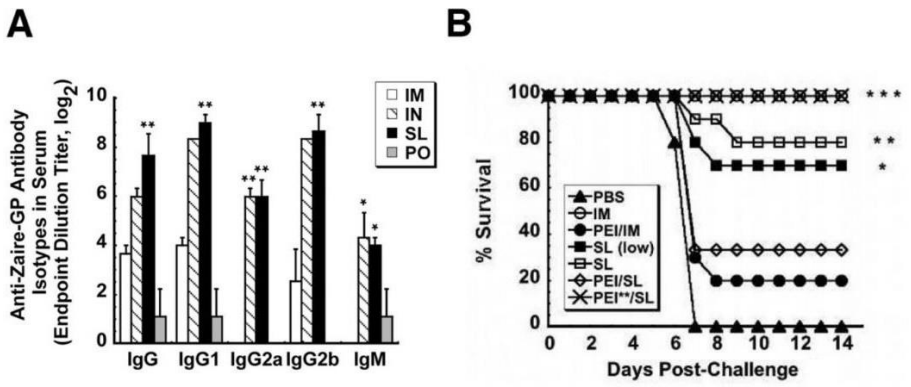

Figure 1.21: Sublingual Immunization Induces a Strong Immune Response and Protective Immunity Following Lethal Ebola Challenge in Mice.

Serum collected from mice with prior exposure to adenovirus serotype 5 (PEI) immunity 42 days after immunization with 1 x 10^8 infectious particles of a recombinant adenovirus expressing Ebola Zaire glycoprotein by various routes (**A**). Samples were evaluated for the presence of antigen specific IgG subclasses, IgM, and IgA by ELISA. Results are expressed as average values ± the standard error of the means. End point titers are expressed as the reciprocal $\log_2$ titer of the last dilution giving an OD at 450 nm of 0.1 units higher than the background. Naïve mice and those with PEI were challenged with a lethal dose of 1,000 pfu mouse-adapted Ebola Zaire (30,000 x LD_{50}) by intraperitoneal injection 28 days after immunization with a single dose of 1 x 10^8 infectious particles of vaccine (**B**). S.L. (low) is a separate group which was immunized with 1 x 10^7 infectious particles of vaccine. PEI was induced by intramuscular injection of 2.5 x 10^{11} particles of adenovirus in all groups 30 days prior to vaccination, except for the treatment group indicated as PEI**. This group was given 5 x 10^{10} adenovirus particles intramuscularly 30 days prior to vaccination. Significance was evaluated with respect to the PEI/IM treatment group. *, $p<0.05$, **, $p<0.01$, ***,$p<0.001$, one-way ANOVA, Bonferroni/Dunn post-hoc analysis. Figure from ref (309).

Aim 1. Development and Characterization of a Novel, Thin Film Vaccine. This was achieved by evaluating the effects of a range of temperatures, from -80°C to 40°C, on infectious titer, in formulations with and without surfactant to determine whether it plays a direct role in the stabilization of adenovirus. These studies were paired with analytical techniques, such as Fourier-Transform Infrared Spectroscopy (FTIR), Scanning Electron Microscopy (116), Differential Scanning Calorimetry (DSC), X-Ray Diffraction (XRD), tensile strength, percent elongation, and viscosity, which outlined how excipients contributed to the physical properties of films, assessed virus-excipient interactions within the film matrix and determined the impact that environmental moisture on thermostability of live virus at elevated temperatures (Chapter 2).

Aim 2. Identification of the Mechanism by which Surfactant Stabilizes Live Virus in the Film Matrix. Characterization of our novel surfactant was conducted through the use of dynamic light scattering (DLS), critical micelle concentration (CMC) determination using the pyrene fluorescent probe technique, and impact of chain length on stabilization of adenovirus. These studies were followed by an evaluation of the unique interactions between our surfactant and adenovirus using Transmission Electron Microscopy (TEM), Bio-Layer Interferometry (BLI), Isothermal Titration Calorimetry (ITC), and amino acid saturation studies paired with sodium dodecyl sulfate–polyacrylamide gel electrophoresis and zeta potential evaluation, which revealed aggregation prevention as the main mechanism behind surfactant-mediated stabilization. Thermal Gravimetric Analysis (TGA) and Karl Fischer titration was also employed to evaluate how the addition of the other formulation components contributed to the interactions between adenovirus and our surfactant. Principles established for adenovirus stability were

applied to develop formulations for a live virus with significantly different physical characteristics than the adenovirus, H1N1 influenza (Chapter 3).

Aim 3. *Ex vivo and In vivo* Evaluation of Thermostable Film Matrix. A proof-of-concept study was used to evaluate whether the sublingual and buccal routes of vaccination were suitable alternatives to traditional administration routes in mice. Following this study, we evaluated whether the addition of natural adjuvants would improve the bioavailability of the vaccine dose in the buccal mucosa using a verified model of the human buccal mucosa to assess permeability and cytokine response. Lastly, an in-depth evaluation of the antigen specific systemic and mucosal immune response alongside protective efficacy of thin film formulations against high-dose Influenza challenge, following buccal, sublingual, and intramuscular vaccine delivery with and without a natural adjuvant was performed (Chapter 4).

1.13 References

1. J. Louten, in *Essential Human Virology*. (Elsevier Inc, Kennesaw, GA, 2016), chap. 8, pp. 133-134.
2. F. Fenner *et al.*, in *Smallpox and Its Eradication*. (World Health Organization, Geneva, 1988), pp. 1371-1409.
3. G. S. Marshall, Vaccine Hesitancy, History, and Human Nature: The 2018 Stanley A. Plotkin Lecture. *Journal of the Pediatric Infectious Diseases Society* **8**, 1-8 (2018).
4. P. D. Minor, Live attenuated vaccines: Historical successes and current challenges. *Virology* **479-480**, 379-392 (2015).
5. J. F. Mosley, 2nd, L. L. Smith, P. Brantley, D. Locke, M. Como, Vaxchora: The First FDA-Approved Cholera Vaccination in the United States. *P T* **42**, 638-640 (2017).
6. O. S. Kumru *et al.*, Vaccine instability in the cold chain: Mechanisms, analysis and formulation strategies. *Biologicals* **42**, 237-259 (2014).
7. A. S. Lauring, J. O. Jones, R. Andino, Rationalizing the development of live attenuated virus vaccines. *Nat Biotechnol* **28**, 573-579 (2010).

8. A. J. Cann *et al.*, Reversion to neurovirulence of the live-attenuated Sabin type 3 oral pollovirus vaccine. *Nucleic Acids Research* **12**, 7787-7792 (1984).
9. L. Pöyhönen, J. Bustamante, J.-L. Casanova, E. Jouanguy, Q. Zhang, Life-Threatening Infections Due to Live-Attenuated Vaccines: Early Manifestations of Inborn Errors of Immunity. *Journal of Clinical Immunology* **39**, 376-390 (2019).
10. World Health Organization, Introduction of inactivated poliovirus vaccine into oral poliovirus vaccine-using countries. *Weekly Epidemiological Record* **78**, 241-252 (2020).
11. World Health Organization, BCG vaccine: WHO position paper. *Weekly Epidemiological Record* **79**, 25-40 (2004).
12. World Health Organization, Measels vaccines: WHO position paper. *Weekly Epidemiological Record* **84**, 349-360 (2009).
13. World Health Organization, Rotavirus vaccines: an update. *Weekly Epidemiological Record* **84**, 533-538 (2009).
14. World Health Organization, Yellow fever vaccine: WHO position paper. *Weekly Epidemiological Record* **78**, 349-360 (2003).
15. L. Varghese *et al.*, Contraindication of live vaccines in immunocompromised patients: an estimate of the number of affected people in the USA and the UK. *Public Health* **142**, 46-49 (2017).
16. J. A. Whitaker, K. Valles, P. K. Tosh, G. A. Poland, in *Vaccinations,* Gregory A. Poland, Ed. (Elsevier, 2019), pp. 139-162.
17. A. Sabbaghi, S. M. Miri, M. Keshavarz, M. Zargar, A. Ghaemi, Inactivation methods for whole influenza vaccine production. *Reviews in Medical Virology* **29**, e2074 (2019).
18. B. Sanders, M. Koldijk, H. Schuitemaker, Inactivated Viral Vaccines. *Vaccine Analysis: Strategies, Principles, and Control*, 45-80 (2014).
19. J. Hawken, S. B. Troy, Adjuvants and inactivated polio vaccine: A systematic review. *Vaccine* **30**, 6971-6979 (2012).
20. S. I. Samson *et al.*, Immunogenicity of high-dose trivalent inactivated influenza vaccine: a systematic review and meta-analysis. *Expert Rev Vaccines* **18**, 295-308 (2019).
21. M. Paulke-Korinek *et al.*, Persistence of antibodies six years after booster vaccination with inactivated vaccine against Japanese encephalitis. *Vaccine* **33**, 3600-3604 (2015).
22. B. L. Innis *et al.*, Protection Against Hepatitis A by an Inactivated Vaccine. *JAMA* **271**, 1328-1334 (1994).
23. D. J. Hicks, A. R. Fooks, N. Johnson, Developments in rabies vaccines. *Clinical & Experimental Immunology* **169**, 199-204 (2012).
24. P. E. Kilgore, A. M. Salim, M. J. Zervos, H.-J. Schmitt, Pertussis: Microbiology, Disease, Treatment, and Prevention. *Clinical Microbiology Reviews* **29**, 449 (2016).
25. A. L. Lopez *et al.*, Immunogenicity and Protection From a Single Dose of Internationally Available Killed Oral Cholera Vaccine: A Systematic Review and Metaanalysis. *Clinical Infectious Diseases* **66**, 1960-1971 (2017).
26. D. R. Howlader *et al.*, A brief review on the immunological scenario and recent developmental status of vaccines against enteric fever. *Vaccine* **35**, 6359-6366 (2017).
27. C. E. Demeure *et al.*, Yersinia pestis and plague: an updated view on evolution, virulence determinants, immune subversion, vaccination, and diagnostics. *Genes & Immunity* **20**, 357-370 (2019).
28. K. Kardani, A. Bolhassani, S. Shahbazi, Prime-boost vaccine strategy against viral infections: Mechanisms and benefits. *Vaccine* **34**, 413-423 (2016).

29. A. Vartak, S. J. Sucheck, Recent Advances in Subunit Vaccine Carriers. *Vaccines* **4**, (2016).
30. I. P. Nascimento, L. C. C. Leite, Recombinant vaccines and the development of new vaccine strategies. *Braz J Med Biol Res* **45**, 1102-1111 (2012).
31. J. Beláková, M. Horynová, M. Krupka, E. Weigl, M. Raska, DNA vaccines: are they still just a powerful tool for the future? *Archivum immunologiae et therapiae experimentalis* **55**, 387-398 (2007).
32. R. Bastola *et al.*, Vaccine adjuvants: smart components to boost the immune system. *Archives of Pharmacal Research* **40**, 1238-1248 (2017).
33. D. Baxter, Active and passive immunity, vaccine types, excipients and licensing. *Occupational Medicine* **57**, 552-556 (2007).
34. R. Rappuoli, E. De Gregorio, A sweet T cell response. *Nature Medicine* **17**, 1551-1552 (2011).
35. R. Rappuoli, Glycoconjugate vaccines: Principles and mechanisms. *Science Translational Medicine* **10**, eaat4615 (2018).
36. S. Davis, D. Feikin, H. L. Johnson, The effect of Haemophilus influenzaetype B and pneumococcal conjugate vaccines on childhood meningitis mortality: a systematic review. *BMC Public Health* **13**, S21 (2013).
37. H. Ewald *et al.*, The Clinical Effectiveness of Pneumococcal Conjugate Vaccines: A Systematic Review and Meta-analysis of Randomized Controlled Trials. *Dtsch Arztebl Int* **113**, 139-146 (2016).
38. C. A. Robertson, J. Hedrick, E. Bassily, D. P. Greenberg, Persistence of bactericidal antibodies 4 years after a booster dose of quadrivalent meningococcal diphtheria toxoid conjugate vaccine (MenACWY-D). *Vaccine* **37**, 1016-1020 (2019).
39. F. Berti, F. Micoli, Improving efficacy of glycoconjugate vaccines: from chemical conjugates to next generation constructs. *Current opinion in immunology* **65**, 42-49 (2020).
40. P. M. Moyle, I. Toth, Modern subunit vaccines: development, components, and research opportunities. *ChemMedChem* **8**, 360-376 (2013).
41. Food and Drug Administration. (2020).
42. R. H. Griesenauer, M. S. Kinch, An overview of FDA-approved vaccines & their innovators. *Expert Rev Vaccines* **16**, 1253-1266 (2017).
43. B. Afrough, S. Dowall, R. Hewson, Emerging viruses and current strategies for vaccine intervention. *Clin Exp Immunol* **196**, 157-166 (2019).
44. E. Prompetchara, C. Ketloy, T. Palaga, Immune responses in COVID-19 and potential vaccines: Lessons learned from SARS and MERS epidemic. *Asian Pacific journal of allergy and immunology* **38**, 1-9 (2020).
45. P. Lostroh, in *Molecular and Cellular Biology of Viruses* CRC Press, Ed. (Boca Raton, FL, 2019), pp. 1-18.
46. A. N. Clements, R. E. Harbach, History of the discovery of the mode of transmission of yellow fever virus. *Journal of vector ecology : journal of the Society for Vector Ecology* **42**, 208-222 (2017).
47. D. R. Wessner, The Origins of Viruses. *Nature Education* **3**, 37 (2010).
48. R. W. Horne, J. M. Hobart, I. P. Ronchetti, Application of the negative staining-carbon technique to the study of virus particles and their components by electron microscopy. *Micron (1969)* **5**, 233-261 (1974).

49. J. D. Almeida, A CLASSIFICATION OF VIRUS PARTICLES BASED ON MORPHOLOGY. *Can Med Assoc J* **89**, 787-798 (1963).
50. P. Lenihan, H. F. Bassett, E. D. Weavers, Demonstration by electron microscopy of parvovirus-like particles in canine parvovirus myocarditis. *The Veterinary record* **107**, 201-202 (1980).
51. A. Augustyn *et al.*, in *Encyclopaedia Britannica*. (Encyclopaedia Britannica, 2019).
52. J. Wellehan, G. Cortes-Hinojosa, in *Fowler's Zoo and Wild Animal Medicine Current Therapy, Volume 9*, R. Eric Miller, Nadine Lamberski, Paul P. Calle, Eds. (W.B. Saunders, 2019), pp. 597-602.
53. C. J. Burrell, C. R. Howard, F. A. Murphy, in *Fenner and White's Medical Virology (Fifth Edition)*, Christopher J. Burrell, Colin R. Howard, Frederick A. Murphy, Eds. (Academic Press, London, 2017), pp. 383-394.
54. K. Saunders, G. P. Lomonossoff, In Planta Synthesis of Designer-Length Tobacco Mosaic Virus-Based Nano-Rods That Can Be Used to Fabricate Nano-Wires. *Front Plant Sci* **8**, 1335-1335 (2017).
55. G. W. Long, J. Nobel, Jr., F. A. Murphy, K. L. Herrmann, B. Lourie, Experience with electron microscopy in the differential diagnosis of smallpox. *Appl Microbiol* **20**, 497-504 (1970).
56. D. Raoult *et al.*, The 1.2-megabase genome sequence of Mimivirus. *Science (New York, N.Y.)* **306**, 1344-1350 (2004).
57. C. Xiao *et al.*, Structural Studies of the Giant Mimivirus. *PLOS Biology* **7**, e1000092 (2009).
58. H. Sobhy, A comparative review of viral entry and attachment during large and giant dsDNA virus infections. *Archives of Virology* **162**, 3567-3585 (2017).
59. D. Kazlauskas, M. Krupovic, Č. Venclovas, The logic of DNA replication in double-stranded DNA viruses: insights from global analysis of viral genomes. *Nucleic acids research* **44**, 4551-4564 (2016).
60. K. A. White, L. Enjuanes, B. Berkhout, RNA virus replication, transcription and recombination. *RNA Biol* **8**, 182-183 (2011).
61. M. Comas-Garcia, Packaging of Genomic RNA in Positive-Sense Single-Stranded RNA Viruses: A Complex Story. *Viruses* **11**, 253 (2019).
62. Y. J. Tao, Q. Ye, RNA Virus Replication Complexes. *PLOS Pathogens* **6**, e1000943 (2010).
63. N. Arnberg *et al.*, Adenovirus Type 37 Binds to Cell Surface Sialic Acid Through a Charge-Dependent Interaction. *Virology* **302**, 33-43 (2002).
64. G. R. Nemerow, P. L. Stewart, Role of αv Integrins in Adenovirus Cell Entry and Gene Delivery. *Microbiology and Molecular Biology Reviews* **63**, 725-734 (1999).
65. E. De Clercq, Antiviral agents active against influenza A viruses. *Nature reviews. Drug discovery* **5**, 1015-1025 (2006).
66. J. L. Shirley, Y. P. de Jong, C. Terhorst, R. W. Herzog, Immune Responses to Viral Gene Therapy Vectors. *Molecular Therapy* **28**, 709-722 (2020).
67. Y. Kobayashi, Y. Suzuki, Compensatory Evolution of Net-Charge in Influenza A Virus Hemagglutinin. *PLoS One* **7**, e40422 (2012).
68. C. P. Gerba, W. Q. Betancourt, Viral Aggregation: Impact on Virus Behavior in the Environment. *Environmental Science & Technology* **51**, 7318-7325 (2017).

69. M. A. Croyle, K. Gerding, K. S. Quick, Role of Container/Closure System and Formulation on Agitation-Induced Aggregation Phenomena in Recombinant Adenoviral Products. *BioProcessing* **2**, 35-41 (2003).
70. E. K. Jeong, J. E. Bae, I. S. Kim, Inactivation of influenza A virus H1N1 by disinfection process. *American Journal of Infection Control* **38**, 354-360 (2010).
71. G. Maheshwari, R. Jannat, L. McCormick, D. Hsu, Thermal inactivation of adenovirus type 5. *Journal of Virological Methods* **118**, 141-146 (2004).
72. J. Bernaud *et al.*, Characterization of AAV vector particle stability at the single-capsid level. *J Biol Phys* **44**, 181-194 (2018).
73. R. K. Evans *et al.*, Development of stable liquid formulations for adenovirus-based vaccines. *Journal of Pharmaceutical Sciences* **93**, 2458-2475 (2004).
74. D. Loewe *et al.*, Forced Degradation Studies to Identify Critical Process Parameters for the Purification of Infectious Measles Virus. *Viruses* **11**, 725 (2019).
75. J. E. Benbough, Some Factors Affecting the Survival of Airborne Viruses. *Journal of General Virology* **10**, 209-220 (1971).
76. A. C. Lowen, J. Steel, Roles of Humidity and Temperature in Shaping Influenza Seasonality. *Journal of Virology* **88**, 7692 (2014).
77. Y. Ma *et al.*, Effects of temperature variation and humidity on the death of COVID-19 in Wuhan, China. *Science of The Total Environment* **724**, 138226 (2020).
78. S. Wanning, R. Süverkrüp, A. Lamprecht, Pharmaceutical spray freeze drying. *International Journal of Pharmaceutics* **488**, 136-153 (2015).
79. C. D. Lytle, J.-L. Sagripanti, Predicted Inactivation of Viruses of Relevance to Biodefense by Solar Radiation. *Journal of Virology* **79**, 14244 (2005).
80. B. K. Mayer, Y. Yang, D. W. Gerrity, M. Abbaszadegan, The Impact of Capsid Proteins on Virus Removal and Inactivation During Water Treatment Processes. *Microbiol Insights* **8**, 15-28 (2015).
81. C.-C. Tseng, C.-S. Li, Inactivation of viruses on surfaces by ultraviolet germicidal irradiation. *J Occup Environ Hyg* **4**, 400-405 (2007).
82. K. J. Card *et al.*, UV Sterilization of Personal Protective Equipment with Idle Laboratory Biosafety Cabinets During the Covid-19 Pandemic. *medRxiv*, 2020.2003.2025.20043489 (2020).
83. I. H. Hamzavi *et al.*, Ultraviolet germicidal irradiation: Possible method for respirator disinfection to facilitate reuse during the COVID-19 pandemic. *Journal of the American Academy of Dermatology* **82**, 1511-1512 (2020).
84. G. Kampf, Efficacy of ethanol against viruses in hand disinfection. *Journal of Hospital Infection* **98**, 331-338 (2018).
85. J. S. Oxford, C. W. Potter, C. McLaren, W. Hardy, Inactivation of influenza and other viruses by a mixture of virucidal compounds. *Appl Microbiol* **21**, 606-610 (1971).
86. R. W. Doms, in *Viral Pathogenesis (Third Edition)*, Michael G. Katze, Marcus J. Korth, G. Lynn Law, Neal Nathanson, Eds. (Academic Press, Boston, 2016), pp. 29-40.
87. J. Rexroad, R. K. Evans, C. R. Middaugh, Effect of pH and ionic strength on the physical stability of adenovirus type 5. *Journal of Pharmaceutical Sciences* **95**, 237-247 (2006).
88. M. A. Croyle, X. Cheng, J. M. Wilson, Development of formulations that enhance physical stability of viral vectors for gene therapy. *Gene Therapy* **8**, 1281-1290 (2001).
89. R. L. Poulson, S. M. Tompkins, R. D. Berghaus, J. D. Brown, D. E. Stallknecht, Environmental Stability of Swine and Human Pandemic Influenza Viruses in Water

under Variable Conditions of Temperature, Salinity, and pH. *Appl Environ Microbiol* **82**, 3721 (2016).
90. P. R. Junankar, R. J. Cherry, Temperature and pH dependence of the haemolytic activity of influenza virus and of the rotational mobility of the spike glycoproteins. *Biochimica et biophysica acta* **854**, 198-206 (1986).
91. B. Bobály, E. Sipkó, J. Fekete, Challenges in liquid chromatographic characterization of proteins. *Journal of Chromatography B* **1032**, 3-22 (2016).
92. K. A. Dill, J. L. MacCallum, The Protein-Folding Problem, 50 Years On. *Science (New York, N.Y.)* **338**, 1042 (2012).
93. T. N. Shamsi, T. Athar, R. Parveen, S. Fatima, A review on protein misfolding, aggregation and strategies to prevent related ailments. *International Journal of Biological Macromolecules* **105**, 993-1000 (2017).
94. M. J. Davies, The oxidative environment and protein damage. *Biochimica et Biophysica Acta (BBA) - Proteins and Proteomics* **1703**, 93-109 (2005).
95. S. W. Hovorka, C. Schöneich, Oxidative degradation of pharmaceuticals: Theory, mechanisms and inhibition. *Journal of Pharmaceutical Sciences* **90**, 253-269 (2001).
96. A. B. Robinson, C. J. Rudd, in *Current Topics in Cellular Regulation*, Bernard L. Horecker, Earl R. Stadtman, Eds. (Academic Press, 1974), vol. 8, pp. 247-295.
97. R. Bischoff, H. V. J. Kolbe, Deamidation of asparagine and glutamine residues in proteins and peptides: structural determinants and analytical methodology. *Journal of Chromatography B: Biomedical Sciences and Applications* **662**, 261-278 (1994).
98. L. J. J. Hansen, R. Daoussi, C. Vervaet, J. P. Remon, T. R. M. De Beer, Freeze-drying of live virus vaccines: A review. *Vaccine* **33**, 5507-5519 (2015).
99. W. Wang, S. Ohtake, Science and art of protein formulation development. *International Journal of Pharmaceutics* **568**, 118505 (2019).
100. N.-Y. Fang *et al.*, Effects of osmolytes on arginine kinase from Euphausia superba: A study on thermal denaturation and aggregation. *Process Biochemistry* **49**, 936-947 (2014).
101. A. Arsiccio, R. Pisano, Stability of Proteins in Carbohydrates and Other Additives during Freezing: The Human Growth Hormone as a Case Study. *The Journal of Physical Chemistry B* **121**, 8652-8660 (2017).
102. S. Ajito, H. Iwase, S.-i. Takata, M. Hirai, Sugar-Mediated Stabilization of Protein against Chemical or Thermal Denaturation. *The Journal of Physical Chemistry B* **122**, 8685-8697 (2018).
103. M. Kudou, K. Shiraki, S. Fujiwara, T. Imanaka, M. Takagi, Prevention of thermal inactivation and aggregation of lysozyme by polyamines. *European Journal of Biochemistry* **270**, 4547-4554 (2003).
104. N. K. Budhavaram, J. A. Miller, Y. Shen, J. R. Barone, Protein Substitution Affects Glass Transition Temperature and Thermal Stability. *Journal of Agricultural and Food Chemistry* **58**, 9549-9555 (2010).
105. M. F. Sabar *et al.*, Synthesis and Bioactivity Study of 30KDa Linear PEG-Interferon and its Comparison with Tri-Branched PEG-Interferon. *Journal- Chemical Society of Pakistan* **35**, (2012).
106. D. Prashar, D. Cui, D. Bandyopadhyay, Y.-Y. Luk, Modification of Proteins with Cyclodextrins Prevents Aggregation and Surface Adsorption and Increases Thermal Stability. *Langmuir* **27**, 13091-13096 (2011).

107. R. Liebner, M. Meyer, T. Hey, G. Winter, A. Besheer, Head to Head Comparison of the Formulation and Stability of Concentrated Solutions of HESylated versus PEGylated Anakinra. *Journal of Pharmaceutical Sciences* **104**, 515-526 (2015).
108. S. V. Thakkar *et al.*, Excipients Differentially Influence the Conformational Stability and Pretransition Dynamics of Two IgG1 Monoclonal Antibodies. *Journal of Pharmaceutical Sciences* **101**, 3062-3077 (2012).
109. S. P. Choudhari, K. P. Pendleton, J. D. Ramsey, T. G. Blanchard, W. D. Picking, A Systematic Approach Toward Stabilization of CagL, a Protein Antigen from Helicobacter Pylori That is a Candidate Subunit Vaccine. *Journal of Pharmaceutical Sciences* **102**, 2508-2519 (2013).
110. S. Shi *et al.*, Biophysical Characterization and Stabilization of the Recombinant Albumin Fusion Protein sEphB4–HSA. *Journal of Pharmaceutical Sciences* **101**, 1969-1984 (2012).
111. N. A. Kim, S. Hada, R. Thapa, S. H. Jeong, Arginine as a protein stabilizer and destabilizer in liquid formulations. *International Journal of Pharmaceutics* **513**, 26-37 (2016).
112. J. J. Hung *et al.*, Improving Viscosity and Stability of a Highly Concentrated Monoclonal Antibody Solution with Concentrated Proline. *Pharmaceutical research* **35**, 133 (2018).
113. W. Wang *et al.*, Effects of osmolytes on Pelodiscus sinensis creatine kinase: A study on thermal denaturation and aggregation. *International Journal of Biological Macromolecules* **60**, 277-287 (2013).
114. H. Yuan *et al.*, The pH stability of foot-and-mouth disease virus. *Virology Journal* **14**, 233 (2017).
115. J.-M. Mayotte, T. Grabs, S. Sutliff-Johansson, K. Bishop, The effects of ionic strength and organic matter on virus inactivation at low temperatures: general likelihood uncertainty estimation (GLUE) as an alternative to least-squares parameter optimization for the fitting of virus inactivation models. *Hydrogeology Journal* **25**, 1063 (2017).
116. T. Hasan *et al.*, Osmolytes in vaccine production, flocculation and storage: a critical review. *Human vaccines & immunotherapeutics* **15**, 514-525 (2019).
117. T. Perevozchikova, H. Nanda, D. P. Nesta, C. J. Roberts, Protein Adsorption, Desorption, and Aggregation Mediated by Solid-Liquid Interfaces. *Journal of Pharmaceutical Sciences* **104**, 1946-1959 (2015).
118. M. M. Castellanos, J. A. Pathak, R. H. Colby, Both protein adsorption and aggregation contribute to shear yielding and viscosity increase in protein solutions. *Soft matter* **10**, 122-131 (2014).
119. K. Talley, E. Alexov, On the pH-optimum of activity and stability of proteins. *Proteins* **78**, 2699-2706 (2010).
120. S. Ohtake, Y. Kita, T. Arakawa, Interactions of formulation excipients with proteins in solution and in the dried state. *Advanced drug delivery reviews* **63**, 1053-1073 (2011).
121. T. A. Khan, H. C. Mahler, R. S. Kishore, Key interactions of surfactants in therapeutic protein formulations: A review. *European journal of pharmaceutics and biopharmaceutics : official journal of Arbeitsgemeinschaft fur Pharmazeutische Verfahrenstechnik e.V* **97**, 60-67 (2015).
122. T. W. Randolph, L. S. Jones, in *Rational Design of Stable Protein Formulations: Theory and Practice*, John F. Carpenter, Mark C. Manning, Eds. (Springer US, Boston, MA, 2002), pp. 159-175.

123. J. S. Bee, T. W. Randolph, J. F. Carpenter, S. M. Bishop, M. N. Dimitrova, Effects of Surfaces and Leachables on the Stability of Biopharmaceuticals. *Journal of Pharmaceutical Sciences* **100**, 4158-4170 (2011).
124. P. A. Gunning *et al.*, Effect of surfactant type on surfactant--protein interactions at the air-water interface. *Biomacromolecules* **5**, 984-991 (2004).
125. F. Poncin-Epaillard *et al.*, Surface treatment of polymeric materials controlling the adhesion of biomolecules. *J Funct Biomater* **3**, 528-543 (2012).
126. *Excipients Included in U.S. Vaccines, by Vaccine* (2019).
127. P. Maffre *et al.*, Effects of surface functionalization on the adsorption of human serum albumin onto nanoparticles – a fluorescence correlation spectroscopy study. *Beilstein Journal of Nanotechnology* **5**, 2036-2047 (2014).
128. J. Gilbert, O. Campanella, O. G. Jones, Electrostatic Stabilization of β-lactoglobulin Fibrils at Increased pH with Cationic Polymers. *Biomacromolecules* **15**, 3119-3127 (2014).
129. A. A. Yaroslavov, A. V. Sybachin, A. A. Efimova, Stabilization of electrostatic polymer-colloid complexes. *Colloids and Surfaces A: Physicochemical and Engineering Aspects* **558**, 1-7 (2018).
130. R. Imamura, H. Mori, Protein-Stabilizing Effect of Amphiphilic Block Copolymers with a Tertiary Sulfonium-Containing Zwitterionic Segment. *ACS Omega* **4**, 18234-18247 (2019).
131. A. M. Azevedo, J. M. S. Cabral, D. M. F. Prazeres, T. D. Gibson, L. P. Fonseca, Thermal and operational stabilities of Hansenula polymorpha alcohol oxidase. *Journal of Molecular Catalysis B: Enzymatic* **27**, 37-45 (2004).
132. H. Zhang *et al.*, PPARβ/δ activation inhibits angiotensin II-induced collagen type I expression in rat cardiac fibroblasts. *Archives of Biochemistry and Biophysics* **460**, 25-32 (2007).
133. J. Mondal *et al.*, How osmolytes influence hydrophobic polymer conformations: A unified view from experiment and theory. *Proceedings of the National Academy of Sciences* **112**, 9270 (2015).
134. V. Kadajji, G. Betageri, Water Soluble Polymers for Pharmaceutical Applications. *Polymers* **3**, (2011).
135. J. C. Lee, S. N. Timasheff, The stabilization of proteins by sucrose. *The Journal of biological chemistry* **256**, 7193-7201 (1981).
136. T. Arakawa, Y. Kita, J. F. Carpenter, Protein–Solvent Interactions in Pharmaceutical Formulations. *Pharmaceutical research* **8**, 285-291 (1991).
137. L. Chang, M. J. Pikal, Mechanisms of protein stabilization in the solid state. *Journal of pharmaceutical sciences* **98 9**, 2886-2908 (2009).
138. B. M. Baynes, D. I. Wang, B. L. Trout, Role of arginine in the stabilization of proteins against aggregation. *Biochemistry* **44**, 4919-4925 (2005).
139. D. M. Matthias, J. Robertson, M. M. Garrison, S. Newland, C. Nelson, Freezing temperatures in the vaccine cold chain: a systematic literature review. *Vaccine* **25**, 3980-3986 (2007).
140. B. Adhikari *et al.*, Earthquakes, Fuel Crisis, Power Outages, and Health Care in Nepal: Implications for the Future. *Disaster medicine and public health preparedness* **11**, 625-632 (2017).

141. M. N. Yakum, J. Ateudjieu, F. R. Pélagie, E. A. Walter, P. Watcho, Factors associated with the exposure of vaccines to adverse temperature conditions: the case of North West region, Cameroon. *BMC Research Notes* **8**, 277 (2015).
142. T. Kitamura *et al.*, Assessment of temperatures in the vaccine cold chain in two provinces in Lao People's Democratic Republic: a cross-sectional pilot study. *BMC Research Notes* **11**, 261 (2018).
143. A. Ashok, M. Brison, Y. LeTallec, Improving cold chain systems: Challenges and solutions. *Vaccine* **35**, 2217-2223 (2017).
144. I. P. Garber Cohen, P. R. Castello, F. L. G. Flecha, Ice-induced partial unfolding and aggregation of an integral membrane protein. *Biochimica et Biophysica Acta (BBA) - Biomembranes* **1798**, 2040-2047 (2010).
145. U. Kartoglu, N. K. Ozguler, L. J. Wolfson, W. Kurzatkowski, Validation of the shake test for detecting freeze damage to adsorbed vaccines. *Bulletin of the World Health Organization* **88**, 624-631 (2010).
146. J. F. Carpenter, J. H. Crowe, The mechanism of cryoprotection of proteins by solutes. *Cryobiology* **25**, 244-255 (1988).
147. R. Surís-Valls, I. K. Voets, The Impact of Salts on the Ice Recrystallization Inhibition Activity of Antifreeze (Glyco)Proteins. *Biomolecules* **9**, 347 (2019).
148. A. E. Rydeen, E. M. Brustad, G. J. Pielak, Osmolytes and Protein–Protein Interactions. *Journal of the American Chemical Society* **140**, 7441-7444 (2018).
149. D. A. J. Tyrrell, B. Ridgwell, Freeze-drying of Certain Viruses. *Nature* **206**, 115-116 (1965).
150. M. Hollings, R. A. Lelliott, Preservation of some plant viruses by freeze-drying. *Plant Pathology* **9**, 63-66 pp. (1960).
151. L. M. Kraft, E. C. Pollard, Lyophilization of Poliomyelitis Virus. Heat Inactivation of Dry MEF1 Virus. *Proceedings of the Society for Experimental Biology and Medicine* **86**, 306-309 (1954).
152. S. D. Allison, T. J. Anchordoquy, in *Nonviral Vectors for Gene Therapy: Methods and Protocols*, Mark A. Findeis, Ed. (Humana Press, Totowa, NJ, 2001), pp. 225-252.
153. W. Wang, Lyophilization and development of solid protein pharmaceuticals. *International Journal of Pharmaceutics* **203**, 1-60 (2000).
154. W. Abdelwahed, G. Degobert, S. Stainmesse, H. Fessi, Freeze-drying of nanoparticles: Formulation, process and storage considerations. *Advanced drug delivery reviews* **58**, 1688-1713 (2006).
155. J. C. Kasper, G. Winter, W. Friess, Recent advances and further challenges in lyophilization. *European Journal of Pharmaceutics and Biopharmaceutics* **85**, 162-169 (2013).
156. A. Wasserman, R. Sarpal, B. Phillips, in *Vaccine Development and Manufacturing*. (2014), pp. 263-285.
157. W. R. Liu, R. Langer, A. M. Klibanov, Moisture-induced aggregation of lyophilized proteins in the solid state. *Biotechnology and bioengineering* **37**, 177-184 (1991).
158. M. E. Brewster, M. S. Hora, J. W. Simpkins, N. Bodor, Use of 2-Hydroxypropyl-β-cyclodextrin as a Solubilizing and Stabilizing Excipient for Protein Drugs. *Pharmaceutical research* **8**, 792-795 (1991).
159. B. S. Chang, C. S. Randall, Y. S. Lee, Stabilization of Lyophilized Porcine Pancreatic Elastase. *Pharmaceutical research* **10**, 1478-1483 (1993).

160. L. L. Chang, M. J. Pikal, Mechanisms of protein stabilization in the solid state. *J Pharm Sci* **98**, 2886-2908 (2009).
161. J. L. Cleland, T. W. Randolph, Mechanism of polyethylene glycol interaction with the molten globule folding intermediate of bovine carbonic anhydrase B. *The Journal of biological chemistry* **267**, 3147-3153 (1992).
162. L. Kreilgaard *et al.*, Effect of Tween 20 on freeze-thawing- and agitation-induced aggregation of recombinant human factor XIII. *J Pharm Sci* **87**, 1597-1603 (1998).
163. M. Mattern, G. Winter, U. Kohnert, G. Lee, Formulation of proteins in vacuum-dried glasses. II. Process and storage stability in sugar-free amino acid systems. *Pharm Dev Technol* **4**, 199-208 (1999).
164. F. Tian *et al.*, Spectroscopic evaluation of the stabilization of humanized monoclonal antibodies in amino acid formulations. *International Journal of Pharmaceutics* **335**, 20-31 (2007).
165. B. Chen *et al.*, Influence of Histidine on the Stability and Physical Properties of a Fully Human Antibody in Aqueous and Solid Forms. *Pharmaceutical research* **20**, 1952-1960 (2003).
166. T. T. Wyatt, H. A. B. Wösten, J. Dijksterhuis, in *Advances in Applied Microbiology*, Sima Sariaslani, Geoffrey M. Gadd, Eds. (Academic Press, 2013), vol. 85, pp. 43-91.
167. X. Tang, M. J. Pikal, Design of Freeze-Drying Processes for Pharmaceuticals: Practical Advice. *Pharmaceutical research* **21**, 191-200 (2004).
168. P. M. J. Costantino Henry R, *Lyophilization of biopharmaceuticals* Biotechnology: Pharmaceutical Aspects (American Association of Pharmaceutical Sciences, Arlington, VA, 2004).
169. S. M. Patel, T. Doen, M. J. Pikal, Determination of end point of primary drying in freeze-drying process control. *AAPS PharmSciTech* **11**, 73-84 (2010).
170. S. C. Schneid, H. Gieseler, W. J. Kessler, S. A. Luthra, M. J. Pikal, Optimization of the secondary drying step in freeze drying using TDLAS technology. *AAPS PharmSciTech* **12**, 379-387 (2011).
171. S. Khairnar, R. Kini, M. Harwalkar, K. Salunkhe, S. Chaudhari, A Review on Freeze Drying Process of Pharmaceuticals. *International Journal of Research in Pharmacy and science* **IJRPS 2013**, 76-94 (2012).
172. R. Lang *et al.*, Rational Design of a Stable, Freeze-Dried Virus-Like Particle-Based Vaccine Formulation. *Drug Development and Industrial Pharmacy* **35**, 83-97 (2009).
173. J. C. May, E. Grim, R. M. Wheeler, J. West, Determination of residual moisture in freeze-dried viral vaccines: Karl Fischer, gravimetric and thermogravimetric methodologies. *Journal of Biological Standardization* **10**, 249-259 (1982).
174. World Health Organization, "The Proper Handling and Use of Vaccine Diluents," *Vaccine Diluents* (World Health Organization, Geneva, Switzerland, 2015).
175. Immunization Action Coalition, "Vaccines with Diluents: How to Use Them," (Immunization Action Coalition, Saint Paul, Minnesota, 2017).
176. C. Czerkinsky *et al.*, Mucosal immunity and tolerance: relevance to vaccine development. *Immunological reviews* **170**, 197-222 (1999).
177. A. Flood, M. Estrada, D. McAdams, Y. Ji, D. Chen, Development of a Freeze-Dried, Heat-Stable Influenza Subunit Vaccine Formulation. *PLoS One* **11**, e0164692-e0164692 (2016).

178. G. Kanojia *et al.*, Developments in the formulation and delivery of spray dried vaccines. *Human vaccines & immunotherapeutics* **13**, 2364-2378 (2017).
179. A. Ziaee *et al.*, Spray drying of pharmaceuticals and biopharmaceuticals: Critical parameters and experimental process optimization approaches. *European Journal of Pharmaceutical Sciences* **127**, 300-318 (2019).
180. I. Roy, M. N. Gupta, Freeze-drying of proteins: some emerging concerns. *Biotechnology and applied biochemistry* **39**, 165-177 (2004).
181. S. H. Wang, S. M. Kirwan, S. N. Abraham, H. F. Staats, A. J. Hickey, Stable Dry Powder Formulation for Nasal Delivery of Anthrax Vaccine. *Journal of Pharmaceutical Sciences* **101**, 31-47 (2012).
182. M. Ameri, Y.-F. Maa, Spray Drying of Biopharmaceuticals: Stability and Process Considerations. *Drying Technology* **24**, 763-768 (2006).
183. G. Kanojia *et al.*, A Design of Experiment approach to predict product and process parameters for a spray dried influenza vaccine. *International Journal of Pharmaceutics* **511**, 1098-1111 (2016).
184. S. Ohtake *et al.*, Heat-stable measles vaccine produced by spray drying. *Vaccine* **28**, 1275-1284 (2010).
185. D. A. LeClair, E. D. Cranston, Z. Xing, M. R. Thompson, Optimization of Spray Drying Conditions for Yield, Particle Size and Biological Activity of Thermally Stable Viral Vectors. *Pharmaceutical research* **33**, 2763-2776 (2016).
186. V. Saluja *et al.*, A comparison between spray drying and spray freeze drying to produce an influenza subunit vaccine powder for inhalation. *Journal of Controlled Release* **144**, 127-133 (2010).
187. Y.-F. Maa, L. Zhao, L. G. Payne, D. Chen, Stabilization of alum-adjuvanted vaccine dry powder formulations: Mechanism and application. *Journal of Pharmaceutical Sciences* **92**, 319-332 (2003).
188. W. F. Tonnis *et al.*, Improved storage stability and immunogenicity of hepatitis B vaccine after spray-freeze drying in presence of sugars. *European Journal of Pharmaceutical Sciences* **55**, 36-45 (2014).
189. J. Huang *et al.*, Protective Immunity in Mice Achieved with Dry Powder Formulation and Alternative Delivery of Plague F1-V Vaccine. *Clinical and Vaccine Immunology* **16**, 719 (2009).
190. S. P. Sellers, G. S. Clark, R. E. Sievers, J. F. Carpenter, Dry powders of stable protein formulations from aqueous solutions prepared using supercritical CO(2)-assisted aerosolization. *J Pharm Sci* **90**, 785-797 (2001).
191. J. Kissmann *et al.*, Stabilization of measles virus for vaccine formulation. *Human vaccines* **4**, 350-359 (2008).
192. J. Burger *et al.*, Stabilizing Formulations for Inhalable Powders of Live-Attenuated Measles Virus Vaccine. *Journal of aerosol medicine and pulmonary drug delivery* **21**, 25-34 (2008).
193. S. P. Cape *et al.*, Preparation of active proteins, vaccines and pharmaceuticals as fine powders using supercritical or near-critical fluids. *Pharmaceutical research* **25**, 1967-1990 (2008).
194. United States Pharmacopeial Convention, in *USP35 NF30, 2012: U. S. Pharmacopoeia National Formulary*. (USP35 NF30, 2012), vol. 35, pp. 765-783.

195. M. Preis, C. Woertz, P. Kleinebudde, J. Breitkreutz, Oromucosal film preparations: classification and characterization methods. *Expert opinion on drug delivery* **10**, 1303-1317 (2013).
196. M. Montenegro-Nicolini, J. O. Morales, Overview and Future Potential of Buccal Mucoadhesive Films as Drug Delivery Systems for Biologics. *AAPS PharmSciTech* **18**, 3-14 (2017).
197. B. M. A. Silva, A. F. Borges, C. Silva, J. F. J. Coelho, S. Simões, Mucoadhesive oral films: The potential for unmet needs. *International Journal of Pharmaceutics* **494**, 537-551 (2015).
198. K. K. Peh, C. F. Wong, Polymeric films as vehicle for buccal delivery: swelling, mechanical, and bioadhesive properties. *Journal of pharmacy & pharmaceutical sciences : a publication of the Canadian Society for Pharmaceutical Sciences, Societe canadienne des sciences pharmaceutiques* **2**, 53-61 (1999).
199. E. Y. Chi, S. Krishnan, T. W. Randolph, J. F. Carpenter, Physical Stability of Proteins in Aqueous Solution: Mechanism and Driving Forces in Nonnative Protein Aggregation. *Pharmaceutical research* **20**, 1325-1336 (2003).
200. T. J. Kamerzell, R. Esfandiary, S. B. Joshi, C. R. Middaugh, D. B. Volkin, Protein-excipient interactions: mechanisms and biophysical characterization applied to protein formulation development. *Advanced drug delivery reviews* **63**, 1118-1159 (2011).
201. J. O. Morales, J. T. McConville, Manufacture and characterization of mucoadhesive buccal films. *European journal of pharmaceutics and biopharmaceutics : official journal of Arbeitsgemeinschaft fur Pharmazeutische Verfahrenstechnik e.V* **77**, 187-199 (2011).
202. J. O. Morales, J. T. McConville, Novel strategies for the buccal delivery of macromolecules. *Drug Development and Industrial Pharmacy* **40**, 579-590 (2014).
203. L. A. Felton, Mechanisms of polymeric film formation. *International Journal of Pharmaceutics* **457**, 423-427 (2013).
204. K. Huntrakul, N. Harnkarnsujarit, Effects of plasticizers on water sorption and aging stability of whey protein/carboxy methyl cellulose films. *Journal of Food Engineering* **272**, 109809 (2020).
205. F. Carvalho, M. Bruschi, R. Evangelista, M. Gremiao, Mucoadhesive drug delivery systems. *Brazilian Journal of Pharmaceutical Sciences* **46**, 1-17 (2010).
206. Y. Lu, E. Zhang, J. Yang, Z. Cao, Strategies to improve micelle stability for drug delivery. *Nano Res* **11**, 4985-4998 (2018).
207. I. Bajrovic, S. C. Schafer, D. K. Romanovicz, M. A. Croyle, Novel technology for storage and distribution of live vaccines and other biological medicines at ambient temperature. *Science Advances* **6**, eaau4819 (2020).
208. H. Sohi, A. Ahuja, F. J. Ahmad, R. K. Khar, Critical evaluation of permeation enhancers for oral mucosal drug delivery. *Drug Development and Industrial Pharmacy* **36**, 254-282 (2010).
209. E. Moghimipour, A. Ameri, S. Handali, Absorption-Enhancing Effects of Bile Salts. *Molecules* **20**, 14451-14473 (2015).
210. K. Kesarwani, R. Gupta, A. Mukerjee, Bioavailability enhancers of herbal origin: an overview. *Asian Pac J Trop Biomed* **3**, 253-266 (2013).
211. S. Kobayashi, S. Kondo, K. Juni, Permeability enhancing effect of oleic acid and its mechanism in human alveolar A549 cells. *European Journal of Pharmaceutical Sciences* **4**, 267-272 (1996).

212. V. Kumar, R. Chari, V. K. Sharma, D. S. Kalonia, Modulation of the thermodynamic stability of proteins by polyols: significance of polyol hydrophobicity and impact on the chemical potential of water. *Int J Pharm* **413**, 19-28 (2011).
213. S. Sharma, A. A. Singh, A. Majumdar, B. S. Butola, Tailoring the mechanical and thermal properties of polylactic acid-based bionanocomposite films using halloysite nanotubes and polyethylene glycol by solvent casting process. *Journal of Materials Science* **54**, 8971-8983 (2019).
214. P. Kanaujia, P. Poovizhi, W. K. Ng, R. B. H. Tan, Preparation, Characterization and Prevention of Auto-oxidation of Amorphous Sirolimus by Encapsulation in Polymeric Films Using Hot Melt Extrusion. *Current Drug Delivery* **16**, 663-671 (2019).
215. B. S. Yadav, S. Koppoju, S. R. Dey, S. R. Dhage, Microstructural investigation of inkjet printed Cu(In,Ga)Se2 thin film solar cell with improved efficiency. *Journal of Alloys and Compounds* **827**, 154295 (2020).
216. V. Leung *et al.*, Thermal Stabilization of Viral Vaccines in Low-Cost Sugar Films. *Scientific Reports* **9**, 7631 (2019).
217. J. A. Stinson *et al.*, Thin silk fibroin films as a dried format for temperature stabilization of inactivated polio vaccine. *Vaccine* **38**, 1652-1660 (2020).
218. M. J. Mistilis *et al.*, Long-term stability of influenza vaccine in a dissolving microneedle patch. *Drug Delivery and Translational Research* **7**, 195-205 (2017).
219. Y.-C. Kim, F.-S. Quan, R. W. Compans, S.-M. Kang, M. R. Prausnitz, Formulation and coating of microneedles with inactivated influenza virus to improve vaccine stability and immunogenicity. *Journal of Controlled Release* **142**, 187-195 (2010).
220. C. Hervé, B. Laupèze, G. Del Giudice, A. M. Didierlaurent, F. Tavares Da Silva, The how's and what's of vaccine reactogenicity. *npj Vaccines* **4**, 39 (2019).
221. I. F. Cook, Sex differences in injection site reactions with human vaccines. *Human vaccines* **5**, 441-449 (2009).
222. E. De Gregorio, E. Caproni, J. B. Ulmer, Vaccine adjuvants: mode of action. *Frontiers in immunology* **4**, 214 (2013).
223. J.-M. Zhang, J. An, Cytokines, inflammation, and pain. *Int Anesthesiol Clin* **45**, 27-37 (2007).
224. K. L. Rock, E. Reits, J. Neefjes, Present Yourself! By MHC Class I and MHC Class II Molecules. *Trends in immunology* **37**, 724-737 (2016).
225. S. C. Gilbert, T-cell-inducing vaccines - what's the future. *Immunology* **135**, 19-26 (2012).
226. G. Mutua *et al.*, Safety and Immunogenicity of a 2-Dose Heterologous Vaccine Regimen With Ad26.ZEBOV and MVA-BN-Filo Ebola Vaccines: 12-Month Data From a Phase 1 Randomized Clinical Trial in Nairobi, Kenya. *The Journal of infectious diseases* **220**, 57-67 (2019).
227. J. Zhu, H. Yamane, W. E. Paul, Differentiation of effector CD4 T cell populations (*). *Annual review of immunology* **28**, 445-489 (2010).
228. C. Kim, F. Fang, C. M. Weyand, J. J. Goronzy, The life cycle of a T cell after vaccination - where does immune ageing strike? *Clin Exp Immunol* **187**, 71-81 (2017).
229. C.-A. Siegrist, P.-H. Lambert, in *The Vaccine Book (Second Edition)*, Barry R. Bloom, Paul-Henri Lambert, Eds. (Academic Press, 2016), pp. 33-42.
230. J. O. Josefsberg, B. Buckland, Vaccine process technology. *Biotechnology and bioengineering* **109**, 1443-1460 (2012).

231. N. K. Jain *et al.*, Formulation and stabilization of recombinant protein based virus-like particle vaccines. *Advanced drug delivery reviews* **93**, 42-55 (2015).
232. J. Mohr, Y. P. Chuan, Y. Wu, L. H. Lua, A. P. Middelberg, Virus-like particle formulation optimization by miniaturized high-throughput screening. *Methods (San Diego, Calif.)* **60**, 248-256 (2013).
233. R. Khandia *et al.*, Modulation of Dengue/Zika Virus Pathogenicity by Antibody-Dependent Enhancement and Strategies to Protect Against Enhancement in Zika Virus Infection. *Frontiers in immunology* **9**, 597-597 (2018).
234. G. R. Doyle, J. A. McCutcheon, *Clinical Procedures for Safer Patient Care* (British Columbia Institute of Technology 2012).
235. J. N. Zuckerman, The importance of injecting vaccines into muscle. Different patients need different needle sizes. *BMJ* **321**, 1237-1238 (2000).
236. P. He, Y. Zou, Z. Hu, Advances in aluminum hydroxide-based adjuvant research and its mechanism. *Hum Vaccin Immunother* **11**, 477-488 (2015).
237. C. A. Shaw *et al.*, Aluminum-induced entropy in biological systems: implications for neurological disease. *Journal of toxicology* **2014**, 491316 (2014).
238. F. E. Shaw, Jr. *et al.*, Effect of anatomic injection site, age and smoking on the immune response to hepatitis B vaccination. *Vaccine* **7**, 425-430 (1989).
239. F. de Lalla, E. Rinaldi, D. Santoro, G. Pravettoni, Immune response to hepatitis B vaccine given at different injection sites and by different routes: a controlled randomized study. *European journal of epidemiology* **4**, 256-258 (1988).
240. T. Tapiainen, J. D. Cherry, U. Heininger, Effect of injection site on reactogenicity and immunogenicity of acellular and whole-cell pertussis component diphtheria-tetanus-pertussis vaccines in infants. *Vaccine* **23**, 5106-5112 (2005).
241. L. Zhang, W. Wang, S. Wang, Effect of vaccine administration modality on immunogenicity and efficacy. *Expert Rev Vaccines* **14**, 1509-1523 (2015).
242. Y. Gillet, P. Habermehl, S. Thomas, C. Eymin, A. Fiquet, Immunogenicity and safety of concomitant administration of a measles, mumps and rubella vaccine (M-M-RvaxPro) and a varicella vaccine (VARIVAX) by intramuscular or subcutaneous routes at separate injection sites: a randomised clinical trial. *BMC medicine* **7**, 16 (2009).
243. F. L. Ruben *et al.*, Choosing a Route of Administration for Quadrivalent Meningococcal Polysaccharide Vaccine: Intramuscular versus Subcutaneous. *Clinical Infectious Diseases* **32**, 170-172 (2001).
244. A. Fisch *et al.*, Immunogenicity and safety of a new inactivated hepatitis A vaccine: a clinical trial with comparison of administration route. *Vaccine* **14**, 1132-1136 (1996).
245. B. Malik, G. Rath, A. K. Goyal, Are the anatomical sites for vaccine administration selected judiciously? *International Immunopharmacology* **19**, 17-26 (2014).
246. M. T. Ochoa, A. Loncaric, S. R. Krutzik, T. C. Becker, R. L. Modlin, "Dermal dendritic cells" comprise two distinct populations: CD1+ dendritic cells and CD209+ macrophages. *J Invest Dermatol* **128**, 2225-2231 (2008).
247. A. K. Shakya, M. Y. E. Chowdhury, W. Tao, H. S. Gill, Mucosal vaccine delivery: Current state and a pediatric perspective. *J Control Release* **240**, 394-413 (2016).
248. J. K. Salmon, C. A. Armstrong, J. C. Ansel, The skin as an immune organ. *West J Med* **160**, 146-152 (1994).
249. W. T. Godbey, in *An Introduction to Biotechnology*, W. T. Godbey, Ed. (Woodhead Publishing, 2014), pp. 275-312.

250. S. H. T. Jorritsma, E. J. Gowans, B. Grubor-Bauk, D. K. Wijesundara, Delivery methods to increase cellular uptake and immunogenicity of DNA vaccines. *Vaccine* **34**, 5488-5494 (2016).
251. A. Tanghe *et al.*, Tuberculosis DNA vaccine encoding Ag85A is immunogenic and protective when administered by intramuscular needle injection but not by epidermal gene gun bombardment. *Infect Immun* **68**, 3854-3860 (2000).
252. R. Weiss *et al.*, Gene gun bombardment with gold particles displays a particular Th2-promoting signal that over-rules the Th1-inducing effect of immunostimulatory CpG motifs in DNA vaccines. *Vaccine* **20**, 3148-3154 (2002).
253. X. Zhou, L. Zheng, L. Liu, L. Xiang, Z. Yuan, T helper 2 immunity to hepatitis B surface antigen primed by gene-gun-mediated DNA vaccination can be shifted towards T helper 1 immunity by codelivery of CpG motif-containing oligodeoxynucleotides. *Scandinavian journal of immunology* **58**, 350-357 (2003).
254. D. J. Irvine, A. Aung, M. Silva, Controlling timing and location in vaccines. *Advanced drug delivery reviews*, S0169-0409X(0120)30065-X (2020).
255. M. C. Diehl *et al.*, Tolerability of intramuscular and intradermal delivery by CELLECTRA(®) adaptive constant current electroporation device in healthy volunteers. *Human vaccines & immunotherapeutics* **9**, 2246-2252 (2013).
256. L. Lambricht *et al.*, Clinical potential of electroporation for gene therapy and DNA vaccine delivery. *Expert opinion on drug delivery* **13**, 295-310 (2016).
257. A. Z. Alkilani, M. T. C. McCrudden, R. F. Donnelly, Transdermal Drug Delivery: Innovative Pharmaceutical Developments Based on Disruption of the Barrier Properties of the stratum corneum. *Pharmaceutics* **7**, 438-470 (2015).
258. C. I. Shin, S. D. Jeong, N. S. Rejinold, Y. C. Kim, Microneedles for vaccine delivery: challenges and future perspectives. *Ther Deliv* **8**, 447-460 (2017).
259. A. Pattani *et al.*, Microneedle mediated intradermal delivery of adjuvanted recombinant HIV-1 CN54gp140 effectively primes mucosal boost inoculations. *J Control Release* **162**, 529-537 (2012).
260. W. C. Weldon *et al.*, Microneedle vaccination with stabilized recombinant influenza virus hemagglutinin induces improved protective immunity. *Clin Vaccine Immunol* **18**, 647-654 (2011).
261. L. Y. Chu *et al.*, Enhanced Stability of Inactivated Influenza Vaccine Encapsulated in Dissolving Microneedle Patches. *Pharmaceutical research* **33**, 868-878 (2016).
262. E. V. Vassilieva *et al.*, Improved immunogenicity of individual influenza vaccine components delivered with a novel dissolving microneedle patch stable at room temperature. *Drug Deliv Transl Res* **5**, 360-371 (2015).
263. A. Vrdoljak *et al.*, Induction of broad immunity by thermostabilised vaccines incorporated in dissolvable microneedles using novel fabrication methods. *Journal of Controlled Release* **225**, 192-204 (2016).
264. X. Chen *et al.*, Improving the reach of vaccines to low-resource regions, with a needle-free vaccine delivery device and long-term thermostabilization. *J Control Release* **152**, 349-355 (2011).
265. G. Ma, C. Wu, Microneedle, bio-microneedle and bio-inspired microneedle: A review. *Journal of Controlled Release* **251**, 11-23 (2017).
266. C. F. Kuper *et al.*, The role of nasopharyngeal lymphoid tissue. *Immunology today* **13**, 219-224 (1992).

267. H. Yusuf, V. Kett, Current prospects and future challenges for nasal vaccine delivery. *Human Vaccines & Immunotherapeutics* **13**, 34-45 (2017).
268. M. A. Clark, M. A. Jepson, B. H. Hirst, Exploiting M cells for drug and vaccine delivery. *Advanced drug delivery reviews* **50**, 81-106 (2001).
269. I. Shannon, C. L. White, J. L. Nayak, Understanding Immunity in Children Vaccinated With Live Attenuated Influenza Vaccine. *J Pediatric Infect Dis Soc* **9**, S10-s14 (2020).
270. R. Dhere *et al.*, A pandemic influenza vaccine in India: from strain to sale within 12 months. *Vaccine* **29 Suppl 1**, A16-21 (2011).
271. C. Calzas, C. Chevalier, Innovative Mucosal Vaccine Formulations Against Influenza A Virus Infections. *Frontiers in immunology* **10**, (2019).
272. D. Albrecht, M. Iwashima, D. Dillon, S. Harris, J. Levy, A Phase 1, Randomized, Open-Label, Safety, Tolerability, and Comparative Bioavailability Study of Intranasal Dihydroergotamine Powder (STS101), Intramuscular Dihydroergotamine Mesylate, and Intranasal DHE Mesylate Spray in Healthy Adult Subjects. *Headache* **60**, 701-712 (2020).
273. J. H. Ryu *et al.*, Chitosan oral patches inspired by mussel adhesion. *J Control Release* **317**, 57-66 (2020).
274. P. Watts, A. Smith, M. Hinchcliffe, in *Mucosal Delivery of Biopharmaceuticals*, Bruno Sarmento, José das Neves, Eds. (Springer, Boston, MA, 2014), pp. 499-516
275. L. Casettari, L. Illum, Chitosan in nasal delivery systems for therapeutic drugs. *J Control Release* **190**, 189-200 (2014).
276. M. A. Gill, E. P. Schlaudecker, Perspectives from the Society for Pediatric Research: Decreased Effectiveness of the Live Attenuated Influenza Vaccine. *Pediatric research* **83**, 31-40 (2018).
277. H. Jang, T. M. Ross, Preexisting influenza specific immunity and vaccine effectiveness. *Expert Rev Vaccines* **18**, 1043-1051 (2019).
278. K. Edwards, P. H. Lambert, S. Black, Narcolepsy and Pandemic Influenza Vaccination: What We Need to Know to be Ready for the Next Pandemic. *The Pediatric infectious disease journal* **38**, 873-876 (2019).
279. D. J. Lewis *et al.*, Transient facial nerve paralysis (Bell's palsy) following intranasal delivery of a genetically detoxified mutant of Escherichia coli heat labile toxin. *PLoS One* **4**, e6999 (2009).
280. Z.-B. Wang, J. Xu, Better Adjuvants for Better Vaccines: Progress in Adjuvant Delivery Systems, Modifications, and Adjuvant-Antigen Codelivery. *Vaccines* **8**, 128 (2020).
281. H. B. Lee *et al.*, Oral Immunization of FMDV Vaccine Using pH-Sensitive and Mucoadhesive Thiolated Cellulose Acetate Phthalate Microparticles. *Tissue engineering and regenerative medicine* **15**, 1-11 (2018).
282. G. Azzali, Structure, lymphatic vascularization and lymphocyte migration in mucosa-associated lymphoid tissue. *Immunological reviews* **195**, 178-189 (2003).
283. M. F. Cesta, Normal Structure, Function, and Histology of Mucosa-Associated Lymphoid Tissue. *Toxicologic Pathology* **34**, 599-608 (2006).
284. B. Homayun, X. Lin, H.-J. Choi, Challenges and Recent Progress in Oral Drug Delivery Systems for Biopharmaceuticals. *Pharmaceutics* **11**, 129 (2019).
285. H. Cheroutre, F. Lambolez, D. Mucida, The light and dark sides of intestinal intraepithelial lymphocytes. *Nature Reviews Immunology* **11**, 445-456 (2011).

286. T. Magrone, E. Jirillo, Development and Organization of the Secondary and Tertiary Lymphoid Organs: Influence of Microbial and Food Antigens. *Endocrine, metabolic & immune disorders drug targets* **19**, 128-135 (2019).
287. T. Sun, A. Nguyen, J. L. Gommerman, Dendritic Cell Subsets in Intestinal Immunity and Inflammation. *Journal of immunology (Baltimore, Md. : 1950)* **204**, 1075-1083 (2020).
288. A. N. Vlasova, S. Takanashi, A. Miyazaki, G. Rajashekara, L. J. Saif, How the gut microbiome regulates host immune responses to viral vaccines. *Curr Opin Virol* **37**, 16-25 (2019).
289. R. A. Kuschner *et al.*, A phase 3, randomized, double-blind, placebo-controlled study of the safety and efficacy of the live, oral adenovirus type 4 and type 7 vaccine, in U.S. military recruits. *Vaccine* **31**, 2963-2971 (2013).
290. D. Amicizia, L. Arata, F. Zangrillo, D. Panatto, R. Gasparini, Overview of the impact of Typhoid and Paratyphoid fever. Utility of Ty21a vaccine (Vivotif®). *Journal of preventive medicine and hygiene* **58**, E1-e8 (2017).
291. Advisory Committee on Immunization Practices, "Typhoid Immunization Recommendations of the Advisory Committee on Immunization Practices (ACIP)," (1994).
292. S.-H. Kim, Y.-S. Jang, The development of mucosal vaccines for both mucosal and systemic immune induction and the roles played by adjuvants. *Clin Exp Vaccine Res* **6**, 15-21 (2017).
293. P. Pereira, V. Vetter, B. Standaert, B. Benninghoff, Fifteen years of experience with the oral live-attenuated human rotavirus vaccine: reflections on lessons learned. *Expert Rev Vaccines*, 1-15 (2020).
294. O. S. Folorunso, O. M. Sebolai, Overview of the Development, Impacts, and Challenges of Live-Attenuated Oral Rotavirus Vaccines. *Vaccines (Basel)* **8**, (2020).
295. T. Nakagomi, O. Nakagomi, A critical review on a globally-licensed, live, orally-administrable, monovalent human rotavirus vaccine: Rotarix. *Expert opinion on biological therapy* **9**, 1073-1086 (2009).
296. J. J. Liau, S. Hook, C. A. Prestidge, T. J. Barnes, A lipid based multi-compartmental system: Liposomes-in-double emulsion for oral vaccine delivery. *European journal of pharmaceutics and biopharmaceutics : official journal of Arbeitsgemeinschaft fur Pharmazeutische Verfahrenstechnik e.V* **97**, 15-21 (2015).
297. S.-J. Cao *et al.*, Nanoparticles: Oral Delivery for Protein and Peptide Drugs. *AAPS PharmSciTech* **20**, 190-190 (2019).
298. E. M. Pridgen, F. Alexis, O. C. Farokhzad, Polymeric nanoparticle technologies for oral drug delivery. *Clin Gastroenterol Hepatol* **12**, 1605-1610 (2014).
299. V. M. Kurup, J. Thomas, Edible Vaccines: Promises and Challenges. *Mol Biotechnol* **62**, 79-90 (2020).
300. M. S. Khan, F. A. Joyia, G. Mustafa, Seeds as Economical Production Platform for Recombinant Proteins. *Protein and peptide letters* **27**, 89-104 (2020).
301. S. Pillet *et al.*, Immunogenicity and safety of a quadrivalent plant-derived virus like particle influenza vaccine candidate-Two randomized Phase II clinical trials in 18 to 49 and ≥50 years old adults. *PLoS One* **14**, e0216533 (2019).
302. S. Rosales-Mendoza, V. A. Márquez-Escobar, O. González-Ortega, R. Nieto-Gómez, J. I. Arévalo-Villalobos, What Does Plant-Based Vaccine Technology Offer to the Fight against COVID-19? *Vaccines (Basel)* **8**, (2020).

303. M. N. Uddin, A. Allon, M. A. Roni, S. Kouzi, Overview and Future Potential of Fast Dissolving Buccal Films as Drug Delivery System for Vaccines. *Journal of pharmacy & pharmaceutical sciences : a publication of the Canadian Society for Pharmaceutical Sciences, Societe canadienne des sciences pharmaceutiques* **22**, 388-406 (2019).
304. H. Kraan *et al.*, Buccal and sublingual vaccine delivery. *Journal of Controlled Release* **190**, 580-592 (2014).
305. N. Narang, J. Sharma, Sublingual mucosa as a route for systemic drug delivery. *International Journal of Pharmacy and Pharmaceutical Sciences* **3**, 18-22 (2011).
306. S. Hua, Advances in Nanoparticulate Drug Delivery Approaches for Sublingual and Buccal Administration. *Frontiers in Pharmacology* **10**, (2019).
307. T. J. De Marco, I. Blomsnes, Effect of various conditions on the sublingual absorption of para-aminosalicylic acid. *Oral surgery, oral medicine, and oral pathology* **37**, 320-326 (1974).
308. J. Upadhyay, R. B. Upadhyay, P. Agrawal, S. Jaitley, R. Shekhar, Langerhans cells and their role in oral mucosal diseases. *N Am J Med Sci* **5**, 505-514 (2013).
309. J. H. Choi *et al.*, A single sublingual dose of an adenovirus-based vaccine protects against lethal Ebola challenge in mice and guinea pigs. *Molecular pharmaceutics* **9**, 156-167 (2012).
310. C. Czerkinsky, J. Holmgren, in *Mucosal Vaccines: Modern Concepts, Strategies, and Challenges*, Pamela A. Kozlowski, Ed. (Springer Berlin Heidelberg, Berlin, Heidelberg, 2012), pp. 1-18.
311. V. F. Patel, F. Liu, M. B. Brown, Advances in oral transmucosal drug delivery. *Journal of Controlled Release* **153**, 106-116 (2011).
312. D. J. Aframian, T. Davidowitz, R. Benoliel, The distribution of oral mucosal pH values in healthy saliva secretors. *Oral Diseases* **12**, 420-423 (2006).
313. P. W. Wertz, C. A. Squier, Cellular and molecular basis of barrier function in oral epithelium. *Critical reviews in therapeutic drug carrier systems* **8**, 237-269 (1991).
314. H. S. Oberoi, Y. M. Yorgensen, A. Morasse, J. T. Evans, D. J. Burkhart, PEG modified liposomes containing CRX-601 adjuvant in combination with methylglycol chitosan enhance the murine sublingual immune response to influenza vaccination. *Journal of Controlled Release* **223**, 64-74 (2016).
315. J. A. White *et al.*, Serum and mucosal antibody responses to inactivated polio vaccine after sublingual immunization using a thermoresponsive gel delivery system. *Human vaccines & immunotherapeutics* **10**, 3611-3621 (2014).
316. A. Borde, A. Ekman, J. Holmgren, A. Larsson, Effect of protein release rates from tablet formulations on the immune response after sublingual immunization. *European Journal of Pharmaceutical Sciences* **47**, 695-700 (2012).
317. J.-H. Song *et al.*, Sublingual vaccination with influenza virus protects mice against lethal viral infection. *Proc Natl Acad Sci U S A* **105**, 1644-1649 (2008).
318. J. Y. Kim, Y. Choi, H. H. Nguyen, M. K. Song, J. Chang, Mucosal immunization with recombinant adenovirus encoding soluble globular head of hemagglutinin protects mice against lethal influenza virus infection. *Immune Netw* **13**, 275-282 (2013).
319. P. N. Boyaka, Inducing Mucosal IgA: A Challenge for Vaccine Adjuvants and Delivery Systems. *The Journal of Immunology* **199**, 9 (2017).
320. L. B. Lawson, E. B. Norton, J. D. Clements, Defending the mucosa: adjuvant and carrier formulations for mucosal immunity. *Current opinion in immunology* **23**, 414-420 (2011).

321. C. Hervouet *et al.*, Sublingual immunization with an HIV subunit vaccine induces antibodies and cytotoxic T cells in the mouse female genital tract. *Vaccine* **28**, 5582-5590 (2010).
322. Vaccine Innovation Prioritisation Strategy, "Sublingual Dosage Forms," (Geneva, Switzerland, 2019).
323. ClinicalTrials.gov. (National Library of Medicine Bethesda, MD, 2016).
324. G. Passalacqua, D. Bagnasco, G. W. Canonica, 30 years of sublingual immunotherapy. *Allergy* **75**, 1107-1120 (2020).
325. P. Demoly, G. Passalacqua, M. A. Calderon, T. Yalaoui, Choosing the optimal dose in sublingual immunotherapy: Rationale for the 300 index of reactivity dose. *Clinical and Translational Allergy* **5**, 44 (2015).
326. K. Aran *et al.*, An oral microjet vaccination system elicits antibody production in rabbits. *Science Translational Medicine* **9**, eaaf6413 (2017).
327. C. L. McNeilly *et al.*, Microprojection arrays to immunise at mucosal surfaces. *J Control Release* **196**, 252-260 (2014).
328. Y. Zhen *et al.*, Multifunctional liposomes constituting microneedles induced robust systemic and mucosal immunoresponses against the loaded antigens via oral mucosal vaccination. *Vaccine* **33**, 4330-4340 (2015).
329. T. Wang *et al.*, Mannosylated and lipid A-incorporating cationic liposomes constituting microneedle arrays as an effective oral mucosal HBV vaccine applicable in the controlled temperature chain. *Colloids and Surfaces B: Biointerfaces* **126**, 520-530 (2015).
330. J. Mašek *et al.*, Multi-layered nanofibrous mucoadhesive films for buccal and sublingual administration of drug-delivery and vaccination nanoparticles - important step towards effective mucosal vaccines. *Journal of Controlled Release* **249**, 183-195 (2017).
331. J. H. Choi, S. C. Schafer, A. N. Freiberg, M. A. Croyle, Bolstering Components of the Immune Response Compromised by Prior Exposure to Adenovirus: Guided Formulation Development for a Nasal Ebola Vaccine. *Molecular Pharmaceutics* **12**, 2697-2711 (2015).
332. J. H. Choi *et al.*, A Single Dose Respiratory Recombinant Adenovirus-Based Vaccine Provides Long-Term Protection for Non-Human Primates from Lethal Ebola Infection. *Molecular Pharmaceutics* **12**, 2712-2731 (2015).

Chapter 2: Novel Technology for Storage and Distribution of Live Vaccines and Other Biological Medicines at Ambient Temperature[1]

2.1 Introduction

Vaccines have often been described as the greatest human intervention supporting global health, second only to clean drinking water (1). In 1900, 53% of deaths in the United States were due to infectious disease (2). In 2010, that number dramatically fell to 3%. However, many vaccines are rarely designed to meet the needs of every global community. This is highlighted by the fact that, in 2015, more than half of the leading causes of death in low-income countries were the result of infectious disease while less than 10% of deaths in high-income countries were attributed to similar causes (3). One of the primary reasons for this disparity is limited uptake of vaccines with nearly 20 million infants worldwide not receiving routine immunizations, such as three doses of diphtheria-tetanus-pertussis (DTP) vaccine (4). To date, the vaccine requisites of developing countries have not been adequately met for a variety of reasons including issues associated with fragile healthcare systems, conflict resolution, policy making, program management, financing, supply chain and distribution across large urban areas and to the most remote locations (5). Each of these issues contributed in some part to the delay in the distribution of experimental vaccines and therapeutics against Ebola during the 2014-2016 outbreak (6, 7). The ramifications of these roadblocks were also seen in the 2016-2017

[1] This chapter was published in Science Advances: I. Bajrovic, S. C. Schafer, D. K. Romanovicz, M. A. Croyle, Novel technology for storage and distribution of live vaccines and other biological medicines at ambient temperature. Science Advances 6, eaau4819 (2020). I.B., S.C.S., and M.A.C. designed the project. I.B. conceptualized and designed the experiments and performed the stability, rate of release, FTIR, and DSC studies and the analysis. D.K.R. prepared samples for SEM, collected images, and participated in their analysis in conjunction with S.C.S., I.B., and M.A.C. I.B. performed cell culture and adenovirus amplification. S.C.S. assisted with preparation of the figures and the Supplementary Materials. I.B. and M.A.C. wrote and edited the manuscript.

meningitis outbreak in Nigeria where the cost and limited supply of a vaccine contributed to the mortality and spread of disease (8). A more long-term example of this effect is exemplified by the prevalence of deaths in children less than 5 years of age from rotavirus infection in India and Sub-Saharan African countries over the last decade due to their inability to access the vaccine without external subsidiaries (9).

Much of the cost of a given vaccine is product specific and dictated by the nature of the antigen, immunogen or pathogen of interest and the complexity of large-scale production processes (10). Distribution and administration costs also significantly add to the price of a vaccine. These costs are often not product specific as most vaccines are temperature sensitive and require cold-chain maintenance, which entails transporting, storing, and monitoring them at a recommended temperature from the point of production to the point of use (11). In total, the cost of distribution and administration often exceeds the cost of vaccine production, making them the most prohibitive barriers to global immunization campaigns. One simulation model found that of the $64 billion needed to introduce 18 vaccines to 94 countries within a 10 year timeframe, $38 billion would be utilized to support distribution and administration alone (12). Even when developing countries can access vaccines, such as those available through the Expanded Program on Immunization (EPI) and other programs (13), maintenance and monitoring of required cold chain conditions are not guaranteed due to varying access to equipment and resources needed to maintain optimal environmental conditions (14, 15). For example, during the inspection of vaccinating facilities in Cameroon, only 76% had a functional thermometer in use. Of those, 20% had recorded temperatures that fell outside those recommended by vaccine manufacturers. This was primarily due to vulnerabilities in the power

grid and lack of alternative sources of electricity, as was also found in other regions around the globe (16, 17).

Development of a technology that could significantly minimize resources needed for distribution and administration of vaccines would notably enhance access to these medicines and improve global health. Breakthroughs in formulation development and technology that have effectively stabilized live bacteria, viruses and recombinant proteins at ambient temperatures offer a viable solution to improving global distribution of vaccines (18-20). It has been predicted that if the original 5-in-1 Pentavalent Vaccine was reformulated as a fully thermostable preparation, its availability in developing countries could reach nearly 100% (21). The majority of vaccines recommended for low- and middle-income countries by the World Health Organization are packaged in glass and plastic vials, often with diluents and related materials (22). Thus, the amount of revenue and manpower required for storage and monitoring of these preparations is significant and may be prohibitive for stockpiling in preparation for widespread infectious disease outbreaks for many regions around the world. Most require reconstitution with specific solvents prior to administration and are predominantly given by injection (22). This requires the participation of numerous health care professionals which adds to the cost of any vaccination campaign and can also be a source of vaccine failure and wastage due to human error in developed as well as low- and middle-income countries (23, 24). Vaccines developed for mucosal administration provide a reasonable alternative to parenteral vaccination strategies. They are needle-free, eliminating the need for and associated costs of trained personnel for vaccine administration. They are also capable of inducing both localized and systemic immune responses by facilitating transport of vaccine and associated antigens throughout the mucosa-associated lymphoid tissue (MALT) (25). For some pathogens, mucosal immunity may also be

necessary to improve the durability or long-term protection offered by a vaccine (26). They also heighten patient acceptance and compliance in both industrialized and developing countries (25, 27). However, only 4 of the vaccines currently available are delivered by the mucosal route (28).

In this report, we summarize our efforts to develop a novel platform that can significantly reduce costs associated with storage, distribution and administration of vaccines and other biological drug products. Initially, more than 400 formulations were screened for their ability to enhance the immune response of an adenovirus-based Ebola vaccine (29). Formulations providing favorable *in vivo* data were then assessed for their ability to stabilize recombinant adenoviruses in a thin, peelable film matrix (Figure 2.1A and B). One formulation was found to stabilize adenovirus for a period of 3 years at room temperature (Figure 2.1C). This formulation, reconstituted and given via the respiratory route to non-human primates, offered full protection from a lethal dose of Ebola (30) but was never utilized for the primary purpose for which it was designed, immunization by the sublingual (SL) or the buccal (BU) route. Additional studies revealed that this platform was also capable of preserving live bacteria at room temperature for 8 months with minimal loss of viability upon reconstitution (Figure 2.1D). Further investigation revealed that the performance of a primary antibody (Figure 2.1E) and an antibody-enzyme conjugate (Figure 2.1F) embedded in our thin film at room temperature was superior to that of the same product stored in the manufacturer's liquid formulation stored under the same conditions. Subsequent mechanistic studies with a recombinant adenoviral vector have allowed us to identify criteria vital for long-term stabilization that can be applied and adapted for other biological products.

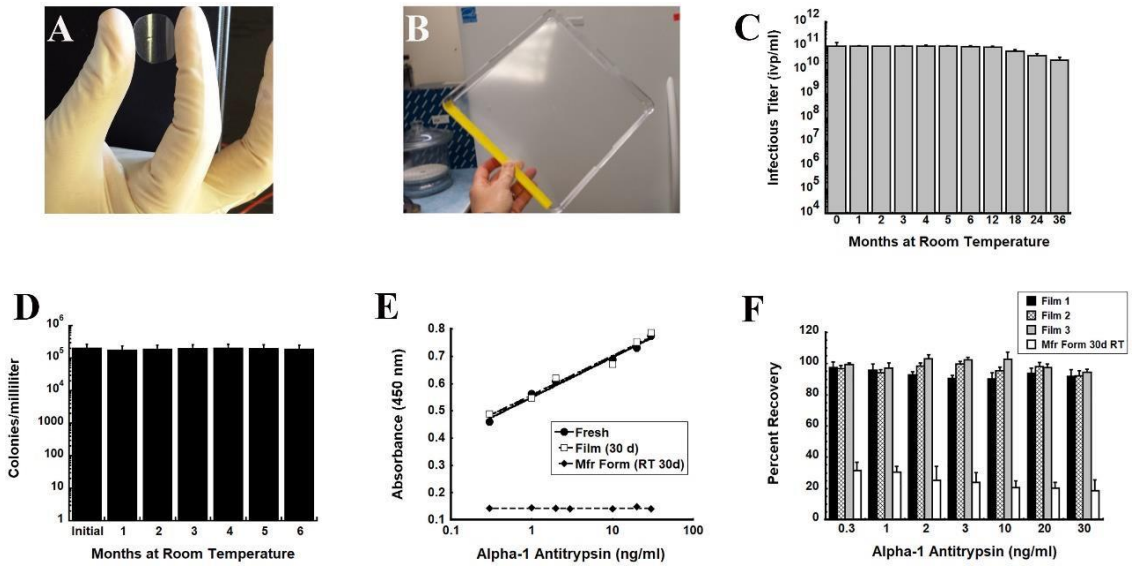

Figure 2.1: Film Technology Stabilizes Live Microorganisms and Biological Compounds for Extended Periods of Time at Ambient Temperatures.

(**A**) Prototype unit dose film useful for assessment of long-term stability as described in this manuscript. (**B**) Prototype large scale film that can be utilized for stockpiling and storage and sectioned into multiple single dose films for distribution. (**C**) Thirty-six month stability profile of recombinant adenovirus in solid film matrix. Replicate films (n=5 / time point) were stored at 20 °C, reconstituted with sterile water and infectious titer assessed with a standard limiting dilution assay (19). (**D**) Six month stability profile of film containing live bacteria at 20°C. Films (n=5 / time point) were reconstituted with sterile saline and solutions plated on nutrient rich agar. Colonies were counted for assessment of recovery of live bacteria from the film. (**E**) Binding affinity of primary antibody (178260, Millipore) stabilized in thin film and stored at room temperature (RT) for 30 days is superior to that of the manufacturer's product stored as a liquid under the same conditions. Solutions made from rehydrated films were utilized in an alpha-1 anti-trypsin (A1AT) ELISA assay in triplicate as described (31). Correlation coefficients (r^2) for standard curves made with fresh stock stored at 4 °C (Fresh), antibody reconstituted from

film after storage for 30 days at 20 °C (Film) and antibody stored in the manufacturer's liquid formulation after storage for 30 days at 20 °C (Mfr. Form) was 0.99, 0.99 and 0.10 respectively. (**F**) Recovery of binding affinity of AP192P, a donkey anti-mouse IgG antibody, horseradish peroxidase (HRP) conjugate (Millipore) after storage in a thin film at 20 °C. Percent recovery is the relative absorbance reading generated by an assay utilizing secondary antibody from reconstituted films with that of fresh stock as supplied by the manufacturer for each given concentration of A1AT standard. Results were also compared with manufacturer's stock stored at RT (instead of -20 °C as recommended). Each of the bars in the graph represent readings obtained from antibody recovered from 3 separate films in a given experiment and data reflect the averages ± the standard error of the mean of data collected from 3 separate experiments.

2.2 Materials and Methods

2.2.1 Materials

Dulbecco's phosphate-buffered saline (DPBS), Trizma® base (2-Amino-2-(hydroxymethyl)-1,3-propanediol), potassium ferricyanide, potassium ferrocyanide, glutaraldehyde (grade I, 25% in water) fetal bovine serum (FBS, qualified, US origin), glycerol, and D-sorbitol (USP grade) were purchased from Sigma Aldrich (St. Louis, MO). Poly(maleic anhydride-alt-1-octadecene) substituted with 3-(dimethylamino)propylamine was purchased from Anatrace (Maumee, OH). Dulbecco's modified Eagle's medium (DMEM), was purchased from Mediatech (Manassas, VA). Hydroxypropyl Methyl Cellulose 4*KM (HPMC) was kindly provided by the Dow Chemical Company (Midland, MI). Penicillin (10,000 IU) and streptomycin (10,000µg/mL) were purchased from Gibco Life Technologies (Grand Island, NY). 5-Bromo-4-chloro-3-indolyl-β-d-galactoside (X-gal) was purchased from Gold Biotechnology

(St.Louis, MO). All other chemicals were of analytical reagent grade and purchased from Thermo Fisher Scientific (Pittsburgh, PA) unless specified otherwise.

2.2.2 Adenovirus Production and Purification

First-generation adenovirus serotype 5 expressing E. coli beta-galactosidase under the control of a cytomegalovirus (CMV) promoter was amplified in human embryonic kidney (HEK) 293 cells (ATCC CRL-1573) and purified from secondary lysates according to established methods (19). Preparations with a ratio of infectious to physical viral particles of 1:100 were utilized in the studies summarized here.

2.2.3 Formulation Screening

Base formulations were prepared in bulk with various solvents. Additional excipients were added to base and homogenized prior to addition of virus. A virus concentration of 1.25 x 10^{12} v.p./film was selected so that subtle changes in infectious titer could be detected with a standard limiting dilution/infectious titer assay and histochemical staining (19). Films were dispensed into 1 ml unit dose molds (or 100 ul unit dose for mouse studies) using an E3 Repeater pipette (Eppendorf, Hauppauge, NY) and dried in 8 hours, (1ml film) and 4 hours (100 ul film) under ambient temperature and pressure (20 °C, 1 atm) and aseptic conditions. Once dry, films were reconstituted in and infectious titer assays performed on HeLa cells (ATCC# CCL-2). Percent recovery was calculated as:

$$\%\ Recovery = \frac{\log\left(infectious\ titer\ of\ t = 1\right)}{\log(infectious\ titer\ of\ t = 0)} \times 100$$

where t=1 is the infectious titer of a film that was reconstituted after drying and t=0 is the infectious titer of virus in the same formulation prior to drying.

2.2.4 Rate of Release Analysis

Films were placed in sterile chambers containing 1 ml of saline (pH 7) warmed to 37 °C. Buffers in each chamber were stirred (60 rpm) and 10µL samples collected every 5 minutes for a period of 2 hours. Equal amounts of blank buffer were added to each chamber after sampling to maintain a constant volume. Samples were also taken of virus containing liquid film formulations that did not undergo drying and of virus in PBS alone which were also stirred at 37 °C. Results from these controls were used to normalize data for changes in titer due to temperature, physical agitation and formulation effects.

2.2.5 Young's Modulus and Percent Elongation

Films were prepared and dried under ambient temperature and pressure (20 °C, 1 atm) under aseptic conditions. The following day they were evaluated for their respective young's modulus and percent elongation using a TA XT Plus Texture Analyzer (TA Instruments; New Castle, Delaware). Samples of each film (12.0 × 2.54 cm) were fixed on tensile grips (TA-108S-5) and a TA-8 (1/4" diameter ball) probe was used. The test speed was constant at 0.6 mm/ min. The young's modulus values for each preparation were calculated using the following equation (32):

$$Youngs\ Modulus = \frac{F \times L}{A \times \Delta L}$$

F is the force required to break the film, L is the original length of the film and A is cross-sectional area of the film. The ΔL value represents the amount by which the length of the film changed during the elongation process.

Percent elongation was calculated using the following equation (33):

$$\%Elongation = \frac{extension\ to\ break}{original\ length\ of\ sample\ between\ clamps} \times 100$$

2.2.6 Viscosity Measurements

Liquid formulations with and without virus were prepared fresh on the day of testing and evaluated for their respective viscosity with a Rheometer AE G2 viscometer (TA Instruments; New Castle, Delaware) using cone plates (40 mm diameter with cone angle of 1.99°). The viscometer was calibrated using a certified viscosity reference standard (466.5 mPa*s, National Institute for Standard Technology). Each sample was then added between the cone plates at the determined optimal volume (0.700mL) and measurements were taken at 25°C.

2.2.7 Short-Term Stability

Solid State. Virus containing films were prepared in bulk and in parallel with the following liquid formulations: Control buffer A (10% glycerol/PBS) and in Control buffer B (PBS). A fraction of each production lot was stored at 4, 20, 37, 40 and 50°C. Samples stored at 4 and 20 °C were reconstituted and infectious titer assessed on days 1, 3, 7, 14, 28, 48, and 84 while the titer of those stored at 37 °C were assessed on days 1-7, 10, and 14. Samples stored at 40 and 50 °C were reconstituted and infectious titer assessed on days 1 through 5. *Liquid State.* Virus was added to replicate sterile containers containing liquid formulations and stored with replicate Control A and Control B preparations at 4, 20, 40 and 50 °C. Infectious titer for each preparation was assessed on the same schedule as described for films at each respective storage temperature. *Relative Humidity.* Films were prepared in bulk and a fraction of each production lot was stored 40°C in a VWR 6292 vacuum oven to achieve an atmosphere of 0% RH, a convection oven to achieve an atmosphere of 20% RH (Precision, 2EG, Winchester, VA) and an incubator (VWR Symphony 5.3A) to achieve an atmosphere of 97% RH. Humidity was

monitored over time using an Ambient Weather WS-3000-X5 Wireless Thermo-Hygrometer (Chandler, AZ). Samples were reconstituted and infectious titer assessed on day 3.

2.2.8 Freeze-Thaw Studies

Films were prepared in bulk and placed at -80 °C once drying was complete. After 24 hours, all samples were thawed to room temperature, 20 °C. Replicate (n=3) samples were reconstituted and infectious titer of virus assessed while remaining films were returned to the freezer. This cycle was repeated daily for 16 days, with infectious titer assays performed on replicate films on days 2-8, 12, and 16

2.2.9 Scanning Electron Microscopy

Films were prepared and, when drying was complete, they were coated with 12nm Pt/Pd in a Cressington 208HR sputter coater and subsequently photographed on a Zeiss Supra 40V Scanning Electron Microscope (Zeiss; Jena, Germany).

2.2.10 Differential Scanning Calorimetry

DSC was conducted on films with and without virus using a DSC-Q2000 calorimeter (TA Instruments; New Castle, Delaware). Films were cut, weighed and samples (5-10 mg) stored in crimped black die pans prior to analysis.

2.2.11 X-ray Powder Diffraction

A Rigaku MiniFlex 600 II was employed to study the crystallinity of dry powder excipients and of films. The generator operating voltage and current were 40 kV and 15mA, respectively. The scanning step was 0.04° and the 2θ scanning range was 5-50°. A Silicon Zero Diffraction Dish was used for films, which were held in place using an aluminum holder.

2.2.12 Fourier Transform Infrared Spectroscopy

FTIR spectroscopy was conducted on films prepared with and without virus using a Nicolet™ iS™ 50 FT-IR Spectrometer (ThermoFisher Scientific; Waltham, Massachusetts). Films were placed under the probe and scans were conducted in the 4000–800 cm^{-1} region using an ATR method with a diamond/ZnSe prism.

2.2.13 Statistical Analysis

Statistical analysis of data was performed using JMP (JMP Statistical Software from SAS, Cary, NC). Differences with respect to treatment were calculated using unpaired two-tailed Student's t tests. Differences were determined to be significant when the probability of chance explaining the results was reduced to less than 5% ($P < 0.05$).

2.3 Results

To identify factors key for recovery and preservation of virus infectivity in a novel thin film dosage form, over 30 combinations of buffers and excipients were evaluated according to a fractional factorial design. Excipients utilized in our multi-component films fall into three specific categories: base, binder and surfactant. For simplicity, multi-component formulations will be referred to by number throughout the text as they are listed in Table 2.1. Preliminary studies identified the importance of solvent, base concentration, the presence of binders and surfactants and final formulation pH on recovery of infectious virus upon reconstitution of films. Additional studies illustrate the role film components play in the preservation of live virus during exposure to stressors such as repeated freeze-thaw cycles and elevated temperatures. The final series of studies summarized here aim to identify mechanistic explanations for virus stabilization during the film forming process.

2.3.1 Identifying Key Formulation Components for Stability: Solvent, Excipient Selection and pH.

Initial screening studies were designed to evaluate the role of several different aqueous solvent systems in the maintenance of infectivity of live, recombinant adenovirus during the drying process. Films prepared in unbuffered formulations were least effective at preserving virus titer (Figure 2.2). Infectious virus was not recovered from films produced with the lowest amount of base excipient in the absence of buffering agents (Figure 2.2A). Use of phosphate buffered saline (PBS) to prepare films containing the lowest concentration of base significantly improved recovery of infectious virus particles (73%, Figure 2.2A). PBS also improved recovery of virus from films made with medium (92%, Figure 2.2B) and high (75%, Figure 2.2C) base concentrations with respect to those prepared in an unbuffered solvent.

Table 2.1: Summary of Formulations

Solvents: Red=Unbuffered Solution, Blue=PBS, Green=Tris.

	HPMC			Sorbitol	Glycerol	PMAL
Concentration	0.5%	1.5%	3%	2%	2%	1%
1						
2						
3						
4						
5						
6						
7						
8						
9						
10						
11						
12						
13						

Table 2.1: Summary of Formulations continued

14						
15						
16						
17						
18						
19						
20						
21						
22						
23						
24						
25						
26						
27						
28						
29						
30						
31						
32						
33						
34						
35						
36						

Preparations made with Tris buffer with low and medium base concentrations demonstrated recoveries of live virus of greater than 95% (Figures 2.2A and 2.2B). Preparations made with this buffer experienced a drop in pH of ~ 1.1 units regardless of base concentration during the drying process while those made with PBS and unbuffered solution demonstrated drops in pH of 2.5 and 3 units respectively (data not shown).

Since films prepared with Tris buffer were the most efficient in maintaining virus infectivity during the drying process, a second series of screening studies was initiated to identify the impact base concentration had on virus recovery during drying (Figure 2.2D). Films prepared with the lowest base concentration were able to retain 80 $\pm$ 17% of the original titer

after drying while those prepared with moderate and high base concentrations recovered 90 ± 6.5 and 93 ± 5.4% of infectious virus particles respectively. With the realization that films containing base alone could not support full recovery of infectious virus upon reconstitution, two different binders were added to the medium base formulation and evaluated for their ability to improve infectious titer after drying. The average recovery of films prepared with sorbitol was 97 ± 4.1% (Figure 2.2E). Films prepared with glycerol maintained 88 ± 14% of the original virus titer.

In a final effort to further improve recovery of infectious virus from films after drying, surfactant was added to Tris buffered preparations containing either base formulation alone or each of the binding agents described above (Figure 2.2F). Addition of surfactant significantly improved recovery of infectious titer in films containing only the medium concentration of base from 59 ± 4.7% (Formulation 25, Table 2.1) to 84 ± 1%. A similar effect was seen with the highest base concentration with recovery increasing from 72 ± 3.6% (Formulation 31) to 93 ± 4.6%. When sorbitol was added to the medium base preparation (Formulation 27), recovery of infectious virus rose from 96 ± 3.4% to 97 ± 2.1%. The surfactant impacted recovery in a slightly opposite manner when glycerol was also present in the formulation as the original virus concentration fell from 88 ± 14% to 85 ± 1.0% (Formulation 30). Aggregate analysis of data collected during the screening of solvent, base and binder formulations revealed that there was a direct correlation between virus recovery and the pH of the film after drying ($r^2 = 0.996$, Figure 2.2G). Film preparations capable of recovering more than 90% of the original virus titer after drying had final pH values within the range of 6.5 to 7.4. Due to the high variability, flexibility, and difficulty in handling films prepared with the low and high concentrations of base excipient, their use was excluded from the remainder of the studies outlined here.

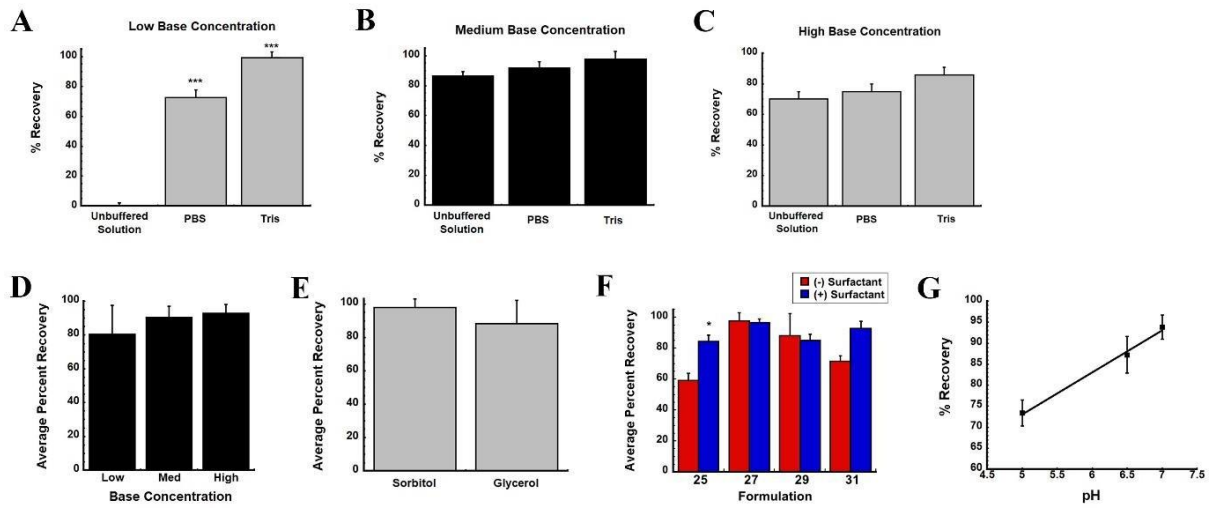

Figure 2.2: Solvent and Excipient Combinations that Preserve Virus Recovery from Film Matrix Maintain Optimal pH During Drying.

Recovery of virus from films containing 0.5% (Low, **A**), 1.5% (Medium, **B**) and 3.0% (High, **C**) concentrations of base excipient prepared in three different solvent systems was evaluated using an infectious titer assay. Once an optimal solvent system was selected, stepwise addition of excipients to the film identified an optimal base excipient concentration (**D**) and binder (**E**). Additional screening revealed that surfactant further improved recovery of infectious virus from the matrix (**F**). Analysis of data collected during each phase of screening revealed that formulations that maintained a final dried pH of 7.0 exhibited the highest recovery of infectious virus from the film (**G**). In each panel, data represents the average $\pm$ the standard deviation of a minimum of 3 films per condition. *$p < 0.05$, **$p < 0.01$, ***$p < 0.001$, two-tailed Student's t test. Formulations are summarized in the figure according to the numbers assigned in Table 2.1.

2.3.2 Role of Surfactant on the Rate of Release of Virus from Films

Films prepared with the base excipient alone released virus at a rate of 6.3×10^6 infectious virus particles (i.v.p)/ml/min after placement in PBS at 37 °C with gentle agitation (Figure 2.3A). Addition of sorbitol increased this rate twofold. When surfactant was also included in the formulation, the rate increased tenfold to 6.0×10^7 i.v.p/ml/min. The entire amount of infectious virus added to films containing both surfactant and sorbitol were released within 5 minutes (Figure 2.3B). Films prepared with base excipient alone (Formulation 25) released 90% of the dose in 5 minutes and only 97% of the total dose after 2 hours. The addition of sorbitol (Formulation 27) resulted in 88% of dose released after 5 minutes but only marginally improved recovery to 98% of the full dose after 2 hours.

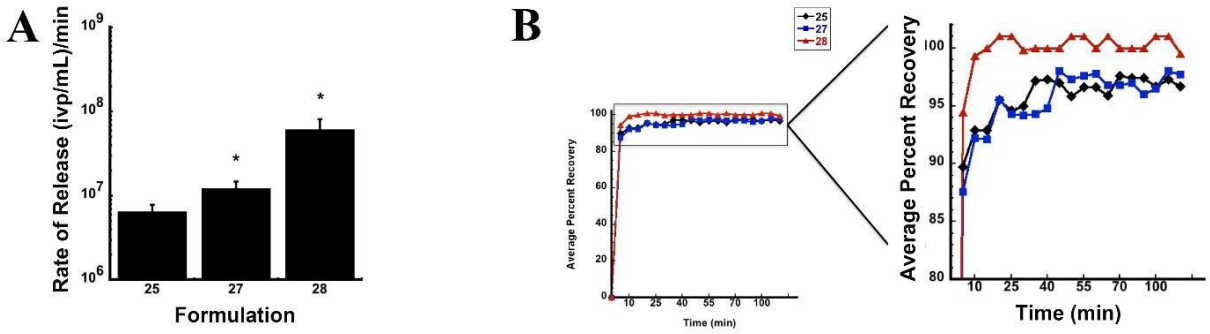

Figure 2.3: Release of Virus from the Film Matrix is Tunable.

(**A**) Virus Release Rate from Films Prepared by Stepwise Addition of Excipients. Films containing 1.25×10^{12} v.p. were placed in warmed (37 °C) PBS with gentle agitation and samples collected over a period of 2 hours. The concentration of infectious virus was determined by a standard infectious titer assay. (**B**) Cumulative Release Profiles of Films Containing Base, Binder and Surfactant Combinations. Data collected during the dissolution of each film was normalized with that generated from virus placed in the correlating liquid formulation and collected over 20 minute intervals to account for any loss attributable to agitation and extended exposure to heat. In each panel, data represents the average $\pm$ the standard deviation of a minimum of three films per condition. *$p < 0.05$, two-tailed Student's t test. Formulations are summarized in the figure according to the numbers assigned in Table 2.1.

2.3.3 Mechanical Properties of Films

During the screening process, the mechanical properties of each film formulation were also assessed as the ductility of a film not only dictates the feasibility of production but also the ease at which it can be handled and manipulated (34). Varying the amount of base, binder and surfactant did not significantly impact the measured elongation of any of the films when a uniform force was applied to them (Figure 2.4). Evaluation of young's modulus of films revealed that glycerol was the only excipient that significantly altered the mechanical properties of the films, making them prone to tearing (Figure 2.5). Thus, due to the difficulty in processing and handling films containing glycerol, sorbitol was selected as the most optimal binder to be utilized for the remainder of the studies summarized in this manuscript. Since the surfactant further improved recovery of virus from the film, a short-term stability study was developed with Formulation 27 and 28.

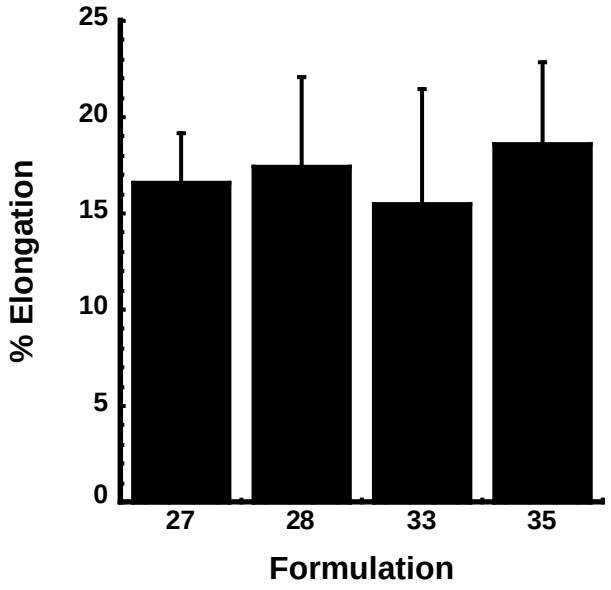

Figure 2.4: Complexity of a Formulation Does Not Significantly Impact Elongation of Thin Films.

Films were prepared under aseptic conditions. and evaluated for their respective mechanical properties using a Texture Analyzer AR G2 instrument. Elongation values were determined directly from the tension versus elongation curve at break. Data represents the average $\pm$ the standard deviation of three films per formulation. Formulations are referenced according to the numbers listed in Table 2.1.

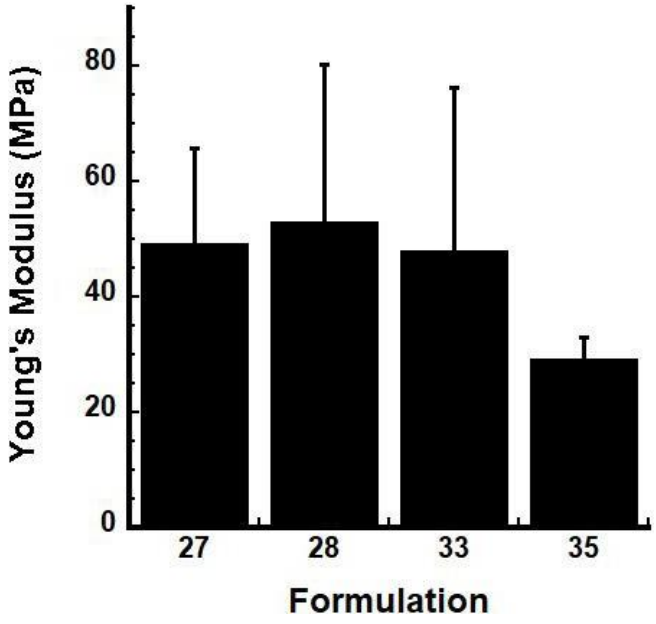

Figure 2.5: Young's Modulus of Thin Films is Influenced by Certain Excipient Combinations.

Films (n=3 per formulation) were prepared under aseptic conditions and evaluated for their respective mechanical properties using a Texture Analyzer AR G2 instrument. Values were calculated for each film using the Young's Modulus equation. Data represents the average $\pm$ the standard deviation of three films per formulation. Formulations are referenced according to the numbers listed in Table 2.1.

2.3.4 Impact of Rehydration Medium on Recovery of Virus Infectivity from Films

Solutions prepared from solubilized films have the potential to be utilized for administration of vaccines and other biologicals by various routes which may dictate the nature of the solvent utilized for rehydration. After the initial screening studies were complete, a small pilot study was initiated to determine if certain solvents, commonly utilized for reconstitution of drug products would be compatible with the film platform. Solvents evaluated were: sterile water for injection (WFI), sterile saline, 100 mM phosphate buffered saline (pH 7.4) and 10 mM Tris buffer (pH 8.1). Cell culture media (DMEM containing 2% FBS) was utilized as a control solvent for comparison. Statistical analysis revealed that there was no significant difference between the recovery of infectious virus with respect to solvent utilized for reconstitution in films prepared with the same formulation and that contained the same amount of virus prior to drying (Figure 2.6). Assessment of film formulations prior to drying revealed that reducing the amount of base excipient with subsequent addition of binder and surfactant significantly reduced the viscosity of each preparation (Figure 2.7). When virus was added, the viscosity of each liquid film formulations fell to half of its initial value. Viscosities of solutions made from reconstituted films were also significantly less than those made prior to drying. Because the film platform can be utilized for a variety of applications, the volume of diluent can be altered to support different routes of administration or to concentrate the virus. Reducing the reconstitution volume by half increased solution viscosity fourfold.

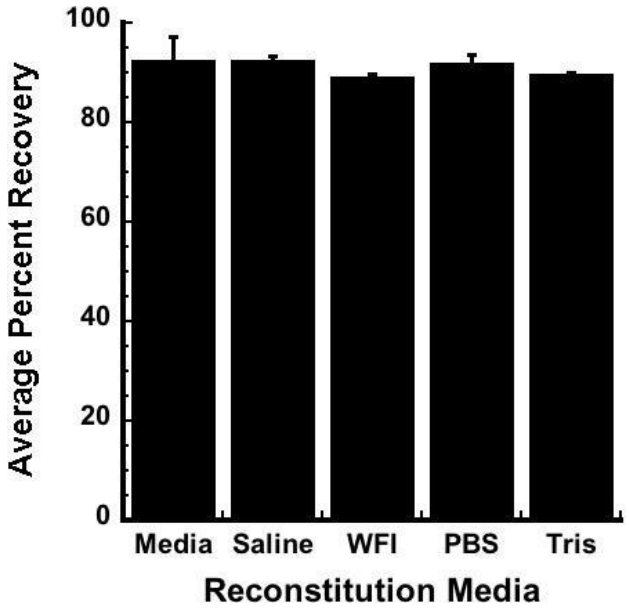

Figure 2.6: Viable Adenovirus Can be Recovered from Films Reconstituted with a Variety of Diluents.

Films containing 1.25×10^{12} adenovirus particles suspended in Formulation 28 were prepared in batch under aseptic conditions. Replicates of three films were reconstituted with the following solutions once drying was complete: DMEM supplemented with 2% FBS (Media), Sterile saline (0.9% NaCl), sterile water for injection (WFI), 100 mM phosphate buffered saline (PBS, pH 7.4) and 10 mM Tris buffer, pH 8.0. Data represents the average $\pm$ the standard deviation. A two-tailed Student's t-test was utilized to determine the lack of significant difference in infectious titer of virus in each reconstituted film ($p > 0.05$).

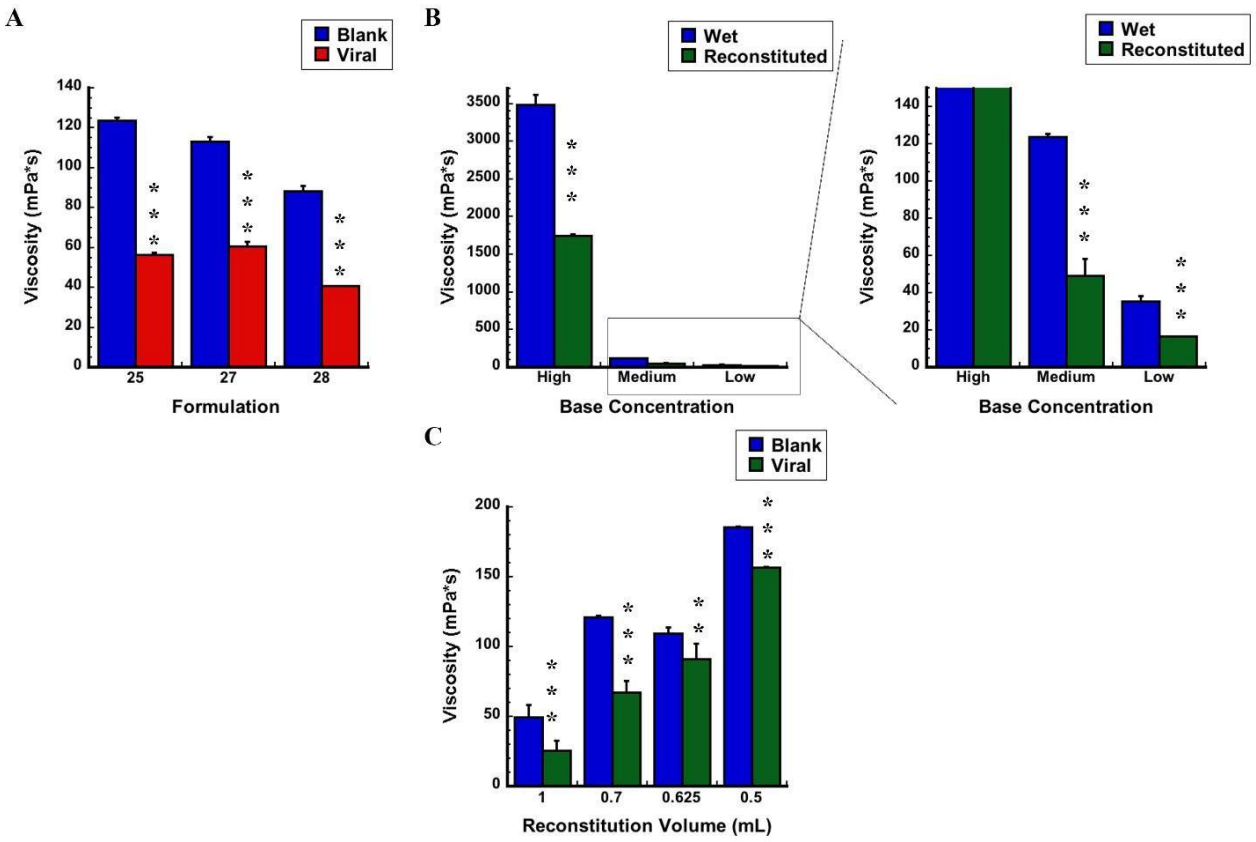

Figure 2.7: Virus, Excipients and Solvent Volume Significantly Impact Viscosity of Solutions Made from Reconstituted Films.

(A) Stepwise addition of excipients reduces formulation viscosity (blue bars). Addition of 1.25 × 10^{12} adenovirus particles to each respective formulation reduced viscosity further (red bars). (B) Base excipient significantly contributes to formulation viscosity (blue bars). Rehydration of films prepared with 1mL of formulation with an equivalent volume of sterile water produces a solution with a viscosity that is notably less than the original solution (green bars). (**C**) Rehydration of films in a volume less than the original formulation volume increases viscosity of solution. Films made with 1 mL of Formulation 28 with (green bars) and without (Blank, blue bars) virus were reconstituted with the same and reduced volumes of sterile water upon drying. In each panel, data represents the average ± the standard deviation of a minimum of three

films/solutions per condition. **p < 0.01, ***p < 0.001, two-tailed Student's t test. Formulations are summarized according to the numbers listed in Table 2.1.

2.3.5 Stability of Adenovirus in an Optimized Film Formulation

The durability of virus stabilized in the optimized film formulation was evaluated by placing films containing 1.25×10^{12} virus particles (v.p.) in a temperature-controlled chamber set at 37 °C. Infectious titer was then evaluated in films reconstituted with sterile media at set timepoints for 14 days (Figure 2.8A). Virus at the same concentration was also stored under the same conditions in a traditional standard liquid formulation (100 mM PBS, pH 7.0, 10% v/v glycerol, Control A) commonly utilized to compare novel formulations (35, 36) and titer assessed over time for comparison. The amount of infectious virus recovered from films stored at 37 °C was ~ 97 $\pm$ 2.6% of the original titer throughout the 14 day study period. Infectious virus could not be detected in the Control A preparation within 24 hours and for the remainder of the study. A longer evaluation of virus stability revealed that films could maintain 100 $\pm$ 2.2 % of their original titer for 84 days at 4 °C (Figure 2.8B). This was in stark contrast to preparations containing the same amount of virus in phosphate buffered saline alone (Control B formulation) in which recovery fell to 67 $\pm$ 0.85 % of its original titer after 25 days at 4 °C. Infectious virus could not be detected in either of the control formulations after 48 days at 4 °C.

In order to determine the role the surfactant played in virus stability, films containing 1.25×10^{12} v.p. were prepared and stored at 20 °C. Infectious titer was compared over time to preparations stored in the same manner containing the same amount of virus in liquid Control A and Control B formulations (Figure 2.8C). All preparations retained full recovery of infectious virus during the first 7 days of storage except for films that did not contain surfactant (92 $\pm$

4.1%). Films containing surfactant did not experience a significant drop in virus infectivity throughout the study period. These films contained 100 $\pm$ 0.14% of their original titer after storage for 84 days at 20 °C. Infectious virus could not be detected in either of the control formulations or in films without surfactant at the 84 day timepoint.

The robust stability profile of films containing surfactant stimulated further evaluation of the ability of this preparation to protect virus under different environmental stressors. Films prepared with and without surfactant were exposed to a series of 16 freeze-thaw cycles by freezing samples at -80 °C and then thawing them to 20 °C. Replicate films were collected at different intervals, rehydrated and infectious titer compared with liquid formulations containing PBS and 10% glycerol (Control A) or PBS alone (Control B) that underwent the same freeze-thaw schedule. By the fourth freeze-thaw cycle, infectious titer of virus formulated in PBS alone fell to 83 $\pm$ 0.4% while all other preparations retained more than 95% of their original titer (Figure 2.8D). Infectious virus could not be detected the Control B formulation by the eighth freeze-thaw cycle while 91 $\pm$ 0.08% of the original titer was detected in the Control A preparation. By the sixteenth freeze-thaw cycle, the infectious titer of films prepared without surfactant fell to 94 $\pm$ 0.5% of their original titer while those containing surfactant did not demonstrate a notable drop in titer (100 $\pm$ 0.7% recovery) after completing the entire freeze-thaw series.

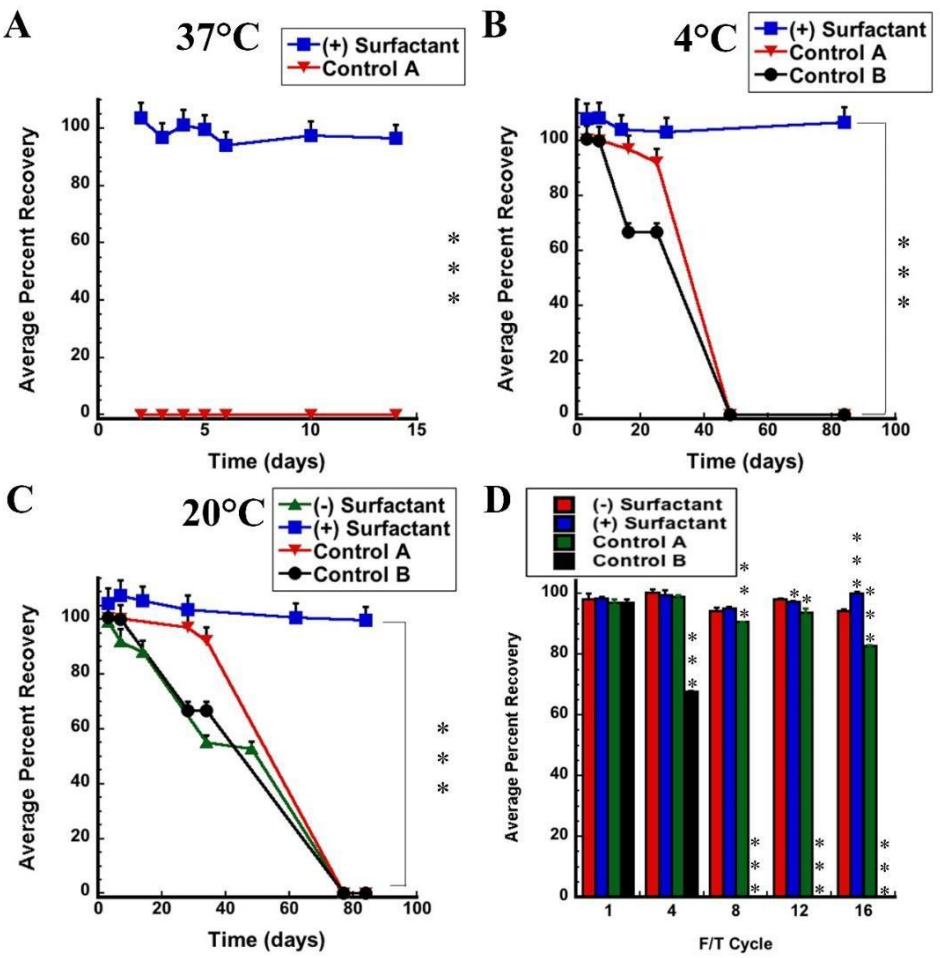

Figure 2.8: Optimized Thin Film Matrix Enhances Adenovirus Stability at Ambient Temperatures and Under Environmental Stressor Conditions.

Films containing 1.25×10^{12} v.p. were prepared in batch and either stored in controlled environmental chambers held at 37 °C (**A**), 4 °C (**B**) and 20 °C (**C**) for 84 days or subjected to a series of 16 freeze-thaw cycles (**D**). Replicates (at least 3 per timepoint) were reconstituted and live virus concentration assessed by a standard infectious titer assay (19). Virus was placed at the same concentration in two standard liquid formulations and infectious titer under each storage condition also assessed for comparison. In each panel, Control A formulation consisted of 100 mM phosphate buffered saline (pH 7.4) and 10% glycerol and Control B formulation consisted of 100 mM phosphate buffered saline alone. In each panel, data represents the average

± the standard deviation. *p < 0.05, ***p < 0.001, two-tailed Student's t test. Formulations are summarized in the figure according to the numbers listed in Table 2.1.

2.3.6 Stability of Adenovirus in Rehydrated Films

Solutions prepared from films could be utilized for a variety of applications such as nasal, oral or ocular delivery of biologicals. Thus, the physical stability of virus in rehydrated films prepared with and without surfactant was assessed at 4 and 20 °C for a period of 84 days. Infectious titer was assessed over time and compared to virus prepared at the same concentration in Control A and B formulations. Infectious titer of all preparations remained at 97% of the original concentration or higher after 14 days at 4 °C except the Control B preparation which fell to 67 ± 1.3% of the original titer and remained at this level through the 25 day timepoint (Figure 2.9A). Infectious virus could not be detected in either control formulation after the 48 day timepoint. In sharp contrast, rehydrated films containing surfactant retained 100 ± 0.6% of their original titer while those without surfactant retained 93 ± 2.0% infectivity at the 84 day timepoint.

The infectious titer of virus stored in control buffer A fell to 89 ± 0.06% of the original titer when stored at 20 °C for 14 days and to 67 ± 4.0% by day 42 (Figure 2.9B). Infectious virus could no longer be detected in the control B preparation after 25 days at room temperature. Rehydrated films that did not contain surfactant retained 95 ± 0.53% of their original infectious virus concentration for 84 days at 20 °C while those containing surfactant did not demonstrate a notable loss of viral titer (100 ± 0.53% recovery) throughout the entire study period. A final series of studies designed to identify the limits at which this formulation stabilized live virus was

conducted at 40 and 50 °C, temperatures that can potentially be reached in cargo compartments during transportation and in the heat of many developing countries (37).

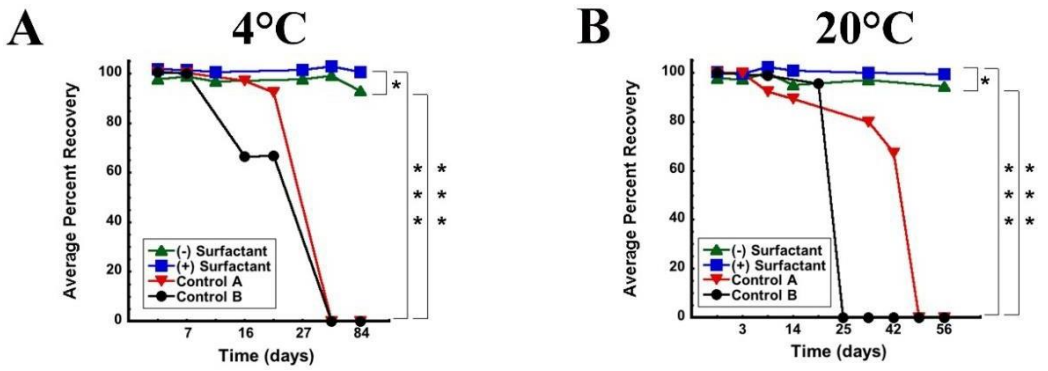

Figure 2.9: Adenovirus Stability Profiles of Liquid Film Formulations During Long Term Storage.

Virus (1.25×10^{12} v.p.) was placed in Formulation 27 and 28 and stored in the liquid form in controlled environmental chambers held at 4 °C (**A**) and 20 °C (**B**) for 84 days. Replicate samples (n= 3) were collected at each timepoint and live virus concentration assessed by a standard infectious titer assay (19). Virus at the same concentration was also placed in two standard liquid formulations and infectious titers under each storage condition also assessed for comparison. Control A formulation consisted of 100 mM phosphate buffered saline (pH 7.4) and 10% glycerol. Control B formulation consisted of 100 mM phosphate buffered saline alone. In each panel, data represents the average $\pm$ the standard deviation. *$p < 0.05$, ***$p < 0.001$, two-tailed Student's t test.

At 40 °C, liquid formulations containing surfactant maintained 91+ 0.95% of their original titer for 5 days, while formulations without surfactant fell to 82 + 1.6% of their original concentration within 3 days (Figure 2.10A and B). Infectious virus could no longer be detected

in control formulations after 24 hours at 40°C. Recovery of infectious virus from the film matrix was significantly impacted at temperatures above 37 °C as films containing surfactant displayed 74± 0.98% of their original titer after 5 days at 40°C and 73± 1.3% of their original titer after 2 days at 50°C (Figure 2.10 C and D). During these studies, environmental monitors indicated that relative humidity significantly fell below 25% when temperature was increased to 50°C. This prompted a pilot study to determine how humidity impacts stability of virus in the film matrix during accelerated stability studies. When samples were stored at 40°C and relative humidity reduced to levels at and below what was observed for the 50°C study, virus titer was reduced by 88% after 3 days under these conditions (Figure 2.11). Additional studies involving assessment of humidity and various packaging systems on viral stability in the film matrix are currently underway.

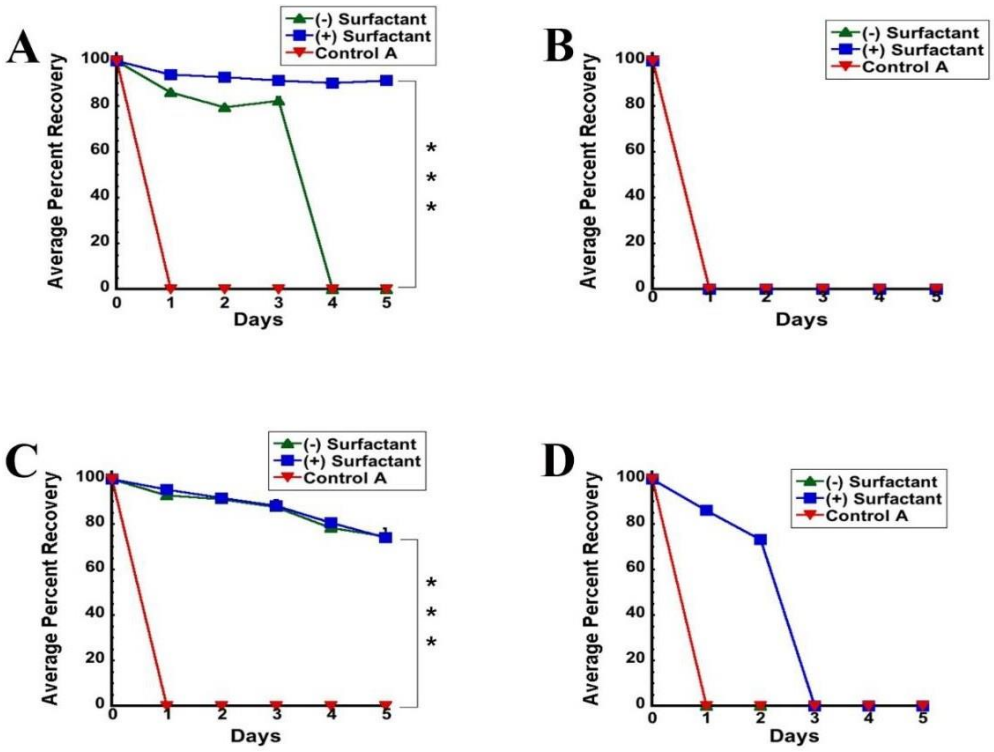

Figure 2.10: Adenovirus Stability Profiles of Rehydrated and Solid Films at Elevated Temperatures.

Virus (1.25×10^{12} v.p.) was placed in Formulation 27 and 28 and stored in the liquid form at 40 (**A**) and 50°C (**B**) and in the solid (film) form at 40 (**C**) and 50°C (**D**) for five days. Replicate samples (n=3) collected at each timepoint and live virus concentration assessed by a standard infectious titer assay (19). Virus was placed at the same concentration in one standard liquid formulation (Control A, 100 mM phosphate buffered saline (pH 7.4) and 10% glycerol) and infectious titers under each storage condition also assessed for comparison. In each panel, data represents the average $\pm$ the standard deviation. *$p < 0.05$, ***$p < 0.001$, two-tailed Student's t test.

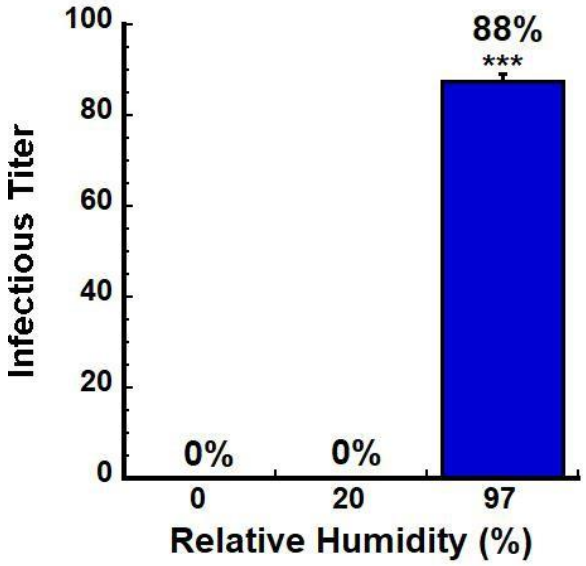

Figure 2.11: Recovery of Live Adenovirus from the Film Matrix at Elevated Temperature is Significantly Impacted by Environmental Humidity.

Virus (1.25×10^{12}) was placed in Formulation 28 and stored in solid (film) form at 40°C for three days at 0, 20, and 97% Relative humidity. Replicate samples (n= 3) were collected at each timepoint and live virus concentration assessed by a standard infectious titer assay (19). In each panel, data represents the average $\pm$ the standard deviation. *$p < 0.05$, ***$p < 0.001$, two-tailed Student's t test.

2.3.7 Physical Characterization of Thin Films

Visualization of films by scanning electron microscopy (SEM) revealed that the surface of those prepared with the base formulation were porous and contained small pockets of varying size throughout the three-dimensional matrix (Figure 2.12 A-C). When films containing virus were dried in the optimized formulation containing sorbitol and surfactant, the surface of the film assumed a glassy state in which virus particles were evenly suspended (Figure 2.12D, arrows).

Differential Scanning Calorimetry (DSC) was used to analyze samples in a step-wise fashion to evaluate the amorphous quality of films (Figure 2.13). The absence of an observable endotherm in each scan indicates that none of the film components melt at temperatures below 150 °C. The glass transition temperature (Tg') of films prepared with base formulation alone was 148.5 °C. Addition of sorbitol to the base did not significantly impact Tg' (148.4 °C) while addition of surfactant to the base and binder fostered a slight shift in Tg' (146.5 °C). The optimized film formulation containing virus had an Tg' of 149.7 °C which correlated with the SEM image of a glassy surface when drying was complete. The results obtained from SEM and DSC were further supported by wide angle X ray diffraction patterns (Figure 2.14). Individual components of the film, most notably sorbitol, were crystalline substances in the dry state and contained diffraction peaks of varying intensity (Figure 2.14A). However, films made with the optimized combination of base, sorbitol and surfactant exhibited a single broad peak of relatively low intensity, characteristic of amorphous compounds (Figure 2.14D). Inclusion of virus in the optimized film platform did not disrupt the amorphous state of the final product (Figure 2.14E).

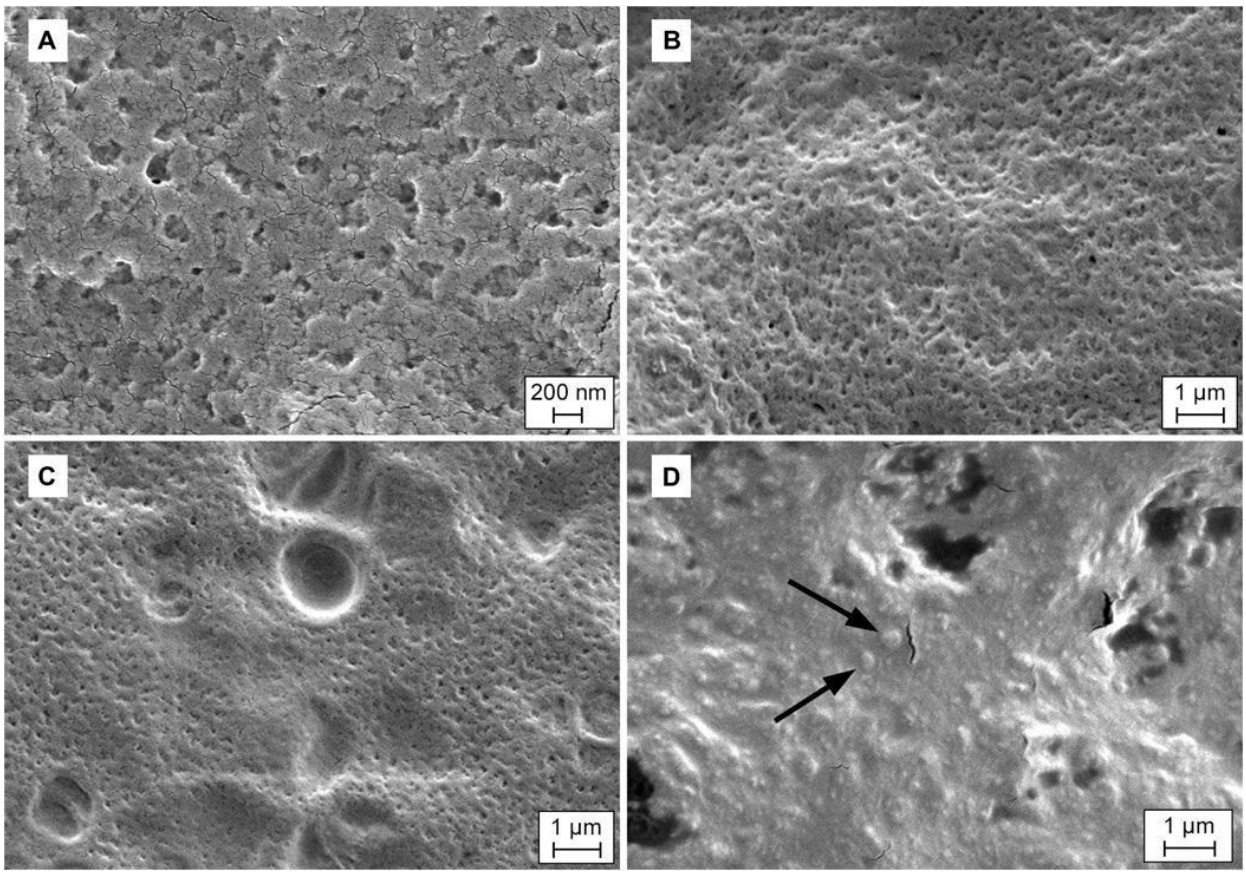

Figure 2.12: Excipient Combinations Transform Porous Film Base into an Amorphous Solid.

(**A)** Scanning electron micrograph of porous surface of thin film consisting only of base excipient (Formulation 25, Table 2.1). (**B**) Surface of two component film (Formulation 14) in the absence of virus. (**C**) Large non-crystalline pockets in film (Formulation 27) which foster stabilization of virus particles. (**D**) Adenovirus particles (arrows) suspended in amorphous film matrix of optimized Formulation 28. Perforations in film surface are artifacts from extended electron bombardment on the surface of the thin film.

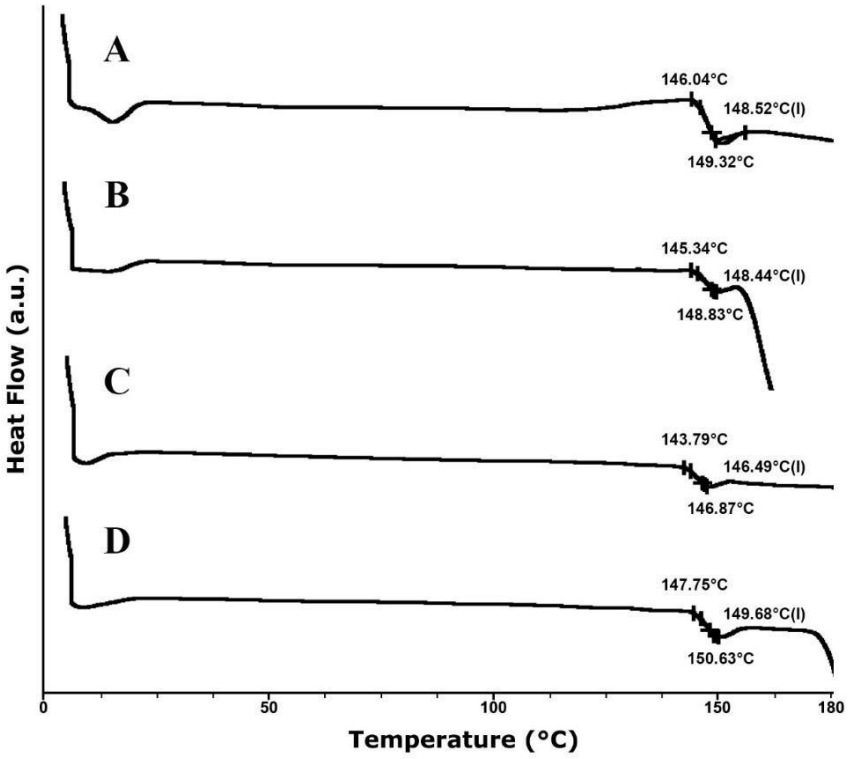

Figure 2.13: DSC Analysis Reveals that Thin Films are Amorphous Solids Across a Wide Temperature Range.

Differential scanning calorimetry profiles taken after sequential addition of excipients to the optimized thin film matrix. (**A**) Base alone (Formulation 25), (**B**) Base and Sorbitol (Formulation 27), (**C**) Optimized formulation (Formulation 28) in the absence of virus and (**D**) containing virus.

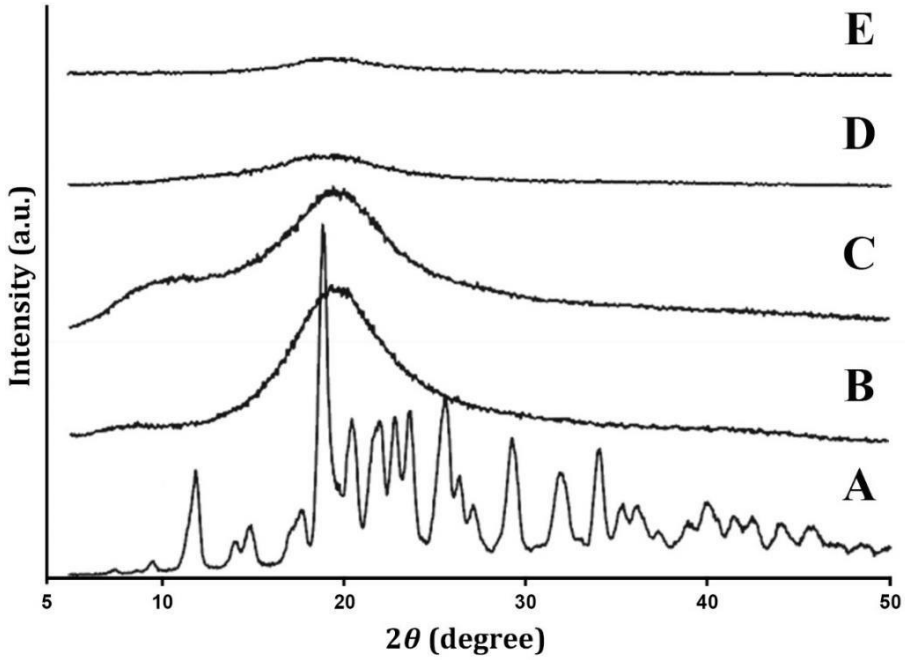

Figure 2.14: X-Ray Scanning Diffraction Reveals Films as Amorphous Solids.
Wide angle diffraction patterns of different components in the optimized thin film matrix. Scans of excipients: (**A**) sorbitol, (**B**) surfactant, (**C**) base as individual dry solids were used as crystallinity references for the composite optimized film (Formulation 28) with (**E**) and without (**D**) virus.

Fourier Transform Infrared (FTIR) spectroscopy was used to identify bond interactions between each of the components of the optimized film and the adenovirus. The most pronounced change in spectra in films prepared with and without virus was found for nitrogen-hydrogen bonds at the wavenumber 3300 (Figure 2.15). Absorbance at this wavelength increased twofold when virus was added to base formulation alone. A similar trend was noted when virus was added to formulation containing base and sorbitol. No significant difference in

absorbance was noted at this wavelength when virus was added to the optimized film formulation, possibly indicating that direct binding of virus particles to the surfactant may be a key factor for stabilization in our optimized thin film matrix.

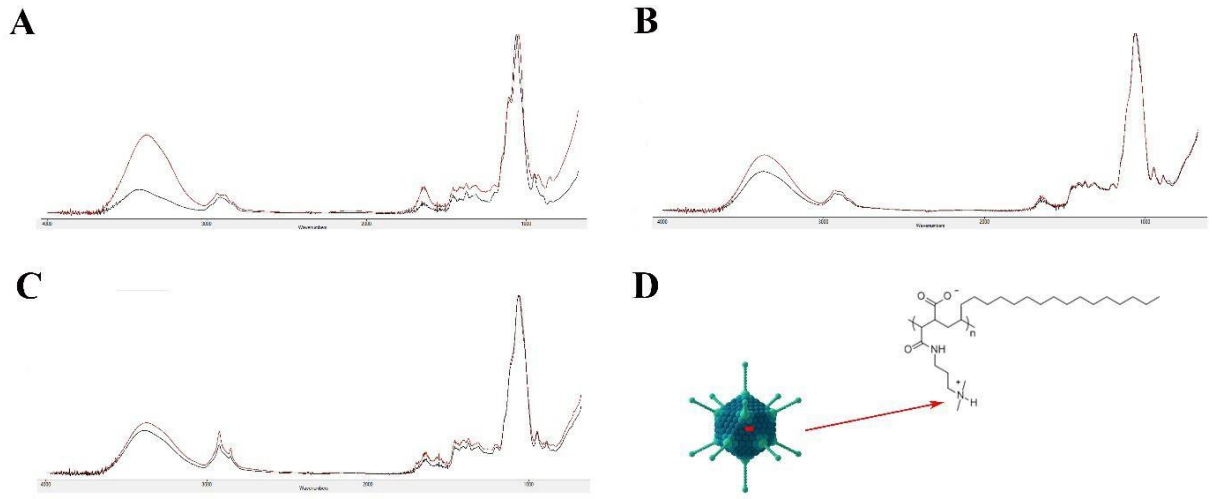

Figure 2.15: Fourier-Transform Infrared (FTIR) Spectroscopy Scans Suggest that Nitrogen-Hydrogen Bonds between Virus and Surfactant May be Key for Stabilization in Thin Film Matrix.

IR absorption spectra in the 4000–800 cm^{-1} region for films containing (**A**) base alone (Formulation 25), (**B**) base and sorbitol (Formulation 27) and (**C**) optimized Formulation 28. In each panel, black traces represent film in the absence of adenovirus. Red traces represent film containing 1.25×10^{12} particles of adenovirus. Panel **D** illustrates the proposed interaction between the cationic region of the surfactant and the negatively charged glutamic acid residues of the adenovirus hexon proteins. Virus image adapted from: Splettstoesser, T. A simplified 3D-generated structure of the adenovirus. Wikimedia Commons accessed 5 March, 2019; Available from: https://commons.wikimedia.org/wiki/File:Adenovirus_3D_schematic.png

2.4 Discussion

In a recent publication, Kristensen et al., in collaboration with the Expanded Program on Immunization, surveyed 158 managers of immunization campaigns in low- and middle- income countries to identify characteristics of vaccines they believed would suit logistical and infrastructure challenges faced within their countries (39). Respondents valued characteristics that prevent heat damage, vaccine wastage and simplified vaccine delivery. The novel platform described here meets the majority of these needs. With respect to heat stability, we have shown that a recombinant adenovirus-based vaccine can be stored at ambient temperature for a significant period of time, which is quite noteworthy (Figure 2.1C). One configuration of the film can accommodate a single dose of vaccine (Figure 2.1A) and is significantly space saving as we have estimated that 350,000 doses of the current BCG (10/20) vaccine, when incorporated in our film, would hold the space of 600 8.5 × 11 inch sheets and weigh ~3 kg, while the same number of vaccine doses in the current platform and packaging (vial + ampule of diluent) would require space a little larger than an American football field (5,749 m^2) for storage and weigh 2,730 kg (40). This platform may also offer additional space saving capability by accommodating more than one antigen as we have also demonstrated that we can also effectively stabilize live bacteria, antibodies, and enzymes at ambient temperatures in the film matrix (Figure 2.1 D-F). While pivotal studies investigating the amount of antigen that can be effectively loaded in a single use film are ongoing, we have shown that our process is capable of providing an even distribution of virus throughout films (Figure 2.16), the amount of virus embedded in a film does not impact recovery upon reconstitution, and that there is a direct correlation ($r^2 = 0.994$, Figure 2.17) between the amount of virus added to and recovered from our optimized film matrix, indicating that vaccines and other biologicals can be stabilized in

large sheets that can be divided into various sizes/doses or single unit dose films that contain a defined amount of antigen.

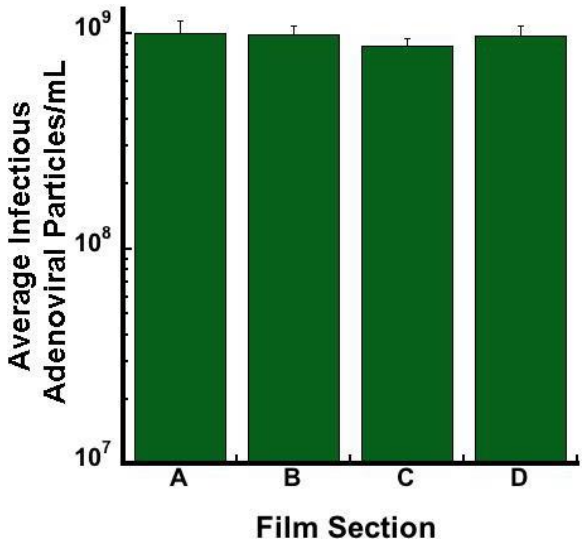

Figure 2.16: Virus is Evenly Distributed Throughout the Film Matrix.

Replicate films made with 1 milliliter of Formulation 28 containing 1.25×10^{12} adenovirus particles were prepared under aseptic conditions. Films were cut into 4 quadrants and each reconstituted with 250 microliters of sterile water for injection. Infectious titer of each rehydrated film was determined using a standard infectious titer assay (19). Data represents the average $\pm$ the standard deviation of a minimum of six films per section. A two-tailed Student's t test was utilized to determine the lack of significance difference in infectious titer of virus in each reconstituted film ($p > 0.05$).

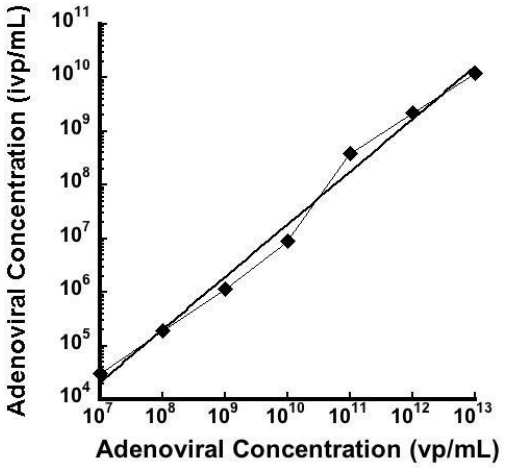

Figure 2.17: The Amount of Virus Embedded in Film Matrix Does Not Impact Recovery of Virus from the Film Matrix.

Physical adenovirus particles (v.p./ml, x axis) were incorporated in thin films prepared with Formulation 28 in concentrations ranging from those obtained immediately after purification (1×10^{13}, 1×10^{12}) to those which reflect reasonable doses for immunization and therapeutic purposes (1×10^{12} - 1×10^{7}). Films were reconstituted immediately upon drying and corresponding infectious titers (y axis) found for each virus concentration, indicating that films can be scaled up or down for manufacturing purposes. Data represents the average $\pm$ the standard deviation of a minimum of six films per concentration.

Thirteen of the current WHO recommended vaccines are distributed as solid products, primarily as lyophilized powders (22, 28). While this method of stabilization has significantly extended the shelf life of vaccines, it remains limited by high production costs necessary to acquire specialized equipment, long processing times of more than 48 hours in some cases and susceptibility of vaccine candidates to the process stressors of freezing and drying (45). Thus,

there is a growing demand in the pharmaceutical and other industries for novel technologies that stabilize proteins and other biologicals through a non-thermal approach (46). While films for oral use are a relatively new dosage form, there are currently 13 approved products available in the U.S. and Europe, which contain small molecules for over the counter use (47). Standard methods for manufacturing films also require the use of specialized equipment for hot melt extrusion or thermal printing and involve use of volatile solvents to accelerate drying (48), which can significantly compromise the integrity of live organisms and other antigens and the subsequent potency of a vaccine. With the intent to develop technology that would be easily transferrable to facilities in resource poor countries, our approach is different in that we identified combinations of excipients that could effectively stabilize a live virus during the film forming process at ambient temperatures, under aseptic conditions in the absence of heat and other external stressors without using highly technical equipment and a drying process which was complete within a single working day. This also holds promise for outbreak and pandemic scenarios as it offers a means for minimizing bottlenecks for production and distribution of large volumes of vaccines and biologicals and, as we have shown here, is flexible for adaptation to different types of products.

In the Kristensen study, resistance to freezing was one of the top 10 features of an ideal vaccine (39). Loss of vaccine potency to freezing is a serious threat to global health as one study noted that, in low-income countries, vaccines were more likely to be exposed to temperatures below recommended ranges during storage while vaccines were more likely to be exposed to freezing temperatures during transit in higher income countries (49). Our optimized thin film matrix successfully protected the adenovirus from disruption during thermocycling for a series of 16 freeze-thaw cycles (Figure 2.8). This is a significant finding as the most promising

formulations described in the literature to date are liquid preparations capable of protecting the virus from 5 and 12 cycles respectively (50, 51). It also suggests that this optimal combination of excipients suspended the virus in a matrix capable of protecting it from a series of environmental stressors. One of the most interesting findings summarized here is the impact that environmental humidity has on adenovirus stability in our film matrix at a given temperature (Figure 2.11). Relative humidity (12) has been reported to affect the stability of a variety of viruses by controlling the amount of water retained, the concentration of solutes, and its pH within the microenvironment of aerosol droplets with some viruses (like the adenovirus) stable in high humidity environments (80% RH) and others (for example influenza) stable at lower humidities (20% RH) (52). While the studies outlined in this manuscript identified a formulation that provides a favorable microenvironment for the adenovirus within the film at certain temperatures and RH environments above 60%, it failed to do so when the RH fell below 25%. Films utilized for each of the stability studies summarized here were packaged in particle free resealable plastic bags under aseptic conditions. Alternative packaging systems that can maintain a favorable internal humidity level when stored in low humidity environments are currently under evaluation in our laboratory to address this important issue. Guidelines set by both the World Health Organization and the International Conference on Harmonization (ICH) specify that long term and accelerated stability studies be conducted at temperatures ranging from 25-40 °C and at 60-75% relative humidity and are relevant for both hot and dry and hot and humid climates (53). Our results suggest that stability data collected from biological preparations stored in low humidity environments might provide results different than those performed according to WHO/ICH guidelines and, if implemented routinely, could significantly improve product stability as they may encounter RH environments as low as 10% in homes and

distribution centers around the globe on a seasonal basis (54) and during transit in arid climates when RH of 10-30% are experienced during daylight hours (55). Additional accelerated stability studies at RH below 25% are also underway with a panel of different viruses in our film matrix and is the subject of an upcoming manuscript.

One of the pivotal findings of this study was the correlation of pH within the film matrix with virus recovery upon drying and with long term stability (Figure 2.2). This principle was previously established within the pH range of 6-8 for recombinant adenovirus-based products prepared in solid and liquid dosage forms (19, 56) and suggests virus degradation within the film matrix may also be pH-mediated. None of the aqueous solvents evaluated in our study were capable of fully maintaining the original pH of the formulation during the film forming process. This was probably due to loss of original pH of the preparation due to concentration of buffering agents and their interaction with other components of the formulation in a manner that prevented them from maintaining pH during the vitrification process (57). One of the prime constituents of successful formulations identified in these studies was the base excipient. A polymer, capable of forming strong intramolecular hydrogen bonds (58), it played a key role in maintaining structural confirmation of the virus capsid. This was evident during the rate of release studies, as films containing this excipient alone failed to completely release the entire dose of virus originally loaded in the film (Figure 2.3). It is also important to note that this excipient significantly enhanced the viscosity of each preparation in the liquid state (Figure 2.7), suggesting that its ability to minimize molecular motility both in the solid and liquid formulations was also key to maintaining long term stability at ambient temperatures.

Sorbitol and glycerol, predominately used in film formulations as plasticizers (59), impacted virus stability in the film matrix very differently. Preparations containing glycerol took

longer to dry, indicating that this reagent had a high a higher capacity for retaining water within the film matrix. We suggest that sorbitol more efficiently contributed to the development of the three-dimensional matrix of the film through strong interactions with the other excipients, replacing their interactions with water, thus accelerating the drying process and leaving the virus suspended in the highly vitreous, yet flexible matrix of the film. The amorphous nature of the film was first visualized by electron microscopy (Figure 2.12) and further confirmed by X-ray diffraction (Figure 2.14). Calorimetric assessment of the optimized film matrix indicates that it has a glass transition temperature above 140 °C, suggesting that at the at each of the temperatures utilized in the assessment of adenovirus stability, none of the excipients were susceptible to crystallization which could compromise the adenovirus capsid and facilitate precipitation of buffer components and other excipients, allowing the virus to remain stably suspended in an amorphous polymer matrix during long term storage. We have shown previously that addition of a zwitterionic surfactant to our preparations at the concentration used here significantly improves the potency of an adenovirus-based Ebola vaccine (29, 30) and attributed it to the fact that it is capable of significantly reducing the energy barrier for the virus to cross the lipid bilayer of the cell membrane (60). Here, we show that it is paramount for conferring stability of virus in the film matrix and rehydrated films when stored at ambient and elevated temperatures (Figures 2.8, 2.9, 2.10). FTIR analysis revealed that complete incorporation of adenovirus only occurred when this excipient was present, as there was no notable change in peak location or absorbance intensity, suggesting that integrity of the virus capsid was maintained through interaction of the positively charged amine group on the surfactant with the negatively charged glutamic acid residues located on the adenovirus hexon protein (61). Despite this, rate of release studies indicate that the presence of the surfactant was

key in achieving rapid and complete release of an infectious dose of virus from the film (Figure 2.3). We envision a model in which the size of the surfactant, incorporated within the amorphous network formed by it and the other excipients of the optimized formulation facilitated rapid hydration of the film and subsequent release of virus through a series of hydrophobic and hydrophilic interactions. Additional mechanistic studies are currently underway to evaluate the strength of the virus-surfactant interaction in both the liquid and solid states and to determine if it also is necessary for stabilization of other viruses within the film matrix.

This report is the first to identify essential parameters for effective stabilization of a live virus in a thin film matrix prepared in aqueous formulations under ambient conditions. We believe these findings will serve as the basis for accelerated design of strategies for thermostabilization of other biologicals like therapeutic antibodies and enzymes in a similar dosage form. The platform described here that effectively stabilizes adenovirus at ambient and elevated temperatures, and releases virus efficiently is notably distinct from all other vaccine platforms described to date. This approach, designed with developing countries in mind, holds great promise to enhance global access to vaccines and other biological medicines by reducing costs associated with their production, distribution and supply chain maintenance. The impact of this is significant given that the World Health Organization (22) estimates that nearly 50% of lyophilized (freeze-dried) and 25% of liquid vaccines are discarded each year due to disruption of the cold chain (21).

2.5 References

1. B. Greenwood, The contribution of vaccination to global health: past, present and future. *Philos Trans R Soc Lond B Biol Sci* **369**, 20130433-20130433 (2014).
2. D. S. Jones, S. H. Podolsky, J. A. Greene, The Burden of Disease and the Changing Task of Medicine. *New England Journal of Medicine* **366**, 2333-2338 (2012).

3. World Health Organization. The top 10 causes of death: Leading causes of death by economy income group. (2018).
4. K. Hardt *et al.*, Vaccine strategies: Optimising outcomes. *Vaccine* **34**, 6691-6699 (2016).
5. A. B. Hill, C. Kilgore, M. McGlynn, C. H. Jones, Improving global vaccine accessibility. *Current Opinion in Biotechnology* **42**, 67-73 (2016).
6. R. J. Carter *et al.*, Implementing a Multisite Clinical Trial in the Midst of an Ebola Outbreak: Lessons Learned From the Sierra Leone Trial to Introduce a Vaccine Against Ebola. *J Infect Dis* **217**, S16-S23 (2018).
7. D. Schopper *et al.*, Research Ethics Governance in Times of Ebola. *Public Health Ethics* **10**, 49-61 (2017).
8. R. Shaker, D. Fayad, G. Dbaibo, Challenges and opportunities for meningococcal vaccination in the developing world. *Hum Vaccin Immunother* **14**, 1084-1097 (2018).
9. Jacqueline E. Tate, Anthony H. Burton, Cynthia Boschi-Pinto, U. D. Parashar, Global, Regional, and National Estimates of Rotavirus Mortality in Children <5 Years of Age, 2000–2013. *Clinical Infectious Disease* **62**, S96-S105 (2016).
10. S. Plotkin, J. M. Robinson, G. Cunningham, R. Iqbal, S. Larsen, The complexity and cost of vaccine manufacturing - An overview. *Vaccine* **35**, 4064-4071 (2017).
11. J. Lloyd, J. Cheyne, The origins of the vaccine cold chain and a glimpse of the future. *Vaccine* **35**, 2115-2120 (2017).
12. A. Portnoy *et al.*, Costs of vaccine programs across 94 low- and middle-income countries. *Vaccine* **33**, A99-A108 (2015).
13. D. R. Feikin, B. Flannery, M. J. Hamel, M. Stack, P. M. Hansen, in *Reproductive, Maternal, Newborn, and Child Health: Disease Control Priorities, Third Edition (Volume 2)*, R. E. Black, R. Laxminarayan, M. Temmerman, N. Walker, Eds. (The International Bank for Reconstruction and Development / The World Bank (c) 2016 International Bank for Reconstruction and Development / The World Bank., Washington (DC), 2016).
14. A. Ashok, M. Brison, Y. LeTallec, Improving cold chain systems: Challenges and solutions. *Vaccine* **35**, 2217-2223 (2017).
15. B. Adhikari *et al.*, Earthquakes, Fuel Crisis, Power Outages, and Health Care in Nepal: Implications for the Future. *Disaster Medicine and Public Health Preparedness* **11**, 625-632 (2017).
16. M. N. Yakum, J. Ateudjieu, F. R. Pélagie, E. A. Walter, P. Watcho, Factors associated with the exposure of vaccines to adverse temperature conditions: the case of North West region, Cameroon. *BMC Research Notes* **8**, 277 (2015).
17. T. Kitamura *et al.*, Assessment of temperatures in the vaccine cold chain in two provinces in Lao People's Democratic Republic: a cross-sectional pilot study. *BMC research notes* **11**, 261-261 (2018).
18. M. Y. Chan, T. S. Dutill, R. M. Kramer, Lyophilization of Adjuvanted Vaccines: Methods for Formulation of a Thermostable Freeze-Dried Product. *Vaccine Adjuvants: Methods and Protocols*, 215-226 (2017).
19. M. A. Croyle, X. Cheng, J. M. Wilson, Development of formulations that enhance physical stability of viral vectors for gene therapy. *Gene Therapy* **8**, 1281-1290 (2001).
20. F. M. C. Cardoso, D. Petrovajova, T. Hornakova, Viral vaccine stabilizers: status and trends. *Acta virologica* **61**, 231-239 (2017).

21. B. Y. Lee *et al.*, The impact of making vaccines thermostable in Niger's vaccine supply chain. *Vaccine* **30**, 5637-5643 (2012).
22. World Health Organization (WHO). (2018).
23. A. Shastay, Administering Just the Diluent or One of Two Vaccine Components Leaves Patients Unprotected. *Home Healthcare Now* **34**, 218-220 (2016).
24. C. Duttagupta, D. Bhattacharyya, P. Narayanan, S. M. Pattanshetty, Vaccine wastage at the level of service delivery: a cross-sectional study. *Public Health* **148**, 63-65 (2017).
25. A. K. Shakya, M. Y. E. Chowdhury, W. Tao, H. S. Gill, Mucosal vaccine delivery: Current state and a pediatric perspective. *J Control Release* **240**, 394-413 (2016).
26. R. W. Cross, C. E. Mire, H. Feldmann, T. W. Geisbert, Post-exposure treatments for Ebola and Marburg virus infections. *Nature Reviews Drug Discovery* **17**, 413-434 (2018).
27. K. Schulze *et al.*, in *How to Overcome the Antibiotic Crisis : Facts, Challenges, Technologies and Future Perspectives*, Marc Stadler, Petra Dersch, Eds. (Springer International Publishing, Cham, 2016), pp. 207-234.
28. World Health Organization, *International Travel and Health*. Chapter 6 Vaccine-Preventable Diseases and Vaccines (WHO Press, Geneva, Switzerland 2017).
29. J. H. Choi, S. C. Schafer, A. N. Freiberg, M. A. Croyle, Bolstering Components of the Immune Response Compromised by Prior Exposure to Adenovirus: Guided Formulation Development for a Nasal Ebola Vaccine. *Mol Pharm* **12**, 2697-2711 (2015).
30. J. H. Choi *et al.*, A Single Dose Respiratory Recombinant Adenovirus-Based Vaccine Provides Long-Term Protection for Non-Human Primates from Lethal Ebola Infection. *Mol Pharm* **12**, 2712-2731 (2015).
31. H. T. Le, Q.-C. Yu, J. M. Wilson, M. A. Croyle, Utility of PEGylated recombinant adeno-associated viruses for gene transfer. *Journal of Controlled Release* **108**, 161-177 (2005).
32. G. W. Radebaugh, J. L. Murtha, T. N. Julian, J. N. Bondi, Methods for evaluating the puncture and shear properties of pharmaceutical polymeric films. *International Journal of Pharmaceutics* **45**, 39-46 (1988).
33. J. C. Visser *et al.*, Quality by design approach for optimizing the formulation and physical properties of extemporaneously prepared orodispersible films. *International Journal of Pharmaceutics* **485**, 70-76 (2015).
34. M. Preis, K. Knop, J. Breitkreutz, Mechanical strength test for orodispersible and buccal films. *International Journal of Pharmaceutics* **461**, 22-29 (2014).
35. M. Pelliccia *et al.*, Additives for vaccine storage to improve thermal stability of adenoviruses from hours to months. *Nat Commun* **7**, 13520-13520 (2016).
36. M. A. Croyle, Q.-C. Yu, J. M. Wilson, Development of a Rapid Method for the PEGylation of Adenoviruses with Enhanced Transduction and Improved Stability under Harsh Storage Conditions. *Human Gene Therapy* **11**, 1713-1722 (2000).
37. S. Mercier, S. Villeneuve, M. Mondor, I. Uysal, Time–Temperature Management Along the Food Cold Chain: A Review of Recent Developments. *Comprehensive Reviews in Food Science and Food Safety* **16**, 647-667 (2017).
38. H. T. Rupniak *et al.*, Characteristics of four new human cell lines derived from squamous cell carcinomas of the head and neck. *Journal of the National Cancer Institute* **75**, 621-635 (1985).

39. D. D. Kristensen, K. Bartholomew, S. Villadiego, K. Lorenson, What vaccine product attributes do immunization program stakeholders value? Results from interviews in six low- and middle-income countries. *Vaccine* **34**, 6236-6242 (2016).
40. World Health Organization. (WHO Press, Geneva, Switzerland, 2017).
41. D. Liebowitz, J. D. Lindbloom, J. R. Brandl, S. J. Garg, S. N. Tucker, High titre neutralising antibodies to influenza after oral tablet immunisation: a phase 1, randomised, placebo-controlled trial. *The Lancet Infectious Diseases* **15**, 1041-1048 (2015).
42. G. Koopman *et al.*, Correlation between Virus Replication and Antibody Responses in Macaques following Infection with Pandemic Influenza A Virus. *Journal of virology* **90**, 1023-1033 (2016).
43. S. Pillet *et al.*, Cellular immune response in the presence of protective antibody levels correlates with protection against 1918 influenza in ferrets. *Vaccine* **29**, 6793-6801 (2011).
44. S. J. Samet, S. M. Tompkins, Influenza Pathogenesis in Genetically Defined Resistant and Susceptible Murine Strains. *Yale J Biol Med* **90**, 471-479 (2017).
45. T. Werk *et al.*, New Processes for Freeze-Drying in Dual-Chamber Systems. *PDA Journal of Pharmaceutical Science and Technology* **70**, 191 (2016).
46. L. Mirmoghtadaie, S. Shojaee Aliabadi, S. M. Hosseini, Recent approaches in physical modification of protein functionality. *Food Chemistry* **199**, 619-627 (2016).
47. J. O. Morales, D. J. Brayden, Buccal delivery of small molecules and biologics: of mucoadhesive polymers, films, and nanoparticles. *Current Opinion in Pharmacology* **36**, 22-28 (2017).
48. B. Fonseca-Santos, M. Chorilli, An overview of polymeric dosage forms in buccal drug delivery: State of art, design of formulations and their in vivo performance evaluation. *Materials Science and Engineering: C* **86**, 129-143 (2018).
49. C. M. Hanson, A. M. George, A. Sawadogo, B. Schreiber, Is freezing in the vaccine cold chain an ongoing issue? A literature review. *Vaccine* **35**, 2127-2133 (2017).
50. R. K. Evans *et al.*, Development of stable liquid formulations for adenovirus-based vaccines. *Journal of Pharmaceutical Sciences* **93**, 2458-2475 (2004).
51. S. S. Renteria, C. C. Clemens, M. A. Croyle, Development of a nasal adenovirus-based vaccine: Effect of concentration and formulation on adenovirus stability and infectious titer during actuation from two delivery devices. *Vaccine* **28**, 2137-2148 (2010).
52. R. H. M. Price, C. Graham, S. Ramalingam, Association between viral seasonality and meteorological factors. *Sci Rep* **9**, 929-929 (2019).
53. W. H. O. E. C. o. S. f. P. Preparations, "Fifty Second Report on Stability Testing of Active Pharmaceutical Ingredients and Finished Pharmaceutical Products.," *WHO Technical Report* (Geneva, Switzerland. , 2018).
54. J. L. Nguyen, D. W. Dockery, Daily indoor-to-outdoor temperature and humidity relationships: a sample across seasons and diverse climatic regions. *Int J Biometeorol* **60**, 221-229 (2016).
55. G. E. Walsberg, Small Mammals in Hot Deserts: Some Generalizations Revisited. *BioScience* **50**, 109-120 (2000).
56. J. Rexroad, T. T. Martin, D. McNeilly, S. Godwin, C. Russell Middaugh, Thermal Stability of Adenovirus type 2 as a Function of pH. *Journal of Pharmaceutical Sciences* **95**, 1469-1479 (2006).

57. G. Gomez, M. J. Pikal, N. Rodriguez-Hornedo, Effect of initial buffer composition on pH changes during far-from-equilibrium freezing of sodium phosphate buffer solutions. *Pharmaceutical research* **18**, 90-97 (2001).
58. V. G. Kadajji, G. V. Betageri, Water Soluble Polymers for Pharmaceutical Applications. *Polymers* **3**, (2011).
59. R. Gheribi *et al.*, Development of plasticized edible films from Opuntia ficus-indica mucilage: A comparative study of various polyol plasticizers. *Carbohydrate Polymers* **190**, 204-211 (2018).
60. Y. Lu, L. Jipeng, D. Lu, The mechanism for the complexation and dissociation between siRNA and PMAL: a molecular dynamics simulation study based on a coarse-grained model. *Molecular Simulation* **43**, 1-9 (2017).
61. S. Karlin, V. Brendel, Charge configurations in viral proteins. *Proceedings of the National Academy of Sciences* **85**, 9396 (1988).

Chapter 3: Mechanistic Evaluation of Adenoviral Stabilization in Novel Thin Film Technology

3.1 Introduction

Live, attenuated viral [LAV] vaccines contain a weakened version of naturally infectious viruses and successfully elicit a strong cellular and antibody mediated immune response, while significantly reducing pathogenicity. There are currently several available attenuated viral vaccines that protect against a variety of viruses such as Varicella, Herpes Zoster, Rotavirus, Influenza, and Yellow Fever. A drawback linked with production, storage, and distribution of LAVs is their susceptibility to irreversible changes to the three-dimensional functional shape of viral proteins and loss of immunogenicity, primarily brought on by extreme changes in solution pH and temperature as well as other environmental stressors such as shear stress, light, and surface adsorption (1-3). Therefore, it is not surprising that all approved LAVs require either refrigeration or ultra-low temperatures for long term storage (Appendix Table 1 & 2).

The World Health Organization estimates that over half of the vaccines shipped annually are discarded due to a disruption in the cold-chain during shipment and transportation (4). Heat inactivation of viruses has been proven to damage both enveloped and non-enveloped viruses by disrupting the capsid and exposing genomic material to the harsh environment outside of cells (5-7). Viruses have different levels of vulnerability to heat exposure. For example, H1N1 influenza is heat inactivated after exposure to 70°C for 5 minutes while adenovirus serotype 5 is heat inactivated after 20 minutes (8, 9). While heat damage may seem like the only concern, several liquid formulations are also freeze-sensitive (10). If these vaccines are either heated or cooled outside of their storage range, typically 2-8°C, they must be discarded. An estimated 14%

to 35% of refrigerators or transport shipments expose vaccines to freezing temperatures and between 75% and 100% of vaccines are subjected to freezing at some point between production and administration of vaccines (11). We recently demonstrated that a formulation consisting of a polymer base, sugar, and surfactant was able to stabilize adenovirus serotype 5 in both a liquid and thin film format (8). Our novel thin film platform maintained viral stability for three months at 4°C and 20°C as well as for 14 days at 37°C and 5 days at 40°C. Thin films were also able to protect virus through 16 freeze-thaw cycles, wherein films were frozen at -80°C and warmed to 20°C per a cycle. Our formulation successfully protects adenovirus through a range of temperatures without reducing viability which could significantly simplify vaccine transportation and distribution. Another advantage of the thin film platform of particular interest to low- and middle-income countries is the elimination of sharps waste. A vaccine campaign to eliminate measles in the Philippines has estimated that 130,000 kg of sharps waste and an additional 72,000 kg of non-hazardous waste was generated in a little under a month (12). Our technology can easily be stored in envelopes, eliminating the need for needles, glass vials, and syringes and in effect reducing the environmental burden greatly. Lastly, the novel thin film platform can be self-administered and eliminates the need for trained health care-professionals to administer injections during vaccination campaigns. However, out of these three advantages we believe the film's resistance to temperature fluctuations is the most critical and important contribution to the field of vaccine delivery.

The critical role of the surfactant in adenoviral stabilization was evident as films prepared with optimized concentrations of zwitterionic surfactant consistently outperformed formulations lacking the stabilizing excipient at the various temperatures evaluated (13). Films prepared with surfactant also rapidly released all of the infectious virus from the three-dimensional matrix,

while virus remained bound to the platform in the presence of base alone. Fourier transform infrared spectroscopy suggested the key to stabilization of the virus, in the thin film matrix, might be through interactions of the positively charged amine groups of the surfactant with the negatively charged glutamic acid residues located on adenovirus' surface protein, hexon, by the complete incorporation of adenovirus into formulation spectra resulting in no significant shifts in peak absorbance (14). The aim of this report is to understand how the surfactant interacts with the virus and the other formulation components so that the principles can be applied for effective stabilization of other biologics within the film matrix. However, due to the structural complexity of proteins, the direct study of surface protein-excipient interactions is somewhat difficult (15). Moreover, viruses are made up of a series of complex proteins in a specific assembly, further complicating the study of virus-excipient interaction. We hypothesized that via intermolecular interactions the surfactant stabilizes adenovirus within the amorphous thin film network and facilitates the rapid hydration of the film, through the assistance of the other excipients, resulting in complete delivery of the viral load. In this study, we visualized the impact of each component of the formulation on adenovirus capsid stability using transmission electron microscopy. Physical interactions of surfactant with itself and with virus at the concentration used in the film were evaluated through a saturation study and evaluation of the critical micelle concentration. Isothermal titration calorimetry (ITC) and biolayer interferometry (BLI) were utilized to investigate the strength of the interaction between the virus and surfactant and the thermodynamic contribution to stabilization. The contribution of each excipient to moisture content of the formulation was evaluated to determine how hydration of viral proteins contributed to viral stabilization and interaction with formulation components. These studies are summarized here along with the translatability of our novel stabilization technology by

evaluating four additional viruses, different in size, surface charge, and envelope, in the film matrix.

3.2 Materials and Methods

3.2.1 Materials

Dulbecco's PBS, Trizma base [2-amino-2-(hydroxymethyl)-1,3-propanediol], pyrene (puriss. p.a.), potassium ferricyanide, potassium ferrocyanide, glutaraldehyde (grade I, 25% in water), FBS (qualified, U.S. origin), glycerol, sodium azide, choline bicarbonate, SigmaFast BCIP/NBT tablets, calcium alpha-d-heptagluconate, and D-sorbitol [USP (United States Pharmacopeia) grade] were purchased from Sigma-Aldrich (St. Louis, MO). Poly(maleic anhydride-alt-1-octadecene) substituted with 3-(dimethylamino)propylamine was purchased from Anatrace (Maumee, OH). DMEM and MEM were purchased from Mediatech (Manassas, VA). EMEM was purchased from Lonza (Basel, Switzerland). Hydroxypropyl methylcellulose 4*KM was provided by the Dow Chemical Company (Midland, MI). Penicillin (10,000 IU) and streptomycin (10,000 μg/ml) were purchased from Gibco Life Technologies (Grand Island, NY). 5-Bromo-4-chloro-3-indolyl-β-D-galactoside (X-gal) was purchased from Gold Biotechnology (St. Louis, MO). EDC (1-Ethyl-3-[3-dimethylaminopropyl] carbodiimide hydrochloride), S-NHS (N-hydroxysulfosuccinimide), Ethanolamine, Acetate Buffer, and Kinetics Buffer were purchased from ForteBio (Fremont, CA). Anti-Influenza A Antibody (MAB8258B-5) and Streptavidin, Alkaline Phosphatase Conjugate were purchased from Millipore Sigma (Burlington, MA). Hydranal was purchased from Honeywell (Charlotte, NC). Methanol, 99.8% Extra Dry was purchased from Acros Organics (Fair Lawn, NJ). Influenza A Virus, A/Puerto Rico/8-9VMC3/1934 (H1N1) was purchased from BEI Resources (Manassas, VA). All other

chemicals were of analytical reagent grade and purchased from Thermo Fisher Scientific (Pittsburgh, PA) unless specified otherwise.

3.2.2 Adenovirus Production and Purification

First-generation adenovirus serotype 5 expressing E. coli beta-galactosidase under the control of a cytomegalovirus (CMV) promoter was amplified in human embryonic kidney (HEK) 293 cells (ATCC CRL-1573) and purified from secondary lysates according to established methods (16). Preparations with a ratio of infectious to physical viral particles (v.p) of 1:100 were utilized in the studies summarized here.

3.2.3 Transmission Electron Microscopy

Formulations were prepared and diluted 1:10 in sterile water. Carbon coated grids (CTU300-CU) were treated with 25 mA plasma for 2 minutes. After treatment, the sample was added to each grid and excess liquid was removed using a filter wedge, followed by the addition of 2% uranyl acetate (pH 4.5). Excess liquid was removed using a filter wedge. Grids were subsequently photographed on a JEOL 2010F transmission electron microscope (JEOL, Peabody, Massachusetts) employing an accelerating potential of 80kV.

3.2.4 Saturation Study

Formulations were prepared in bulk at a virus concentration of 1.25×10^{12} v.p. so that subtle changes in infectious titer could be detected with a standard limiting dilution/infectious titer assay and histochemical staining (16). The following formulations were prepared: (A) 4mg/mL aspartic acid, (B) 4mg/mL glutamic acid, (C) 10mg/mL surfactant (D) 10% glycerol/PBS (E) 10 mg/mL surfactant saturated with 4 mg/mL of Aspartic Acid, and (F) 10 mg/mL surfactant saturated with 4 mg/mL Glutamic Acid. The production lot was stored at 20°C

and infectious titer was assessed on days 1, 3, 5, 7, 14, and 28 on HeLa cells (ATCC# CCL-2). Percent recovery was calculated as:

$$\% \, Recovery = \frac{\log\left(infectious \; titer \; of \; t \; = 1\right)}{\log(infectious \; titer \; of \; t \; = 0)} \times 100$$

where t=1 is the infectious titer of a formulation the day it was evaluated and t=0 is the infectious titer of virus in the same formulation the day it was prepared. Formulations were also prepared without virus to determine the saturation points. They were prepared with or without 2.5% glycerol, and pH was monitored using an Orion Star™ A111 Benchtop pH Meter (ThermoFisher Scientific, Waltham, MA) as well as pH indicator solutions. Lastly, liquid formulations and films were prepared using formulation F with the additional formulation components, hydroxypropyl methyl cellulose and sorbitol and infectious titer was assessed on days 1, 3, 5, and 7.

3.2.5 SDS-PAGE

Samples A-F from the formulation study were prepared and incubated at 25°C for 3 days for t=3 time point and freshly prepared for the t=1 time point. Tris 1M was titrated into samples so that the pH was uniform, and samples were incubated for 10 minutes at 100°C and loaded onto a sodium dodecylsulfate polyacrylamide (SDS-PAGE) stacking gels (3-10%). Protein molecular weight standards in the range of 10,000 – 250,000 Da (Bio-Rad, Hercules, California) served as markers for estimating the molecular weight of Ad proteins. Stacking gels were run at 80 V and stained with the Cytiva PlusOne™ Silver Staning Kit (Cytiva, Marlborough, MA) according to manufacturer's recommendations. Band intensities in the silver stained gels were obtained from images of the gels using Gel Analyzer Version 19.1, however interference from surfactant resulted in large variance of band intensity between gels and therefore only qualitative comments were made regarding band intensity. Bands of freshly prepared formulation D were

assumed to have undergone no protein degradation and were therefore, taken as 100% of the initial intensity in relation to bands in different formulations.

3.2.6 Dynamic Light Scattering and Zeta Potential

PMAL C-16 was dissolved in sterile DI water at a concentration of 10 mg/mL and sterile filtered. Cuvettes were washed 3x with sterile DI water and 3x with ethanol and dried using compressed air. Samples were placed in cuvettes and measured using a Zetasizer Nano Series (Malvern Panalytical, Malvern, UK). Data was analyzed with the Malvern Zetasizer Software version 8.00.4813.

For zeta potential measurements, formulations A-F were prepared, as described above, in Tris buffer and evaluated using Zetasizer Nano Series folded capillary cells and a Zetasizer Nano Series (Malvern, Malvern, UK). Samples of PMAL C-8 and C-12 were also prepared in Tris buffer for analysis of zeta potential. Data was analyzed with the Malvern Zetasizer Software version 8.00.4813 using the Smoluchowski approximation.

3.2.7 Biolayer Interferometry

All analyses were carried out on an Octet Red96E machine (ForteBio, Fremont, California). Adenovirus stock was dialyzed to remove glycerol that would interfere with the AR2G biosensors and subsequently inactivated. Ultraviolet inactivation of adenovirus was monitored, during treatment of adenovirus with λ 365 nm, using an infectious titer assay over a period of four hours. Adenovirus serotype 5 immobilization scouting, on AR2G biosensors, was performed using acetate buffer pH 4, 5, and 6 and surfactant was prepared in kinetics buffer, purchased from Biacore. After unsuccessful immobilization, the orientation of Ad and surfactant

was revered. Kinetics buffer purchased from Biacore was used as running and regeneration buffer.

3.2.8 Isothermal Titration Calorimetry

All analyses were carried out on a Microcal PEAQ-ITC System (Malvern, Malvern, UK). Adenovirus stock was dialyzed to remove glycerol that would interfere with binding parameters and PMAL was diluted in dialysate to minimize differences between buffers the samples were suspended in. Adenovirus was inactivated using the same protocol as described above. Fifteen, 2.5 µL injections of PMAL were added to a cell containing adenovirus, using a reference power of 10 µcal/sec. Analysis was conducted using MicroCal PEAQ-ITC Analysis software (Malvern, Malvern, UK).

3.2.9 Critical Micelle Concentration

Contact Angle Goniometer. Formulations were prepared in water and dropped onto a PFTE (Polytetrafluoroethylene) sheet. Contact angle was subsequently measured by taking images with a FTA200 contact angle goniometer (First Ten Angstroms, Newark, California) and using the NT/2000/XP software.

Pyrene Fluorescent Probe. Pyrene was dissolved in methanol and then spiked into surfactant at a concentration of 1µM. Solutions of surfactant were prepared from 1.28 mM to 2.5 x 10^{-3} mM by two-fold serial dilutions. Fluorescence was measured at 25°C using an Infinite 200 spectrophotometer (Tecan, Männedorf, Switzerland). Pyrene was excited by light at 336 nm and emission observed at 373 nm and 384 nm with an integration time of 2 s. The ratio of the

fluorescence intensity at these 2 wavelengths (I1/I3) was used to determine critical micelle concentrations.

3.2.10 Chain Length

Films were prepared with base, sorbitol, and surfactant with varying chain lengths 8, 12, and 16. Once drying was complete, all samples (n=3) were reconstituted and infectious titer of virus and zeta potential was assessed, as described above.

3.2.11 Moisture Content Analysis

Thermal Gravimetric Analysis. Films were prepared with base (B), base and sorbitol (17), base, sorbitol, and surfactant (BSS), and base, sorbitol, surfactant, and virus (BSSV). Upon complete drying, the next day films were weighed and loaded into stainless steel pans (Catalog #: 0319-1525) and analysis was carried out using the TA Instruments Q500 TGA (TA Instruments, New Castle, DE). A standard run was conducted (10°C ramp every minute up to 550°C) under Nitrogen gas. Data analysis was conducted using the Universal V4.5A TA Instruments software.

Volumetric Karl Fischer Titration. All analysis was performed on a V10S Volumetric Karl Fischer Titrator (Mettler Toledo, Columbus, OH). Films (1mL) were prepared using standard protocols previously outlined (13). Extraction solvent was prepared by mixing 10 mL anhydrous methanol and 10 mL of anhydrous formamide, the weight of the reconstitution volume (1 mL) was recorded (m_{sol}). The weight of each film was also recorded (m_{ext}). The film was then added to a scintillation vial which was sealed with an aluminum seal using 13 mm crimpers. Meanwhile, 20 mL of sterile DI water was heated to 50°C and vials were placed in the solution, and vortexed occasionally, until films dissolved. Special care was given to ensure that vials did

not flip or float in water and that the sample was not sticking to the walls of the vial. Next, the moisture content of blank extraction solvent was determined by first weighing the sample (m1), injecting half of it into the titration vessel, and weighing the sample again (m2). The weight of the sample injected was entered, determined by subtracting m1 from m2, and the moisture content was provided by the instrument (B%). The same procedure was followed for the film and the moisture content was recorded (C%). The following calculation was used to determine the moisture content of the film based on all the values recorded:

$$Moisture\ Content\ (\%) = C \times \left(\frac{msol + mext}{mext}\right) - \left(\frac{B \times msol}{mext}\right)$$

3.2.12 Alternative Virus Screen

Films were prepared with Adenovirus (n=3) at a concentration of 1.25 x 10^{12} vp/mL , Influenza (n=3) at a concentration of 3 x 10^{8} pfu/mL , Respiratory Syncytial Virus (n=4) at a concentration of 2 x 10^{6} pfu/mL , and Herpes Simplex Virus (n=4) at a concentration of 7 log pfu/mL. The following day they were reconstituted, and infectious titer was assessed.

3.2.13 Flu Excipient Optimization

Choline. Films were prepared with base, sugar, and varying concentrations of choline: 0.1, 1, 3, 5, and 8.5% w/v. The following day they were reconstituted, and infectious titer was assessed on MDCK cells (ATCC #CCL-34). Average percent recovery was determined using the above equation.

Heptagluconate. Films were prepared with base and 1% w/v Calcium α-D-Heptagluconate hydrate. The following day they were reconstituted, and infectious titer was

assessed on MDCK cells (ATCC #CCL-34). Average percent recovery was determined using the above equation.

3.2.14 Cytotoxicity Assay

Cytotoxicity was assessed by measuring the amount of adenosine triphosphate (ATP), an indicator of metabolically active cells, in cultures using a Cell Titer-Glo Luminescent Cell Viability assay kit (Promega, Madison, WI) according to the manufacturer's instructions. Data generated from this assay was used to evaluate the cytotoxicity of formulation with 5% w/v choline after exposure to human buccal cells (TR-146) for 30 min, 60 min, and 120 min.

3.2.15 Stability of Influenza Film

Formulations and films, consisting of base and 1% w/v Calcium α-D-Heptagluconate hydrate were prepared in bulk at a virus concentration of 3 x 10^8 $CEID_{50}$ so that subtle changes in infectious titer could be detected with a standard limiting dilution/infectious titer assay and histochemical staining. They were stored at 4°C and 20°C for 21 days and the infectious titer was assessed on MDCK cells (ATCC #CCL-34). Percent recovery was calculated as described above.

3.2.16 Statistics

Statistical analysis of data was performed using JMP (JMP Statistical Software from SAS, Cary, NC). Differences with respect to treatment were calculated using unpaired two-tailed Student's *t* tests. Differences were determined to be significant when the probability of chance explaining the results was reduced to less than 5% ($P < 0.05$).

3.3 Results

3.3.1 Visualization of Formulation Components Using Transmission Electron Microscopy

We began our evaluation of the physical impact of each excipient on adenovirus by monitoring adenovirus capsids with transmission electron microscopy (18) after addition of each formulation component in a stepwise fashion. TEM revealed large aggregates of adenovirus present in formulations consisting of only base (Figure 3.1 A and B) and base and sorbitol (Figure 3.1 C and D). The addition of surfactant prevented viral aggregation and each individual virion appears 1.5 to 2.5 times larger in size, possibly due to variable interaction of surfactant (Figure 3.1 E and F). In order to understand what the new structures seemingly coating the virus might be, a new formulation consisting only of surfactant and adenovirus in Tris buffer was prepared. In the absence of other excipients, we observed several of the same circular structures, roughly 9 nm in size, surrounding adenovirus capsids, and preventing viral aggregation by the formation of large structures (Figure 3.1 G and H). These large structures varied in width (513 ± 57 nm). We hypothesized that these structures may be surfactant surrounding the adenoviral capsids, and in the presence of all formulation components, fully coating virions (Figure 3.1 E and F).

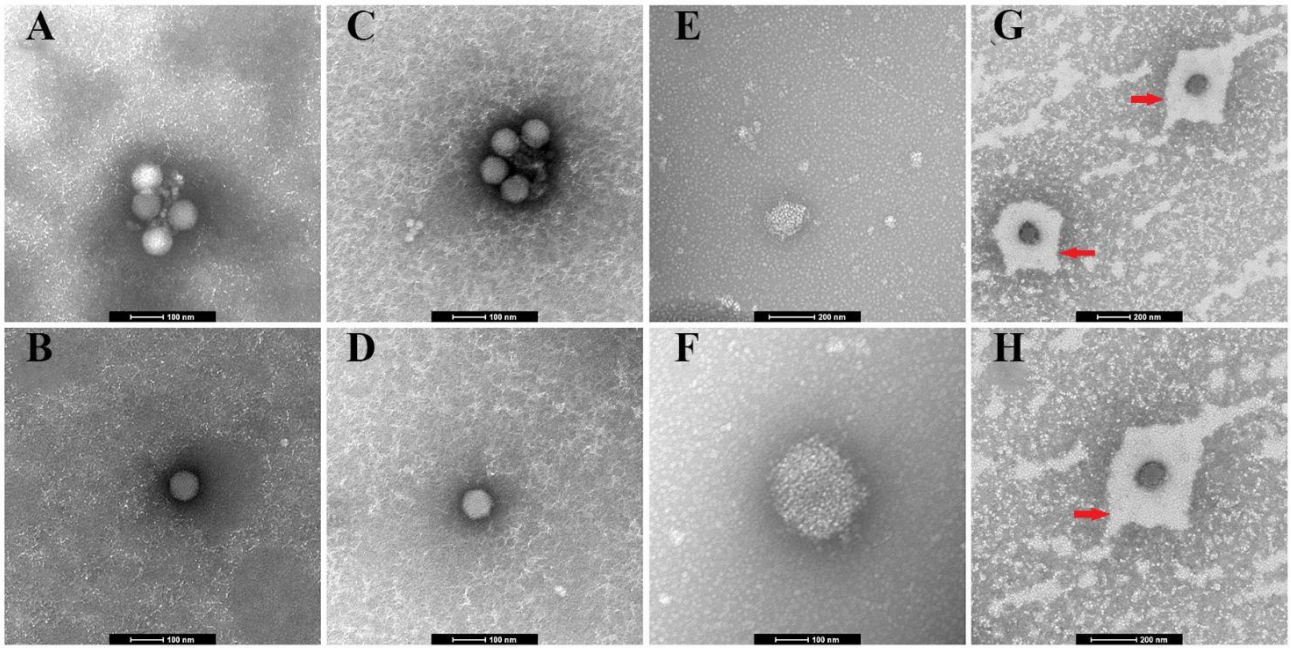

Figure 3.1: Surfactant prevents aggregation and forms micelle like structures around virus particles.

(**A**|**B**) Transmission electron micrograph of formulation consisting only of HPMC excipient and adenovirus particles. Adenovirus diameter size was estimated as 96 ± 5 nm in Panel A of Figure 1 and 95 ± 4 nm in Panel B. (**C**|**D**) Formulation consisting of HPMC and Sorbitol in the presence of virus does not prevent aggregation. Adenovirus particles are sized at 91 ± 4 nm and 93 ± 5 nm in Panels C and D, respectively. (**E**|**F**) Formulation consisting of HPMC, Sorbitol and Surfactant in the presence of virus prevents viral aggregation and results in capsids which are seemingly coated in varying degrees with surfactant and larger in size. Estimated virus size in Panel E is 168 ± 24 nm and in Panel F is 239 ± 15 nm. (**G**|**H**) Adenovirus particles surrounded by surfactant which prevent aggregation. Average size of capsids in panel G is 96 ± 2 nm and in panel H is 98 ± 1 nm. The estimated size of the circular structures is 9 ± 1 nm. The red arrows point towards circular structures surrounding adenovirus capsids. It is important to note that the capsids likely appear darker due to how bright the surrounding circular structures are, creating a strong contrast in panels G and H. ImageJ software was used to estimate sizing.

3.3.2 Saturation of Surfactant via Saturation with Amino Acids

Since the presence of surfactant significantly impacts a variety of physiochemical properties of the thin film matrix, we designed a study to evaluate the effect of surfactant saturation on adenoviral stability. Glutamic acid (E) and aspartic acid (D) are two amino acids predominantly responsible for the negative charge on the hexon protein of adenovirus serotype 5 (14). Saturation of potential sites that were utilized to interact with and stabilize adenovirus was performed to investigate the interactions between negatively charged residues located on the hexon protein of the adenovirus capsids and the positively charged arm of the zwitterionic surfactant in our novel formulation.

The pH served as an indicator for saturation of surfactant with the amino acids studied. To determine the point of saturation, the pH of the solution was employed. Solutions were prepared in Tris buffer (pH 8.1) with glutamic acid or aspartic acid at maximum solubility, resulting in pH 3 and 3.5 respectively, and titrated into a solution of surfactant concentrated at 10 mg/mL in Tris buffer (pH 8.1) until the pH changed. This concentration of surfactant was selected for the study as it was the optimized concentration previously used in formulations that stabilized adenovirus at ambient temperatures (13). As is it important to remain above the pKa of the side chain of glutamic acid (4.25) and aspartic acid (3.86) to maintain the negative charge, the optimal pH of surfactant saturated solutions was selected as pH 5.5. This was low enough to mask the protective effects of the surfactant, as adenovirus is stable in pH 6-8 (16, 19), but high enough to maintain the appropriate surface charge on all molecules in solution. The addition of 1.3 mg/mL of glutamic acid or 1 mg/mL of aspartic acid to surfactant was identified as the ideal concentration to achieve pH 5.5 (Figure 3.2 A and B). However, laboratory stocks of adenovirus are stored at 5 x 10^{12} vp/mL using PBS buffer containing 10% glycerol, as a cryoprotectant, for

storage at -80°C (20-22). Therefore, formulations prepared for the saturation study with adenoviral stock contained 2.5% glycerol in PBS, a 1:4 dilution accounting for the addition of adenovirus at a concentration of 1.25×10^{12} vp/mL, and needed to be evaluated for the impact of these additional components on the pre-defined saturation point. Preparations of glutamic acid or aspartic acid were prepared at maximum solubility and titrated into a solution of surfactant concentrated at 10 mg/mL in Tris with 2.5% glycerol, initially pH 6.5, until the pH changed. Our studies revealed that only concentrations of 4mg/mL of glutamic acid or aspartic acid were strong enough to lower the pH of solutions containing surfactant at 10mg/mL in Tris prepared with 2.5% glycerol in PBS, to 5.5 (Figure 3.2 C and D).

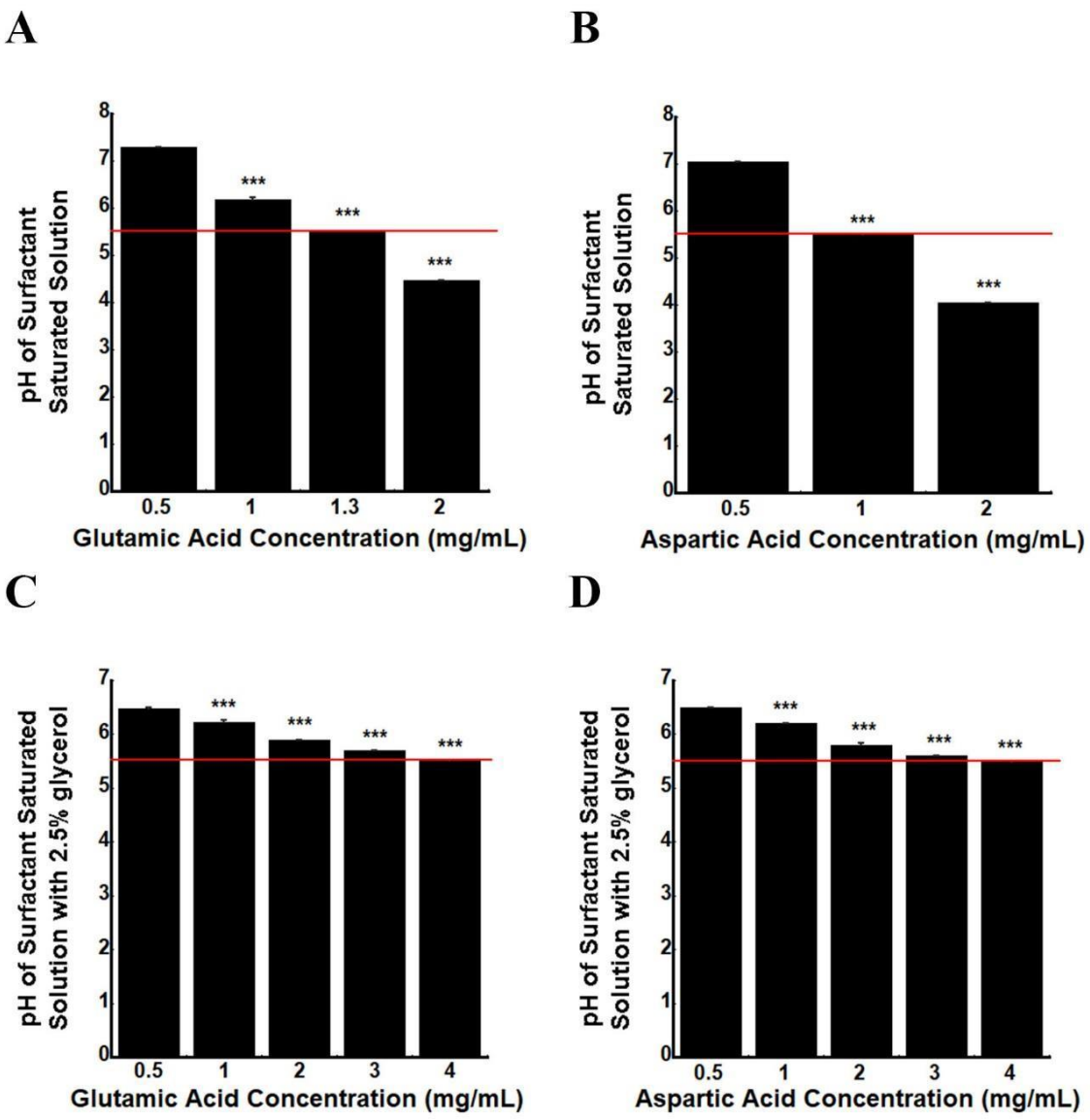

Figure 3.2: Presence of Glycerol Increases the pH Saturation Point of Surfactant.

Formulations containing 10 mg/mL of surfactant in Tris buffer were prepared and varying concentrations of glutamic acid (**A**) and aspartic acid (**B**) were titrated in until a target pH of 5.5 was observed (demarked by a red line). Formulations containing 10 mg/mL of surfactant in Tris buffer were then prepared with 2.5% glycerol in PBS and varying concentrations of glutamic acid (**C**) and aspartic acid (**D**) were titrated in until a pH of 5.5 was observed, to account for the

addition of this excipient in adenovirus stock. Data represents the average ± the standard deviation, n=3. ***$p < 0.001$, two-tailed Student's t test.

Upon determination of the saturation point, virus at a concentration of 1.25×10^{12} vp, with 2.5% glycerol, was added to solutions of glutamic acid- or aspartic acid-saturated surfactant and studied at 20°C and infectious titer was monitored for 28 days. Control preparations consisting of glutamic acid, aspartic acid, surfactant, and Tris buffer were also prepared with a virus concentration of 1.25×10^{12} vp. pH was monitored in conjunction with recovery of adenovirus and did not fluctuate during the sampling period (Table 3.1). After 28 days, controls prepared with surfactant alone (Sample C) or Tris buffer (Sample D) retained 99 ± 0.5 % and 98 ± 1.1% of their original infectious titer, respectively. Virus in the aspartic acid control solution (Sample A) fell to 86 ± 0.3 % after 14 days, while aspartic acid-saturated surfactant formulations (Sample E) retained 97 ± 0.5 % of their original titers. However, within only three days glutamic acid-saturated surfactant (Sample F) had no detectable recovery while glutamic acid controls (Sample B) retained 91 ± 0.4% of their original titer (Figure 3.3 A). When we prepared the complete formulation with glutamic acid saturated surfactant, there seemed to be a buffering effect (Figure 3.3 B). After three days, solid film formulations retained 74% ± 0.5% of the original infectious titer, while liquid formulations were significantly more effective at protecting adenovirus from glutamic acid saturated surfactant (92 ± 0.3%; $p<0.001$). The infectious titer continued to drop and by the end of 7 days only 64% ± 0.6% and 90 ± 0.7% of the original titer was retained in film and liquid preparations, respectively.

In order to determine if the impact on transduction efficiency of adenovirus incubated with glutamic acid-saturated surfactant after 3 days at 20°C was linked to post-translational

modifications of adenoviral structural proteins, we performed sodium dodecyl sulfate polyacrylamide gel electrophoresis (SDS-PAGE). Figure 3C provides a diagram of the current understanding of the adenovirus capsid based on cryo-electron microscopy and crystallography (23). Adenovirus in 2.5% glycerol and PBS freshly prepared, D t=0, was used as the standard for comparison of structural protein integrity and showed at least 14 unique protein bands (Figure 3.3 D). Seven proteins (demarked as, *) were detected that could not be confidently corelated with known adenoviral structural proteins. The 7 structural proteins identified include II, III, IIIa, IV, V, VI, and VIII. However, we did not include VI and VIII in our analysis as the smearing of the silver stain due to surfactant made it difficult to discern bands in all the samples. Control samples prepared with surfactant appeared to have a slightly higher molecular weight than all other samples (Figure 3.3 D & E). This is likely an artifact of the surfactant competing with SDS and therefore running through the gel at a slower rate than the other samples. Additionally, protein IIIa had reduced band sharpness and only four unidentified protein bands were present in samples prepared with surfactant (Figure 3.3 D). SDS-PAGE did not reveal any significant changes in the protein bands observed for samples prepared with aspartic acid (Sample E) or glutamic acid (Sample F) saturated surfactant in comparison to control adenovirus at either time point (Figure 3.3 E). However, this technique did confirm that the hypothesized protective effects of surfactant were blocked by the saturation of surfactant with either amino acid, as all 14 bands were present in comparable molecular weight (Figure 3.3 E). No major differences were detected between the day 0 and day 3 time points for any of the samples containing surfactant or the amino acid samples prepared without surfactant (Sample A: aspartic acid, Sample B: glutamic acid) relative to the adenoviral control (Figure 3.3 D).

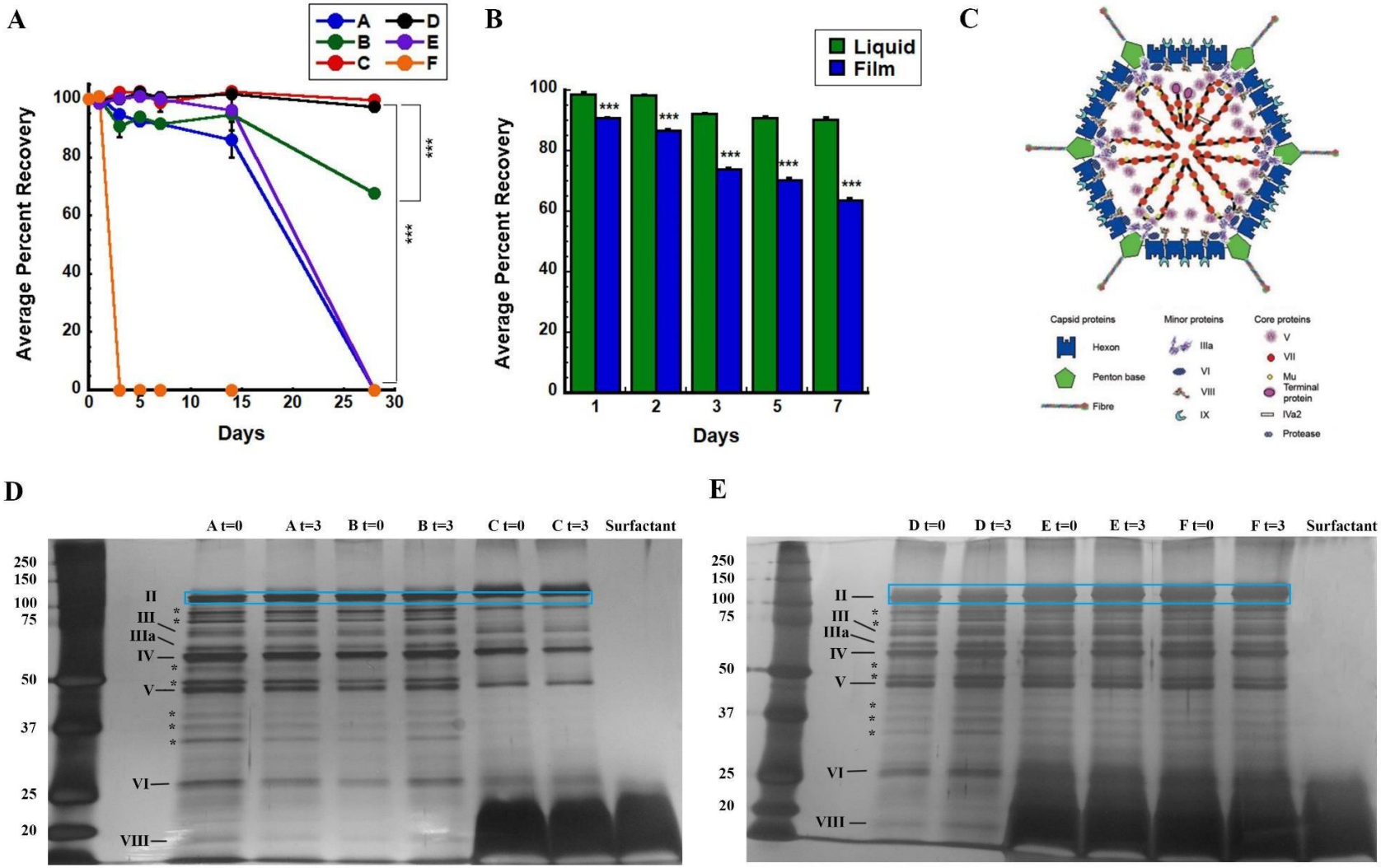
A
A
B
C
D
E
F
Average Percent Recovery
Days
***
B
Liquid
Film
Average Percent Recovery
Days
***
C
Capsid proteins
Hexon
Penton base
Fibre
Minor proteins
IIIa
VI
VIII
IX
Core proteins
V
VII
Mu
Terminal protein
IVa2
Protease
D
A t=0
A t=3
B t=0
B t=3
C t=0
C t=3
Surfactant
250
150
100
75
50
37
25
20
II
III
IIIa
IV
V
VI
VIII
E
D t=0
D t=3
E t=0
E t=3
F t=0
F t=3
Surfactant
250
150
100
75
50
37
25
20
II
III
IIIa
IV
V
VI
VIII

Figure 3.3: Further evaluation indicates affinity between surfactant and glutamic acid residues on virus capsid.

Formulations containing 1.25×10^{12} v.p. were prepared in batch and stored at 20 °C for 28 days. Formulations are labeled in the figure according to the letters listed in Table 1. (**A**) Saturation of Surfactant Impacts Adenoviral Transduction Efficiency. Replicates (at least 3 per timepoint) were reconstituted and live virus concentration assessed by a standard infectious titer assay. Virus was placed at the same concentration in two standard liquid formulations and infectious titer under each storage condition also assessed for comparison. Sample C consisted of 10 mg/mL Surfactant and Sample D consisted of 100 mM phosphate buffered saline and 2.5% glycerol. Data represents the average ± the standard deviation. ***$p < 0.001$, two-tailed Student's t test. (**B**) Complete Formulation Reduces the Impact of Glutamic-Acid Saturated Surfactant on Transduction Efficiency. Replicates (at least 3 per timepoint) were reconstituted and live virus concentration assessed by a standard infectious titer assay. Virus was placed at the same concentration in liquid and film formulations containing: hydroxypropyl methyl cellulose, sorbitol, and 10mg/mL surfactant saturated with 4mg/mL glutamic acid. Infectious titer was assessed for comparison. Data represents the average ± the standard deviation. ***$p < 0.001$, two-tailed Student's t test. (**C**) Adenovirus Structure from ref (23). (**D & E**) Silver Stained Gels of Saturation Study Samples Following SDS-PAGE. Lanes from left to right on the first gel are molecular weight standards, aspartic acid and adenovirus at day 0 (A t=0), aspartic acid and adenovirus at day 3 (A t=3), glutamic acid and adenovirus at day 0 (B t=0), glutamic acid and adenovirus at day 3 (B t=3), surfactant and adenovirus at day 0 (C t=0), surfactant and adenovirus at day 3 (C t=3), and surfactant (**C**). Lanes from left to right on the second gel are molecular weight standards, adenovirus at day 0 (D t=0), adenovirus at day 3 (D t=3), aspartic acid-surfactant and adenovirus at day 0 (E t=0), aspartic acid-surfactant and adenovirus at day 3 (E t=3), glutamic acid-surfactant and

adenovirus at day 0 (F t=0), glutamic acid-surfactant and adenovirus at day 3 (F t=3), and surfactant (**D**). Ad protein subunits were assigned according to their appearance order on the gel as well as reference by Ahi (24). Proteins that differ from known Ad structural proteins were designated with an asterisk (*).

Table 3.1: Saturation Study Formulation pH

Formulation	pH
A Aspartic Acid (4mg/mL) + Ad	5
B Glutamic Acid (4mg/mL) + Ad	5
C Surfactant (10 mg/mL) + Ad	6.5
D Ad	7
E Aspartic Acid (4mg/mL) +Surfactant (10 mg/mL) + Ad	5.5
F Glutamic Acid (4mg/mL) +Surfactant (10 mg/mL) + Ad	5.5

Since we could not identify any post-translational modifications to adenoviral structural proteins following SDS-page analysis, we decided to investigate the samples from the saturation study for non-covalent interactions. Zeta potential measurements were performed to analyze the magnitude of electrostatic repulsion between the charged particles in solution and whether the repulsion contributes to the interactions between adenovirus and the surfactant. The magnitudes are reported as absolute values, as zeta potential deals with surface potential. The positive and/or negative findings are not robust and should not be related with surface charge or charge density, due to the variance in sample pH (25). The zeta potential of aspartic acid and adenovirus (Sample A, 7 mV), glutamic acid and adenovirus (Sample B, 4 mV), and glutamic acid saturated with surfactant and adenovirus (Sample F, 16 mV) did not significantly change over 3 days at 20°C ($p>0.05$, Figure 3.4A). However, the zeta potential of adenovirus in 2.5% glycerol (Sample D) and adenovirus prepared with surfactant (Sample C) significantly decreased from 20 mV to 15 mV ($p<0.01$) and from 11 mV to 3 mV ($p<0.001$), respectively, from day zero to day three (Figure 3.4A). Conversely, the zeta potential of aspartic acid saturated with surfactant (Sample E) significantly increased from 11 to 16 mV from day zero to day three ($p<0.01$). The zeta potential of all the samples was significantly lower than adenovirus in 2.5% glycerol at day zero (A, B, E: $p<0.001$; C, F: $p<0.01$; Figure 3.4B). However, after three days samples A, B, and C had significantly lower ($p<0.001$) zeta potentials than adenoviral control, and samples E and F had slightly (but significantly) higher zeta potentials ($p<0.01$; Figure 3.4C).

Evaluating the zeta potential of the formulation prepared without adenovirus, provided additional insight into observed zeta potentials. Surfactant without the presence of adenovirus has a zeta potential of 3 mV (Figure 3.4D). Aspartic acid and glutamic acid saturated with surfactant, without the addition of virus, have significantly higher zeta potentials, 19mV and 24

mV, respectively, than the zeta potential of surfactant alone (Figure 3.4D). Additionally, glutamic acid saturated with surfactant results in a significantly higher zeta potential than aspartic acid saturated with surfactant ($p<0.05$).

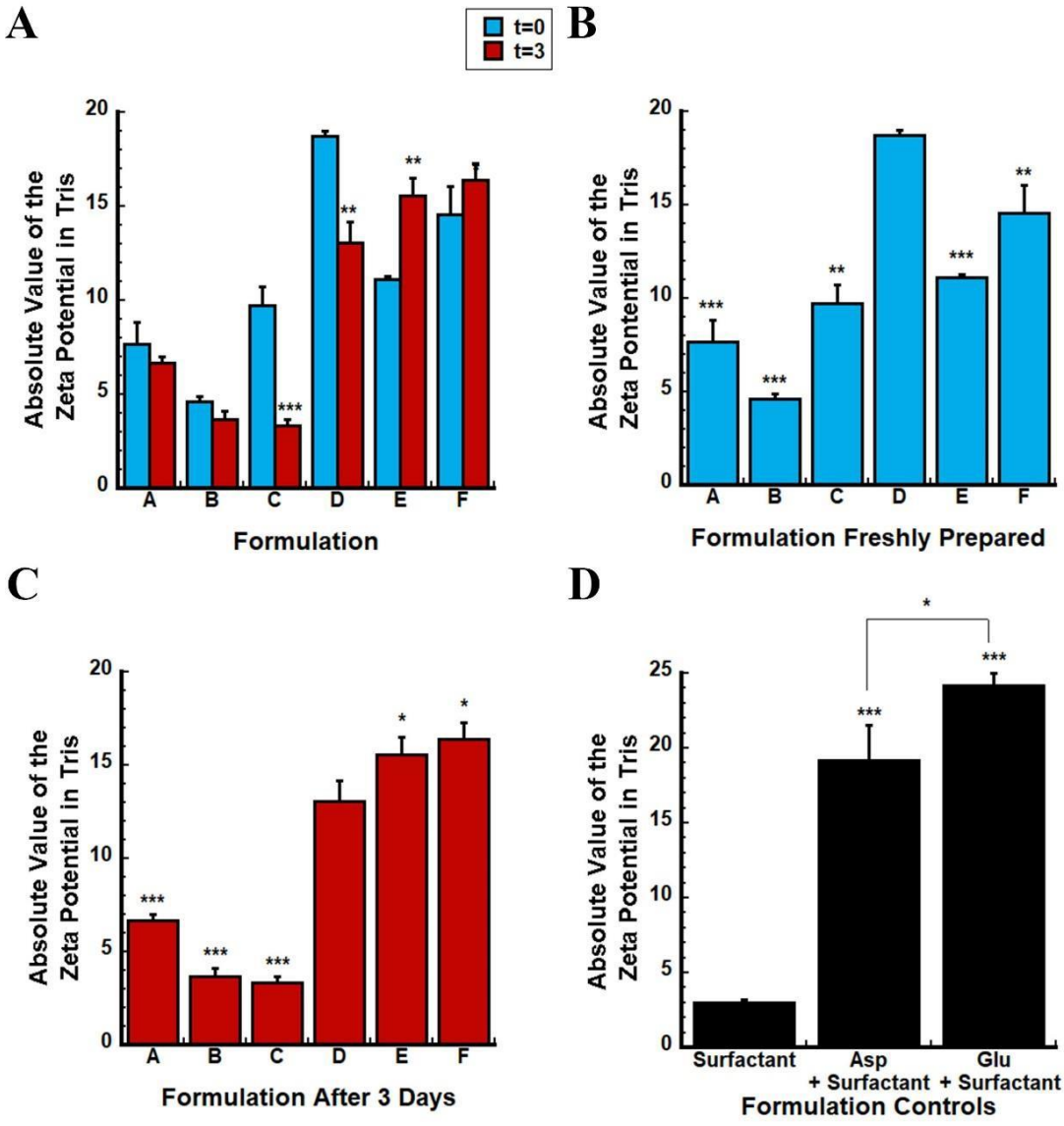

Figure 3.4: The Magnitude of the Zeta Potential of Adenovirus-Surfactant Formulations Hints at Surfactant Adsorption to Adenoviral Surface as a Mechanism of Aggregation Prevention.

Formulations containing 1.25×10^{12} v.p. were prepared in batch and stored at 20 °C for 28 days. Formulations are labeled in the figure according to the letters listed in Table 3.1. Zeta potential

measurements were collected using a Zetasizer Nanoseries for each formulation and compared to the initial zeta potential recorded (**A**). Zeta potential measurements for freshly prepared samples were compared to adenoviral control (**B**). Zeta potential measurements for samples after three days were compared to adenoviral control (**C**). Control formulations prepared without adenovirus were evaluated for zeta potential (**D**). Data represents the average ± the standard deviation, n=3. *p<0.05, **p<0.01, ***p < 0.001, two-tailed Student's t test.

3.3.3 Binding Affinity of Surfactant and Adenovirus

While the zeta potential measurements provide insight into electrostatic repulsion, they do not provide information on direct virus – surfactant interactions (25). In order to evaluate if the surfactant interacts with adenovirus in a quantifiable way, we initially used biolayer interferometry (BLI). Adenovirus was originally immobilized on biosensors at a concentration of 20 µg/mL and a surfactant concentration 10 times the expected Kd, 229 pM based on studies with similar regions of interest on the hexon protein (26), was prepared. However, after unsuccessful immobilization we tried increasing the concentration of adenovirus to 52.5 µg/mL, which corresponds to the amount of virus we have in our optimal formulations but did not see an increase in immobilization at any of the pH's (4-6) tested (Figure 3.5B). Various pH's are tested in order to ensure the protein of interest is in a desirable confirmation to bind AR2G receptors, namely below the pI. Since the pI of Adenovirus 5 has been previously recorded as 4.5 (27) and capsid stability below pH 4 remains largely questionable, we were concerned that lowering the pH further would be detrimental to protein stability and further pH scouting was not optimal (28, 29). Therefore, we then attempted switching the orientation, and successfully immobilized the surfactant (Figure 3.5C, Step 3) at a concentration of 1 mg/mL in acetate buffer at pH6, and

prepared adenovirus at 52.5 µg/mL, 105 µg/mL, and 210 µg/mL, and evaluated responses for an increase in binding affinity (Figure 3.5C). However, we were still unable to see a notable increase in binding of adenovirus to the surfactant, which would be indicated by a steep increase in the slope between steps 5 (Baseline) and 6 (Binding). To confirm that the protein integrity had not been damaged due to UV inactivation, which was a part of the identified procedure from which these studies were modeled (26), we did not UV-inactivate the virus and used of 210 µg/mL, but still detected no change in binding affinity.

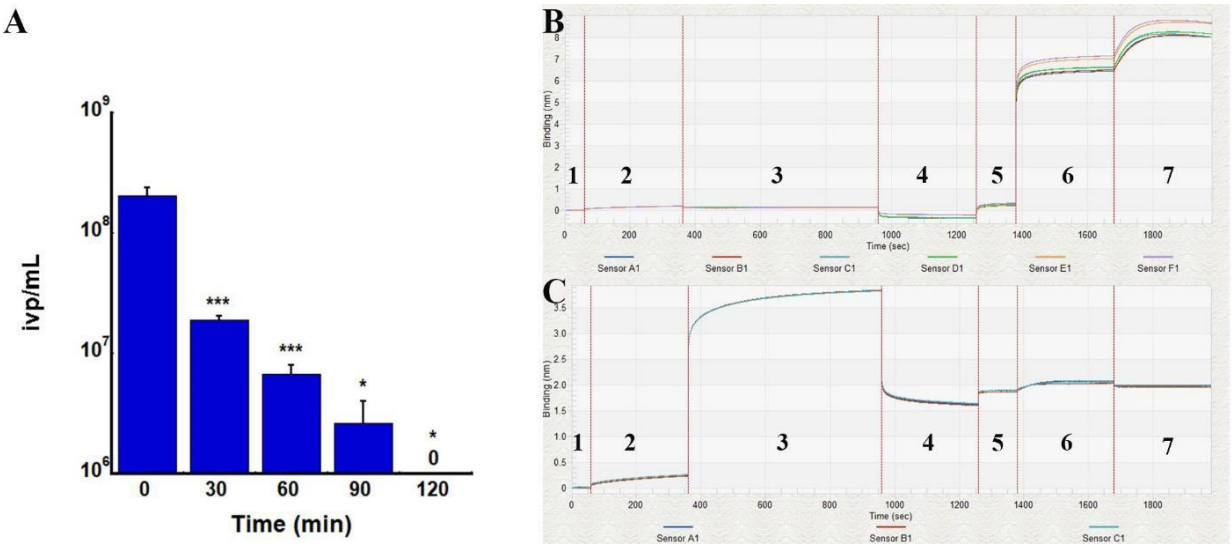

Figure 3.5: Biolayer Interferometry Fails to Detect Notable Adenovirus-Surfactant Interactions.

UV inactivation of adenovirus takes two hours of exposure to λ 365 nm adapted from previous protocol (30) (**A**). Adenovirus was unsuccessfully immobilized on AR2G biosensors and surfactant binding analyzed as indicated by the lack of the sharp increase in slope at step 3 (**B**). Surfactant was immobilized on AR2G biosensors and adenovirus binding analyzed without a detectable affinity as indicated by a lack of a sharp increase in slope at step 6 (**C**). The kinetic responses are shown in binding (18) vs. time in seconds (s). Numbers on graph are associated with individual steps of kinetic analysis: (1) Equilibration of biosensors (2) Activation of

biosensors (3) Immobilization of protein on biosensors (4) Quench (31) reaction of protein immobilization (5) Baseline stabilization in running buffer prior to binding analysis (6) Binding of ligand to protein immobilized on biosensors (7) Dissociation of bound ligand from protein.

Since evaluation of the affinity between surfactant and adenovirus was not quantifiable using BLI, we used isothermal titration calorimetry as it is more sensitive for detecting lower affinities. A concentration of 100 mg/mL of surfactant was selected as this is the solubility limit in Tris and it would guarantee that the surfactant would quickly reach the same concentration it is in the formulation (10 mg/mL) in the cell containing the protein of the ITC experiment. Adenovirus was prepared in the same concentration it is used in our optimized formulation, an estimated 2 nM (32). However, at this concentration we were unable to observe saturation of protein and lowered the concentration to 1 nM and observed a plateau at the end of the thermogram, indicating saturation of proteins was likely occurring. We obtained a dissociation constant (Kd) of $2.25 \times 10^{-9} \pm 0.848 \times 10^{-9}$ M, after accounting for various controls, between the adenovirus and the surfactant. The relevant controls include surfactant injected into buffer, buffer injected into adenovirus, and buffer injected into buffer. We also observed endothermic peaks and a ΔG of -11.8 ± 0.252 kcal/mol, ΔH of -0.578 ± 0.125 kcal/mol, and a $-T\Delta S$ of -11.267 ± 0.289 kcal/mol (Figure 3.6). However, while the thermodynamic values and Kd did not vary between replicate runs, we detected large variation for each individual run. For example, the delta H output for one run was recorded as $0.486 \pm 3.3 \times 10^{8}$ kcal/mol and the Kd $3.06 \times 10^{-9} \pm 1.6$ M. We hypothesize this variation, as well as the large molar ratio detected between interaction of the surfactant and adenovirus, is due to the heterogenous nature of our system: an intact adenovirus capsid and a surfactant which is polydisperse in nature.

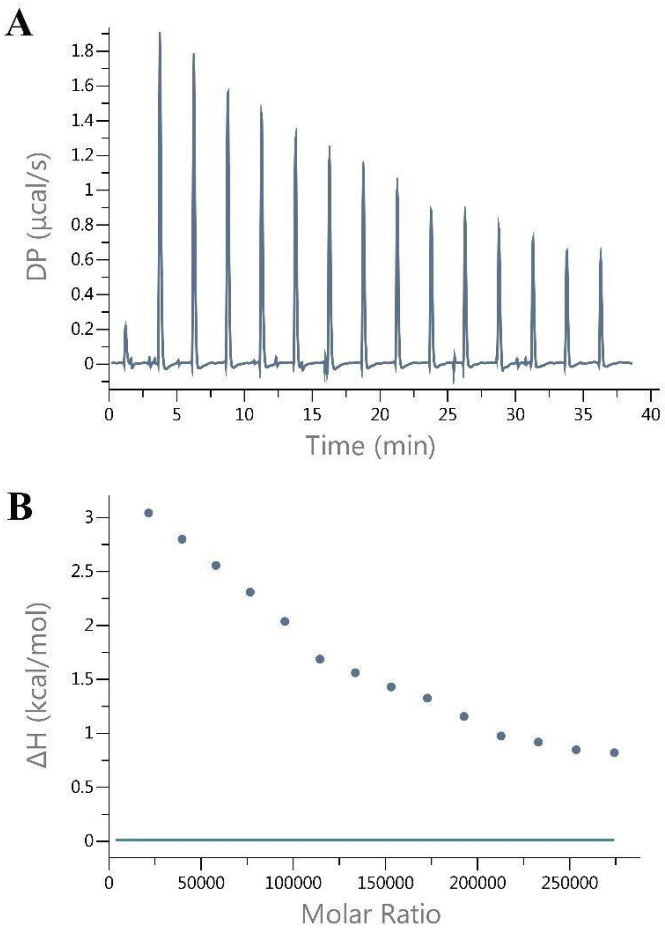

Figure 3.6: Isothermal Titration Calorimetry Reveals Nanomolar Affinity Between Adenovirus and Surfactant.

Surfactant was prepared at a concentration of 1.5 mM in Tris buffer dialysate, and adenovirus was dialyzed in Tris buffer at an estimated concentration 1 nM. Representative ITC results (**A**) and fitting curves (**B**) for surfactant binding to adenovirus are displayed.

3.3.4 A Closer Look at Surfactant and Critical Micelle Concentration

While we have been able to observe the vital role that surfactant plays in adenoviral stabilization at ambient temperatures and the prevention of viral aggregation by TEM, very little information has been published about the properties of the novel surfactant in our thin film

formulation. Poly (maleic anhydride-alt-1-octadecene) substituted with 3-(dimethylamino) propylamine (PMAL), is a zwitterionic surfactant with a formula weight varying from 39,000 to 65,000. Analysis by dynamic light scattering (DLS) resulted in a multi-modal distribution of the surfactant, at the concentration used in our formulation, with intensity peaks at 1.480, 24.44, and 2414 nm and a polydispersity index (PDI) of 0.431 (Figure 3.7). Therefore, the average diameter provided by cumulant analysis (8nm) is unreliable.

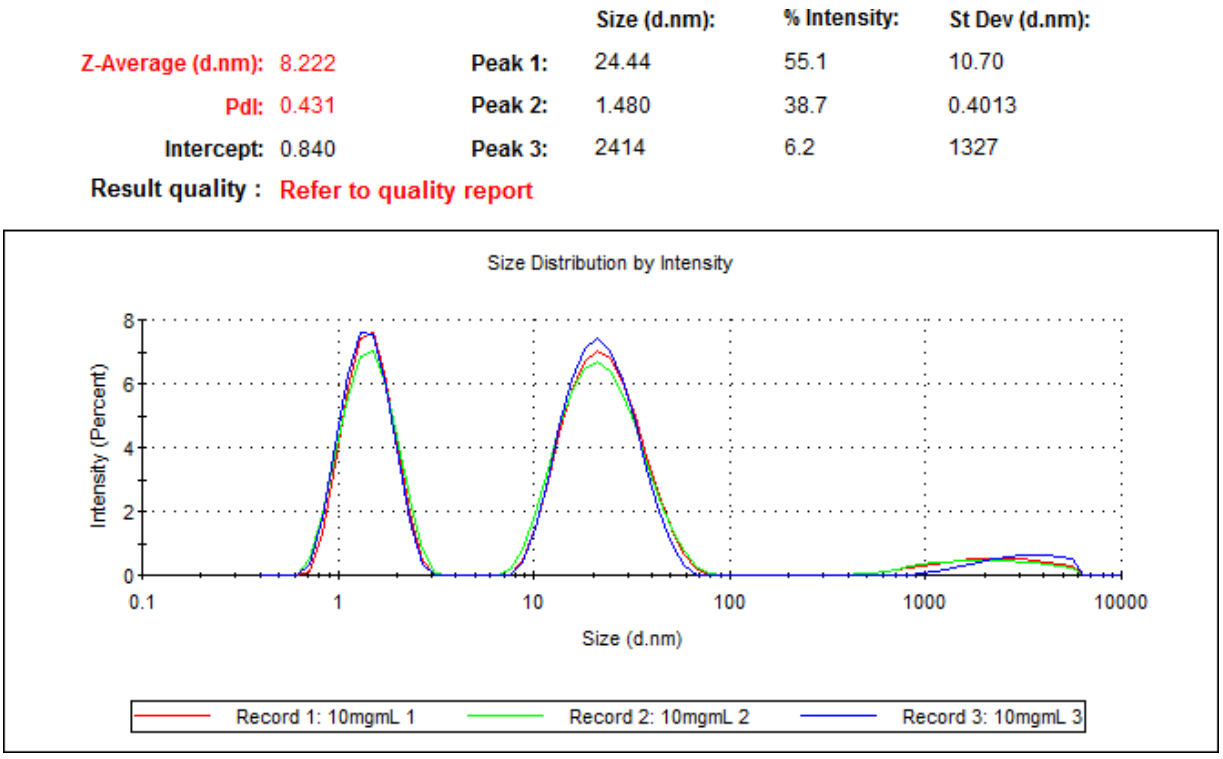

Figure 3.7: Dynamic Light Scattering (DLS) fails to provide insight into the size distribution of polydisperse polymer.

Surfactant samples were prepared by dissolving 10 mg/mL of surfactant in sterile deionized water and filter sterilizing samples through a 0.22µm filter. Subsequent analysis was performed on a Zetasizer Nano (Malvern).

Since we were unable to use DLS to provide reliable characterization information regarding the size of PMAL C-16, we decided to determine the critical micelle concentration (CMC) of our surfactant. The CMC provides important information regarding whether monomers, micelles, or a combination of both are present in formulations and in what format they may be interacting with adenovirus. Due to the viscosity of our optimized formulation, 88 mPa*s (13), we only analyzed the CMC of surfactant in water or in Tris buffer, as the addition of all other formulation components would interfere with the sensitivity of CMC detection. We began our evaluation of PMAL by monitoring the impact of increasing surfactant concentration on the contact angle of solutions using a contact angle goniometer to determine the critical micelle concentration (CMC). As the concentration of a surfactant increases, the contact angle decreases rapidly until the CMC is reached and then stays constant, since the contact angle is a function of surface tension and only the monomeric form contributes to reduction of the surface tension (12). However, due to highly variable results with no clear trend (data not shown) we opted to use a more sensitive technique, rather than attempting to optimize the experimental procedure for improved results. The pyrene fluorescence probe is based on the ratio (I1/I3) of pyrene fluorescence at the first and third vibronic bands (373 and 384 nm) which characteristically increases with increasing polarity. Since pyrene is a hydrophobic molecule pyrene passes from the aqueous phase to the hydrophobic micellar phase with increasing surfactant concentrations, which then lead to a sigmoidal decrease of the I1/I3 ratio (33). The CMC titration of polysorbate 80 (tween 80) was employed as a control and confirmed the accuracy of the pyrene probe technique by indicating 0.015 mM as the CMC in water at 25°C (Figure 3.8A), which is in good agreement with literature values (34, 35). The CMC estimation for the zwitterionic surfactant is provided in mg/mL, as the molecular weight is variable. We

detected a CMC of 2.56 mg/mL in water (Figure 3.8B) and 4.58 mg/mL in Tris (Figure 3.8C). In terms of mM units, the range would then be identified as 0.039 to 0.066 mM for water and 0.07 to 0.117 mM for Tris. This confirms that in Tris, micelles are likely present in solution at a concentration of 10 mg/mL.

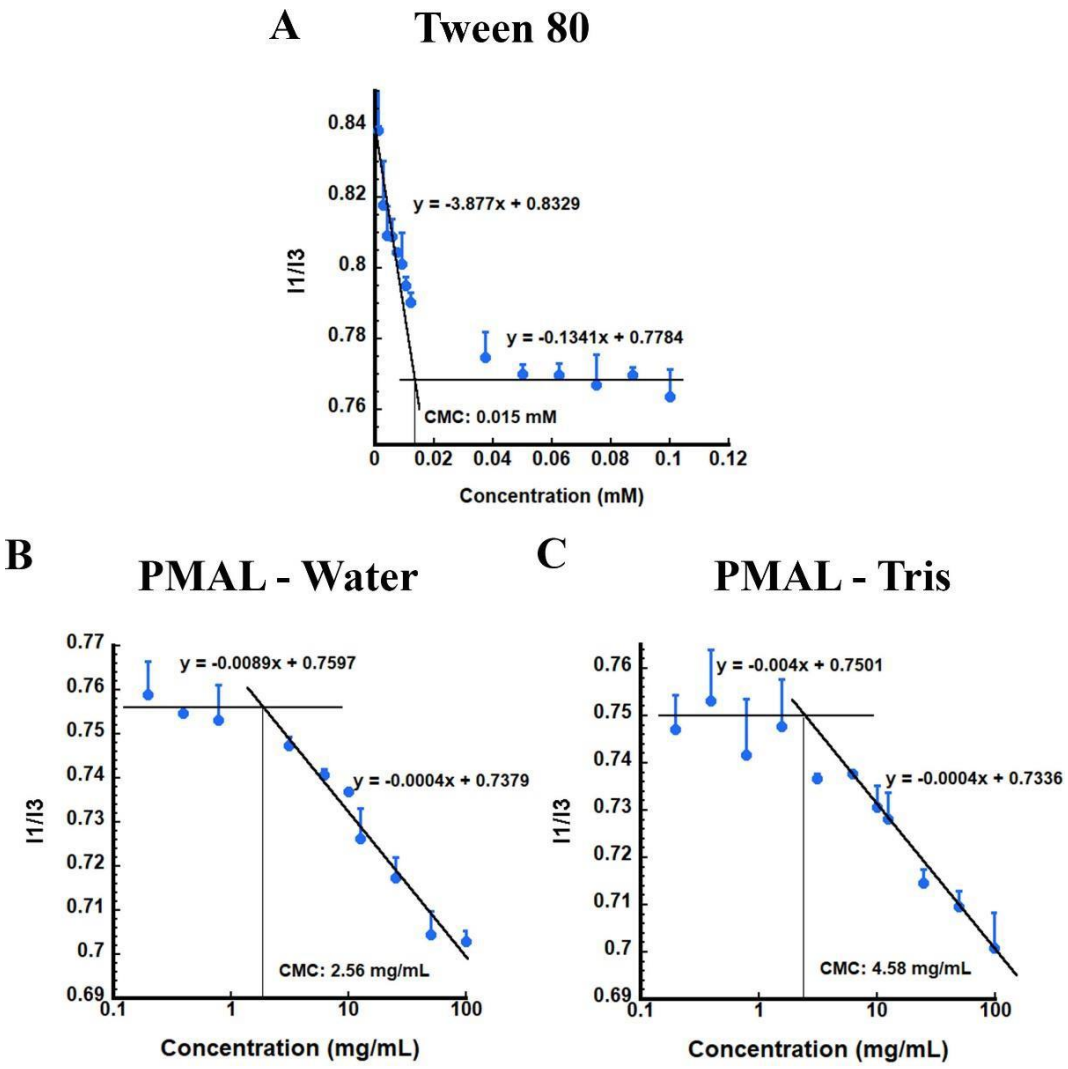

Figure 3.8: Pyrene Fluorescent Probe Confirms Presence of Micelles in Ad-PMAL Formulations.

CMC of Tween 80 was determined to be 0.015 mM, defined as the cross point between the two black lines, using the pyrene probe method (mean ± SD) (**A**). CMC of surfactant in water was determined to be 2.56 mg/mL, defined as the cross point between the two black lines, using the

pyrene probe method (mean ± SD) (**B**). CMC of surfactant in Tris was determined to be 4.58 mg/mL, defined as the cross point between the two black lines, using the pyrene probe method (mean ± SD) (**C**).

Since we have determined the likely presence of micelles in Tris buffer, we decided to evaluate the impact of carbon chain length on adenoviral recovery as the chain length of surfactants affects micelle size. We prepared formulations with the two additional commercially available chain lengths of our surfactant (C8 and C12) and compared them with the surfactant chain length we have been using in the thin film formulation (C16). Films prepared with C8 had the lowest recovery of original infectious titer, 86 ± 0.2 % (Figure 3.9A). C12 containing films maintained 92 ± 0.3 % of their original titer, however C16 films were the most efficient at stabilizing virus by preserving a significantly higher infectious recovery, 97 ± 2.1 %, than both C8 ($p<0.01$) and C12 ($p<0.05$) containing films (Figure 3.9A). Additionally, C12 films had a significantly higher average percent recovery than C8 films ($p<0.05$, Figure 3.9A). We also evaluated if the varying chain lengths had an impact on the magnitude of the zeta potential. Formulations of adenovirus and surfactant C8 and C12 had a zeta potential of 6 mV and 7 mV, respectively, which was significantly lower than the zeta potential of C16 formulations (11 mV; C8 $p<0.05$; C12 $p<0.01$; Figure 3.9B).

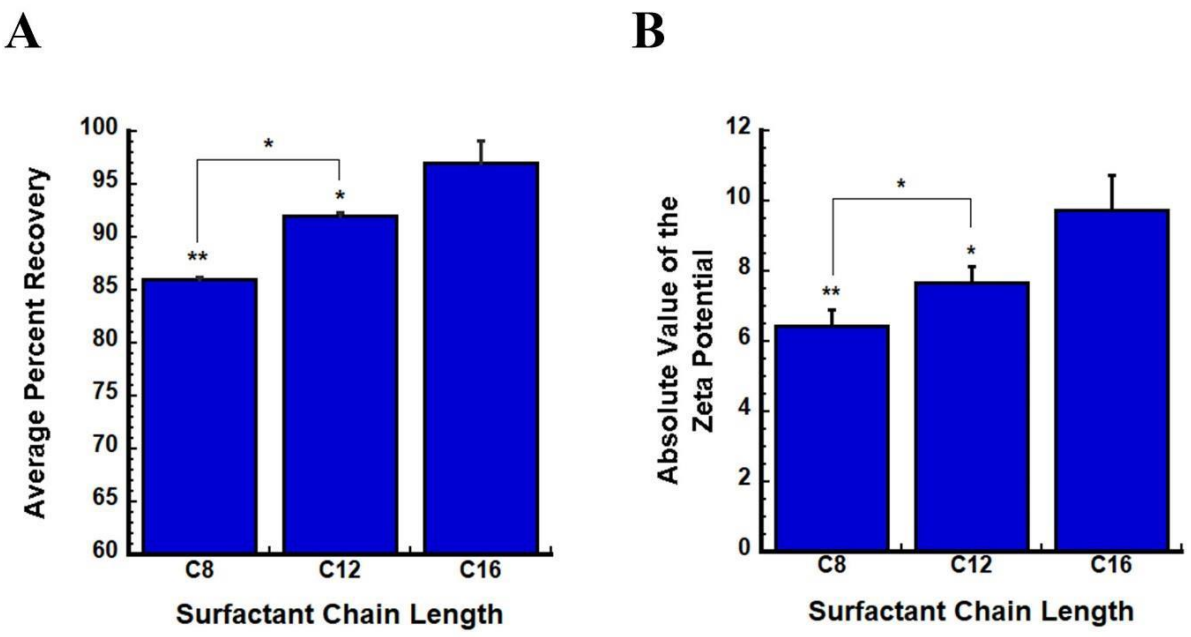

Figure 3.9: Chain Length of Surfactant Impacts Recovery and Zeta Potential from Film Post-Drying.

Recovery of virus from films containing surfactant consisting of chain length 8 (C8), 12 (C12), or 16 (C16) was evaluated using an infectious titer assay **(A).** The magnitude of the zeta potential measurements progressively increased as the carbon chain length increased (**B**). Data represents the average ± the standard deviation, n=3, and was compared to chain length 16 for significance. *p < 0.05, **p<0.01, two-tailed Student's t test.

3.3.5 Evaluation of Complete Formulation

Upon evaluation of the surfactant separate from other formulation components, we wanted to assess the contribution of each component, through the stepwise addition of excipients, to the thermal stability and moisture content of the complete, optimized formulation. Evaluation of the thermal stability, with thermal gravimetric analysis (TGA), provides insight into the strength of the interactions of the formulation components based on how much heat is

required to break the matrix that we hypothesized formed (13) via the association of formulation excipients. Figure 10 displays a sample thermogram, obtained via TGA, from the analysis of: B(base), BS (base and sorbitol), BSS (base, sorbitol, and surfactant), and BSSV (base, sorbitol, surfactant, and virus) which shows that the first thermal transition is over at around 140°C, indicative of physioadsorbed water evaporation (36), and immediately followed by thermal degradation for BSS and BSSV samples, as shown by the dramatic weight loss of the sample (Figure 3.10 C &D). However, samples without surfactant complete the first thermal transition around the same temperature, but thermal degradation does not begin until 180°C (Figure 3.10 A & B).

Moisture content plays an important role in protein stability as hydrolysis can lead to the break-down of proteins and impact stability of viruses over time (16, 37-39). Analysis of the impact of excipients on total water retained, by the end of the first thermal transition, revealed that the addition of sorbitol (17) and surfactant (BSS) resulted in a significant increase in moisture retained in the film, 9.03% ± 0.02% ($p<0.05$) and 9.71% ± 0.514% ($p<0.05$) respectively, relative to films prepared with base alone (B: 7.67% ± 0.292%, Figure 3.11A). The addition of adenovirus to the complete formulation containing base, sorbitol, and surfactant (BBSV) resulted in an increase in the total water retained, 13.34% ± 1.345%, as well (Figure 3.11A).

As TGA analysis provides an estimation of water retained based on the change in weight of the sample by 150°C, this technique may not be specific enough for determination of water content. We analyzed the difference between the moisture content for BSSV samples determined with volumetric Karl Fisher (KF) titration and compared it to the total mass of water retained determined by TGA and found that both techniques produced comparable results (TGA: 13.34%

± 1.345%; KF: 13.53 ± 017%, $p>0.05$, Figure 3.11B). As the KF results had lower variability, we used that technique to determine whether increase in moisture content of films prepared with adenovirus was due to the addition of glycerol, as our laboratory prepares adenoviral stocks containing glycerol. While there was a higher moisture content in films prepared with 2.5% glycerol in PBS (13.0% ± 0.297%) than films without glycerol, films prepared with adenovirus had a slightly (but significantly) higher moisture content (13.53% ± 0.17%, $p<0.05$; Figure 3.11C).

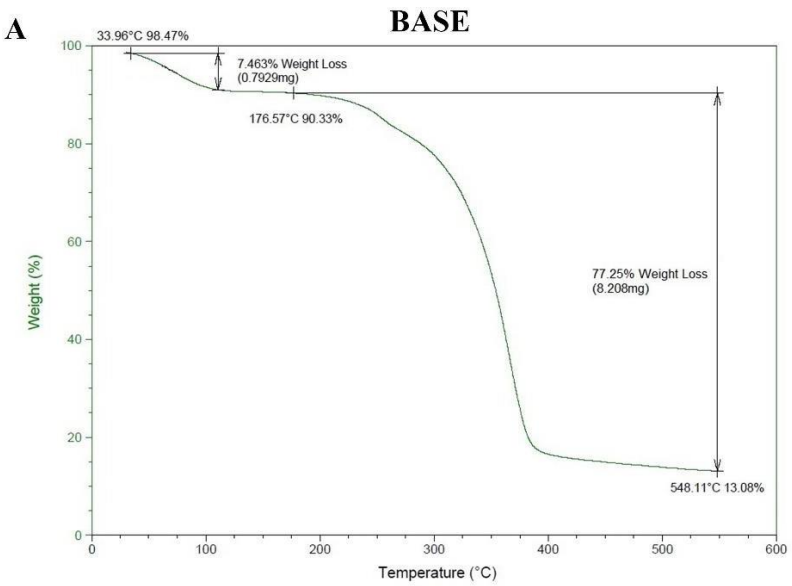
A
BASE
33.96°C 98.47%
7.463% Weight Loss
(0.7929mg)
176.57°C 90.33%
77.25% Weight Loss
(8.208mg)
548.11°C 13.08%
Weight (%)
Temperature (°C)

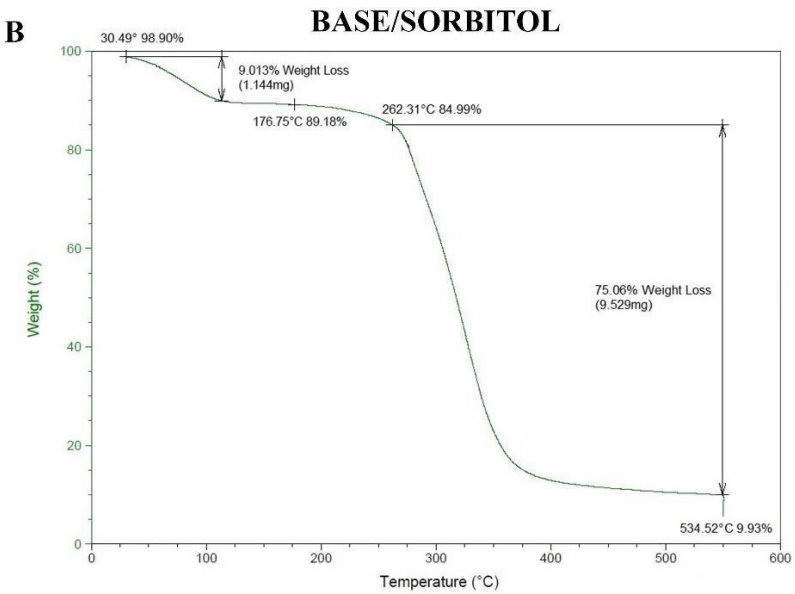
B
BASE/SORBITOL
30.49° 98.90%
9.013% Weight Loss
(1.144mg)
176.75°C 89.18%
262.31°C 84.99%
75.06% Weight Loss
(9.529mg)
534.52°C 9.93%
Weight (%)
Temperature (°C)

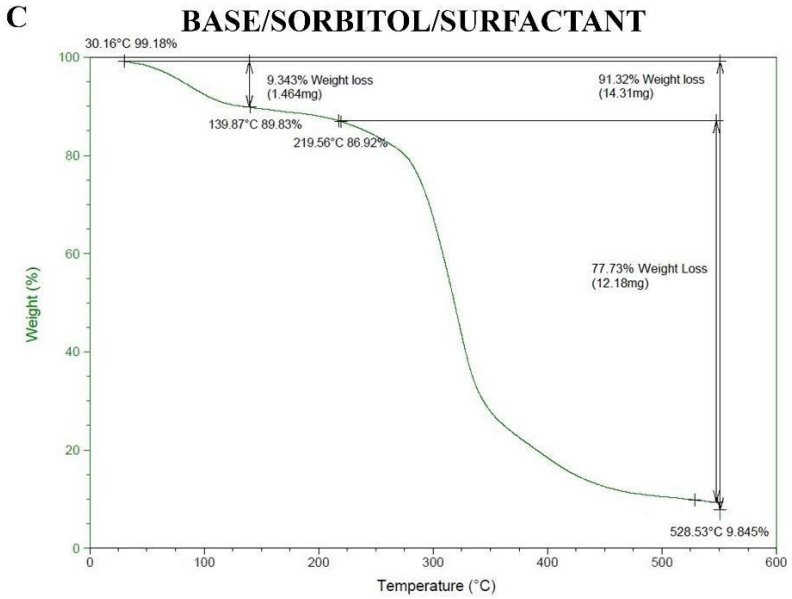
C
BASE/SORBITOL/SURFACTANT
30.16°C 99.18%
9.343% Weight loss
(1.464mg)
139.87°C 89.83%
219.56°C 86.92%
91.32% Weight loss
(14.31mg)
77.73% Weight Loss
(12.18mg)
528.53°C 9.845%
Weight (%)
Temperature (°C)

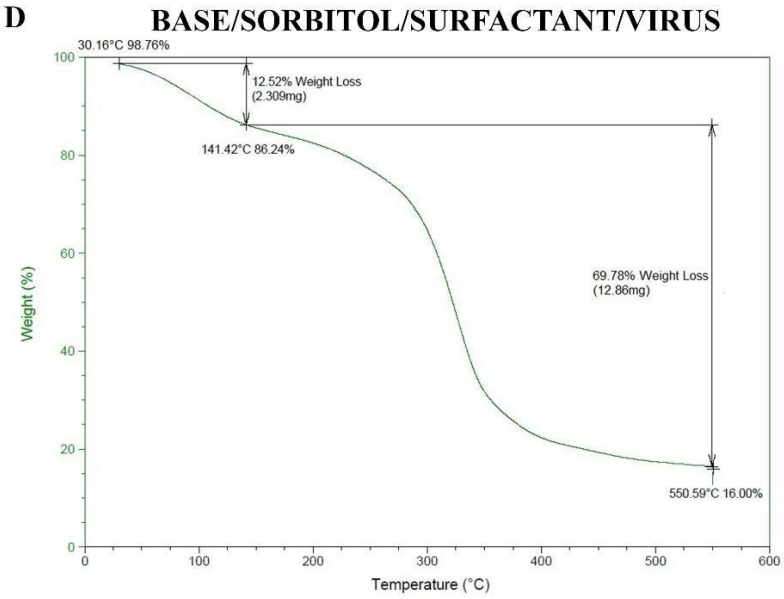
D
BASE/SORBITOL/SURFACTANT/VIRUS
30.16°C 98.76%
12.52% Weight Loss
(2.309mg)
141.42°C 86.24%
69.78% Weight Loss
(12.86mg)
550.59°C 16.00%
Weight (%)
Temperature (°C)

Figure 3.10: Excipients work together to maintain uniform moisture content in dried films. Sample thermal gravimetric analysis profiles taken after sequential addition of excipients to the optimized thin film matrix. **(A)** Base alone, **(B)** Base and Sorbitol, **(C)** Optimized formulation in the absence of virus and **(D)** containing virus formulated in 2.5% glycerol.

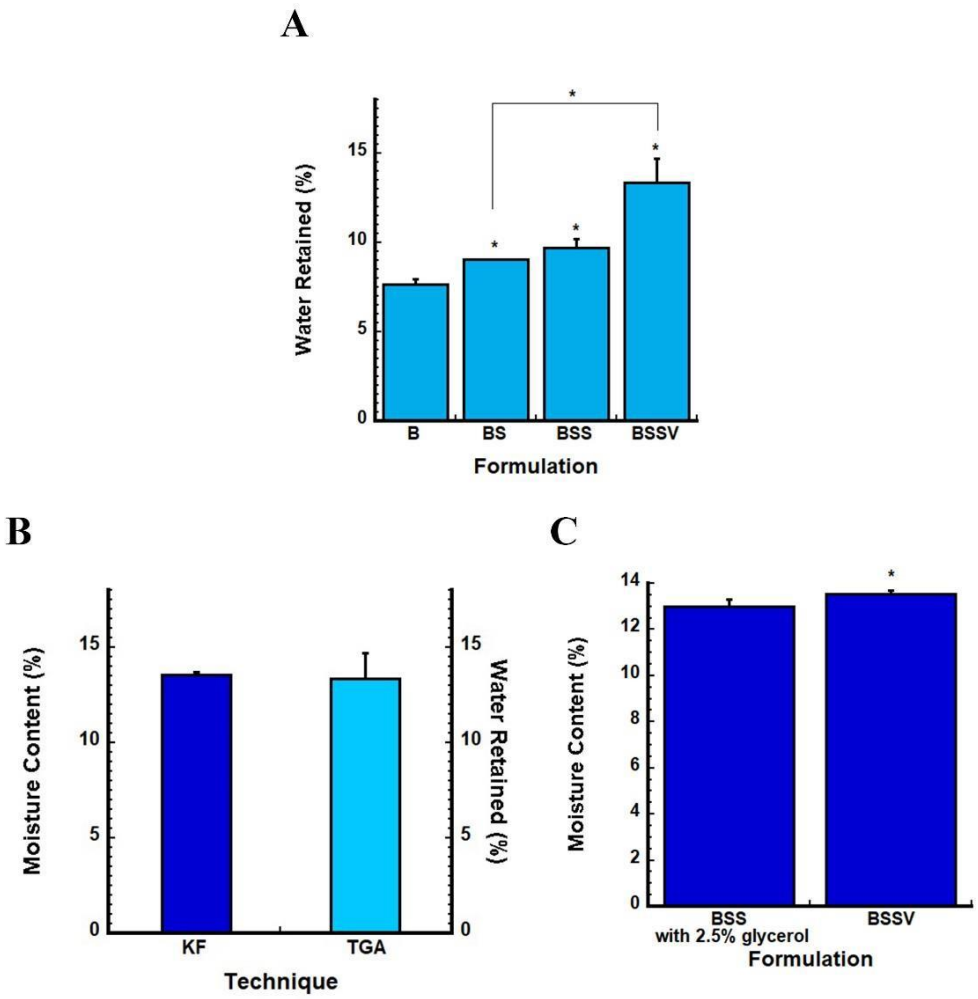

Figure 3.11: Moisture content is significantly impacted by the presence of sorbitol and surfactant in thin film formulation.

Formulations were prepared with base (B), base and sorbitol (17), base sorbitol and surfactant (BSS), and base, sorbitol, and surfactant with adenovirus (BSSV). TGA analysis revealed that

the stepwise addition of formulation excipients results in an increase in water retained (**A**). Volumetric KF Titration and TGA yield comparable values for moisture content for BSSV samples (**B**). The addition of 2.5% glycerol to account for adenoviral stock preparations in thin films containing base, sorbitol, and surfactant results in an increase in moisture content using KF (**C**). Data represents the average ± the standard deviation for a minimum of n=3. *p<0.05, **p< 0.01, ***p<0.001, two-tailed Student's t test.

3.3.6 Translatability of Thin Film Platform

Since our previous studies illustrated the importance of surfactant in formulations for adenoviral stabilization, we wanted to evaluate how viruses with alternative properties are impacted by formulation components and if the thin film platform is versatile. We compared the infectious titer for the following viruses in our novel formulation: adenovirus (Ad), adeno-associated virus (AAV), respiratory syncytial virus (RSV), herpes simplex virus (HSV), and influenza (H1N1). Table 3.2 provides an overview of size, presence of envelope, surface charge, and genomic material for each virus. The observed stability profile with the surfactant for Ad (97 ± 2.1%), AAV (98.1 ± 2.4%), RSV (95 ± 0.78%), and HSV (98 ± 1%) was not as high for the influenza virus (63 ± 5.1%) (Figure 3.12A). So, we evaluated how stepwise addition of each formulation component, base (BV), base with sorbitol (BSV), and base with sorbitol and surfactant (BSSV), impacted recovery of H1N1 to see if it would provide additional insight into the reduced recovery. The addition of each formulation component, BV: 75 ± 1% (74%, 75%), BSV: 68 ± 2.1% (66%, 69%), and BSSV: 63 ± 5.1%, resulted in a notable decrease of the average percent recovery compared to unformulated H1N1 (Control, 97.8 ± 2.4%, Figure 3.12B). Data is provided as the average ± standard deviation since this is most representative of the

spread of the data as well the actual values for each sample, since n=2 for samples BV and BSV. We also found that the removal of sorbitol from the formulation did not improve recovery of influenza either (62 ± 0.5%, data not shown). This was surprising as previous studies with adenovirus have shown that the stepwise addition of each excipient resulted in gradually improved recovery of virus, with the recovery of adenovirus in base alone starting below 60% and increasing to 90% with the addition of sorbitol and 98% with the addition of surfactant (13). As the base is essential for film formation, this indicated that either an alternative excipients were needed to improve the recovery of H1N1 from films.

Table 3.2: Viruses evaluated for compatibility with the thin film matrix

Virus	Size (18)	Enveloped	Surface Charge	Genomic Material	Reference
Adenovirus (Ad)	70 - 100	No	Negative	dsDNA	(40)
Adeno-associated virus (AAV)	25	No	Negative	ssDNA	(41)
Respiratory syncytial virus (RSV)	150 -250	Yes	Negative	ssRNA	(42)
Herpes simplex virus (HSV)	150 - 240	Yes	Negative	dsDNA	(43)
Influenza (H1N1)	80 - 120	Yes	Positive	ssRNA	(44)

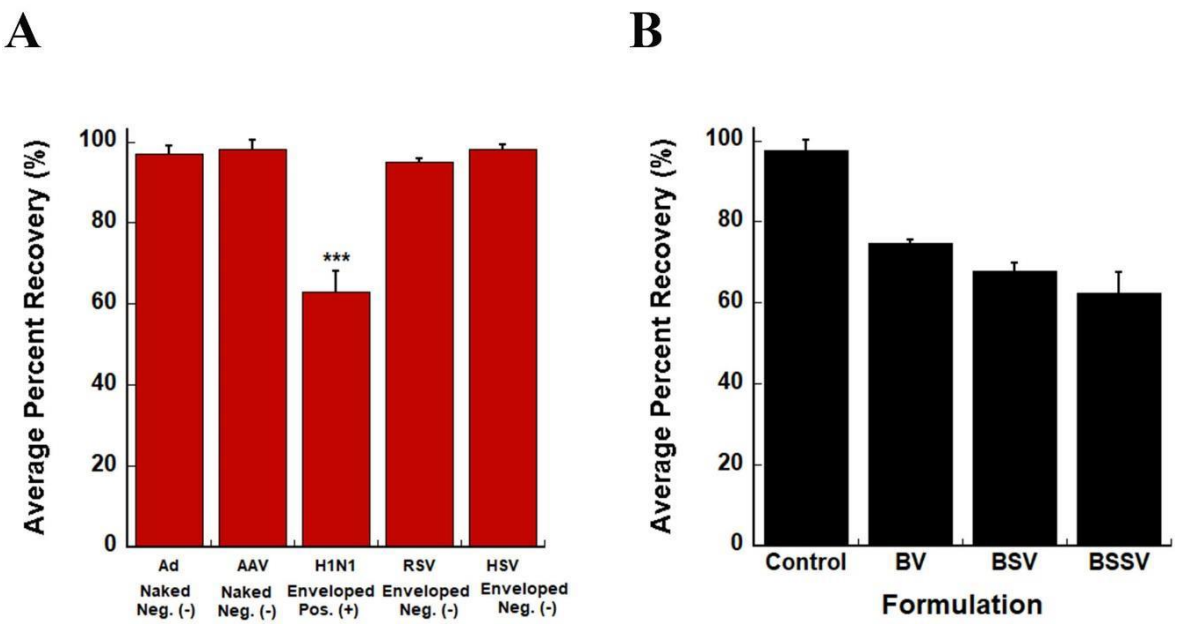

Figure 3.12: Thin Film Platform is Incompatible with Influenza Virus.

Recovery of adenovirus (Ad), adeno-associated virus (AAV), influenza (H1N1), respiratory syncytial virus (RSV), and herpes simplex virus from optimized thin film platform evaluated using infectious titer assays for a minimum of n=3, ***p< 0.001, two-tailed Student's t test (**A**). Stepwise addition of formulation excipients results in decreased recovery (**B**). Control is unformulated H1N1, BV is base with H1N1, BSV is base with sorbitol and H1N1, BSSV is base with sorbitol, surfactant, and H1N1. Data represents the average ± the standard deviation. Statistical analysis was not performed as n=2 and would not be meaningful.

Due to the predominately positive surface charge of H1N1, likely due to positively charged surface protein Hemagglutinin, we began our troubleshooting with the surfactant. Since our surfactant is zwitterionic in charge, we hypothesized that the reduction in recovery was due to partial viral inactivation, mitigated by the negatively charged arm of the surfactant interacting with Hemagglutinin. We prepared formulations with alternative concentrations of choline, a

positively charged surfactant (Figure 3.13A), anticipating that is would not adversely interact with H1N1. The least successful concentration, 0.5% w/v choline, only retained 80 ± 0.95% (79%, 80%) of the original infectious titer (Figure 3.13B). Higher concentrations resulted in improved recovery of infectious titer: 1%w/v choline maintained 99 ± 2% (98%, 101%), 3% w/v choline maintained 96 ± 0.5% (96%, 97%), 5% w/v choline maintained 102 ± 0.45% (102%, 103%) and 8.5% choline w/v maintained 94 ± 2.8% (92%, 96%). However, after 3 days at 25°C there was no detectable infectious titer in the films containing any concentration of choline and the pH had increased from 7.5 to 8.5. Additionally, a cytotoxicity study conducted on TR146 cells, an *in vitro* model of the human SL and BU mucosa (45), revealed that 5% w/v choline films, without H1N1, resulted in a significant reduction in viable cells ($3.7 \times 10^{-6} \pm 1.1 \times 10^{-6}$ RLU; $p<0.001$) after only 30 minutes, relative to untreated cells ($2 \times 10^{7} \pm 4.18 \times 10^{5}$ RLU; Figure 3.13C). At the end of the two-hour sampling period, 5% w/v films without H1N1 had reduced the amount of viable cells even further ($1.4 \times 10^{-5} \pm 3.8 \times 10^{-4}$ RLU). We hypothesized that choline was increasing cellular uptake of H1N1 by solubilizing cell membranes, as has been documented in the literature, and therefore improving recovery from films but also increasing cytotoxic response (46, 47). As previous studies have shown that the formulation with the original surfactant are not cytotoxic (13), choline was abandoned as a viable replacement.

Calcium α-d-heptagluconate dihydrate (heptagluconate) (Figure 3.13D) was identified as an alternative excipient for evaluation as previous studies have found that this excipient, in combination with sodium carboxy methyl cellulose, successfully stabilized H1N1 influenza (48). As the base in our formulation is similar to carboxy methyl cellulose we hypothesized that this excipient may be a better addition to our base than sorbitol or the surfactant we currently use. Films prepared, dried, and reconstituted the following day with our base and heptagluconate

maintained 99 ± 4.2% (96%, 102%) of the original infectious titer and pH of 6.5, which substantially higher than the original formulation and comparable to choline (Figure 3.13E). A preliminary stability study revealed that liquid formulations and films stored at 4°C retained 100 ± 0.3% (100%, 100.4%) and 97 ± 1.5% (98%, 96%), respectively, of the original infectious titer for 21 days (Figure 3.13F). The liquid formulations and films stored at 25°C retained 84 ± 1.4% (83%, 85%) and 71 ± 0.71% (70%, 71%), respectively, of the original infectious titer at this time. There were no detectable changes in pH. The addition of heptagluconate to sorbitol and our base, surfactant and our base, or sorbitol, surfactant and our base, resulted in crystallized films, which were not suitable for evaluation.

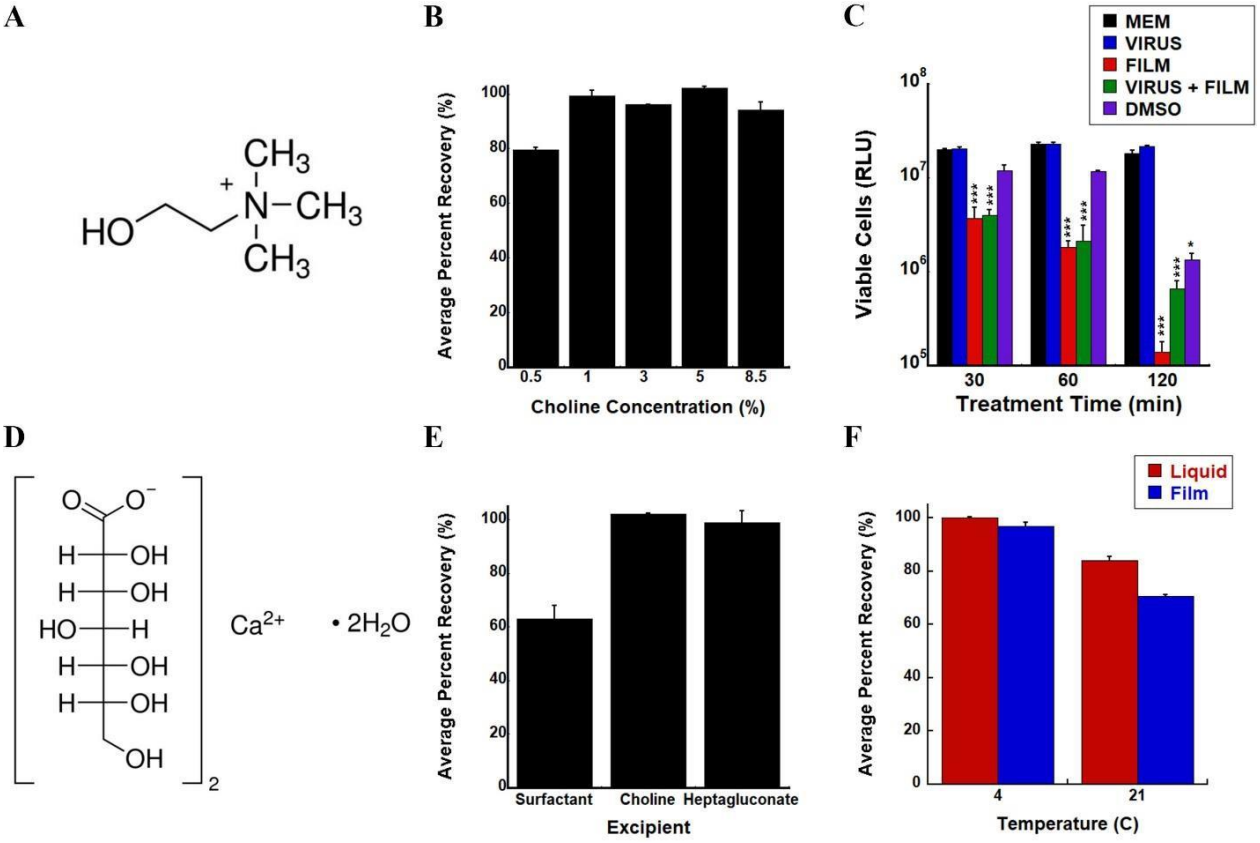

Figure 3.13: Thin Film Formulation Improved for Influenza Stabilization.

Structure of Choline (**A**). Varying concentrations (w/v) of choline optimize recovery of influenza from films containing HPMC and sorbitol (**B**). Cell activity was assessed by measuring the amount of adenosine triphosphate (ATP) in cultures using a Cell Titer-Glo Luminescent Cell Viability assay kit from Promega (**C**). TR-146 were treated for 30, 60, and 120 min with MEM media, influenza virus (virus), choline films, choline films with influenza, and DMSO. Data represents the average ± the standard deviation, n=3. *p < 0.05, **p< 0.01, ***p < 0.001, two-tailed Student's t test. Structure of Calcium α-D-heptagluconate dihydrate (**D**). Optimized formulation containing surfactant (1% w/v), HPMC/sorbitol/choline (5% w/v), and HPMC/calcium α-d-heptagluconate dihydrate (5%w/v) were evaluated for their effect on influenza stabilization using a traditional infectious titer assay (**E**). Influenza (3×10^8 ivp/mL) was placed in formulations consisting of HPMC and choline and stored in the liquid form and film in controlled environmental chambers held at 4° and 20°C for 21 days. Replicate samples (n=2) were collected at each time point, and live virus concentration was assessed by a standard infectious titer assay (**F**). Statistical analysis was not performed as n=2 and would not be meaningful for Panels B, E, and F.

3.4 Discussion

Effective stabilization of vaccines at ambient and elevated temperatures is a critical step towards providing global access to immunization. A variety of pharmaceutical excipients have been identified as protein stabilizers and have been used in formulations to prevent the viral degradation at 2-8°C and ultra-low temperatures (Appendix Table 1 & 2). Sugars, polymers, and surfactants have been used for their ability to prevent adsorption to surfaces, aggregation, and/or

hydrolysis of viral proteins via electrostatic interactions, micelle formation, or hydrogen bonding (49). We recently demonstrated that a multi-component formulation consisting of a polymer base, sugar, and surfactant was able to protect adenovirus serotype 5 from temperature-mediated degradation in both a liquid and thin film format (13). In order to better understand how each excipient contributed to the stabilization of adenovirus, a stepwise analysis of each formulation component was conducted. We found that the pH range of 6 to 8 within the thin film matrix correlated to more successful stabilization of adenovirus (13, 16, 19). We also found that the pH of the final formulation was reduced when drying was complete. This was most likely due to the concentrations of buffering agents and their interactions with formulation excipients during the film forming process (13, 50). The polymer base played a key role in maintaining the three dimensional and structural conformation of adenovirus capsids due to its ability to form strong intramolecular hydrogen bonds (13, 51). This was evident when formulations prepared with this excipient alone failed to successfully release the entire viral dose loaded into the film (13). The polymer base also resulted in significantly more viscous formulations, possibly contributing to minimal molecular mobility and stability. With the addition of sorbitol to the polymer base, we observed improved stability of adenovirus likely due to the excipient's contribution to the three-dimensional matrix of the film via strong interactions with the polymer base and sorbitol. Sorbitol and surfactant also decreased drying time of thin films (13). We hypothesized that this occurred due to the ability of excipients to replace water molecules and interact with other excipients, while maintaining a minimal level of surface protein hydration to prevent denaturation of the virus capsids. The resulting film was an amorphous solid with a high glass transition temperature, preventing excipient crystallization (13). However, while the vital role of the surfactant in adenoviral stabilization was evident, the mechanism of stabilization remained

unclear. Consistently, formulations prepared with surfactant stabilized adenovirus at 4°C and 20°C for three months and 40°C for 5 days more efficiently than formulations lacking the surfactant (13). The aim of these studies was to characterize the surfactant and determine how it interacts with adenoviral capsids, as well as the other formulation excipients, to maintain stability. We also explored the translatability of our novel thin film platform by evaluating viruses with various properties.

Poly (maleic anhydride-alt-1-octadecene) substituted with 3-(dimethylamino) propylamine (PMAL, C-16), the zwitterionic surfactant in our novel thin film formulation, belongs to a new class of surfactants known as amphipols. Since amphipols are relatively new compounds, there is a limited amount of characterization information currently published on these surfactants. While PMAL C-12, chain length 12, has previously been used to protect detergent solubilized-ATPase from the catalytic activity of the detergent by preventing aggregation of complexes (52), and PMAL C-8, chain length 8, has been used to solubilize a number of membrane proteins for characterization (53-56), there are no published articles, to date, characterizing PMAL C-16. The most important characteristic of surfactants is the critical micelle concentration (CMC) because proteins interact very differently with monomeric and micellar conformations of surfactants (57). For example, ionic surfactants, and some nonionic and zwitterionic surfactants, denature proteins below their CMC. We found that while the CMC of PMAL in water (2.56 mg/mL, or 0.0039 mM to 0.066 mM) was lower than the CMC in Tris (4.58 mg/mL, or 0.070 to 0.117 mM; Figure 3.8), formulations of PMAL-Ad were still above the CMC and likely had micelles present in solution. Tris buffer has previously been documented to increase the CMC of SDS, likely by reducing the hydrophobic interactions of the surfactant with itself (58). It is difficult to determine if micelles are present in the complete optimized

formulation (13), due to the viscosity and addition of other formulation excipients. However, it has previously been established that premicellar aggregation of amphipols begins at concentrations four times lower than those indicated by fluorescent spectroscopy methods (59-61) and that premicellar aggregates are present in all stable working concentrations of amphipols (62). Therefore, we believe that if micelles are not present in the complete formulation, premicellar aggregates likely are and still contribute to the overall stability of adenovirus. We also evaluated the impact of shorter alkyl chain lengths, PMAL C-8 and PMAL C-12, on stabilization of adenovirus and found that with decreasing chain length infectious titer decreased (Figure 3.9). This may be related to their reduced ability to form micelles as the shorter the hydrophobic chain, the less likely micelle formation will occur because the hydrophobicity of the surfactant decreases, effectively reducing the affinity for self-association (63, 64). However, we also observed a reduction in the zeta potential with decreasing alkyl chain length (Figure 3.9). This is indicative of weaker repulsive forces resulting in formulation aggregation (25). Taken together, we hypothesize due to the reduced ability of C8 and C12 to form micelles, in comparison to C-16, and overall reduced hydrophobic nature, that premicellar aggregates are less effective at stabilizing adenovirus than the more hydrophobic C-16 amphipol. It is important to note that the I1/I3 ratio for both Tween 80 control and PMAL samples was less than one at the concentrations tested. This is indicative of a hydrophobic environment in which fluorescence intensity emissions of pyrene at wavelength 383 are greater than those at 373 (65). After testing alternative organic solvents, like dimethyl sulfoxide to attempt to increase the ratio above 1, adjusting the gain on the instrument, as well as testing a variety of clear polystyrene plates available, we were unable to generate a I1/I3 ratio greater than 1 with an accurate estimation of the Tween 80 control. Therefore, we decided to report the values of the CMC, that were

generated using the protocol described in the methods section, which resulted in an accurate estimation of the CMC of Tween 80, for PMAL C-16. However, future studies should validate the estimation we determined using the pyrene fluorescent probe technique either on a different instrument or via alternative methodologies which focus on other properties impacted by micelle formation such as conductivity and rheology. The contact angle or surface tension of increasing surfactant concentration solutions may also be attempted again on an alternative surface, as PFTE resulted in random results which were not reproducible. This may be because while PMAL is neutral overall, it is zwitterionic and carries both positive and negative charges meaning it may have adsorbed to the surface of the PFTE sheets. The polydisperse, heterogenous nature of PMAL, however, may also provide additional difficulties in using surface properties in the determination of CMC.

After determining the CMC and impact of chain length, we began to explore the interaction of adenovirus with our amphipol, PMAL. Amphipols were originally synthesized to adsorb onto the surface of membrane proteins in order to solubilize and stabilize them for in-vitro evaluation (66-68). We observe a similar behavior between our amphipol, PMAL, and adenovirus capsids via zeta potential measurements. Zeta potential measurements can be described as the electrical potential at the slipping plane, which is the boundary which separates the rest of the solution from the part of the solution that is attached to the surface of the particle (25). After three days at room temperature, formulations consisting of adenovirus and PMAL had a zeta potential equal to that of formulations containing only our surfactant in buffer, indicating that surfactant may have adsorbed to the surface, or is surrounding the surface, of adenovirus capsids and that the zeta potential of surfactant is dominating the readout after 3 days (Figure 3.4). TEM images support this hypothesis by depicting surfactant surrounding adenoviral

capsids and preventing viral aggregation (Figure 3.1). It is important to note that sample preparation required a 1:10 dilution in water for clear visualization of adenovirus capsids and may not be representative of the formulation at increased concentrations of surfactant. This behavior corresponds with the strong stability of adenovirus in PMAL-only formulations for 28 days at room temperature as well as fewer unidentified protein bands following SDS-PAGE analysis (Figure 3.3). As there was no impact on transduction efficiency of adenovirus, we believe the 3 unidentified protein bands missing from PMAL-adenovirus formulations, relative to adenoviral controls, may be loose protein contaminates which can cause viral particle inactivation via aggregation (69), and that the presence of surfactant displaces these impurities from the viral surface and contributes to stabilization. We also hypothesize that the reduced band sharpness of protein IIIa in PMAL-adenovirus formulations (Figure 3.3) is likely linked to the protective effects of the surfactant preventing complete denaturation of proteins, since there was no reduction in transduction efficiency. It is important to note that membrane proteins, for which amphipols were originally designed to adsorb to the surface of, have a hydrophobic surface (67) and the adenoviral capsid consists of proteins which have both hydrophobic and hydrophilic regions (70). This likely impacts the affinity of PMAL to the surface of the adenovirus capsid, relative to a purely hydrophobic membrane protein surface. Furthermore, due to the polydisperse, heterogenous nature of the surfactant at the concentration used in our formulations (Figure 3.7) the zeta potential measurements are not robust enough to definitively conclude that the surfactant uniformly adsorbs to the capsid surface, as previous studies have shown that larger agglomerates (1000 nm) can predominantly govern the estimated zeta potential overshadowing smaller species in polydisperse samples (71). Hence, further studies were conducted to evaluate surfactant affinity and association with adenoviral capsids.

Amphipols were designed to stabilize and solubilize membrane proteins by binding the hydrophobic surface of the protein at multiple contact points via non-covalent interactions. This results in slow dissociation rates and permanent binding of the membrane proteins. They will only unbind membrane proteins in the presence of a competing surfactant or lipid that has a high affinity for the target protein (67). With the concept of competitive inhibition in mind, we designed a saturation study wherein adenovirus was incubated with amino acid saturated surfactant. Glutamic acid and aspartic acid residues have previously been identified as two amino acids contributing to the overall negative charge of the hexon protein on adenovirus capsids (14, 70) and were used to determine whether PMAL had a unique affinity to the amino acids, and in turn the hexon protein. We hypothesized that we would see a steady decline in the stability of adenovirus samples prepared with amino-acid saturated surfactant due to the inability of the surfactant to interact with, and stabilize, adenovirus capsids. Surprisingly, infectious titer in samples prepared with adenovirus and glutamic-acid saturated surfactant was undetectable after only three days (Figure 3.3). Since glutamic acid only differs in structure from aspartic acid by the addition of one methylene group and pH controls did not follow the same trend, we repeated the study to guarantee that the effect we were seeing was reproducible. Through two additional runs of the study, we confirmed that glutamic acid was interacting with surfactant in a unique way which resulted in reduced transduction efficiency. We were able to determine that post-translational modifications were not responsible for the impact on transduction efficiency, as all samples incubated with amino acid-saturated surfactant or amino-acid controls had no difference in band pattern, relative to adenoviral controls, following SDS-PAGE analysis (Figure 3.3). Furthermore, the pH (5.5) could not be solely responsible for the impact on transduction efficiency as formulations prepared with aspartic acid-saturated surfactant, aspartic acid, and

glutamic acid had equal or lower pH values (Table 3.1) but did not result in reduced transduction efficiency until later time points (Figure 3.3). A possible explanation for the unique affinity of PMAL to glutamic acid might be linked to the reason amphipol's were originally designed: to adsorb to hydrophobic surfaces. Since glutamic acid has one additional methylene group, making it slightly more hydrophobic than aspartic acid, PMAL may have created a stronger complex with glutamic acid and subsequently irreversibly bound adenovirus, reducing transduction efficiency. Glutamic acid and PMAL may have also formed a complex that inadvertently impacts adenovirus transduction efficiency by inducing aggregation of viral capsids or by some other undetermined mechanism. Zeta potential measurements provided additional insights on the stability of the amino-acid complexes formed, based on their repulsive forces, and support this hypothesis. Guidelines classifying the stability of nanoparticle solutions, based on zeta potential measurements, have commonly been used in the literature and are defined as: ± 0 to 10 mV (highly unstable), ± 10 to 20 mV (relatively stable), ± 20 to 30 mV (moderately stable), and > ± 30 (highly stable) (25). Based on these categories after three days, glutamic acid saturated surfactant is a moderately stable solution, aspartic acid saturated surfactant and adenoviral control are relatively stable solutions, and aspartic acid, glutamic acid, and surfactant adenoviral controls are highly unstable solutions (Figure 3.4). According to these classifications, the magnitude of the zeta potentials, the impact on transduction efficiency and SDS-PAGE, the likely presence of micelles or premicellar aggregates, and TEM images we hypothesize that surfactant surrounds the adenovirus capsid in micelle form and prevents viral aggregation (Figure 3.14A) or forms a bilayer vesicle. While we are unsure of the exact orientation of surfactant relative to adenovirus, we hypothesize that the interaction between PMAL and adenovirus is partially driven by electrostatic interactions (13, 14). Since the hydrophilic regions

of the hexon protein have previously been identified (70) as having a stronger negative charge (-12.3 to -20.97) than the hydrophobic regions (-3.62 to -5.85) we believe it is unlikely that nonionic and hydrophobic tails of the zwitterionic PMAL are facing the adenoviral surface, whether micelles or premicellar aggregates are present, and suggested the conformations above as the two most likely orientations of surfactant-adenovirus interactions. As the zeta potential is significantly higher for glutamic acid saturated surfactant than all other samples, we also hypothesize that the strength of repulsion in turn may impact transduction efficiency and make it difficult for adenovirus to infect cells (Figure 3.14B). However, as aspartic-acid saturated surfactant did not have a significantly lower zeta potential, there are likely additional factors contributing to the reduction in transduction efficiency. It is also important to note while the zeta potential measurements provide insight into electrostatic repulsion, they do not provide information on any attractive van der Waals forces, meaning a formulation can be stable and prevent aggregation with a low zeta potential (25). This, coupled with the polydispersity of our surfactant at the concentration used in our formulation, is why we used biolayer interferometry (BLI) and isothermal titration calorimetry (ITC) to better characterize the affinity between adenovirus and surfactant.

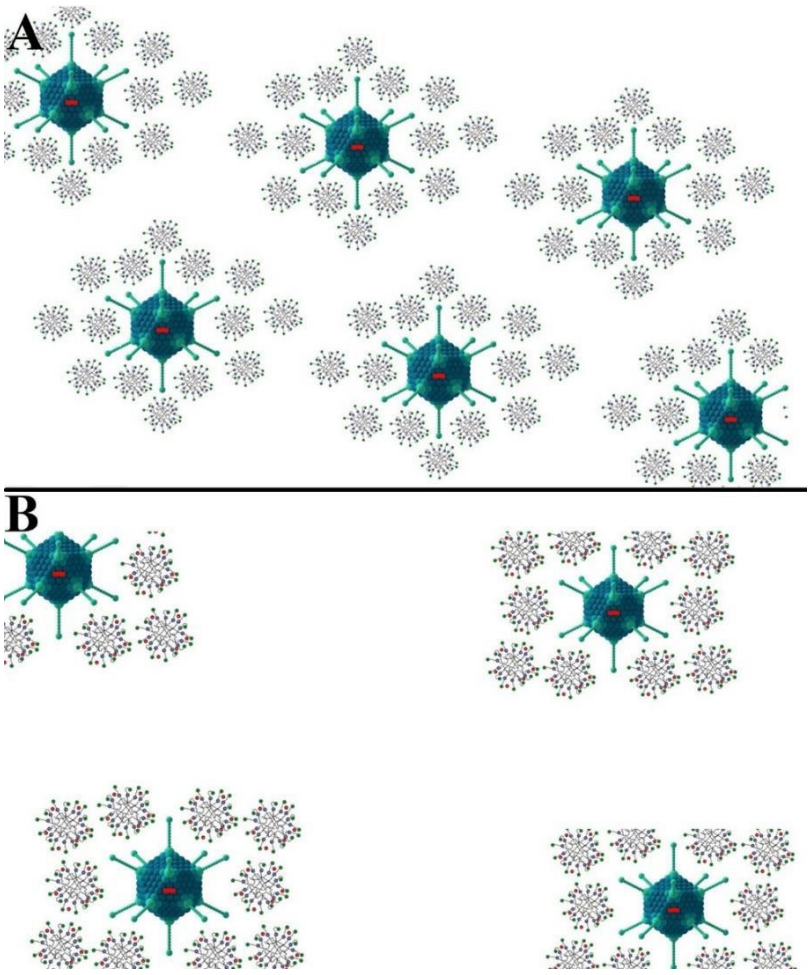

Figure 3.14: Hypothesized Mechanism of Surfactant Mitigated Adenoviral Stabilization. A schematic drawing based on a data collected thus far, on the mechanism of adenoviral stabilization via surfactant interactions (**A**). A potential hypothesis, displaying moderate repulsive forces, of formulations containing glutamic acid saturated surfactant impact on adenovirus transduction efficiency (**B**). Micelle structures are from reference (72). Virus image adapted from: Splettstoesser, T. A simplified 3D-generated structure of the adenovirus. Wikimedia Commons accessed 5 March 2019; available at: https://commons.wikimedia.org/wiki /File:Adenovirus_3D_schematic.png.

Biolayer interferometry (BLI) is an optical technique which is used to detect molecular interactions that analyzes the interference pattern of white light reflected from the biosensor surface and an internal reference layer. When molecules bind to the immobilized protein on the biosensor tip the optical thickness increases and there is a shift in the interference pattern which is measured in real time. We used Amine Reactive 2nd generation (AR2G) biosensors to characterize the interaction between PMAL and adenovirus, wherein proteins are immobilized by EDC-catalyzed amide bond formation (EDC: 1-ethyl-3-[dimethylaminopropyl] carbodiimide hydrochloride). This results in a covalent bond forming between a reactive amine on the protein of interest and the carboxy-terminated biosensor surface (73). Following immobilization, biosensors are incubated in various concentrations of surfactant to determine binding affinity. While biomolecular interaction analysis techniques typically use a single protein as an analyte, Kalyuzhniy et al. successfully conducted surface plasmon resonance spectroscopy (SPR) on intact adenovirus capsids as a part of their analysis of bond formation between human coagulation factor (FX) and adenovirus capsids as well as hexon proteins (26). Although SPR utilizes a similar approach to studying molecular interactions as BLI, due to the use of microfluidics, BLI is a higher throughput technique which allows 96 samples to be run in parallel in half an hour. We designed our BLI studies with this in mind, however, were unable to detect or quantify the strength of interaction, after several attempts at optimization (Figure 3.5). This led us to conclude that either the amine on the surfactant was no longer in a favorable orientation, or that the interactions between the virus and surfactant were outside the quantifiable range of BLI. We turned to an alternative technique, Isothermal Titration Calorimetry (ITC) because it is more efficient at quantifying binding of weaker interactions and measures the heat change generated due to two molecules binding in solution (74). We were able to detect the Kd

($2.25 \times 10^{-9} \pm 0.848 \times 10^{-9}$ M) and thermodynamic parameters (ΔG: -11.8 ± 0.252 kcal/mol, ΔH: -0.578 ± 0.125 kcal/mol, $-T\Delta S$: -11.267 ± 0.28; Figure 3.6) of surfactant titrated into adenovirus. Taken together, these values would suggest that the interaction between the surfactant and adenovirus may be thermodynamically favorable and entropically driven, pointing towards hydrophobic interactions such as desolvation of the protein surface (75). Considering the hypothesized interaction between surfactant and adenovirus in Figure 3.14 A, we believe this corresponds with the assembly of surfactant, in the form of micelles or premicellar aggregates, on or around the surface of adenovirus capsids which displaces water molecules from the viral surface. This results in the prevention of hydrolysis during long term storage and eventual viral inactivation. Additionally, the high affinity detected using ITC, confirms that PMAL was likely no longer in a favorable orientation to bind adenovirus capsids after immobilization using BLI (Figure 3.6). It is important to note, that the large variability detected during each run of ITC makes it difficult to make a confident assertion based on this data alone. We believe since the surfactant is polydisperse at the concentration in our formulation (Figure 3.7) and has a formula weight described as 39,000 to 65,000, which made estimating the molar concentration difficult and imprecise, that this may be a source of the variability. Additionally, adenovirus is a complex arrangement of several proteins and not a single peptide sequence. We believe this may also explain the high molar ratio we observed, indicating several binding points all over the adenovirus capsid (Figure 3.6). The difference in initial concentration between PMAL and adenovirus, in an attempt to mimic the micellar conditions of the formulation may also result in false positives, increasing the molar ratio. Reversing the orientation of the experiment may eliminate the need for a large disparity between protein and ligand concentrations, wherein the ligand (PMAL) is in the cell and the protein (Adenovirus) is titrated in during the ITC run.

However, it is our belief, that the system we are attempting to analyze is too heterogenous for ITC data to be meaningful and reliable. While these studies provide an interesting starting point, future analysis will likely require the identification of specific peptide sequences for analysis of interactions between the amphipol and adenovirus, prior to additional ITC characterization. This can be done using cryo-EM analysis and single particle reconstruction (26, 76) or fluorescent labeling (77, 78). Furthermore, in-house synthesis, or purchase of PMAL synthesized with a controlled molecular weight should help reduce the heterogeneity of the system being analyzed.

Upon evaluation of surfactant interactions with adenovirus capsids isolated from the other formulation components, we wanted to determine how the addition of formulation components impacts the observations of surfactant affinity to adenovirus. Due to the reduction of transduction efficiency of adenovirus in glutamic acid-saturated surfactant formulations, we evaluated if the same effect was present in formulations containing all the formulation components. We saw improved transduction efficiency in liquid formulations containing glutamic-acid saturated surfactant (Figure 3.3). However, films were more negatively impacted by the presence of glutamic acid saturated surfactant than liquid formulations. We hypothesize that the polymer base and sorbitol weaken the affinity between PMAL and glutamic acid and mitigate the impact on transduction efficiency in liquid formulations more efficiently as the removal of moisture, during the drying process, likely reduces some of the buffering effects of interactions between to the amphipol and virus. A second look at the FTIR data from a previous study conducted by our laboratory (13) also supported the hypothesis that additional formulation components buffer the interactions of excipients with adenovirus. We initially noted the increase in absorbance spectra as virus was added to base, base and sorbitol, and the optimized formulation, linked to the density of functional groups increasing, was decreasing as additional

excipients were added. We interpreted this as a potential sign of enhanced integration of adenovirus in the film. However, we also want to highlight the significant peak shift which occurred in the N-H wave range (3300-3500) of spectra of films prepared in base and adenovirus (13). Complexation of adenovirus with base results in bond stretching, characterized by peak shift from 3421 cm^{-1} in films without virus to 3376 cm^{-1} in films with virus. This shift is reduced in FTIR spectra of films prepared with HPMC and sorbitol (3384 cm^{-1} in films without virus to 3366cm^{-1} in films with virus) and is not present in the spectra of films prepared with all three formulation components. TGA analysis reveals that the addition of PMAL and virus, containing 2.5% glycerol as a cryopreservative, in films results in earlier thermal degradation, as well (Figure 3.10). Furthermore, when determining the saturation points by pH testing with amino acid-saturated surfactant and formulations containing adenovirus, we saw that the presence of glycerol created a buffering affect wherein higher amino acid concentrations were need to reduce the pH of the formulations to the targeted pH, 5.5 (Figure 3.2). Taken together, this suggests that the complete formulation disrupts the individual interactions observed between the surfactant and adenovirus as well as the base and adenovirus. While this may seem unfavorable, the affinity of adenovirus' penton fiber for CAR (coxsackievirus-adenovirus receptor) receptors on cells, which is where the virus first attaches to the cell (79), has a dissociation constant of 10^{-9} to 10^{-10} M (80). Therefore, the virus should not have a greater affinity for the surfactant or any formulation component, than CAR cell receptors, as it might have a deleterious effect on transduction efficiency and inhibit release of the virus from the stabilization matrix.

Moisture content also plays a role in excipient interactions and viral stabilization. It has been established in lyophilization processes, wherein water is removed from a formulation via freezing and sublimation, roughly 1-3% of moisture content is optimal for the successful

stabilization of viruses as there is some moisture associated with internal capsid structures, which if depleted will result in protein denaturation and capsid disruption (16, 37, 38, 81). However, in our preparations we observed stability of adenovirus at 4°C and 20°C for three months (13) and optimized formulations initially had a significantly higher moisture content, validated by two techniques (13%; Figure 3.10 and 3.11). The stepwise addition of formulation excipients revealed that the moisture content of films increased due to the addition of sorbitol and virus (Figure 3.10 and 3.11). However, we were able to determine that the increase in moisture content from optimized (base/sorbitol/surfactant) films prepared without virus to optimized films prepared with virus was likely linked to the presence of glycerol in adenoviral stocks, and not the addition of the virus itself (Figure 3.11). Increase in moisture content of films prepared with sorbitol and glycerol, which are plasticizers is well established in the literature (82, 83) and glycerol specifically has been documented to impact moisture content more so than sorbitol (83). This is supported by our studies as the addition of sorbitol to base resulted in a 2% increase in moisture content, but the addition of glycerol resulted in a 4% increase in moisture content (Figure 3.11). Observations from the optimization process have also highlighted the importance of glycerol in thin film preparations, as films stored for more than 1 month without glycerol tend to crystallize, while those prepared with the plasticizer maintain a clear physical morphology. In summary, the initial moisture content of films is not detrimental to adenoviral stability, as would be expected based on the literature, and is likely linked to the intermolecular interactions at play between formulation components which stabilize adenovirus. Future studies will track the impact of long-term storage on moisture content, thermal degradation, and absorbance spectra of films, as that may provide additional insight into the mechanism of adenoviral stabilization in our novel thin film matrix.

A universal vaccine delivery platform would streamline the vaccine production process and could simplify vaccine design. Therefore, the efficacy of the thin film platform at stabilizing alternative viruses, with different properties (Table 3.2), was evaluated. Enveloped viruses, respiratory syncytial virus (RSV) and herpes simplex virus (HSV), as well as non-enveloped adeno-associated virus (AAV), were efficiently stabilized in the thin film matrix likely due to their negative surface charge (Figure 3.12). However, incorporation of influenza (H1N1) in the thin film matrix, did not result in successful stabilization. We theorized this may be because of the positively charged Hemagglutinin surface protein (84) interaction with the negatively charged arm of the zwitterionic surfactant leading to partial viral inactivation, as Hemagglutinin binds cell receptors and drives viral entry (85). Additionally, the main difference between H1N1 and the other viruses examined was the presence of a positive surface charge. Choline was identified as an alternative surfactant which carried a predominantly positive charge and would theoretically have a higher affinity to Neuraminidase surface proteins of Influenza, which are negatively charged. While the infectious titer improved significantly in optimized concentrations of choline, the surfactant was toxic to buccal cells and infectious titer declined over time (Figure 3.13). The is most likely due to the ability of choline to solubilize cell membranes in the presence of influenza and illicit cytotoxic effects (46, 47). Furthermore, influenza is sensitive to alkaline pH's and the shift in pH over time likely resulted in decreased stability (86, 87). Calcium α-D-Heptagluconate dihydrate (heptagluconate), on the other hand, maintained a neutral pH more efficiently and prevented viral degradation of influenza's infectious titer over time at 4°C (Figure 3.13). However, films containing heptagluconate were not as successful at stabilizing influenza at room temperature. Optimization of excipient concentration or addition of other excipients may result in improved recovery of H1N1 from the thin film matrix. Mistilis et

al. demonstrated similar efficacy in formulations prepared sodium carboxy methyl cellulose and heptagluconate with the addition of arginine (48). While arginine has previously been used in many approved formulations (Appendix Table 1 and 2) for its ability to prevent protein aggregation and improve stability (49), it resulted in film crystallization and was not compatible with the film forming ingredient in our thin film matrix. It is important to note that additional replicates will also need to be analyzed, as there were preliminary screening studies only duplicate samples were analyzed.

Characterizing how formulation components contribute to the overall stability of adenovirus proved quite challenging due to the polydisperse and heterogeneous nature of the surfactant utilized in our formulations. While we were unable to conclusively determine the exact mechanism of interaction between PMAL and adenovirus, all of our acquired data supports the likely conclusion that PMAL surrounds the viral surface, preventing aggregation and limiting contact with water molecules via hydrophobic interactions. Furthermore, the difficulty stabilizing influenza supports the theory that charge based, non-covalent interactions also contribute to the affinity of adenovirus to PMAL. It is our belief that these studies provide key insights into the future characterization of intermolecular interactions and that obtaining a more homogenous sample of surfactant will simplify and streamline future characterization.

3.5 References

1. M. G. Mateu, Virus engineering: functionalization and stabilization. *Protein Engineering, Design and Selection* **24**, 53-63 (2010).
2. C. P. Gerba, W. Q. Betancourt, Viral Aggregation: Impact on Virus Behavior in the Environment. *Environmental Science & Technology* **51**, 7318-7325 (2017).
3. M. E. Krause, E. Sahin, Chemical and physical instabilities in manufacturing and storage of therapeutic proteins. *Current Opinion in Biotechnology* **60**, 159-167 (2019).

4. U. Kartoglu, *Monitoring Vaccine Wastage at a Country Level*. (World Health Organization Geneva, Switzerland, 2005).
5. Raymond W Nims, M. Plavsic, Intra-family and inter-family comparisons for viral susceptibility to heat inactivation. *Journal of Microbial and Biochemical Technology* **5**, 136-141 (2013).
6. J. Dijkstra, C. P. de Jager, in *Practical Plant Virology: Protocols and Exercises*, Jeanne Dijkstra, Cees P. de Jager, Eds. (Springer Berlin Heidelberg, Berlin, Heidelberg, 1998), pp. 102-104.
7. S. Gard, O. MaalØE, in *General Virology*, F. M. Burnet, W. M. Stanley, Eds. (Academic Press, 1959), pp. 359-427.
8. E. K. Jeong, J. E. Bae, I. S. Kim, Inactivation of influenza A virus H1N1 by disinfection process. *American journal of infection control* **38**, 354-360 (2010).
9. G. Maheshwari, R. Jannat, L. McCormick, D. Hsu, Thermal inactivation of adenovirus type 5. *Journal of Virological Methods* **118**, 141-146 (2004).
10. C. M. Hanson, A. M. George, A. Sawadogo, B. Schreiber, Is freezing in the vaccine cold chain an ongoing issue? A literature review. *Vaccine* **35**, 2127-2133 (2017).
11. Ümit Kartoglu, Nejat Kenan Özgüler, Lara J Wolfson, W. Kurzatkowski, Validation of the shake test for detecting freeze damage to adsorbed vaccines. *Bulletin of the World Health Organization*, 624-631 (2010).
12. J. Emmanuel, M. Ferrer, F. Ferrer, "Disposal of Mass Immunization Waste Without Incineration," (Department of Health, Manila, Philippines, 2004).
13. I. Bajrovic, S. C. Schafer, D. K. Romanovicz, M. A. Croyle, Novel technology for storage and distribution of live vaccines and other biological medicines at ambient temperature. *Science Advances* **6**, eaau4819 (2020).
14. S. Karlin, V. Brendel, Charge configurations in viral proteins. *Proceedings of the National Academy of Sciences* **85**, 9396 (1988).
15. N. A. Malik, Surfactant–Amino Acid and Surfactant–Surfactant Interactions in Aqueous Medium: a Review. *Applied Biochemistry and Biotechnology* **176**, 2077-2106 (2015).
16. M. A. Croyle, X. Cheng, J. M. Wilson, Development of formulations that enhance physical stability of viral vectors for gene therapy. *Gene Therapy* **8**, 1281-1290 (2001).
17. R. J. Carter *et al.*, Implementing a Multisite Clinical Trial in the Midst of an Ebola Outbreak: Lessons Learned From the Sierra Leone Trial to Introduce a Vaccine Against Ebola. *J Infect Dis* **217**, S16-S23 (2018).
18. W. Abdelwahed, G. Degobert, S. Stainmesse, H. Fessi, Freeze-drying of nanoparticles: Formulation, process and storage considerations. *Advanced Drug Delivery Reviews* **58**, 1688-1713 (2006).
19. J. Rexroad, T. T. Martin, D. McNeilly, S. Godwin, C. Russell Middaugh, Thermal Stability of Adenovirus type 2 as a Function of pH. *Journal of Pharmaceutical Sciences* **95**, 1469-1479 (2006).
20. R. J. C. Harris, *Biological applications of freezing and drying*. (New York: Academic Press Inc., 1954), pp. xii + 415 pp.
21. J. E. Boyd, in *Gene Therapy Technologies, Applications and Regulations*, John Wiley, Ed. (Chichester, 1999), pp. 383-400.
22. P. E. Cruz *et al.*, Screening of Novel Excipients for Improving the Stability of Retroviral and Adenoviral Vectors. *Biotechnology Progress* **22**, 568-576 (2006).

23. W. C. Russell, Adenoviruses: update on structure and function. *The Journal of general virology* **90**, 1-20 (2009).
24. Y. S. Ahi, S. K. Mittal, Components of Adenovirus Genome Packaging. *Front Microbiol* **7**, 1503-1503 (2016).
25. S. Bhattacharjee, DLS and zeta potential – What they are and what they are not? *Journal of Controlled Release* **235**, 337-351 (2016).
26. O. Kalyuzhniy *et al.*, Adenovirus serotype 5 hexon is critical for virus infection of hepatocytes in vivo. *Proceedings of the National Academy of Sciences* **105**, 5483 (2008).
27. B. Michen, T. Graule, Isoelectric points of viruses. *Journal of Applied Microbiology* **109**, 388-397 (2010).
28. M. A. Croyle, B. J. Roessler, B. L. Davidson, J. M. Hilfinger, G. L. Amidon, Factors that Influence Stability of Recombinant Adenoviral Preparations for Human Gene Therapy. *Pharmaceutical Development and Technology* **3**, 373-383 (1998).
29. J. Rexroad, R. K. Evans, C. R. Middaugh, Effect of pH and ionic strength on the physical stability of adenovirus type 5. *Journal of Pharmaceutical Sciences* **95**, 237-247 (2006).
30. S. M. Callahan, P. Wonganan, M. A. Croyle, Molecular and macromolecular alterations of recombinant adenoviral vectors do not resolve changes in hepatic drug metabolism during infection. *Virol J* **5**, 111-111 (2008).
31. A. B. Hill, C. Kilgore, M. McGlynn, C. H. Jones, Improving global vaccine accessibility. *Current Opinion in Biotechnology* **42**, 67-73 (2016).
32. R. W. Ruigrok, M. V. Nermut, P. J. Andree, The molecular mass of adenovirus type 5 as determined by means of scanning transmission electron microscopy (STEM). *J Virol Methods* **9**, 69-78 (1984).
33. J. Aguiar, P. Carpena, J. A. Molina-Bolívar, C. Carnero Ruiz, On the determination of the critical micelle concentration by the pyrene 1:3 ratio method. *Journal of Colloid and Interface Science* **258**, 116-122 (2003).
34. D. Al-Koofee, Effect of Temperature Changes on Critical Micelle Concentration for Tween Series Surfactant. *Global Journal of Science Frontier Research Chemistry* **13**, (2013).
35. A. B. Mandal, B. U. Nair, D. Ramaswamy, Determination of the critical micelle concentration of surfactants and the partition coefficient of an electrochemical probe by using cyclic voltammetry. *Langmuir* **4**, 736-739 (1988).
36. N. Saadatkhah *et al.*, Experimental methods in chemical engineering: Thermogravimetric analysis—TGA. *The Canadian Journal of Chemical Engineering* **98**, 34-43 (2020).
37. D. Greiff, Stabilities of suspensions of influenza virus dried by sublimation of ice in vacuo to different contents of residual moisture and sealed under different gases. *Appl Microbiol* **20**, 935-938 (1970).
38. D. Greiff, Protein structure and freeze-drying: The effects of residual moisture and gases. *Cryobiology* **8**, 145-152 (1971).
39. J. K. Towns, Moisture content in proteins: its effects and measurement. *Journal of Chromatography A* **705**, 115-127 (1995).
40. M. A. Kennedy, R. J. Parks, Adenovirus virion stability and the viral genome: size matters. *Mol Ther* **17**, 1664-1666 (2009).
41. E. D. Horowitz *et al.*, Biophysical and ultrastructural characterization of adeno-associated virus capsid uncoating and genome release. *Journal of virology* **87**, 2994-3002 (2013).

42. T. J. Utley *et al.*, Respiratory syncytial virus uses a Vps4-independent budding mechanism controlled by Rab11-FIP2. *Proceedings of the National Academy of Sciences* **105**, 10209 (2008).
43. R. F. Laine *et al.*, Structural analysis of herpes simplex virus by optical super-resolution imaging. *Nature Communications* **6**, 5980 (2015).
44. J. Vajda, D. Weber, D. Brekel, B. Hundt, E. Müller, Size distribution analysis of influenza virus particles using size exclusion chromatography. *Journal of Chromatography A* **1465**, 117-125 (2016).
45. H. T. Rupniak *et al.*, Characteristics of Four New Human Cell Lines Derived From Squamous Cell Carcinomas of the Head and Neck2. *JNCI: Journal of the National Cancer Institute* **75**, 621-635 (1985).
46. K. Patel, C. A. Pasternak, Permeability changes elicited by influenza and Sendai viruses: separation of fusion and leakage by pH-jump experiments. *The Journal of general virology* **66 (Pt 4)**, 767-775 (1985).
47. D. Rengstl, B. Kraus, M. Van Vorst, G. D. Elliott, W. Kunz, Effect of choline carboxylate ionic liquids on biological membranes. *Colloids Surf B Biointerfaces* **123**, 575-581 (2014).
48. M. J. Mistilis *et al.*, Long-term stability of influenza vaccine in a dissolving microneedle patch. *Drug Deliv Transl Res* **7**, 195-205 (2017).
49. W. Wang, S. Ohtake, Science and art of protein formulation development. *International Journal of Pharmaceutics* **568**, 118505 (2019).
50. G. Gomez, M. J. Pikal, N. Rodriguez-Hornedo, Effect of initial buffer composition on pH changes during far-from-equilibrium freezing of sodium phosphate buffer solutions. *Pharmaceutical research* **18**, 90-97 (2001).
51. V. G. Kadajji, G. V. Betageri, Water Soluble Polymers for Pharmaceutical Applications. *Polymers* **3**, (2011).
52. M. Picard *et al.*, Protective and Inhibitory Effects of Various Types of Amphipols on the Ca2+-ATPase from Sarcoplasmic Reticulum: A Comparative Study. *Biochemistry* **45**, 1861-1869 (2006).
53. K. W. Huynh *et al.*, CryoEM structure of the human SLC4A4 sodium-coupled acid-base transporter NBCe1. *Nat Commun* **9**, 900 (2018).
54. K. P. K. Lee, J. Chen, R. MacKinnon, Molecular structure of human KATP in complex with ATP and ADP. *eLife* **6**, (2017).
55. S. Schoebel *et al.*, Cryo-EM structure of the protein-conducting ERAD channel Hrd1 in complex with Hrd3. *Nature* **548**, 352-355 (2017).
56. C. E. Paulsen, J. P. Armache, Y. Gao, Y. Cheng, D. Julius, Structure of the TRPA1 ion channel suggests regulatory mechanisms. *Nature* **520**, 511-517 (2015).
57. D. Otzen, Protein-surfactant interactions: A tale of many states. *Biochimica et biophysica acta* **1814**, 562-591 (2011).
58. B. S. Gupta, C.-R. Shen, M.-J. Lee, Effect of biological buffers on the colloidal behavior of sodium dodecyl sulfate (SDS). *Colloids and Surfaces A: Physicochemical and Engineering Aspects* **529**, 64-72 (2017).
59. H. Zettl, Y. Portnoy, M. Gottlieb, G. Krausch, Investigation of Micelle Formation by Fluorescence Correlation Spectroscopy. *The Journal of Physical Chemistry B* **109**, 13397-13401 (2005).

60. M. Méndez-Pérez, B. Vaz, L. García-Río, M. Pérez-Lorenzo, Polymeric Premicelles as Efficient Lipophilic Nanocarriers: Extending Drug Uptake to the Submicellar Regime. *Langmuir* **29**, 11251-11259 (2013).
61. D. Lombardo, M. A. Kiselev, S. Magazù, P. Calandra, Amphiphiles Self-Assembly: Basic Concepts and Future Perspectives of Supramolecular Approaches. *Advances in Condensed Matter Physics* **2015**, 151683 (2015).
62. R. Hadgiivanova, H. Diamant, Premicellar aggregation of amphiphilic molecules: Aggregate lifetime and polydispersity. *The Journal of chemical physics* **130**, 114901 (2009).
63. T. Tadros, in *Encyclopedia of Colloid and Interface Science*, Tharwat Tadros, Ed. (Springer Berlin Heidelberg, Berlin, Heidelberg, 2013), pp. 209-210.
64. B. Brycki *et al.*, Effect of the alkyl chain length on micelle formation for bis(N-alkyl-N,N-dimethylethylammonium)ether dibromides. *Comptes Rendus Chimie* **22**, 386-392 (2019).
65. G. K. Bains, S. H. Kim, E. J. Sorin, V. Narayanaswami, The extent of pyrene excimer fluorescence emission is a reflector of distance and flexibility: analysis of the segment linking the LDL receptor-binding and tetramerization domains of apolipoprotein E3. *Biochemistry* **51**, 6207-6219 (2012).
66. M. Zoonens, J.-L. Popot, Amphipols for each season. *J Membr Biol* **247**, 759-796 (2014).
67. J. L. Popot *et al.*, Amphipols From A to Z. *Annual Review of Biophysics* **40**, 379-408 (2011).
68. J.-L. Popot, Amphipols, Nanodiscs, and Fluorinated Surfactants: Three Nonconventional Approaches to Studying Membrane Proteins in Aqueous Solutions. *Annual Review of Biochemistry* **79**, 737-775 (2010).
69. W. Wang, A. A. Ignatius, S. V. Thakkar, Impact of Residual Impurities and Contaminants on Protein Stability. *Journal of Pharmaceutical Sciences* **103**, 1315-1330 (2014).
70. Q. G. Li, K. Lindman, G. Wadell, Hydropathic characteristics of adenovirus hexons. *Arch Virol* **142**, 1307-1322 (1997).
71. S. Skoglund *et al.*, Difficulties and flaws in performing accurate determinations of zeta potentials of metal nanoparticles in complex solutions-Four case studies. *PloS one* **12**, e0181735-e0181735 (2017).
72. E. Drinkel, F. D. Souza, H. D. Fiedler, F. Nome, The chameleon effect in zwitterionic micelles: Binding of anions and cations and use as nanoparticle stabilizing agents. *Current Opinion in Colloid & Interface Science* **18**, 26-34 (2013).
73. ForteBio, "Dip and Read Amine Reactive Second-Generation (AR2G) Biosensors," (Menlo Park, CA).
74. K. E. Hevener *et al.*, in *Methods in Enzymology*, Charles A. Lesburg, Ed. (Academic Press, 2018), vol. 610, pp. 265-309.
75. D. J. Butcher, G. R. Moe, Role of hydrophobic interactions and desolvation in determining the structural properties of a model alpha beta peptide. *Proc Natl Acad Sci U S A* **93**, 1135-1140 (1996).
76. J. Wang *et al.*, Cryo-EM structures of PAC1 receptor reveal ligand binding mechanism. *Cell Research* **30**, 436-445 (2020).
77. C. J. Breen, M. Raverdeau, H. P. Voorheis, Development of a quantitative fluorescence-based ligand-binding assay. *Sci Rep* **6**, 25769-25769 (2016).

78. R. Sridharan, J. Zuber, S. M. Connelly, E. Mathew, M. E. Dumont, Fluorescent approaches for understanding interactions of ligands with G protein coupled receptors. *Biochimica et biophysica acta* **1838**, 15-33 (2014).
79. C. Lyle, F. McCormick, Integrin αvβ5 is a primary receptor for adenovirus in CAR-negative cells. *Virol J* **7**, 148 (2010).
80. V. Legrand *et al.*, Fiberless recombinant adenoviruses: virus maturation and infectivity in the absence of fiber. *Journal of virology* **73**, 907-919 (1999).
81. J. K. Towns, Moisture content in proteins: its effects and measurement. *Journal of chromatography. A* **705**, 115-127 (1995).
82. P. Bergo, I. Moraes, P. J. A. Sobral, Effects of plasticizer concentration and type on moisture content in gelatin films. *Food Hydrocolloids* **32**, 412–415 (2013).
83. M. L. Sanyang, S. M. Sapuan, M. Jawaid, M. R. Ishak, J. Sahari, Effect of plasticizer type and concentration on physical properties of biodegradable films based on sugar palm (arenga pinnata) starch for food packaging. *J Food Sci Technol* **53**, 326-336 (2016).
84. Y. Kobayashi, Y. Suzuki, Compensatory evolution of net-charge in influenza A virus hemagglutinin. *PLoS One* **7**, e40422 (2012).
85. M. Hoffmann, S. Pöhlmann, Cell Entry of Influenza A Viruses: Sweet Talk between HA and CaV1.2. *Cell Host & Microbe* **23**, 697-699 (2018).
86. R. L. Poulson, S. M. Tompkins, R. D. Berghaus, J. D. Brown, D. E. Stallknecht, Environmental Stability of Swine and Human Pandemic Influenza Viruses in Water under Variable Conditions of Temperature, Salinity, and pH. *Applied and environmental microbiology* **82**, 3721-3726 (2016).
87. P. R. Junankar, R. J. Cherry, Temperature and pH dependence of the haemolytic activity of influenza virus and of the rotational mobility of the spike glycoproteins. *Biochimica et biophysica acta* **854**, 198-206 (1986).

Chapter 4: Novel Oral Film Technology Induces Protective Immunity Against Influenza in Mice and Enhances Permeability

4.1 Introduction

During the 20th century it is estimated that 300 million people died of smallpox, roughly three times higher than the total death toll of World War I and II combined (1). The development and careful distribution of a vaccine resulted in the complete eradication of smallpox on May 8, 1980. Development of vaccines against other infectious diseases like polio, measles, mumps, rubella, and meningitis, have also reduced their associated mortality rates by 97-99% (2). However, infectious diseases are still the second cause of death worldwide, disproportionately affecting individuals in low and middle income (LMIC) countries (3-6). While some of these deaths are linked to pathogens for which a vaccine has not been developed, an estimated 1.5 million people die annually from vaccine-preventable diseases (7). This can be partially attributed to the need for trained personnel to administer vaccines and the lack of thermostable vaccines, which become easily inactivated if they are exposed to temperatures outside of their recommended range (Vaccine Appendix Table 1 & 2) and have to be discarded (8, 9). In order to prevent thermal inactivation due to a disruption in the cold-chain, complex maintenance and monitoring protocols are developed which impact the associated costs (10, 11). Over half of the costs linked with implementing vaccine programs originate from service delivery and supply chain maintenance expenditures (12). This highlights the need for significant improvement in vaccine technology and administration.

Many pathogens enter the body through mucosal routes. For example, SARS-CoV-2 and Influenza initiate infection through the nose and mouth passing through the mucous membranes in the respiratory tract (13-15). The development of immunologically strong mucosal barriers can prevent infection at the entry point and stimulate both local and systemic immunity. However, of the 58 approved vaccines against viral pathogens in the United States, 51 are currently given by subcutaneous or intramuscular injection (Appendix Table 2). This generally results in a notable antibody-mediated immune response with limited cellular and mucosal immunity (16, 17). Conversely, mucosal immunization routes generally induce production of local antibodies and T-cell mediated responses, and sometimes a robust systemic response (18). In order to be effective, antigens travel through the gastrointestinal tract and are processed by antigen presenting cells via M cells in Peyer's patches (19). Oral vaccination strategies were first established with the use of the Sabin polio vaccine (OPV). Since then oral vaccines for Rotavirus, Cholera, Adenovirus, and Typhoid Fever have been developed (20). However, oral vaccine formulations must be able to protect the antigen from biological and physiochemical barriers. This includes various enzymes like pepsin and trypsin as well the variable pH, 1.0 to 7.0, of the gastrointestinal tract (21, 22). Buccal and sublingual administration of vaccines offers a distinct advantage over classical oral delivery as antigens can be processed by local antigen presenting cells while evading the barriers of the gastrointestinal tract (23). The presence of these specialized resident antigen presenting cells, Langerhans cells, and direct access to submandibular lymph nodes makes both routes an excellent candidate for vaccine delivery. However, the thickness of the human buccal mucosa, 500-800 μm (24, 25), and high salivary flow rate associated with the sublingual route, 0.3-0.4 mL/min without stimulation and 4 to 7 mL/min with stimulation (25, 26), have prevented these routes from being exploited to their full

potential. To date, there are no approved vaccines in the United States that target the sublingual or buccal mucosa. Phase I clinical trials have explored sublingual vaccine delivery for influenza, cholera, human papillomavirus, and tuberculosis (27). The majority of these immunogens were administered using the injectable vaccine formulation to the sublingual cavity as drops and evaluated for immunogenic effect. However, only one study was actually tailored for formulation to the mucosal delivery route. Nitto Denko Corporation formulated a proprietary tablet, NSV0001, for immunization against seasonal influenza with 15, 30, or 60 µg of hemagglutinin antigen and a novel adjuvant, ND002. The trial was completed in 2017, but the results have not been published (28).

Mucosal vaccines often require adjuvants to overcome the bioavailability limitations associated with oral routes previously mentioned. These adjuvants can act as either permeation enhancers or immunostimulants, and in some cases both (29). While strong candidates for mucosal adjuvants have been identified, for example protonated chitosan which opens tight junctions and stimulates cytokine response, they have not been successfully translated into clinical application (30, 31). One of the hurdles for approval is the associated safety of the compounds and while four adjuvants, (aluminum, AS04/AS01$_B$, MF59, CpG 1018) have been approved for human use in injectable vaccines in the United States, they have been linked with narcolepsy, thyroiditis, and Guillain-Barre syndrome (32-34). Common flavorings, such as cinnamaldehyde and vanillin, may provide a safer alternative to organically synthesized or modified adjuvants and have been previously identified to stimulate transient receptor potential (TRP) channels (35-38). This may prove to be significant as TRP channels, located in the epithelial lining of the oronasal cavity, are voltage-gated cation channels that belong to a 28-protein superfamily, and play a role in dendritic cell activation (TRPA), antigen presentation

(TRPA), T cell differentiation (TRPA), B cell growth, proliferation, and survival (TRPV and TRPM), and cytokine release (TRPV and TRPM) (39, 40). Therefore, a way to overcome the risk associated with already approved adjuvants is to use natural compounds, if proven to be immunostimulants, to pave the way for safe, immunogenic mucosal vaccines.

We have evaluated the utility of sublingual administration of a recombinant adenovirus serotype 5-based vaccine against the Ebola virus as a method of noninvasive immunization that bypasses the gastrointestinal tract (41). In this case, depositing 10μL of a liquid formulation under the tongue of mice elicited a notable cellular (T_{H1}) and humoral (T_{H2}) response and improved survival from a lethal dose of mouse adapted Ebola, with respect to the same vaccine given by the intramuscular route. These findings prompted us to utilize our novel thin film dosage form (42) to target the sublingual and buccal regions of the oral mucosa, minimizing the chance of accidental swallowing of the formulation, and to strictly compare the immune response induced by each route of administration. To achieve this goal, we performed a proof of concept study illustrating the utility of our thin film as an oral dosage form. We then used human buccal explants, derived from oral epithelial cells that were cultured to form multilayered, highly differential models of the human buccal epithelium, to evaluate the bioavailability of H1N1 Influenza virus in formulated oral films and to determine if the addition of TRP agents would be improve the cytokine response and bioavailability and therefore induce a greater immune response *in vivo*. The results are summarized here along with a thorough evaluation of the humoral immune response and protective immunity generated by sublingual and buccal immunization.

4.2 Materials and Methods

4.2.1 Materials

Dulbecco's PBS, Trizma base [2-amino-2-(hydroxymethyl)-1,3-propanediol], FBS (qualified, U.S. origin), glycerol, D-sorbitol [USP (United States Pharmacopeia) grade], sodium azide, SigmaFast BCIP/NBT tablets, cinnamaldehyde (W228613-100G-K), capsaicin (M2028-250MG), and vanillin (V1104-2G) were purchased from Sigma-Aldrich (St. Louis, MO). Eugenol (97-53-0) was purchased from Acros Organics (Fair Lawn, NJ). AM 0902 and GSK 2193874 were purchased from Tocris Bioscience (Bristol, UK). Poly(maleic anhydride-alt-1-octadecene) substituted with 3-(dimethylamino)propylamine was purchased from Anatrace (Maumee, OH). MEM was purchased from Mediatech (Manassas, VA). EMEM was purchased from Lonza (Basel, Switzerland). Hydroxypropyl methylcellulose 4*KM was provided by the Dow Chemical Company (Midland, MI). Penicillin (10,000 IU) and streptomycin (10,000 μg/ml) were purchased from Gibco Life Technologies (Grand Island, NY). EpiOral^{TM} human buccal explants were purchased from MatTek Life Sciences (Ashland, MA). Anti-Influenza A Antibody (MAB8258B-5) and Streptavidin, Alkaline Phosphatase Conjugate were purchased from Millipore Sigma (Burlington, MA). Influenza A Virus A/Puerto Rico/8-9VMC3/1934 (H1N1) was purchased from BEI resources (Manassas, VA). Purified oligonucleotide primers were custom synthesized by Sigma Life Science (Woodlands, TX). All other chemicals were of analytical reagent grade and purchased from Thermo Fisher Scientific (Pittsburgh, PA) unless specified otherwise.

4.2.2 Permeability of Films on Epi Oral Explants

The EpiOral™ assay medium was warmed to 37°C and was added to 0.3 mL/well of a sterile 24 well plate. Under sterile conditions, the EpiOral™ tissues were transferred to the 24 well plate (1 sample/well) and placed at 37°C, 5% CO_2 for 1 hour to equilibrate the tissues. Films were prepared following standard protocol (42) and evaluated for changes in pH using pH indicator solution and film thickness using a Mitutoyo Digimatic Micrometer (Kanagawa, Japan). 150uL films were reconstituted in sterile tubes containing 1mL of EpiOralTM assay medium, warmed to 33°C for 15 minutes. Following equilibration of the tissues, tissue integrity was evaluated using an EVOM^2 Epithelial Voltmeter (World Precision Instruments, Sarasota County, FL). Then the reconstituted films were added to the surface of EpiOral™ tissues and the plates were returned to the incubator. After 30 minutes of elapsed permeation time, the entire volume was collected from each of the wells and replaced with fresh, warmed EpiOral™ assay medium. This procedure was repeated for 60, 90, 120, and 180 minutes and 24 hours. At the end of testing, tissue integrity was evaluated again. Results were evaluated using an infectious titer assay on MDCK cells (ATCC #CCL-34). The percent recovery was calculated as:

$$\%\, Recovery = \frac{\log\left(infectious\ titer\ of\ recovered\ dose\right)}{\log(infectious\ titer\ of\ dose\ administered)} \times 100$$

4.2.2.1 RNA Isolation, RT-PCR and qRT-PCR

Each of the EpiOral™ samples was rinsed three time with phosphate buffered saline (PBS, MatTek) and removed from the plastic cylinder with forceps and deposit it in a syringe filled with 140 uL PBS and 560 uL lysis buffer provided in the QIAmp Viral RNA Mini Kit (Qiagen). A 20 gauge needle is attached to the 1mL syringe and the tissues were forced through the needle 25 times for homogenization. Afterwards the samples were incubated at 20°C for 10

minutes and then centrifuged 10 minutes at 14,000 rpm to pellet the tissue debris. Total RNA was isolated using the QIAamp Viral RNA Kit (Qiagen) according to manufacturer's instructions. Isolated RNA was reversed transcribed with random hexamers using the SuperScript® III first-strand synthesis system (Thermo) and a Master Cycler Pro thermal cycler (Eppendorf AG, Hamburg, Germany). Quantification of H1N1 genome RNA was performed using the SYBR® GreenERTM qPCR SuperMix (Thermo) and the ViiA7TM Real-Time PCR system (Applied Biosystems, Carlsbad, CA) with the following cycling conditions: 50 °C for 2 minutes, 95 °C for 10 minutes followed by 40 cycles of 95°C for 15 seconds and 60 °C for 60 seconds. Forward Primer: 5'-GTCCGGCATCATCACCTCAA-3' and Reverse Primer 5'-ACCGGCAATGGCTCCAAATA-3'were used as primer sequences (43). The percentage of the dose retained in tissues was determined by adding the amount of immobilized virus to the amount of virus present in basolateral media and determining the change in total dose percent recovery using the equation provided above.

4.2.2.2 Permeability Coefficient Determination

Calculation of permeability coefficient, kp, as defined by Fick's law, can be calculate from the following equations:

$$kp = \frac{(average\ flux)}{(C_D - C_R)}$$

The flux (moles/cm^2/hr) versus time was determined by assaying the receiver and donor samples for infectious titer on MDCK cells (ATCC #CCL-34) at each time point, the average donor solution concentration at the end of sampling, and the initial concentration of the receiver solution. The tissue area is 0.6 cm^2. Then the average flux was determined by averaging the flux across time intervals after steady state (± 20%) was achieved. C_D is the concentration of the drug

in the donor solution (ivp/mL). C_R is the concentration of the drug in the receiver solution (ivp/mL).

4.2.3 Assessment of Cytokine Response on Epi Oral Explants

The EpiOral™ tissues, assay medium, and films were prepared as described above. After 6 hours of elapsed permeation time, the entire volume was collected from each of the wells and replaced with fresh, warmed EpiOral™ assay medium. This procedure was repeated at 24 hours. At the end of testing, tissue integrity was evaluated again. The samples were evaluated for cytokine levels using the Th1/Th2 Cytokine 11-Plex Human ProcartaPlex™ Panel (Invitrogen) according to manufacturer's instructions for eleven cytokines: IFNγ, IL-12p70, IL-13, IL-1β, IL-2, IL-4, IL-5, IL-6, IL-18, TNFα, and GM-CSF.

4.2.4 In vivo assessment of film performance

All procedures were approved by the Institutional Animal Care and Use Committees at The University of Texas at Austin and are in accordance with the guidelines established by the National Institutes of Health for the humane treatment of animals.

4.2.4.1 Immunization.

Eight-week-old male BALB/c mice were obtained from the Jackson laboratory (Bar Harbor, ME). Animals were housed in a temperature-controlled, 12-hour light-cycled facility at the Animal Research Center of The University of Texas at Austin. Mice were given free access to standard rodent chow (Harlan Teklad, Indianapolis, IN) and tap water. Animals were anesthetized by a single intraperitoneal injection of a 3.9:1 mixture of ketamine (100 mg/ml, Putney, Portland, ME) and xylazine (100 mg/ml, Sigma-Aldrich, St. Louis, MO). Once deep plane anesthesia was achieved, animals were immunized with 2000 CEID50 (Chicken Embryo Infectious Dose 50% endpoint) of influenza A virus, A/Puerto Rico/8-9VMC3/1934 (H1N1)

(BEI Resources, Manassas, VA) by intramuscular and intranasal routes. Films in preliminary studies were prepared with 2000 CEID50 A/Puerto Rico/8-9VMC3/1934 (H1N1) for SL and BU routes. Films in follow-up studies were prepared at the same dose, 2000 CEID50 A/Puerto Rico/8-9VMC3/1934 (H1N1), for sublingual (SL), buccal (BU), buccal with the flavoring cinnamaldehyde (BUF), and buccal inactivated (BUI). BUI films were prepared by heat inactivating the virus for 3 days at 60°C. Intramuscular injection involved direct injection of virus diluted in saline into each gastrocnemius muscle located on the hindlimb (50 µl per muscle). Nasal immunization was performed by slowly dripping virus diluted in saline into each nostril (10 µl per nostril) using a standard micropipette (Gilson, Middleton, WI). For SL immunization, the SL epithelium was swabbed dry and 20 µl of saline was added to act as an adhesive for the film. Each film was subsequently placed under the tongue using sterile forceps. For BU/BUF/BUI immunization, the upper part of the check pouch was swabbed dry and 10 µl of saline was added to each cheek to act as an adhesive for the film. Half of each film was placed on the upper part of each cheek pouch using sterile forceps. For both SL and BU doses, dissolution time was complete within 5 min without the animals swallowing or chewing the film. Animals given the vaccine by the SL or BU routes were maintained in an upright position for 30 min after immunization to minimize choking and accidental swallowing of the vaccine.

4.2.4.2 Challenge with Mouse-Adapted Influenza Virus and Necropsy.

Twenty-eight days post immunization, vaccinated mice were challenged by intranasal administration using 100,000 $CEID_{50}$ A/Puerto Rico/8-9VMC3/1934 (H1N1) using the technique described above. After challenge, animals were monitored for clinical signs of disease and weighed daily for 10 days. At the end of the study, all animals were euthanized by terminal heart stick and serum was collected by centrifugation of whole blood for ten minutes at 10,000 rpm.

Lungs were placed in an antibiotic solution containing Streptomycin (1g) and Penicillin (5 million units) and a tissue grinder was used to process the tissues. Lung homogenates were centrifuged for 20 minutes at 5000 rpm and 4°C and subsequently analyzed using an infectious titer assay on MDCK cells (ATCC #CCL-34).

4.2.4.3 Neutralizing Antibody Assay.

Anti-influenza antibody (neutralizing antibody) titers were assessed in serum samples collected 28 days after vaccination and 10 days after challenge. Heat-inactivated serum was diluted in MEM in twofold increments starting from a 1:20 dilution. Each dilution was mixed with A/Puerto Rico/8-9VMC3/1934 (H1N1) for 1 hour at 37°C and added to MDCK (Madin-Darby canine kidney) cells in Zero-Serum Medium PSGA (Penicillin, Streptomycin, Gentamicin, and Ampicillin) (Quidel, San Diego, CA) on 96-well plates. Two hours later, 100 µl of MEM supplemented with 20% FBS was added to each well. Cells were incubated an additional 24 hours and visualized by histochemical staining. For each sample, the serum dilution that corresponded to a 50% reduction in viral expression was obtained by the method of Reed and Muench as described previously (44). The absence of neutralization in samples containing medium only (negative control) and FBS (serum control) were criteria for qualification of each assay.

4.2.4.4 Characterization of influenza-specific antibodies.

To assess anti-influenza immunoglobulin levels in serum, Immulon 2 HB plates (Thermo Fisher Scientific, Pittsburgh, PA) were coated with influenza A virus, A/Puerto Rico/8-9VMC3/1934 (H1N1) (1 µg per well) in bicarbonate buffer (pH 9.5) overnight at 4°C. Plates were washed three times with PBS containing 0.05% Tween 20 and blocked in PBS containing 1% bovine serum albumin (Sigma-Aldrich) for 1 hour at room temperature. Heat-inactivated

serum samples were diluted 1:5 in sterile PBS. Fifty microliters of each dilution was added to the antigen-coated plates for 4 hours at room temperature. Plates were washed three times with PBS containing 0.05% Tween 20 and incubated with horseradish peroxidase–conjugated goat anti-mouse IgG, IgG_1, IgG_{2a}, IgG_{2b}, and IgA (1:2000; Southern Biotechnology Associates, Birmingham, AL) in separate wells for 2 hours at room temperature. Plates were washed, and 100 μl of substrate solution [o-phenylenediamine (0.4 mg/ml) (Sigma) in 50 mM phosphate-citrate buffer (pH 5.0) with 0.03% (v/v) hydrogen peroxide] was added to each well. The plate was incubated at room temperature for 10 min, and optical densities were read at 450 nm on a microplate reader (GloMax-Multi+ Detection System, Promega, Madison, WI).

4.2.4.5 T_{H1}:T_{H2} Index Calculation

In order to determine whether thin film vaccination induced a T_{H1} (IgG_{2a}) or T_{H2} (IgG_1) polarization, we used the following protocol. The index was calculated as (IgG_{2a}/IgG_1) using OD260 values. According to such calculation, an index calculation < 1 stands for a T_{H2} polarization; an index > 1 stands for a T_{H1} polarization.

4.2.4.6 Assessment of Cytokine Response Following Lethal Influenza Challenge

Whole blood collected at necropsy, following lethal Influenza challenge, was centrifuged for ten minutes at 10,000 rpm and serum was isolated. The serum samples were evaluated for cytokine levels using the Th1/Th2 Cytokine 11-Plex Human ProcartaPlex™ Panel (Invitrogen) according to manufacturer's instructions for eleven cytokines: IFNγ, IL-12p70, IL-13, IL-1β, IL-2, IL-4, IL-5, IL-6, IL-18, TNFα, and GM-CSF.

4.2.4.7 Cytotoxicity Assay

Cytotoxicity was assessed by measuring the amount of adenosine triphosphate (ATP), an indicator of metabolically active cells, in cultures using a Cell Titer-Glo Luminescent Cell Viability assay kit (Promega, Madison, WI) according to the manufacturer's instructions. Data generated from this assay was used to evaluate the cytotoxicity of fresh formulation 28 after exposure to human buccal cells (TR-146) for 30 min, 60 min, and 120 min.

4.2.5 Statistical Analysis

Statistical analysis of data was performed using JMP (JMP Statistical Software from SAS, Cary, NC). Differences with respect to treatment were calculated using unpaired two-tailed Student's t tests. Differences were determined to be significant when the probability of chance explaining the results was reduced to less than 5% ($P < 0.05$).

4.3 Results

4.3.1 Preliminary *In Vivo* Assessment of Film Performance

In order to determine whether our optimized novel thin film can be used as a platform for successful vaccination, we stabilized H1N1 influenza virus in the film matrix and administered it to the buccal and sublingual mucosa of BALB/c mice at a dose of 2000 $CEID_{50}$. Films successfully dissolved within 30-60 seconds after placement in the mouth. Mice given the same dose of unformulated virus by the intranasal (IN) or intramuscular (IM) routes were included for comparison. Analysis of serum collected 28 days post-immunization revealed that there was no significant difference in the level of anti-influenza IgG antibodies between all treatment groups (Figure 4.1A) and that animals immunized by the buccal route had significantly higher levels of neutralizing antibodies with respect to those immunized by IM injection (Figure 4.1B, p <

0.001). The formulation was well tolerated and there was no visible irritation to the buccal or sublingual mucosa after administration and dissolution of films. These observations are in line with a cytotoxicity study conducted on TR146 cells, an *in vitro* model of the human SL and BU mucosa (45), where each formulation component with and without virus failed to induce measurable toxicity over a 2 hour exposure time (Figure 4.1C). These studies are from a recent publication (42).

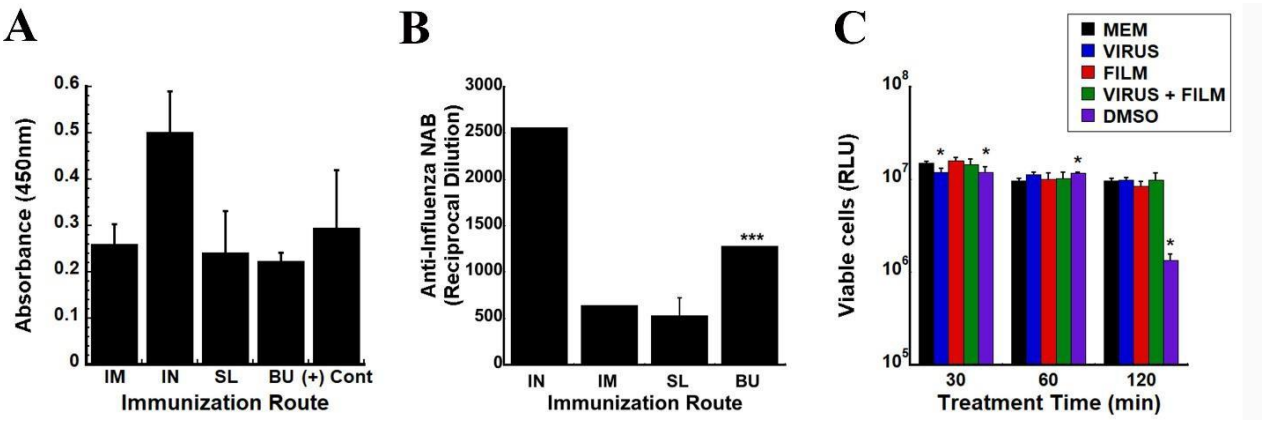

Figure 4.1: Immunogenicity Profiles of Thin Film Vaccine Validates Use in Oral Immunization Strategies.

Individual samples of heat inactivated serum collected 28 days after immunization from BALB/c mice were evaluated for influenza-specific IgG by ELISA (**A**). The average optical density read from samples obtained from each treatment group are presented to serve as a measure of relative antibody concentration. Each assay was validated by readings obtained from a sample collected from mice immunized with the same strain of influenza with an established anti-influenza antibody titer of 1:40 (+ Control, Emory). Readings obtained from samples collected from mice given saline (negative controls) were subtracted from all absorbances. Neutralization capacity of antibodies was assessed by serial dilution of heat inactivated serum with a fixed amount of H1N1 influenza virus prior to infection of MDCK cells (**B**). The reciprocal dilution plotted for each treatment group reflects the dilution at which the ability of the virus to infect target cells was

reduced by 50%. Cell activity was assessed by measuring the amount of adenosine triphosphate (ATP) in cultures using a Cell Titer-Glo Luminescent Cell Viability assay kit from Promega (**C**). TR-146 were treated for 30, 60, and 120 min with MEM media, influenza virus (virus), formulation 28 alone (film), film with virus, and DMSO. In each panel, results are expressed as average values ± the standard error of the mean and are representative of groups containing 4 mice per immunization route. *$p<0.05$, ***$p<0.001$, two-tailed Student's t-test. These studies are from a recent publication (42).

4.3.2 Permeability of Formulations on Epi Oral Explants

By understanding and improving the bioavailability of influenza across the buccal mucosa we may be able to improve the immune response observed. In a previous study, we established that the presence of surfactant in thin film formulations was key to achieving rapid and complete release of an infectious dose of virus upon dissolution (42). However, in order to study the ability of optimized thin film formulations to facilitate transport of vaccine through the oral mucosa in a physiologically relevant manner, permeability of virus across human buccal explants was evaluated (46, 47). Formulated dried films contained 3×10^7 infectious virus particles (ivp) of human H1N1 virus, comparable to the dose contained in live attenuated Flumist® vaccines (48). Unformulated influenza, prepared only in EpiOral^{TM} assay medium, was unable to pass through the human explants into the basolateral chamber during a 3-hour time period (Figure 4.2A). However, films containing an optimized formulation were reconstituted in assay medium and placed on the human explants, 84 ± 0.2 % (83.5%, 83.8%) of the dose successfully permeated through the membrane and into the basolateral chamber. Increasing the dose to 1×10^8 ivp resulted in a lower permeability with 75 ± 1.8 % (74%, 76%) of the dose

successfully passing through human explants. Data is provided as the average ± standard deviation since this is most representative of the spread of the data as well the actual values for each sample, since n=2. The permeability coefficient was also calculated in order to determine the rate at which the virus was able to cross the human explants during the three-hour sampling period. Films prepared with the low dose had a three-fold faster rate of permeation than the films prepared with the high dose (Figure 4.2B). Unformulated virus resulted in limited permeability. After this discovery, we investigated whether the virus was getting trapped in the tissues and if prolonged sampling would impact permeability. We used real time quantitative PCR to quantify the amount of virus remaining in tissue samples after 3 hours. Explants tested with films prepared with the low dose contained 3.5 ± 3.5% (1%, 6%) of the dose immobilized in the tissues (Figure 4.2C). Further increasing the dose of influenza resulted in almost an eight-fold increase, 23 ± 9.2% (17%, 30%), in the amount of virus retained in the tissue. However, without the assistance of formulation excipients, influenza virus was unable to permeate through the buccal explants and 96 ± 7.2% (91%, 100%) of the dose remained in the tissues. Unfortunately, sampling from the apical membrane would disturb the integrity of the tissues, and therefore the missing dose is assumed to be located in the apical chamber. Transepithelial electrical resistance (TEER) was measured and found to be 410 ± 50 ohm*cm^2 at the beginning of the studies and 330 ± 80 ohm*cm^2 at the end of the studies, well within the normal range established in the literature (47).

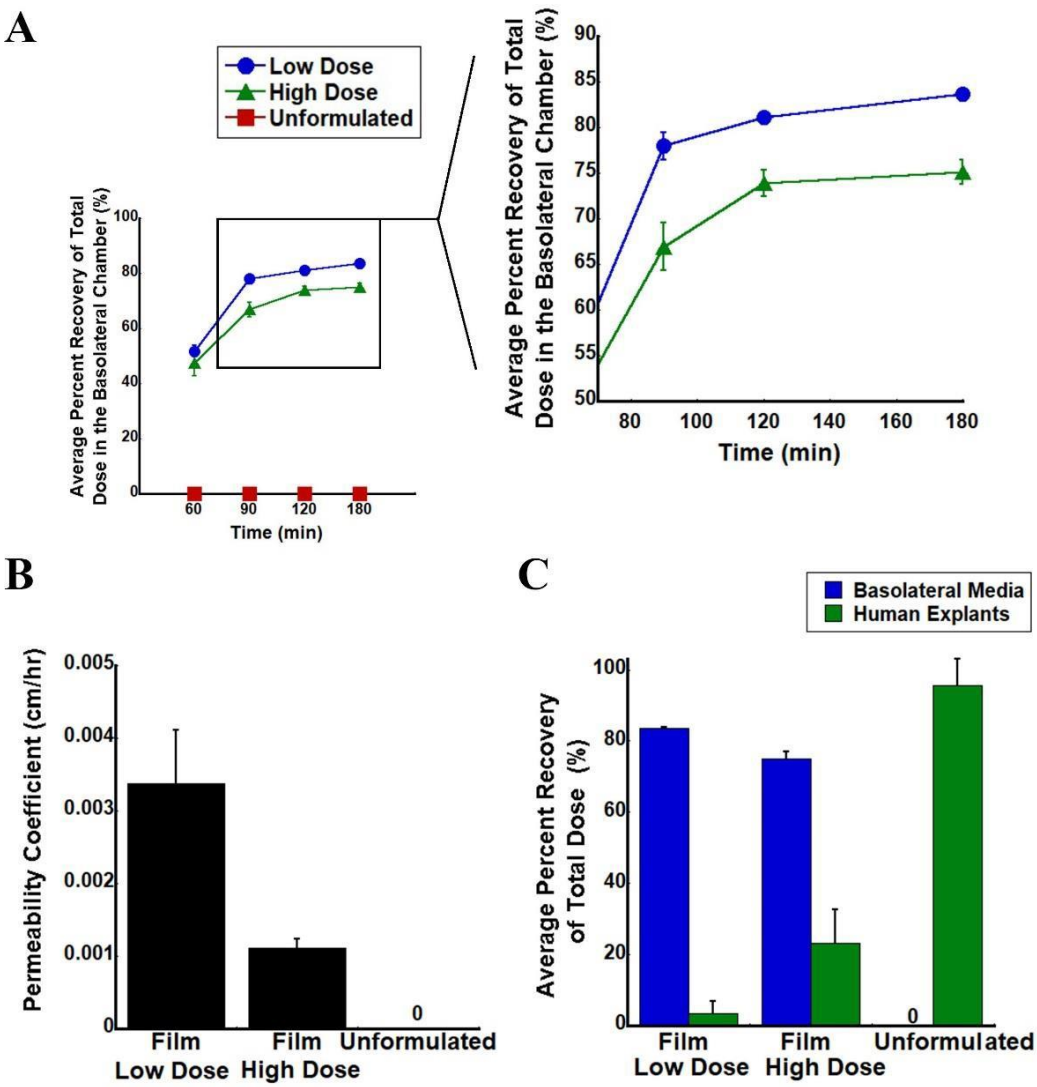

Figure 4.2: Formulations Foster Penetration through the Human Buccal Mucosa.

Films containing 3×10^7 i.v.p. (Low Dose) and 1 x 10^8 i.v.p (High Dose) were reconstituted in EpiOral™ assay medium and placed in the apical chamber of human explants. Virus was prepared with assay medium at the low dose of 3×10^7 i.v.p (Unformulated). (**A**) Cumulative Release Profiles. Samples were collected from the basolateral side of the tissue for 3 hours and the concentration of infectious virus was determined by a standard infectious titer assay. (**B**) Permeation Coefficient. The permeability coefficient was calculated, as defined by Fick's Law, using the infectious titer generated during the three-hour sampling period. See the methods

section for a detailed overview of the equations used. (**C**) Total Dose Distribution. After 24 hours EpiOral^{TM} tissues were rinsed with PBS, lysed via mechanical agitation, and viral RNA was isolated. Then RNA was converted to cDNA and qPCR was performed to determine the amount of virus genomes in each sample. Data collected from tissue isolates was normalized to infectious titer using the ivp/vp ratio. In each panel, data represent the average ± stdev of a minimum of two films per a condition. Statistical analysis was not performed as n=2 and would not be meaningful.

4.3.3 Impact of TRP Activators on Permeability

We also evaluated the effect of flavorings, which may act as natural adjuvants and modulate transient receptor potential (TRP) channels, on virus release and immobilization in human explants. Since each of the selected reagents were not water soluble, we first assessed their impact on physical properties of optimized films. The average pH and drying time of films prepared with flavorings solubilized in either ethanol or DMSO was 6.5 and 6 hours, respectively, and was not significantly different from films prepared without flavorings. Additionally, films prepared with ethanol solubilized compounds had an average thickness of 77 ± 14 µm, which was not significantly different from blank films, 73 ± 7 µm. However, films prepared with DMSO solubilized compounds were significantly thicker, 88 ± 6 µm ($p<0.05$) than films prepared without flavorings. Nevertheless, we did not detect a notable difference in infectious titer between the optimized formulations lacking flavoring and those prepared with flavorings (Figure 4.3A), and proceeded to prepare formulations at the highest activating concentration (Table 4.1) for this study to be able to detect changes in permeability. TRP channel inhibitors were also prepared at the highest known inhibiting concentration and included in

optimized film formulation to ascertain whether changes in permeability could be attributed to TRP activation or were due to an outside factor. Inhibiting concentrations resulted in an average pH of 6.5 and dry time of 6 hours, which is not significantly different than films prepared without inhibitors, however as previously mentioned DMSO solubilized compounds resulted in thicker films. Meanwhile, the infectious titer of optimized formulations was not impacted by the addition of either ethanol or DMSO solubilized flavorings (Figure 4.3B). Therefore, we proceeded to prepare formulations using the highest inhibiting concentration. See Table 4.1 for a list detailing TRP channel activating concentration and Table 4.2 for inhibiting concentrations used in this study.

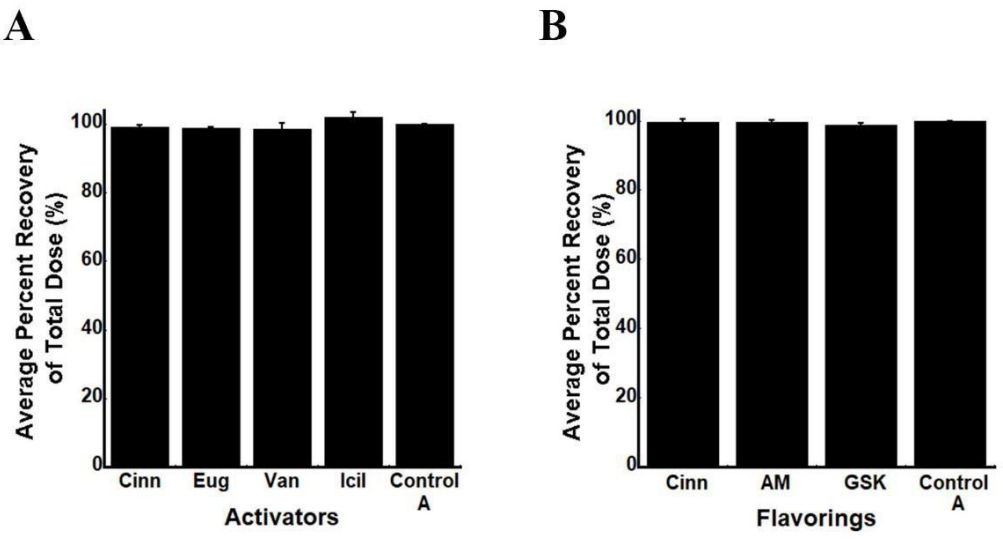

Figure 4.3: Activators and Inhibitors Maintain the Desired Dose of Influenza in Formulation.

Films containing 3×10^7 i.v.p. were prepared with TRP activators Cinnamaldehyde (10^{-2} µM), Eugenol (100 mM), Vanillin (100 µM), and Icilin (100 µM) and compared to formulations prepared without TRP agents (Control A) using a standard infectious titer assay (**A**). Films containing 3×10^7 i.v.p. were prepared with TRP inhibitors Cinnamaldehyde (10 µM), AM 0902

(131 nm), and GSK 2193874 (40 nM) and compared to Control A using a standard infectious titer assay (**B**). In each panel, data represent the average ± stdev.

Table 4.1: Concentrations of TRP Channel Activators Under Evaluation

Compound	Concentration Range	Target Concentration in Formulation	Ref
Eugenol	10 - 100 mM	100 mM	(35)
Vanillin	0.1 - 100 µM	100 µM	(36)
Cinnamaldehyde	10^{-2} – 10^{-3} µM	10^{-2} µM	(37)
Icilin	1 - 100 µM	100 µM	(38)

Table 4.2: Concentrations of TRP Channel Inhibitors Under Evaluation

	Concentration Range	Target Concentration in Formulation	Ref
AM 0902	20 - 131 nM	131 nM	(49)
GSK 2193874	40 – 2000 nM	40 nM*	(50)
Cinnamaldehyde	1 - 10 µM	10 µM	(51)

*This concentration was selected for screening due to studies which highlighted this dose as optimal as opposed to higher concentrations.

Optimized formulations prepared with cinnamaldehyde and vanillin at an activating concentration resulted in 82.7 ± 0.1% (82%, 83%) and 81.8 ± 0.2 % (82, 81.8%), respectively, of the total dose permeating through the membranes. Eugenol and Icilin followed a similar trend, and all of the activators had minimal impact on viral permeation relative to films prepared without activators (Figure 4.4A). Inhibitor GSK 2193874 resulted in a similar amount of virus permeating (81.2% ± 1% | 80%, 82%) through the tissues, and AM 0902 and cinnamaldehyde at inhibiting concentrations followed the same trend (Figure 4.4B). In summary, activators and inhibitors had no notable impact on infectious virus that permeated through the tissues relative to films prepared without either compound. However, there was a large increase in the amount of virus that permeated through the buccal explants with the addition of both activators and

inhibitors in comparison to unformulated virus. The calculated permeability coefficients revealed that films prepared with Icilin facilitated the permeation of virus at a faster rate, during the three-hour sampling period, than blank films across the buccal membrane (Figure 4.4C). TRP inhibitors did not make a notable impact on the rate of viral permeability in comparison to films lacking TRP agents (Figure 4.4D). However, both activators and inhibitors resulted in a faster rate of viral permeation in comparison to unformulated virus. After 24 hours, additional release of virus from the film matrix did not significantly impact the total dose detected in the basolateral membrane. We used qPCR to determine the amount of immobilized virus remaining in the explants and found that TRP activators and inhibitors (Vanillin: 1.3 ± 0.1% | 1.2, 1.4; GSK 2193874: 1 ± 0.9% | 1.6, 0.3%) had a minimal impact on the amount of virus immobilized in the tissues in comparison to blank films, but did decrease the amount of immobilized influenza in comparison to unformulated virus (Figure 4.4 E & F).

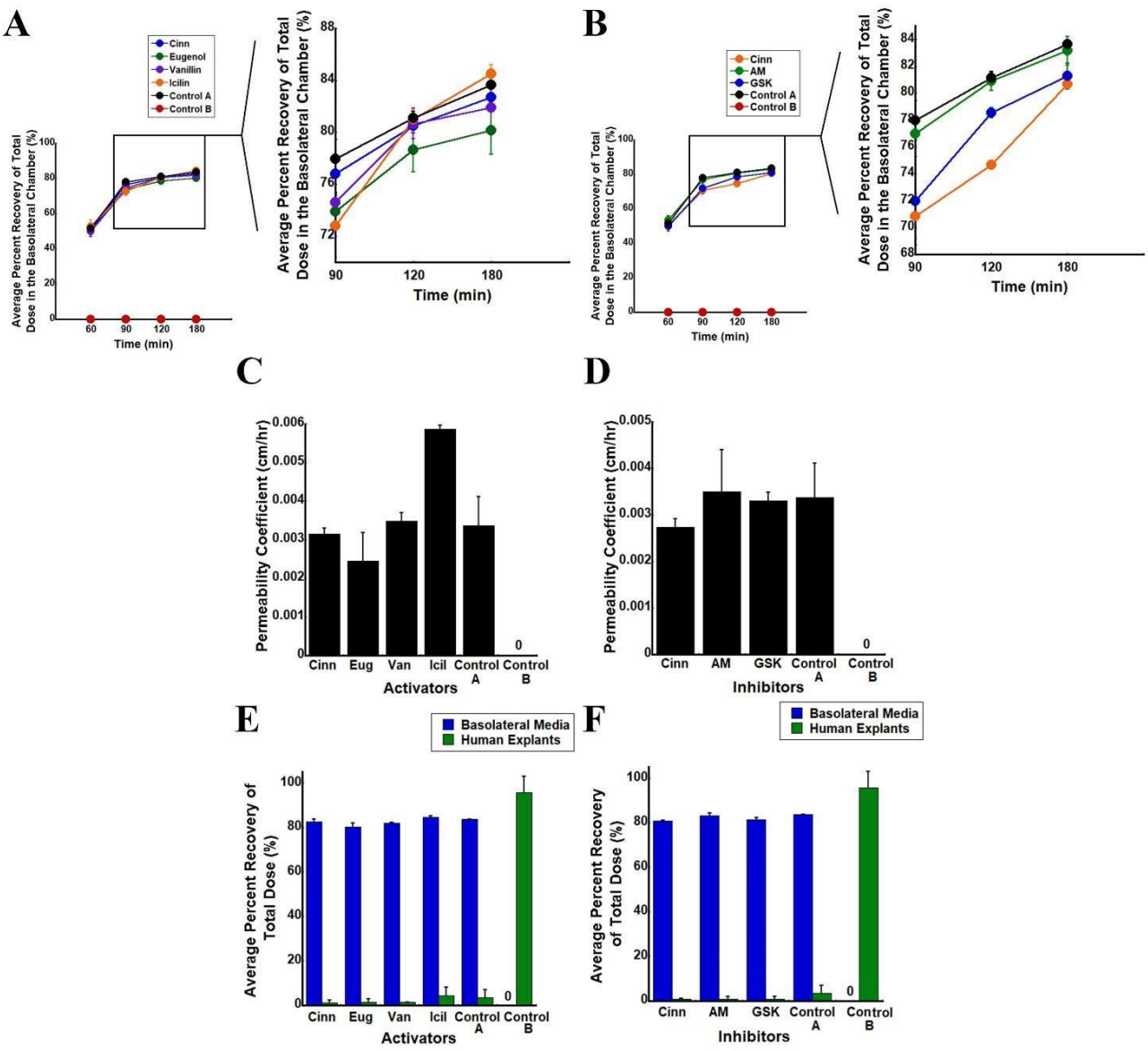

Figure 4.4: Flavorings Facilitate the Penetration of Influenza in Human Buccal Explant Tissues in Comparison to Unformulated Virus.

Films containing 3 x 10^7 i.v.p were prepared with activators or inhibitors, reconstituted in EpiOral^{TM} assay medium, and placed on the apical chamber human explants. Control A consists of blank films containing the same dose of Influenza without TRP agents that were reconstituted in assay medium and placed in the apical chamber of human explants. Control B consists of virus prepared with EpiOral^{TM} assay medium at a dose of 3 × 10^7 i.v.p as well. Cumulative Release

Profiles of (**A**) Activators and (**B**) Inhibitors. Samples were collected from the basolateral side of the tissue for 3 hours and the concentration of infectious virus was determined by a standard infectious titer assay. Permeation Coefficient of (**C**) Activators and (**D**) Inhibitors. The permeability coefficient was calculated, as defined by Fick's Law, using the infectious titer generated during the three-hour sampling period. See the methods section for a detailed overview of the equations used. Total Dose Distribution of (**E**) Activators and (**F**) Inhibitors. After 24 hours, EpiOral^{TM} tissues were rinsed with PBS, lysed via mechanical agitation, and viral RNA was isolated. Then RNA was converted to cDNA and qPCR was performed to determine the amount of virus genomes in each sample. Data collected from tissue isolates was normalized to infectious titer using the ivp/vp ratio. In each panel, data represent the average ± stdev of a minimum of two films per a condition. Statistical analysis was not performed as n=2 and would not be meaningful.

While individual agents did not notably impact transport and permeability of virus, collective evaluation of agents by channel type revealed that TRPM inhibitor cinnamaldehyde reduced the amount of permeated virus in the basolateral membrane by 5% (Figure 4.5A). Due to the variability observed with the amount virus immobilized in the tissues, however, it is difficult to determine reliably whether any of the inhibitors had a sizable impact (Figure 4.5B). The permeability coefficient was reduced three-fold by the presence of TRPM inhibitor relative to TRPM activator (Figure 4.5C). Since none of the inhibitors consistently reduced the permeability coefficient and amount of Influenza in both the tissues and the basolateral media relative to the activators, we determined that the flavorings did not reliably improve or impair viral release from the formulations. Transepithelial electrical resistance (TEER) was measured and found to

be 410 ± 50 ohm*cm^2 at the beginning of the studies and 330 ± 80 ohm*cm^2 at the end of the studies, well within normal range established in the literature (47).

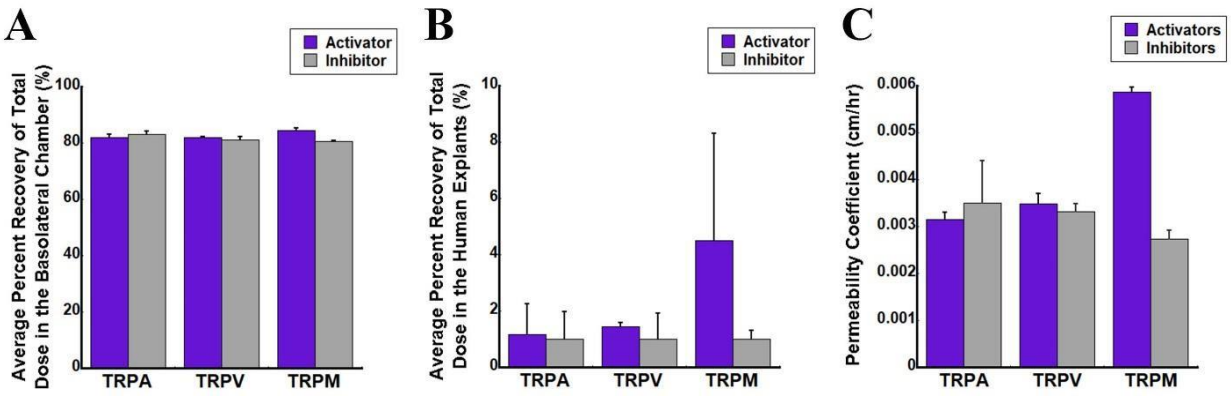

Figure 4.5: TRP Inhibitors Reduce the Rate of Influenza Permeation through Human Explants.

Films containing 3 x 10^7 i.v.p were prepared with activators or inhibitors, reconstituted in EpiOral^{TM} assay medium, and placed on the apical chamber containing human explants. (**A**) The Reductive Effects of TRP Inhibitors on Permeability. An infectious titer assay was used to determine the difference in viral permeability of TRP activators and inhibitors. (**B**) The Reductive Effects of TRP Inhibitors on Viral Immobilization. qPCR was used to determine the difference in immobilized virus between TRP activators and inhibitors. (**C**) The Reductive Effects of TRP Inhibitors on Permeability Coefficients. The permeability coefficient was calculated, as defined by Fick's Law, using the infectious titer generated during the three-hour sampling period. See the methods section for a detailed overview of the equations used. In each panel, data represent the average ± stdev of a minimum of two films per a condition. Statistical analysis was not performed as n=2 and would not be meaningful.

4.3.4 *Ex Vivo* Evaluation of TRP Agents as Potential Vaccine Adjuvants

In the next series of studies, the ability of TRP agents to stimulate or suppress cytokine release in the basolateral chamber of human explants was assessed. We evaluated the basolateral chamber after 6 hours of exposure to reconstituted films prepared with TRP activators and inhibitors, and while all the samples resulted in production of measurable IL-6 and GM-CSF, the results were not meaningfully greater than films prepared without TRP agents or unformulated Influenza (Table 4.3 and 4.4). The additional 9 cytokines evaluated were not detected after six hours of exposure to explants. After 24 hours of exposure, reconstituted films prepared with TRP activators, increased the release of IL-1β in the basolateral chamber of human explants 50-fold relative to films prepared without TRP agents and unformulated virus (Figure 4.6A). Films prepared with inhibiting concentrations of cinnamaldehyde resulted in a 40-fold increase, while those prepared with AM and GSK resulted in a 20-fold increase in the expression of IL-1β (Figure 4.6B). However, due to the variability associated with AM and GSK cytokine levels, the increase in cytokine expression is comparable to films prepared without TRP agents and unreliable. The addition of activators or inhibitors did not significantly impact the amount of IL-6 or GM-CSF cytokines released relative to films prepared without TRP agents, with the average amount of IL-6 production being 140 pg/mL and the average amount of GM-CSF production being 83 pg/mL across all samples (Figure 4.6A & 4.6B). The additional 8 cytokines evaluated were not detected after twenty-four hours of exposure to explants.

We evaluated the reductive effects of TRP inhibitors on cytokine expression relative to TRP activators. A two-fold decrease in IL-1β expression was observed in the basolateral chamber of explants that were exposed to films prepared with TRPV (GSK 2193874) and TRPA (AM 0902) inhibitors relative to films prepared with TRPV (Vanillin) and TRPA

(Cinnamaldehyde) activators (Figure 4.6C). Films prepared with cinnamaldehyde (TRPM inhibitor) reduced expression of IL-1β by 25% in comparison to films prepared with the TRPM activator, Icilin. TRP inhibitors, cinnamaldehyde, AM and GSK each reduced GM-CSF production by one-and-half the original amount TRP activators produced (Figure 4.6D). However, it is important to note that these reductions were not significant due to variability of the samples. The inhibitors had no impact on production of IL-6 relative to their respective activators (Figures 4.6E).

Table 4.3: TRP Channel Activators Effect on Cytokine Response after 6 hours of exposure to EpiOral™ Tissues.

Values are reported as the average amount in pg/mL ± standard deviation of n=2. The eleven cytokines evaluated included: IFNγ, IL-12p70, IL-13, IL-1β, IL-2, IL-4, IL-5, IL-6, IL-18, TNFα, and GM-CSF. Only detected cytokines are listed below.

	Cinnamal-dehyde	Eugenol	Vanillin	Icilin	Control A	Control B
IL-6 (pg/mL)	21.5 ± 0.7	33 ± 7.1	27 ± 0	29 ± 1.4	40.5 ± 13	47.5 ± 8.5
GM-CSF (pg/mL)	37.0 ± 12	28.39 ± 0	33 ± 6.6	37.0 ± 12	37 ± 12	37 ± 12

Table 4.4: TRP Channel Inhibitors Effect on Cytokine Response after 6 hours of exposure to EpiOral™ Tissues.

Values are reported as the average amount in pg/mL ± standard deviation of n=2. The eleven cytokines evaluated included: IFNγ, IL-12p70, IL-13, IL-1β, IL-2, IL-4, IL-5, IL-6, IL-18, TNFα, and GM-CSF. Only detected cytokines are listed below.

	Cinnamal-dehyde	AM 0902	GSK 2193874	Control A	Control B
IL-6 (pg/mL)	31 ± 11	43 ± 14	33.5 ± 0.7	40.5 ± 13	47.5 ± 12
GM-CSF (pg/mL)	55.84 ± 4.5	40.51 ± 17	45.6 ± 0	37 ± 12	37 ± 12

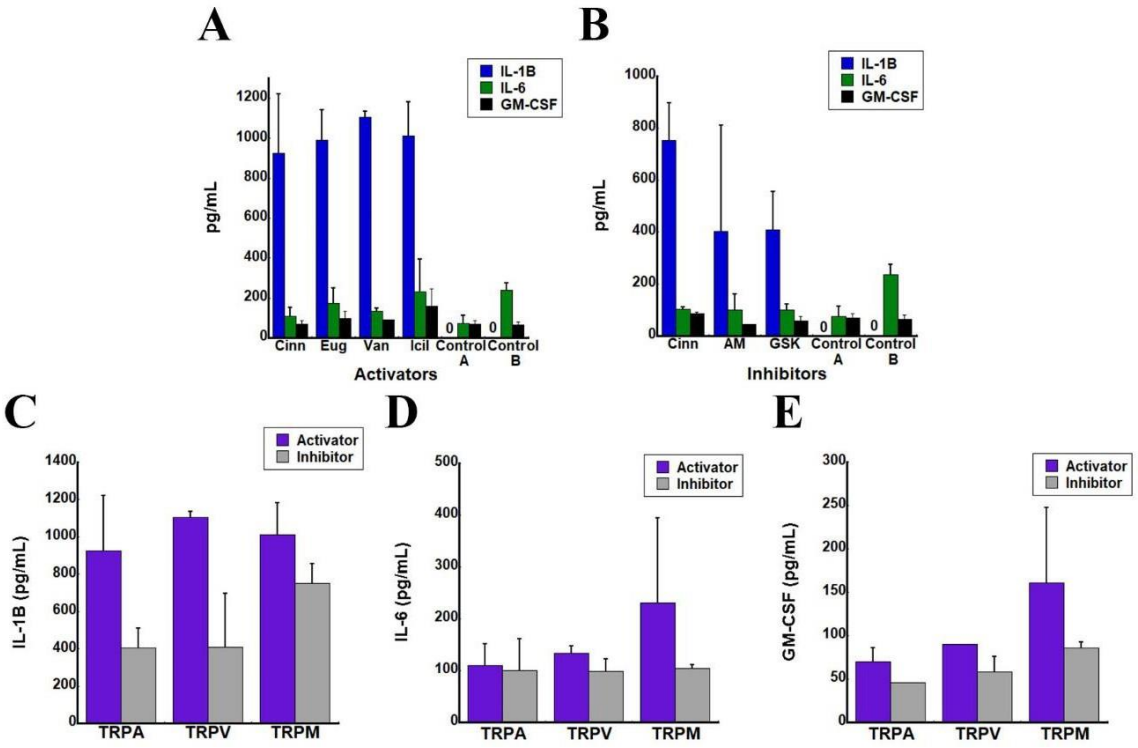

Figure 4.6: TRP Activators Improve Cytokine Response on EpiOral™ Tissues Relative to Films Lacking TRP Agents and Unformulated Virus.

Films containing 3×10^7 i.v.p. were prepared with TRP activating (**A**) and inhibiting (**B**) concentrations, reconstituted in EpiOral™ assay medium and placed on the apical chamber containing EpiOral™ explants. Samples were collected from the basolateral side of the membranes over a period of 24 hours and evaluated for cytokine IL-1β, IL-6, and GM-CSF levels using a ProcartaPlex Multiplex Assay. Control A formulations consisted of influenza at a concentration of 3×10^7 i.v.p in thin film formulations and Control B formulations consisted of 3×10^7 i.v.p influenza in assay medium. The reductive effects of TRP channel inhibitors were compared to inductive effects of activators on cytokine IL-1β (**C**), IL-6 (**D**), and GM-CSF (**E**) levels. In each panel, data represent the average ± stdev of a minimum of two films per condition. Statistical analysis was not performed as n=2 and would not be meaningful.

4.3.5 Thorough Evaluation of Immune Response Elicited by Alternative Immunization Routes

To determine whether the addition of a TRP activator would improve the immune response initially observed and further characterize the impact of alternative routes of vaccination and inactivated vaccine prepared with mouse-adapted-H1N1 virus, we evaluated mice sera 28 days after immunization. The IM route was chosen for comparison since most influenza vaccines currently on the market are given by injection and it is therefore the most clinically relevant route of immunization for influenza vaccines. H1N1 was stabilized in the thin film and given by the buccal (BU) and sublingual (SL) routes to mice at a dose of 2000 $CEID_{50}$. Mice were given the same dose, 2000 $CEID_{50}$, of unformulated virus by the intramuscular route. Additional analysis was conducted on buccally administered films prepared with cinnamaldehyde, a TRPA activator which consistently resulted in cytokine secretion in the basolateral chamber of human explants, and inactivated virus.

Immunization by the intramuscular, sublingual, and buccal routes did not result in a significant difference in total IgG levels 28 days after immunization (Figure 4.7A). However, analysis of IgG isotypes revealed statistical differences between the different immunization routes. Buccal and intramuscular immunization resulted in higher IgG_1 isotypes than the sublingual immunization route ($p<0.001$). There was also a six-fold increase in the anti-influenza-specific IgG_{2a} response ($p<0.05$) and a four-fold increase in the IgG_{2b} response ($p<0.01$) in buccally immunized mice relative to sublingually immunized mice. Immunization by intramuscular injection resulted in significantly lower levels of IgG_{2b} isotypes in comparison to the buccal route ($p<0.05$) and higher levels relative to the sublingual route ($p<0.05$). There was

no significant difference in the level of anti-influenza immunoglobulin total IgG antibodies and isotypes between all buccally immunized mice (Figure 4.7B).

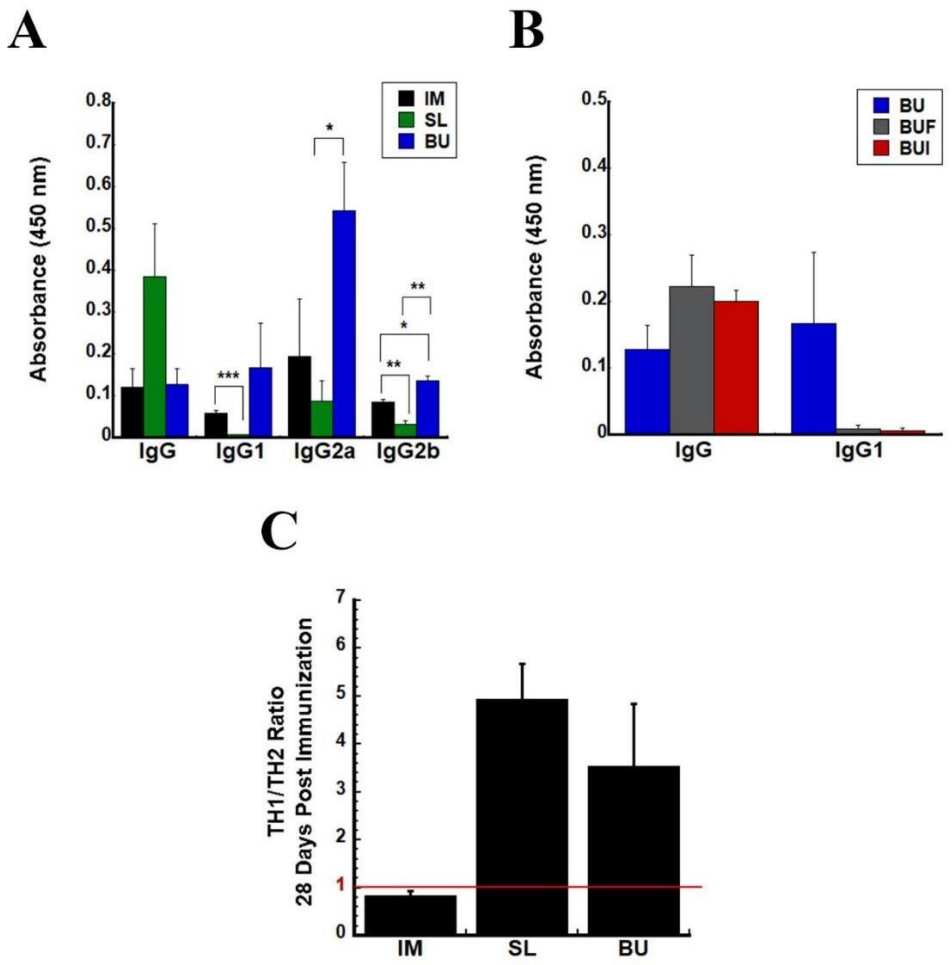

Figure 4.7: Oral Immunization Induces a T_{H1} Mediated Immune Response.

Serum was collected from BALB/c mice immunized by the IM, SL, and BU routes. Standard films were administered to mice by SL and BU routes. Films formulated with cinnamaldehyde (BUF) and inactivated influenza (BUI) were also administered buccally. Characterization of the antigen-specific response was conducted on individual samples which were collected 28 days after immunization (**A&B**) evaluated for influenza-specific IgG isotypes by ELISA. The T_{H1}:T_{H2}

ratio was calculated according to the methods section for immunization routes after 28 days after vaccination (**C**) Ratio < 1 = TH2 polarization. Ratio > 1 = TH1 polarization. In each panel, results are expressed as average values ± the standard error of the mean and are representative of groups containing 3 to 6 mice per immunization route. *p<0.05, **p<0.01, ***p<0.001, two-tailed Student's t-test. two-tailed Student's t test. IM, intramuscular; SL, sublingual; BU, buccal; BUF, buccal with cinnamaldehyde films; BUI, buccal with inactivated virus.

The T_{H1}:T_{H2} ratio was calculated for each immunization group in order to determine whether alternative routes of vaccine administration elicited a specific IgG subclass profile. This ratio compares T_{H1} IgG_{2a} subclass to T_{H2} IgG_1 subclass (52, 53). IgG2b titers were excluded from the ratio calculation as the classification of this IgG isotype is still debated (54, 55). In mice immunized by the intramuscular route 28 days after immunization the antibody response was balanced between $T_H1/T_{H2,}$ with a value close 1 (0.82 ± 0.11). In contrast, mice immunized sublingually or buccally had a distinct T_{H1} profile (Figure 4.7C). The ratios were not calculated for groups wherein no IgG_1 or IgG_{2a} was detected.

In order to determine whether the antibodies detected during isotyping had the ability to neutralize influenza virus, anti-influenza NAB levels were evaluated in serum samples collected 28 days after immunization. Sublingual immunization routes resulted in a significantly higher levels of neutralizing antibodies with respect to those immunized by intramuscular ($p<0.001$) and buccal routes ($p<0.05$) (Figure 4.8A). Analysis of serum following immunization of mice with BUI, BUF, and standard BU films administered to the buccal mucosa revealed that there was no significant difference in the level of anti-influenza NABs between all treatment groups ($p>0.05$, Figure 4.8B).

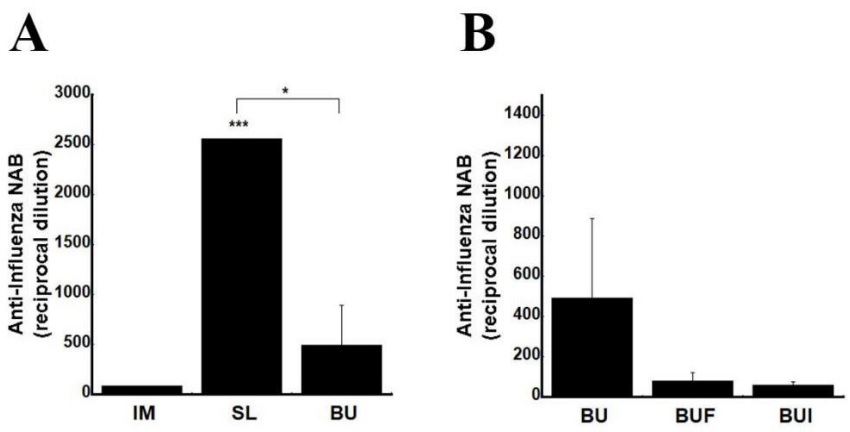

Figure 4.8: Sublingual Immunization Induces Protective Neutralizing Antibody Levels. Neutralization capacity of antibodies was assessed by serial dilution of heat-inactivated serum collected 28 days after immunization (**A &B**) with a fixed amount of H1N1 influenza virus before infection of MDCK (Madin-Darby canine kidney) cells. The reciprocal dilution plotted for each treatment group reflects the dilution at which the ability of the virus to infect target cells was reduced by 50%. In each panel, results are expressed as average values ± standard error and are representative of groups containing 3 to 6 mice per immunization route. IM, intramuscular; SL, sublingual; BU, buccal; BUF, buccal with cinnamaldehyde films; BUI, buccal with inactivated virus.

4.3.6 Evaluation of Protective Immunity Following Influenza Challenge

We began our analysis by evaluating the effects of a high dose influenza challenge, following immunization via various routes, on antibody responses and immunoglobulin isotypes 10 days after challenge and compared to the IM route of vaccination. Anti-influenza specific total IgG levels of mice sublingually immunized doubled relative to intramuscular ($p<0.01$) and buccal ($p<0.001$) immunization routes, following challenge (Figure 4.9A). Sublingual immunization also resulted in significantly higher IgG_{2a} levels relative to intramuscular

immunization ($p<0.05$). Mice BU immunized with inactivated virus or cinnamaldehyde in films, and subsequently challenged, had comparable levels of total IgG and isotypes relative to mice intramuscularly immunized and buccally immunized with standard films, respectively (Figure 4.9A& B). Neutralizing antibody levels NABs dramatically increased across all treatment groups and there were no significant differences between the values ($p>0.05$, Figure 4.9C & D).

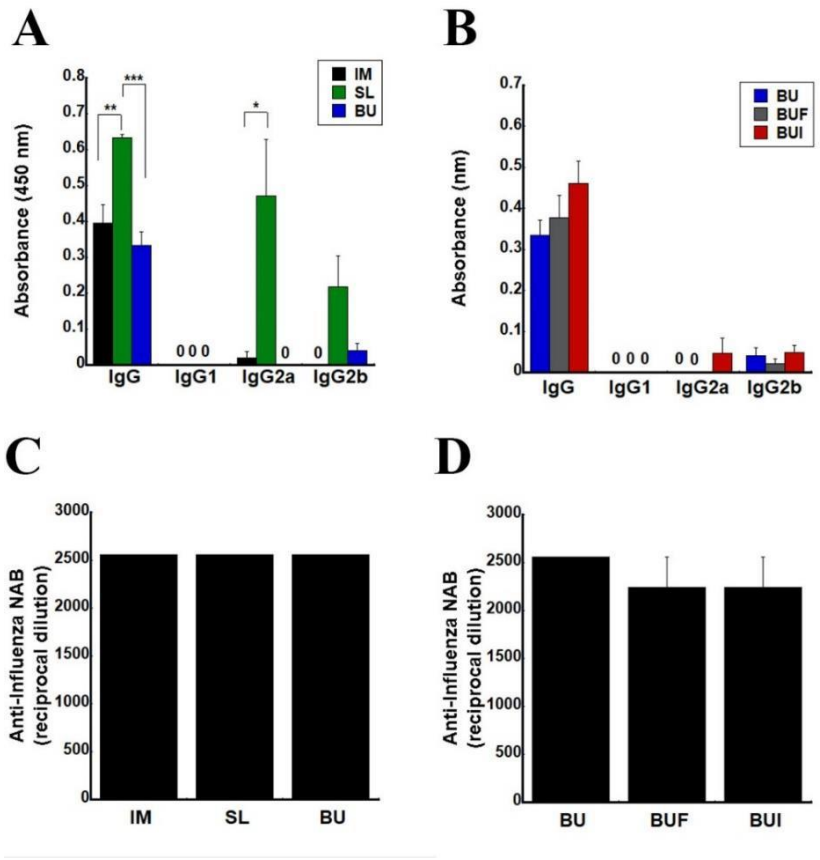

Figure 4.9: Sublingual Immunization Induces a Strong Antibody Immune Response Following Influenza Challenge.

Serum was collected from BALB/c mice immunized by the IM, SL, and BU routes. Standard films were administered to mice by SL and BU routes. Films formulated with cinnamaldehyde (BUF) and inactivated influenza (BUI) were also administered buccally. Characterization of the antigen-specific response was conducted on individual samples which were collected 10 days after influenza challenge (**A&B**) evaluated for influenza-specific IgG isotypes by ELISA.

Neutralization capacity of antibodies was assessed by serial dilution of heat-inactivated serum collected 10 days after influenza challenge (**C&D**) with a fixed amount of H1N1 influenza virus before infection of MDCK (Madin-Darby canine kidney) cells. The reciprocal dilution plotted for each treatment group reflects the dilution at which the ability of the virus to infect target cells was reduced by 50%. In each panel, results are expressed as average values ± the standard error of the mean and are representative of groups containing 3 to 6 mice per immunization route. *$p<0.05$, **$p<0.01$, ***$p<0.001$, two-tailed Student's t-test. two-tailed Student's t test. IM, intramuscular; SL, sublingual; BU, buccal; BUF, buccal with cinnamaldehyde films; BUI, buccal with inactivated virus.

To determine whether the local immune system was stimulated following vaccination by mucosal routes, the oral cavity was rinsed, and the wash was collected for analysis of IgA levels after treatment groups were intramuscularly challenged with a lethal dose of influenza. Influenza-specific IgA induces local immunity and provides a first line of protection against the virus entering through mucosal surfaces (56). IgA levels were not significantly different across any of the treatment groups ($p>0.05$), however the intramuscularly immunized animals had relatively lower IgA levels (Figure 4.10 A&B).

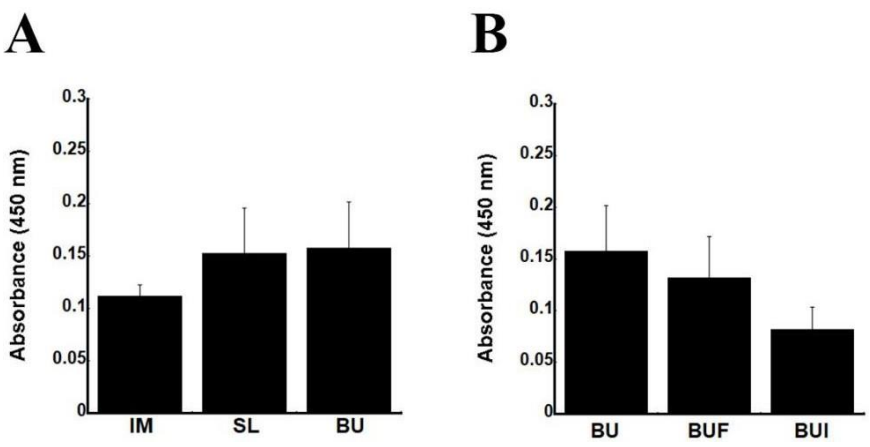

Figure 4.10: Oral Immunization Routes Elicit a Localized Immune Response.
Individual samples of saliva wash collected 10 days after challenge were also evaluated for influenza-specific IgA by ELISA. Intramuscular, sublingual, and buccal immunization routes were evaluated for localized immune response (**A)**. The impact of TRP agent, cinnamaldehyde, and inactivated influenza was evaluated on the localized immune response relative to standard buccal films **(B)**. The average optical density read from samples obtained from each treatment group are presented to serve as a measure of relative antibody concentration. In each panel, results are expressed as average values ± the standard error of the mean and are representative of groups containing 3 to 6 mice per immunization route. *$p<0.05$, two-tailed Student's t test. IM, intramuscular; SL, sublingual; BU, buccal; BUF, buccal with cinnamaldehyde films; BUI, buccal with inactivated virus.

However, the most direct way of evaluating the impact of vaccination route, TRP activator, or inactivated virus on vaccine potency is to assess protection from exposure to a pathogen. We did this by monitoring survival rate, weight loss and the infectious titer of lung homogenates after exposure to a high dose of mouse-adapted H1N1. Animals that lost more than

25% of their total body weight following challenge (57) were humanly sacrificed according to IACUC standards (58). Historical values, produced by our laboratory, from mice given saline and subsequently challenged by the same high dose of influenza were used for percent weight loss and viral load. The challenge study originally conducted had a different set of parameters and mice were not sacrificed until they lost more than 40% of their total body weight, and therefore their survival was not plotted. SL immunization (60% survival) protected mice more efficiently than IM (20% survival) or BU (20% survival) immunization from lethal challenge and resulted in the smallest change in body weight amongst the three groups (Figure 4.11 A, C). Mice in the SL (1.4×10^5 ivp/mL) and BU (1.2×10^5 ivp/mL) treatment group were also slightly more successful at clearing influenza infection from the lungs than mice immunized by traditional IM (1.6×10^5 ivp/mL) route, evident by the infectious titer of influenza found in lung homogenates (Figure 4.11E). However, all immunized groups cleared significantly more virus than PBS controls.

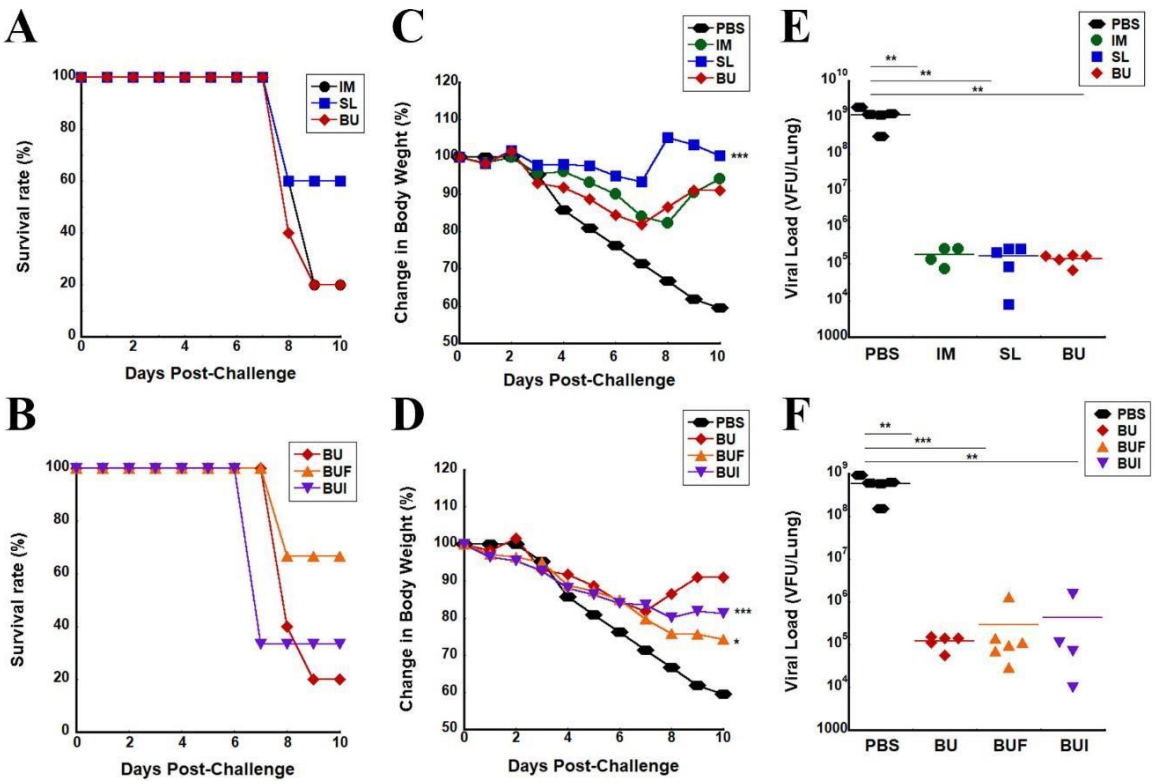

Figure 4.11: Sublingual and Buccal Immunization with Films containing Cinnamaldehyde Results in Protection from Influenza Challenge.

BALB/c mice were challenged with a lethal dose of 100,000 $CEID_{50}$ mouse adapted influenza 28 days after immunization by the IN route. Kaplan–Meier survival curves show SL and BUF groups had the highest survival rate (**A & B**). Body Weight Profiles after Challenge reveal all vaccinated groups had fewer signs of morbidity relative to PBS groups (**C & D**). Lungs were homogenized, following necropsies, and MDCK cells were infected to determine the infectious titer (**E&D**). In all panels, data reflect average values ± the standard error of the mean for 3 to 6 mice per group. IM, intramuscular; SL, sublingual; BU, buccal; BUF, buccal with cinnamaldehyde films; BUI, buccal with inactivated virus.

When mice were immunized buccally with films prepared with TRP activator cinnamaldehyde they were more protected against lethal influenza challenge, survival rate of 66.6%, than mice BU immunized with inactivated virus, survival rate of 33.3%, in films or standard film preparations, survival rate of 20% (Figure 4.11B). While mice in BUF and BUI treatment groups experienced the greatest change in weight, in comparison to BU treatment groups, it is important to note that these mice were on average 2 grams heavier than other mice at the start of the study, and those that survived never went below 20 grams of total body weight (Figure 4.11D). Animals in BUF, BUI, and BU treatment groups had comparable levels of infectious influenza in lung homogenates, but significantly lower viral load compared to PBS controls ($p<0.001$, $p<0.01$, $p<0.01$, respectively) (Figure 4.11F).

A ProcartaPlex Mouse Cytokine assay was used to evaluate the serum of animals after lethal influenza challenge for eleven cytokines. Only IL-18 and IFNγ cytokines had detectable levels in the serum of both survivors and non-survivors. As is commonly seen in samples taken from non-survivors of influenza infection (59-61), serum from these animals contained elevated levels of IL-18 and IFNγ cytokines across all five treatment groups (Figure 4.12). Similarly, as is routinely found in survivors of influenza infection, samples from these groups contained trace amounts of each cytokine. However, there was only a significant difference between cytokine levels in the serum of animals that survived lethal challenge and those that were sacrificed in SL ($p<0.05$) and BUF ($p<0.05$) groups. These groups had the best survival rate in this study, SL (60%) and BUF (66.6%). It is important to note that as some groups only had one survivor or one sacrificed animal, statistical testing was limited.

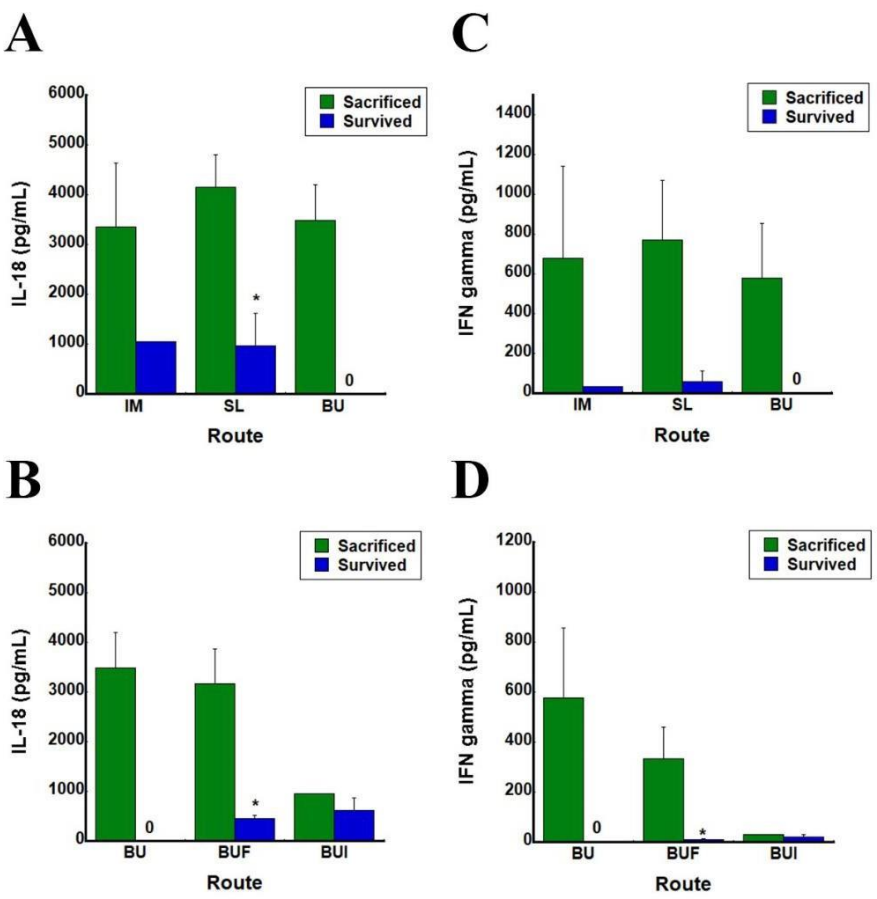

Figure 4.12: Sublingual and Buccal Immunization with Films containing Cinnamaldehyde Result in Significantly Lower Levels of Proinflammatory Cytokines in Survivors of Influenza Challenge.

Samples were taken from survivors 10 days after challenge and from non-survivors at time of death and eleven cytokines were evaluated: IFNγ, IL-12p70, IL-13, IL-1β, IL-2, IL-4, IL-5, IL-6, IL-18, TNFα, and GM-CSF. IL-18 cytokine levels were evaluated for IM, SL, and BU groups (**A**) and BU, BUF, and BUI groups (**B**). IFNγ cytokine levels were evaluated for IM, SL, and BU groups (**C**) and BU, BUF, BUI groups (**D**). In all panels, data reflect average values ± the standard error of the mean for 3 to 6 mice per group. *$p<0.05$, two-tailed Student's t test. IM, intramuscular; SL, sublingual; BU, buccal; BUF, buccal with cinnamaldehyde films; BUI, buccal with inactivated virus.

4.4 Discussion

Of the 26 approved influenza vaccines in the United States, only 3 (Flumist®, Flumist Quadrivalent ®, 2009 H1N1 (MedImmune) utilize a mucosal route (intranasal) for induction of the immune response (Appendix Table 2). After the 2009 pandemic various studies in the US found that in children under the age of 18, Flumist® was not successful in inducing protective immunity against H1N1 viruses, believed to be because of the reduced replication fitness of the H1N1 (A/Bolivia) component in the vaccine (62, 63). This led the Advisory Committee on Immunization Practices (ACIP) and Centers for Disease Control (CDC) to recommend against the use of the vaccine in 2016 (63-65). While the ACIP and CDC lifted the censure on Flumist® in 2018 after a different H1N1 strain (A/Slovenia) was selected, there has been little progress in the development of novel, safe, and effective Influenza vaccines. All new vaccines which have entered the market are designed based on the same strain-specific correlate of protection: strong hemagglutinin inhibition/neutralizing antibody titer (66). Due to this narrow development approach, licensed influenza vaccines provide subprime protection, typically ranging from 10 to 60% from infection (67). By using more than one correlate of protection, such as nasal antibodies (65) or mucosal antibodies along with neutralizing antibody titers, vaccine design may become more balanced, efficient, and representative of robust protective immunity (66). In this study we evaluate an optimized formulation's capability to efficiently deliver a vaccine dose, overcome barriers associated with oral mucosal immunization, and utilize mucosal antibodies, neutralizing antibody titer, and IgG levels as correlates of protection to evaluate the protective immune response to our novel thin film. We also evaluate the ability of a TRP activator to act as a natural adjuvant in the thin film matrix and induce a greater immune response and protective immunity.

Most influenza vaccines currently on the market are given by injection, we believe that the intramuscular route is the true yardstick of success for our formulated film-based vaccine as it represents the most clinically relevant route of immunization for influenza. In our preliminary evaluation, we found that administration of an antigen stabilized in the film matrix by the SL and BU routes is possible in a rodent model and can induce antibody levels comparable to administration of the same antigen by intramuscular injection (Figure 4.1). While these levels may seem low with respect to those observed after immunization by the nasal route, it is important to note that detectable serum antibody titers equal to or above 1:40, as determined by hemagglutination inhibition or neutralizing antibody assays, which we have surpassed here (SL, 1:533; BU, 1:1280; Figure 4.1), are considered predictive of a favorable clinical outcome following exposure to influenza (66, 68-70). It is also important to realize that the virus used in our studies, the mouse adapted PR8 strain, preferentially replicates in the airways, supporting a significantly stronger response after intranasal administration in contrast to that obtained from the other routes of administration (71). For this reason, animals given the virus by the intranasal route were also included in our initial study to validate assays for assessment of the antibody-mediated immune response by the novel SL and BU routes. Additionally, screening films after vaccination revealed that the actual dose administered via sublingual and buccal routes was 1100 $CEID_{50}$ instead of 2000 $CEID_{50}$, and this may have contributed to a weakened response relative to intranasal routes.

In an attempt to evaluate whether bioavailability of the vaccine dose is a barrier to successful immunization, we studied transport of the virus across a physiologically relevant model of human buccal mucosa. Unlike traditional immunization strategies, vaccines delivered to the sublingual or buccal mucosa of humans must pass through thick, nonkeratinized stratified

squamous epithelial tissue before entering the blood stream (72). Saliva and swallowing present additional challenges to successful delivery of solid oral dosage forms (73). The ideal dosage form will overcome these hurdles by exhibiting the following characteristics: adhesion to the oral cavity, regulated and efficient dose release, and unidirectional dose release (74). Mucoadhesive polymers, surfactants, bile salts, and fatty acids have been used in the past to facilitate successful dose release to the blood stream of small molecules (75-77). Recent studies have used chitosan and bilosomes to improve bioavailability of vaccines (78, 79). Our optimized thin film formulation (42) highlighted the importance of mucoadhesive polymer and surfactant, as application of unformulated Influenza A to an established 3D tissue explant culture model of human buccal mucosa (80) resulted in limited bioavailability, while our optimized formulation resulted in permeation of 84% of the total dose (Figure 4.2). We hypothesize that the higher dose resulted in a greater amount of virus being immobilized in the tissues, but lower overall bioavailability, due to the dilution of the formulation components to achieve the target dose. This made the formulations less viscous and more capable of entering the tissue, but reduced the concentration of surfactant. Permeation coefficients for formulated virus were either comparable or greater than values found in the literature for permeation enhancers across porcine or human buccal explants (80-83). It is important to note that due to sensitivity of the buccal tissues, we were not able to sample from the apical chamber of the explants and had to perform a mass balance calculation to determine the concentration of virus in the apical chamber once steady state was achieved (2 hours), which may result in slightly higher permeability coefficients. However, there is an advantage to a portion of the dose remaining in the tissues. The mechanisms of action adjuvants in intramuscular vaccines employ to elicit immune responses include the depot effect and antigen presenting cell (APC) recruitment to the site of injection

(84). The depot effect is the slow release of antigen which provides continual stimulation to the immune system so APCs reaching the site of immunization later can recognize the antigen and present it to T cells (85, 86). Since roughly 3% of the final dose was immobilized when formulated virus was applied to the buccal explants, this could potentially stimulate the immune system in a favorable way following vaccination to buccal routes. We later discovered a miscalculation and the actual dose administered to explants was 600,000 $CEID_{50}$ (low dose) and 2,000,000 $CEID_{50}$ (high dose), roughly 50-fold lower than planned. However, due to the reduced bioavailability observed at the higher dose (Figure 4.2), we believe we discovered a better range for evaluation for future studies on human buccal explants, than previously believed. Additionally, these studies were designed as a preliminary evaluation of the bioavailability of the dose in reconstituted films and subsequent studies to evaluate the impact of solid thin film application to human explants and to produce greater replicates are warranted.

Adjuvants in vaccines have also been used to stimulate the immune system by promoting cytokine production and recruiting APC's to the site of immunization (84). Since transient receptor potential channels (TRP) have previously been proven to play a role in both cytokine production and APC recruitment, we assessed whether common flavorings, TRP activators, may be able to act as natural adjuvants (39, 40). Upon evaluation of cytokines in the basolateral media of human explants, we saw a substantial impact on IL-1β release in response to films prepared with activators cinnamaldehyde (TRPA), vanillin (TRPV), and icilin (TRPM) relative to films prepared without TRP agents (Figure 4.6). Interleukin-1β, a proinflammatory cytokine produced by activated macrophages, is involved in a variety of cellular activities, including cell proliferation, differentiation, and apoptosis and is an indicator of antigen presenting cell recruitment in response to TRP agents (87). Additionally, unformulated controls which had

limited bioavailability resulted in some cytokine recruitment, indicating that the immobilized virus in buccal explants could contribute to the immunogenic profile of the optimized thin film vaccine (Figure 4.2 & 4.4). We also evaluated the effects of films formulated with TRP agents on the recovery (Figure 4.3) and bioavailability (Figure 4.4 & 4.5) of Influenza and did not see any alarming changes. It is important to note that while the addition of TRP inhibitors did not significantly reduce cytokine levels relative to films prepared with activators, we believe this may be due to the presence of organic solvents which are required to solubilize flavorings. Ethanol has previously been linked with upregulation and downregulation of cytokine responses depending on length of exposure (88, 89). Future studies will need to include control films prepared with the same amount of organic solvent but without TRP agents, as well as additional replicates to better characterize the impact of TRP activators and inhibitors.

Upon validation of the thin film as a viable vaccine dosage form and evaluation of the bioavailability of the dose administered to buccal explants, a comprehensive analysis of the immunogenicity profiles of film-stabilized Influenza administered by each route including TRPA activator, cinnamaldehyde, and inactivated virus was performed. Successful whole virus vaccination by mucosal routes has previously been associated with a strong IgG_{2a} response in BALB/c mice and linked to T-helper 1 (T_{H1}) polarized immunity (90, 91). T_{H1} mediated responses have been characterized as superior to T_{H2} as they are better at providing protection against influenza infection as IgG_{2a} antibodies can enhance antigen uptake due to their higher capacity to bind Fc-receptors on antigen-presenting cells (91-95). This is important at mucosal surfaces due to the epithelial barrier through which antigens must cross resulting in reduced bioavailability. The portion of the dose that successfully crosses the barrier is then met with several IgG antibody secreting cells at mucosal surfaces (96, 97). In fact, successful nasal

vaccination often results in IgA and IgG responses (98). This paradigm is partially supported by our studies as mice immunized by sublingual and buccal routes had T_{H1} polarized immune responses and higher neutralizing antibody titers, while intramuscularly immunized mice had a balanced T_{H1}/T_{H2} response and lower neutralizing antibody titer (Figure 4.7 and 4.8). While a balanced T_{H1}/T_{H2} response is normally favorable, since it elicits both cellular and humoral immunity, previous studies have demonstrated that in the case of Influenza it is vital that a vaccine induce a strong T_{H1} response in order to clear infection because T_{H2} antibodies (IgG_1) cannot activate complement cascades and the virus replicates excessively (98, 99). While the intramuscular antibody response resulted in a balanced Th1/Th2 response, the lower magnitude of IgG1 and IgG2a isotypes is likely indicative of weakly binding antibodies, incapable of producing strong protective immunity and therefore is not favored in our studies. When evaluating the IgA response, orally immunized groups had higher levels of mucosal antibodies in saliva wash but the difference was not statistically significant (Figure 4.10). The addition of other adjuvants to films administered to the sublingual route might result in greater mucosal immunity and improved survival.

Following high-dose challenge, sublingually immunized mice were most successful at producing total IgG and IgG2a (Figure 4.9). This correlated with significantly higher neutralizing antibody titers (1:2560) prior to challenge relative to intramuscular (1:80) and buccal (BU 1:493, BUF 1:80, BUI 1:60) routes (Figure 4.8). High levels of IgG_{2a} have previously been associated with repeated exposure to influenza in humans (100-102) and may be an indicator of the successful induction of immune memory following challenge. Additionally, the superiority of the sublingual immune response may be linked to direct access to submandibular lymphnodes which are located underneath the tongue in the ventral cervical subcutaneous region of mice (103, 104).

It is important to note that we later determined the actual dose administered to mice sublingually and buccally was 1500 $CEID_{50}$ which was slightly lower than the dose administered intramuscularly, but higher than the dose from initial studies. This increase in dose from the initial studies was favorable in terms of sublingual vaccination routes but was disadvantageous for buccal routes. Since the buccal mucosa of mice has 8-12 epithelial layers and the sublingual mucosa has 6-8, limited bioavailability is most likely a factor in the reduced efficacy of buccal immunization relative to sublingual (105). Furthermore, a dose that is too high may result in greater dose immobilization in the tissues and lower permeation coefficients, as observed in human buccal explants (Figure 4.2). The oral mucosa of mice is also keratinized which provides an additional permeability barrier to successful dose delivery (105). The reduced efficacy of the inactivated vaccine, on the other hand, may be because the dose was not high enough to illicit a protective immune response. Inactivated vaccines have been proven to be less immunogenic when directly compared to whole-virus vaccines and often require additional adjuvants (106, 107). However, we believe that the variability between dosing and immune response elicited with the thin film in general may also be related to difficulty preparing films small enough for the oral mucosa of mice. Films are currently prepared in stainless-steel molds, with a volume of 245 mm^3, which are then sectioned into 4 equal pieces and administered one at a time until the film is no longer visible. Due to the mechanical manipulation required to administer the dose we believe that inconsistent dosing may be the reason for limited protective efficacy with sublingual and buccal routes, regardless of live or inactivated virus. Three-dimensional printing technology may be the best alternative to preparing molds that can accommodate films of various sizes for future studies and may eliminate the variation observed.

Survival following influenza challenge supported the IgG subclass isotype and neutralizing antibody trends, as 60% of sublingually immunized mice survived lethal challenge (Figure 4.11). While 66.6% of mice immunized buccally with TRP activator cinnamaldehyde survived lethal challenge, they exhibited a 23% greater change in body weight and 58% higher lung viral titers relative to sublingual groups. They were likely more adversely impacted by challenge than sublingually immunized animals, as weight loss and high lung viral titers have been established as sign of influenza pathology (108, 109). However, sublingual and BUF groups outperformed intramuscular, BU, and BUI groups wherein only 20% of mice survived challenge. Cytokine response following lethal influenza challenge also provides insight into the severity of disease. While IL-18 is an inducer of IFNγ and T_{H1} responses, high levels of IL-18 are associated with lethality (110). Interestingly, sublingual and buccal (with cinnamaldehyde) immunization resulted in significantly lower levels of proinflammatory cytokine IL-18 in survivors relative to animals sacrificed following influenza challenge (Figure 4.12). An increasing number of studies have indicated that toll-like receptor (TLR) mediated immune response, which recognizes pathogen associated molecular patterns (PAMPs) and results in either the suppression or upregulation of cytokines, is associated with TRP channel activation and inhibition (111-113). Therefore, the discrepancy between all other indicators of morbidity and cytokine levels in mice buccally immunized with the TRPA agent may be due to a downregulated cytokine response. (114). The concentration of the TRP agent used to prepare films was identified for human TRPA activation and future studies will likely need to explore and optimize the dose of natural flavoring for murine applications. Taken together these findings suggest that sublingual vaccination, even at a slightly lower dose than intramuscular, was the most efficient route at inducing a strong, systemic humoral T_{H1} polarized response and protecting mice from lethal

influenza challenge. Future studies will need to analyze the mucosal and systemic T-cell response associated with alternative vaccination routes to provide additional insight into the mechanism of protection of animals immunized with the optimized thin film platform.

Influenza viruses evade a variety of host immune responses to achieve successful infection, evident through the need of a new flu vaccine every year (98). Therefore, vaccine candidates that can elicit strong, long lasting immune responses which outmaneuver the pathogen are needed. In the studies summarized here, we characterized the bioavailability and immunogenicity of sublingual and buccal delivery of an H1N1 Influenza vaccine that successfully elicited a strong humoral response. We also determined critical factors related to the development of long-lasting, protective immunity of mucosally immunized mice that will provide important insight into the optimization of the thin film vaccine platform in future studies. While some of these findings may be specific to Influenza virus, this platform may be modified for administration of alternative viruses such as respiratory syncytial virus, herpes simplex virus, and adeno-associated virus, all of which have previously been stabilized in the thin film matrix.

4.5 References

1. D. A. Henderson, The eradication of smallpox – An overview of the past, present, and future. *Vaccine* **29**, D7-D9 (2011).
2. R. Rappuoli, H. I. Miller, S. Falkow, Medicine. The intangible value of vaccination. *Science (New York, N.Y.)* **297**, 937-939 (2002).
3. World Health Organization. The top 10 causes of death: Leading causes of death by economy income group. (2018).
4. C. Dye, After 2015: infectious diseases in a new era of health and development. *Philos Trans R Soc Lond B Biol Sci* **369**, 20130426-20130426 (2014).
5. Margaret E Kruk *et al.*, Mortality due to low-quality health systems in the universal health coverage era: a systematic analysis of amenable deaths in 137 countries. *The Lancet* **392**, 2203-2212 (2018).
6. C. Hansen, E. Paintsil, Infectious Diseases of Poverty in Children: A Tale of Two Worlds. *Pediatr Clin North Am* **63**, 37-66 (2016).

7. World Health Organization, in *World Health Statistics*. (2010), chap. Selected Infectious Diseases: Number of Reported Cases, pp. 73-84.
8. B. K. Giersing *et al.*, Challenges of vaccine presentation and delivery: How can we design vaccines to have optimal programmatic impact? *Vaccine* **35**, 6793-6797 (2017).
9. D. E. Phillips, J. L. Dieleman, S. S. Lim, J. Shearer, Determinants of effective vaccine coverage in low and middle-income countries: a systematic review and interpretive synthesis. *BMC Health Serv Res* **17**, 681-681 (2017).
10. S. Plotkin, J. M. Robinson, G. Cunningham, R. Iqbal, S. Larsen, The complexity and cost of vaccine manufacturing - An overview. *Vaccine* **35**, 4064-4071 (2017).
11. D. D. Kristensen, T. Lorenson, K. Bartholomew, S. Villadiego, Can thermostable vaccines help address cold-chain challenges? Results from stakeholder interviews in six low- and middle-income countries. *Vaccine* **34**, 899-904 (2016).
12. A. Portnoy *et al.*, Costs of vaccine programs across 94 low- and middle-income countries. *Vaccine* **33**, A99-A108 (2015).
13. H. Xu *et al.*, High expression of ACE2 receptor of 2019-nCoV on the epithelial cells of oral mucosa. *International Journal of Oral Science* **12**, 8 (2020).
14. B. Killingley, J. Nguyen-Van-Tam, Routes of influenza transmission. *Influenza and Other Respiratory Viruses* **7**, 42-51 (2013).
15. Y. J. Hou *et al.*, SARS-CoV-2 Reverse Genetics Reveals a Variable Infection Gradient in the Respiratory Tract. *Cell* **182**, 429-446.e414 (2020).
16. N. Lycke, M. Bemark, Mucosal adjuvants and long-term memory development with special focus on CTA1-DD and other ADP-ribosylating toxins. *Mucosal immunology* **3**, 556-566 (2010).
17. J. Wang *et al.*, Single mucosal, but not parenteral, immunization with recombinant adenoviral-based vaccine provides potent protection from pulmonary tuberculosis. *Journal of immunology (Baltimore, Md. : 1950)* **173**, 6357-6365 (2004).
18. A. Iwasaki, Exploiting Mucosal Immunity for Antiviral Vaccines. *Annual Review of Immunology* **34**, 575-608 (2016).
19. A. J. McDermott, G. B. Huffnagle, The microbiome and regulation of mucosal immunity. *Immunology* **142**, 24-31 (2014).
20. J. E. Vela Ramirez, L. A. Sharpe, N. A. Peppas, Current state and challenges in developing oral vaccines. *Adv Drug Deliv Rev* **114**, 116-131 (2017).
21. K. M. Van De Graaff, Anatomy and physiology of the gastrointestinal tract. *The Pediatric Infectious Disease Journal* **5**, (1986).
22. D. M. Mudie, G. L. Amidon, G. E. Amidon, Physiological parameters for oral delivery and in vitro testing. *Mol Pharm* **7**, 1388-1405 (2010).
23. H. Kraan *et al.*, Buccal and sublingual vaccine delivery. *Journal of Controlled Release* **190**, 580-592 (2014).
24. S. Hua, Advances in Nanoparticulate Drug Delivery Approaches for Sublingual and Buccal Administration. *Frontiers in Pharmacology* **10**, (2019).
25. M. Sattar, O. M. Sayed, M. E. Lane, Oral transmucosal drug delivery – Current status and future prospects. *International Journal of Pharmaceutics* **471**, 498-506 (2014).
26. S. P. Humphrey, R. T. Williamson, A review of saliva: normal composition, flow, and function. *The Journal of prosthetic dentistry* **85**, 162-169 (2001).
27. Vaccine Innovation Prioritisation Strategy, "Sublingual Dosage Forms," (Geneva, Switzerland, 2019).

28. ClinicalTrials.gov. Identifier: NCT02955030, Evaluation of the Safety and Immunogenicity of a Sublingual Influenza Vaccine NSV0001 in Healthy Male Volunteers. (National Library of Medicine Bethesda, MD, 2016).
29. L. Zeng, Mucosal adjuvants: Opportunities and challenges. *Hum Vaccin Immunother* **12**, 2456-2458 (2016).
30. C. Marques, C. Som, M. Schmutz, O. Borges, G. Borchard, How the Lack of Chitosan Characterization Precludes Implementation of the Safe-by-Design Concept. *Frontiers in Bioengineering and Biotechnology* **8**, (2020).
31. I. M. van der Lubben, J. C. Verhoef, G. Borchard, H. E. Junginger, Chitosan and its derivatives in mucosal drug and vaccine delivery. *European Journal of Pharmaceutical Sciences* **14**, 201-207 (2001).
32. P. Pellegrino, E. Clementi, S. Radice, On vaccine's adjuvants and autoimmunity: Current evidence and future perspectives. *Autoimmunity Reviews* **14**, 880-888 (2015).
33. J. Alijotas-Reig, Human adjuvant-related syndrome or autoimmune/inflammatory syndrome induced by adjuvants. Where have we come from? Where are we going? A proposal for new diagnostic criteria. *Lupus* **24**, 1012-1018 (2015).
34. B. Laupèze, C. Hervé, A. Di Pasquale, F. Tavares Da Silva, Adjuvant Systems for vaccines: 13 years of post-licensure experience in diverse populations have progressed the way adjuvanted vaccine safety is investigated and understood. *Vaccine* **37**, 5670-5680 (2019).
35. J. Vriens, B. Nilius, R. Vennekens, Herbal compounds and toxins modulating TRP channels. *Curr Neuropharmacol* **6**, 79-96 (2008).
36. R. A. Ross, Anandamide and vanilloid TRPV1 receptors. *British Journal of Pharmacology* **140**, 790-801 (2003).
37. S. Mihara, T. Shibamoto, The role of flavor and fragrance chemicals in TRPA1 (transient receptor potential cation channel, member A1) activity associated with allergies. *Allergy, Asthma & Clinical Immunology* **11**, 11 (2015).
38. A. M. Peier *et al.*, A TRP Channel that Senses Cold Stimuli and Menthol. *Cell* **108**, 705-715 (2002).
39. S. Basu, P. Srivastava, Immunological role of neuronal receptor vanilloid receptor 1 expressed on dendritic cells. *Proc Natl Acad Sci U S A* **102**, 5120-5125 (2005).
40. L. L. Nohara, S. R. Stanwood, K. D. Omilusik, W. A. Jefferies, Tweeters, Woofers and Horns: The Complex Orchestration of Calcium Currents in T Lymphocytes. *Frontiers in Immunology* **6**, (2015).
41. J. H. Choi *et al.*, A single sublingual dose of an adenovirus-based vaccine protects against lethal Ebola challenge in mice and guinea pigs. *Mol Pharm* **9**, 156-167 (2012).
42. I. Bajrovic, S. C. Schafer, D. K. Romanovicz, M. A. Croyle, Novel technology for storage and distribution of live vaccines and other biological medicines at ambient temperature. *Science Advances* **6**, eaau4819 (2020).
43. Y. Zhang *et al.*, Influenza Research Database: An integrated bioinformatics resource for influenza virus research. *Nucleic Acids Res* **45**, D466-D474 (2017).
44. J. H. Choi, S. C. Schafer, A. N. Freiberg, M. A. Croyle, Bolstering Components of the Immune Response Compromised by Prior Exposure to Adenovirus: Guided Formulation Development for a Nasal Ebola Vaccine. *Molecular Pharmaceutics* **12**, 2697-2711 (2015).

45. H. T. Rupniak *et al.*, Characteristics of four new human cell lines derived from squamous cell carcinomas of the head and neck. *Journal of the National Cancer Institute* **75**, 621-635 (1985).
46. N. P. Yadev, C. Murdoch, S. P. Saville, M. H. Thornhill, Evaluation of tissue engineered models of the oral mucosa to investigate oral candidiasis. *Microbial Pathogenesis* **50**, 278-285 (2011).
47. J. Kubilus *et al.*, "Characterization and testing of new buccal and gingival tissue models," (MatTek Corporation, Ashland, MA, 2006).
48. FluMist (influenza vaccine live) [package insert]. Gaithersburg, MD: MedImmune; 2019.
49. L. B. Schenkel *et al.*, Optimization of a Novel Quinazolinone-Based Series of Transient Receptor Potential A1 (TRPA1) Antagonists Demonstrating Potent in Vivo Activity. *Journal of medicinal chemistry* **59**, 2794-2809 (2016).
50. M. Cheung *et al.*, Discovery of GSK2193874: An Orally Active, Potent, and Selective Blocker of Transient Receptor Potential Vanilloid 4. *ACS medicinal chemistry letters* **8**, 549-554 (2017).
51. F. Roth-Walter *et al.*, Immune suppressive effect of cinnamaldehyde due to inhibition of proliferation and induction of apoptosis in immune cells: implications in cancer. *PloS one* **9**, e108402 (2014).
52. D. J. Lefeber *et al.*, Th1-Directing Adjuvants Increase the Immunogenicity of Oligosaccharide-Protein Conjugate Vaccines Related to Streptococcus pneumoniae Type 3. *Infection and Immunity* **71**, 6915 (2003).
53. M. L. Visciano, M. Tagliamonte, M. L. Tornesello, F. M. Buonaguro, L. Buonaguro, Effects of adjuvants on IgG subclasses elicited by virus-like Particles. *Journal of Translational Medicine* **10**, 4 (2012).
54. H. L. Weiner, Oral tolerance: immune mechanisms and the generation of Th3-type TGF-beta-secreting regulatory cells. *Microbes and infection* **3**, 947-954 (2001).
55. T. M. McIntyre *et al.*, Transforming growth factor beta 1 selectivity stimulates immunoglobulin G2b secretion by lipopolysaccharide-activated murine B cells. *The Journal of experimental medicine* **177**, 1031-1037 (1993).
56. P. N. Boyaka, Inducing Mucosal IgA: A Challenge for Vaccine Adjuvants and Delivery Systems. *J Immunol* **199**, 9-16 (2017).
57. E. A. Weaver, A. M. Rubrum, R. J. Webby, M. A. Barry, Protection against Divergent Influenza H1N1 Virus by a Centralized Influenza Hemagglutinin. *PloS one* **6**, e18314 (2011).
58. M. Couto, in *Vertebrate Embryogenesis: Embryological, Cellular, and Genetic Methods*, Francisco J. Pelegri, Ed. (Humana Press, Totowa, NJ, 2011), pp. 579-599.
59. J. R. Tisoncik *et al.*, Into the eye of the cytokine storm. *Microbiology and molecular biology reviews : MMBR* **76**, 16-32 (2012).
60. J. S. Peiris, K. P. Hui, H. L. Yen, Host response to influenza virus: protection versus immunopathology. *Current opinion in immunology* **22**, 475-481 (2010).
61. Q. Liu, Y.-h. Zhou, Z.-q. Yang, The cytokine storm of severe influenza and development of immunomodulatory therapy. *Cellular & Molecular Immunology* **13**, 3-10 (2016).
62. M. A. Gill, E. P. Schlaudecker, Perspectives from the Society for Pediatric Research: Decreased Effectiveness of the Live Attenuated Influenza Vaccine. *Pediatric Research* **83**, 31-40 (2018).

63. J. R. Chung *et al.*, Live Attenuated and Inactivated Influenza Vaccine Effectiveness. *Pediatrics* **143**, e20182094 (2019).
64. G. P. Kobinger *et al.*, Assessment of the Efficacy of Commercially Available and Candidate Vaccines against a Pandemic H1N1 2009 Virus. *The Journal of Infectious Diseases* **201**, 1000-1006 (2010).
65. L. A. Grohskopf *et al.*, Prevention and Control of Seasonal Influenza with Vaccines: Recommendations of the Advisory Committee on Immunization Practices-United States, 2018-19 Influenza Season. *MMWR. Recommendations and reports : Morbidity and mortality weekly report. Recommendations and reports* **67**, 1-20 (2018).
66. F. Krammer, J. P. Weir, O. Engelhardt, J. M. Katz, R. J. Cox, Meeting report and review: Immunological assays and correlates of protection for next-generation influenza vaccines. *Influenza Other Respir Viruses* **14**, 237-243 (2020).
67. T. T. Wang, S. Bournazos, J. V. Ravetch, Immunological responses to influenza vaccination: lessons for improving vaccine efficacy. *Current opinion in immunology* **53**, 124-129 (2018).
68. D. Liebowitz, J. D. Lindbloom, J. R. Brandl, S. J. Garg, S. N. Tucker, High titre neutralising antibodies to influenza after oral tablet immunisation: a phase 1, randomised, placebo-controlled trial. *The Lancet Infectious Diseases* **15**, 1041-1048 (2015).
69. G. Koopman *et al.*, Correlation between Virus Replication and Antibody Responses in Macaques following Infection with Pandemic Influenza A Virus. *Journal of virology* **90**, 1023-1033 (2016).
70. S. Pillet *et al.*, Cellular immune response in the presence of protective antibody levels correlates with protection against 1918 influenza in ferrets. *Vaccine* **29**, 6793-6801 (2011).
71. S. J. Samet, S. M. Tompkins, Influenza Pathogenesis in Genetically Defined Resistant and Susceptible Murine Strains. *Yale J Biol Med* **90**, 471-479 (2017).
72. J. O. Morales *et al.*, Challenges and Future Prospects for the Delivery of Biologics: Oral Mucosal, Pulmonary, and Transdermal Routes. *The AAPS journal* **19**, 652-668 (2017).
73. J. A. Bartlett, K. van der Voort Maarschalk, Understanding the oral mucosal absorption and resulting clinical pharmacokinetics of asenapine. *AAPS PharmSciTech* **13**, 1110-1115 (2012).
74. C. P. Jain, G. Joshi, U. Kataria, K. Patel, Enhanced Permeation of an Antiemetic Drug from Buccoadhesive Tablets by Using Bile Salts as Permeation Enhancers: Formulation Characterization, In Vitro, and Ex Vivo Studies. *Sci Pharm* **84**, 379-392 (2016).
75. J. O. Morales, D. J. Brayden, Buccal delivery of small molecules and biologics: of mucoadhesive polymers, films, and nanoparticles. *Current Opinion in Pharmacology* **36**, 22-28 (2017).
76. A. Miquel-Clopés, E. G. Bentley, J. P. Stewart, S. R. Carding, Mucosal vaccines and technology. *Clinical & Experimental Immunology* **196**, 205-214 (2019).
77. T. Caon, L. Jin, C. M. Simões, R. S. Norton, J. A. Nicolazzo, Enhancing the buccal mucosal delivery of peptide and protein therapeutics. *Pharmaceutical research* **32**, 1-21 (2015).
78. A. Shukla, V. Mishra, P. Kesharwani, Bilosomes in the context of oral immunization: development, challenges and opportunities. *Drug Discovery Today* **21**, 888-899 (2016).
79. L. Xing *et al.*, Chemical Modification of Chitosan for Efficient Vaccine Delivery. *Molecules (Basel, Switzerland)* **23**, (2018).

80. J. Boateng, O. Okeke, Evaluation of Clay-Functionalized Wafers and Films for Nicotine Replacement Therapy via Buccal Mucosa. *Pharmaceutics* **11**, (2019).
81. C. Padula, S. Pescina, S. Nicoli, P. Santi, New Insights on the Mechanism of Fatty Acids as Buccal Permeation Enhancers. *Pharmaceutics* **10**, (2018).
82. D. Kottke, H. Majid, J. Breitkreutz, B. B. Burckhardt, Development and evaluation of mucoadhesive buccal dosage forms of lidocaine hydrochloride by ex-vivo permeation studies. *International Journal of Pharmaceutics* **581**, 119293 (2020).
83. H. Abd El Azim, N. Nafee, A. Ramadan, N. Khalafallah, Liposomal buccal mucoadhesive film for improved delivery and permeation of water-soluble vitamins. *International Journal of Pharmaceutics* **488**, 78-85 (2015).
84. S. Awate, L. A. Babiuk, G. Mutwiri, Mechanisms of action of adjuvants. *Frontiers in immunology* **4**, 114-114 (2013).
85. K. Brewer *et al.*, Unique depot formed by an oil based vaccine facilitates active antigen uptake and provides effective tumour control. *Journal of Biomedical Science* **25**, (2018).
86. G. Ahlén *et al.*, In Vivo Electroporation Enhances the Immunogenicity of Hepatitis C Virus Nonstructural 3/4A DNA by Increased Local DNA Uptake, Protein Expression, Inflammation, and Infiltration of CD3+ T Cells. *J Immunol* **179**, 4741-4753 (2007).
87. G. Lopez-Castejon, D. Brough, Understanding the mechanism of IL-1β secretion. *Cytokine Growth Factor Rev* **22**, 189-195 (2011).
88. F. T. Crews *et al.*, Cytokines and Alcohol. *Alcoholism: Clinical and Experimental Research* **30**, 720-730 (2006).
89. C. J. M. Kane *et al.*, Effects of Ethanol on Immune Response in the Brain: Region-Specific Changes in Adolescent Versus Adult Mice. *Alcoholism: Clinical and Experimental Research* **38**, 384-391 (2014).
90. A. O. Hovden, R. J. Cox, L. R. Haaheim, Whole influenza virus vaccine is more immunogenic than split influenza virus vaccine and induces primarily an IgG2a response in BALB/c mice. *Scandinavian Journal of Immunology* **62**, 36-44 (2005).
91. J. F. S. Mann *et al.*, Lipid vesicle size of an oral influenza vaccine delivery vehicle influences the Th1/Th2 bias in the immune response and protection against infection. *Vaccine* **27**, 3643-3649 (2009).
92. J. Hinkula, S. Nyström, C. Devito, A. Bråve, S. E. Applequist, Long-Lasting Mucosal and Systemic Immunity against Influenza A Virus Is Significantly Prolonged and Protective by Nasal Whole Influenza Immunization with Mucosal Adjuvant N3 and DNA-Plasmid Expressing Flagellin in Aging In- and Outbred Mice. *Vaccines (Basel)* **7**, 64 (2019).
93. J. P. Amorij, A. Huckriede, J. Wilschut, H. W. Frijlink, W. L. Hinrichs, Development of stable influenza vaccine powder formulations: challenges and possibilities. *Pharmaceutical research* **25**, 1256-1273 (2008).
94. S. L. Swain *et al.*, CD4+ T-cell memory: generation and multi-faceted roles for CD4+ T cells in protective immunity to influenza. *Immunol Rev* **211**, 8-22 (2006).
95. A. Bot, S. Bot, C. A. Bona, Protective Role of Gamma Interferon during the Recall Response to Influenza Virus. *Journal of Virology* **72**, 6637 (1998).
96. P. Brandtzaeg *et al.*, The B-cell system of human mucosae and exocrine glands. *Immunol Rev* **171**, 45-87 (1999).

97. W.-D. Zhang, W.-H. Wang, S. Jia, The Distribution of SIgA and IgG Antibody-Secreting Cells in the Small Intestine of Bactrian Camels (Camelus bactrianus) of Different Ages. *PloS one* **11**, e0156635 (2016).
98. X. Chen *et al.*, Host Immune Response to Influenza A Virus Infection. *Frontiers in Immunology* **9**, (2018).
99. T. M. Moran, H. Park, A. Fernandez-Sesma, J. L. Schulman, Th2 Responses to Inactivated Influenza Virus Can Be Converted to Th1 Responses and Facilitate Recovery from Heterosubtypic Virus Infection. *The Journal of Infectious Diseases* **180**, 579-585 (1999).
100. A. S. El-Madhun, R. J. Cox, L. R. Haaheim, The Effect of Age and Natural Priming on the IgG and IgA Subclass Responses after Parenteral Influenza Vaccination. *The Journal of Infectious Diseases* **180**, 1356-1360 (1999).
101. M. S. Miller *et al.*, Neutralizing antibodies against previously encountered influenza virus strains increase over time: a longitudinal analysis. *Sci Transl Med* **5**, 198ra107-198ra107 (2013).
102. Y. Adachi *et al.*, Exposure of an occluded hemagglutinin epitope drives selection of a class of cross-protective influenza antibodies. *Nature Communications* **10**, 3883 (2019).
103. C. L. Maruyama, M. M. Monroe, J. P. Hunt, L. Buchmann, O. J. Baker, Comparing human and mouse salivary glands: A practice guide for salivary researchers. *Oral Diseases* **25**, 403-415 (2019).
104. Z. F. H. M. Boonman *et al.*, Intraocular Tumor Antigen Drains Specifically to Submandibular Lymph Nodes, Resulting in an Abortive Cytotoxic T Cell Reaction. *The Journal of Immunology* **172**, 1567 (2004).
105. C. Thirion-Delalande *et al.*, Comparative analysis of the oral mucosae from rodents and non-rodents: Application to the nonclinical evaluation of sublingual immunotherapy products. *PloS one* **12**, e0183398-e0183398 (2017).
106. P. Yang *et al.*, Response of BALB/c mice to a monovalent influenza A (H1N1) 2009 split vaccine. *Cellular & Molecular Immunology* **7**, 116-122 (2010).
107. N. Du *et al.*, Generation and evaluation of the trivalent inactivated reassortant vaccine using human, avian, and swine influenza A viruses. *Vaccine* **26**, 2912-2918 (2008).
108. H. T. Groves *et al.*, Mouse Models of Influenza Infection with Circulating Strains to Test Seasonal Vaccine Efficacy. *Frontiers in Immunology* **9**, (2018).
109. T. Burkholder, C. Foltz, E. Karlsson, C. G. Linton, J. M. Smith, Health Evaluation of Experimental Laboratory Mice. *Curr Protoc Mouse Biol* **2**, 145-165 (2012).
110. C. A. Dinarello, Interleukin-18, a proinflammatory cytokine. *European cytokine network* **11**, 483-486 (2000).
111. E. Hakimizadeh *et al.*, TRPV1 receptor-mediated expression of Toll-like receptors 2 and 4 following permanent middle cerebral artery occlusion in rats. *Iran J Basic Med Sci* **20**, 863-869 (2017).
112. M. Tauseef *et al.*, TLR4 activation of TRPC6-dependent calcium signaling mediates endotoxin-induced lung vascular permeability and inflammation. *The Journal of experimental medicine* **209**, 1953-1968 (2012).
113. C. Maisonneuve, S. Bertholet, D. J. Philpott, E. De Gregorio, Unleashing the potential of NOD- and Toll-like agonists as vaccine adjuvants. *Proceedings of the National Academy of Sciences* **111**, 12294 (2014).

114. R. S. Rudicell *et al.*, Comparison of adjuvants to optimize influenza neutralizing antibody responses. *Vaccine* **37**, 6208-6220 (2019).

Chapter 5: Conclusion

The primary focus of this project was to develop and characterize a thermostable, mucosal-based vaccine platform that can be easily adapted for a variety of vaccine candidates. Experiments were designed to test the hypothesis that stabilizing a live virus-based vaccine in a multi-component formulation containing a novel zwitterionic surfactant, in a liquid state and dried film matrix, would result in improved viral stability after exposure to ambient and elevated temperatures, as well as an improved immune response following mucosal immunization relative to traditional vaccination routes. Thermostabilization of vaccines can significantly simplify vaccine storage and distribution processes, eliminating the need for cold-chain maintenance, and resulting in global access to life-saving vaccines. Despite this benefit, all approved vaccines for use by the Food and Drug Administration must be refrigerated, at minimum, for long term storage in order to guarantee potency. In order to address the need for thermostabilized vaccines, the World Health Organization developed the "Controlled Temperature Chain" (CTC) wherein vaccines are required to be stable at 40°C for at least three days to improve global access to vaccines. In the studies described in this document, I have shown that formulations containing surfactant, in the thin film matrix and liquid state, successfully stabilized live adenovirus at 4°C and 20°C for a minimum of three months, as well as 14 days at 37°C and 5 days at 40°C. The film matrix protected virus through 16 freeze-thaw cycles, during which films were frozen at -80°C and warmed to 20°C per a cycle. Our stabilization platform outperforms the only other vaccines that fit the requirements set forth by CTC, MenAfriVac© and Gardasil© 4, which are stable for four and three days, respectively. Stabilization at elevated temperatures, was found to be closely linked to relative humidity and additional studies are currently in progress to identify

optimal relative humidity parameters for adenovirus, as well as other viruses, for improved stabilization in the thin film matrix.

Successful stabilization of adenovirus in the thin film matrix was linked to the presence of the novel zwitterionic surfactant in optimized formulations. However, the mechanism of stabilization was largely unclear, making it difficult to address the translatability of the platform for additional biologics. To address this issue, I designed a series of studies to investigate the interactions of adenovirus with the novel zwitterionic surfactant and the other formulation components. FTIR scans revealed that in the presence of all the formulation components, adenovirus was likely completely incorporated into the thin film matrix and therefore resulted in no detectable shifts in peak position or intensity. We hypothesized that the incorporation was facilitated by the non-covalent interactions between the positively charged arm of the zwitterionic surfactant and the negative residues located on hexon proteins, previously identified as being responsible for the negative surface charge of adenoviral capsids. Saturation of the surfactant with glutamic acid resulted in reduced transduction efficiency and supported the hypothesis that electrostatic interactions played a role in the interactions between the surfactant and amino acid. The inclusion of influenza, which has a positively charged Hemagglutinin surface protein, in the thin film matrix resulted in reduced transduction efficiency and also provided evidence that electrostatic interactions contributed to viral stabilization in the optimized thin film formulation. Additional evaluation of the intermolecular interactions between the surfactant and adenovirus capsids revealed that the surfactant may surround viral capsids and prevent aggregation as well as displace water molecules and protein contaminants from the capsid surface. Taken together, we hypothesized that hydrophobic and electrostatic interactions likely mitigate the stabilization of adenovirus by preventing aggregation of capsids in solution.

When the additional formulation components were included in the analysis of intermolecular interactions, we found the impact on transduction efficiency was reduced by the presence of glutamic acid saturated surfactant. Furthermore, complete release of the viral load was mitigated by the presence of surfactant in formulations in less than ten minutes, while formulations lacking the novel surfactant did not completely release the viral dose after two hours of sampling dissolution liquid. Additionally, TGA profiles revealed weaker intermolecular interactions in the optimized formulation based on earlier thermal degradation of the entire thin film matrix relative to films prepared without surfactant. Therefore, we concluded that the inclusion of all formulation components buffers the interactions between the surfactant and adenovirus in order to facilitate the successful release of the virus, without having a deleterious impact on stability. These studies provided key insights into viral stabilization which simplified the approach towards improving influenza stabilization in the thin film matrix. However, the heterogeneity and polydispersity of the zwitterionic surfactant presented several roadblocks and challenges in complete characterization of intermolecular interactions. Future characterization studies should obtain a homogenous sample of the surfactant, which will provide fewer sources of variability and more straightforward characterization. The use of fluorescence spectroscopy or cryo-EM analysis and single particle reconstruction will aid in the identification of specific peptide sequences, from adenoviral capsids, involved in intermolecular interactions. This will also likely reduce the heterogeneity of the system and simplify future evaluation of surfactant interactions.

The last phase of this project involved evaluating the ability of the thin film matrix to induce a strong immune response following sublingual or buccal immunization. Administration of vaccines to mucosal routes results in an immunologically strong mucosal barrier that can prevent infection at the entry point of the pathogen and stimulate local and systemic immunity.

Despite this, the overwhelming majority of vaccines approved for use by the FDA utilize traditional immunization routes due to the physiochemical barriers associated with mucosal vaccination. In order to overcome these limitations, novel vaccine dosage forms are typically employed. A preliminary screen demonstrated that vaccination with the thin film platform resulted in a stronger humoral response following mucosal vaccination than with traditional intramuscular vaccination. Additionally, the optimized formulation improved bioavailability of the viral dose across human buccal explants. Further characterization of the immune response also revealed that sublingual routes induced a strong T_{H1} polarized immune response which resulted in greater protective efficacy than intramuscular immunization. Unlike other vaccine platforms in clinical trials for sublingual delivery, the thin film platform specifically targets the oral mucosa instead of employing an intramuscular vaccine for oral mucosal vaccination. Additionally, it significantly reduces biohazardous waste generated by immunization campaigns and promotes self-administration. However, incomplete survival following high dose influenza challenge in rodents strongly suggests that a more uniform production methodology is needed to immunize small animals. Additional studies are currently in progress to identify and create molds suitable for murine immunization in order to eliminate the variability observed.

Appendix Table 1: Bacterial Based Vaccines.

Information and data was adapted from refs (1-3)

Product (Antigen)	Formulation (route)	Storage Temp (°C)	Freeze-Sensitive	Formulation ingredients
Live Attenuated Bacteria				
BCG Vaccine [bacille Calmette-Guerin] (Tuberculosis)	Lyophilization (PC)	2-8	No	glycerin, asparagine, citric acid, potassium phosphate, magnesium sulfate, and iron ammonium citrate, lactose
Dengvaxia (Dengue)	Lyophilization (SC)	2-8	Yes	sodium chloride, amino acids, L-arginine hydrochloride, sucrose, D-trehalose dihydrate, D-sorbitol, trometamol, urea
TICE BCG [bacille Calmette-Guerin] (Tuberculosis)	Lyophilization (ID, PC)	2-8	No	Asparagine, citric acid, lactose, glycerin, iron ammonium citrate, magnesium sulfate, potassium phosphate
(Plague Vaccine)	Liquid (IM)	Not Available	Not Available	formaldehyde, phenol, beef-heart extract, yeast extract, agar, peptones and peptides of soya and casein
Vaxchora (Cholera)	Lyophilization (Oral)	-25 to -15	No	ascorbic acid, Hy-Case SF, sodium chloride, sucrose
Vivotif (Typhoid)	Capsule (Oral)	2-8	No	Amino acids, ascorbic acid, casein, dextrose, galactose, lactose, sucrose, yeast extract
Conjugates, Polysaccharide Carrier				

Menactra (Meningococcal)	Liquid (IM)	2-8	No	Formaldehyde (Each 0.5 mL dose may contain residual amounts of formaldehyde of less than 2.66 µg (0.000532%), by calculation), phosphate buffers
Menveo (Meningococcal)	Lyophilization (IM)	2-8	No	Amino acids, formaldehyde, yeast extract
MenQuadfi (Meningococcal Groups A, C, Y, W)	Liquid (IM)	2-8	Yes	Sodium chloride, sodium acetate, eacg 0.5 mL dose may contain residual amounts of formaldehyde of less than 3 mcg/mL
Prevnar-13 (Pneumococcal)	Liquid (IM)	2-8	Yes	Aluminum phosphate, ammonium sulfate, casamino acid, polysorbate 80, succinate buffer, yeast
Pneumovax 23 (Pneumococcal)	Liquid (IM, SC)	2-8	No	Phenol
Hiberix (*Hib Influenza*)	Lyophilization (IM)	2-8	No	Formaldehyde, lactose
ActHIB (*Hib Influenza*)	Lyophilization (IM)	2-8	No	Ammonium sulfate, formaldehyde, sucrose
PedvaxHIB (*Hib Influenza*)	Liquid (IM)	2-8	Yes	Aluminum hydroxyphosphate sulfate
Subunit, purified bacterial antigens				
Tetanus Toxoid	Liquid (IM, SC)	2-8	No	Sodium chloride, thimerosal
Tetanus Toxoid Adsorbed	Liquid (IM)	2-8	Yes	aluminum phosphate, free formaldehyde
Biothrax (Anthrax)	Liquid (IM, SC)	2-8	Yes	Aluminum hydroxide, amino acids, benzethonium chloride, formaldehyde, inorganic salts and sugars, vitamins

Typhim Vi (Typhoid)	Liquid (IM)	2-8	No	Disodium phosphate, monosodium phosphate, phenol, polydimethylsiloxane, hexadecyltrimethylammonium bromide
Bexsero (Meningococcal)	Liquid (IM)	2-8	Yes	Aluminum hydroxide, sodium chloride, histidine, sucrose
Trumenba (Meningococcal)	Liquid (IM)	2-8	Yes	Polysorbate 80, aluminum phosphate, histidine buffered saline
Menomune (Meningococcal)	Lyophilization (SC)	2-8	No	Lactose, thimerosal
Combination vaccines				
Pediarix (Diphtheria, Tetanus, Pertussis w/Hepatitis B)	Liquid (IM)	2-8	Yes	Aluminum hydroxide, aluminum phosphate, calf serum, lactalbumin hydrolysate, formaldehyde, glutaraldehyde, neomycin sulfate, polymyxin B, polysorbate 80, yeast protein
Infanrix (Diphtheria, Tetanus, Pertussis)	Liquid (IM)	2-8	Yes	Aluminum hydroxide, bovine extract, formaldehyde, glutaraldehyde, polysorbate 80
Tripedia (Diphtheria, Tetanus, Pertussis)	Liquid (IM)	2-8	Yes	Aluminum potassium sulfate, ammonium sulfate, bovine extract, formaldehyde, gelatin, peptone, polysorbate 80, sodium phosphate, thimerosal
Daptacel (Diphtheria, Tetanus, Pertussis)	Liquid (IM)	2-8	Yes	Aluminum phosphate, formaldehyde, Glutaraldehyde, 2-phenoxyethanol
Kinrix (Diphtheria, Tetanus, Pertussis w/ inactivated Polio)	Liquid (IM)	2-8	Yes	Aluminum hydroxide, calf serum, formaldehyde, glutaraldehyde, lactalbumin hydrolysate, neomycin sulfate, polymyxin B, polysorbate 80

Quadracel (Diphtheria, Tetanus, Pertussis, w/ inactivated Polio)	Liquid (IM)	2-8	Yes	aluminum phosphate, polysorbate 80, formaldehyde, glutaraldehyde, bovine serum albumin, 2-phenoxyethanol, neomycin, polymyxin B sulfate
Comvax (*Hib Influenzae*, HepB)	Liquid (IM)	2-8	Yes	Amorphous aluminum hydroxyphosphate sulfate, amino acids, dextrose, formaldehyde, hemin chloride, mineral salts, nicotinamide adenine dinucleotide, potassium aluminum sulfate, sodium borate, soy peptone, yeast protein
(Diphtheria, Tetanus)	Liquid (IM)	2-8	Yes	Aluminum phosphate, formaldehyde
DecaVac (Diphtheria, Tetanus)	Liquid (IM)	2-8	Yes	Aluminum potassium sulfate, bovine muscle tissue, formaldehyde, peptone, thimerosal
TeniVac (Diphtheria, Tetanus)	Liquid (IM)	2-8	Yes	Aluminum phosphate, formaldehyde
TDVAX (Diphtheria, Tetanus)	Liquid (IM)	2-8	Yes	Aluminum, formaldehyde, thimerosal
Adacel (Tetanus Toxoid, Diphtheria, & Acellular pertussis)	Liquid (IM)	2-8	Yes	Aluminum phosphate, ammonium sulfate, formaldehyde, glutaraldehyde, 2-phenoxyethanol
Boostrix (Tetanus Toxoid,	Liquid (IM)	2-8	Yes	Aluminum hydroxide, bovine extract, formaldehyde, glutaraldehyde, polysorbate 80

Diphtheria, & Acellular pertussis)				
Pentacel (Diphtheria and Tetanus, Acellular Pertussis, Inactivated Polio, Haemophilus b)	Liquid (IM)	2-8	Yes	Aluminum phosphate, bovine serum albumin, formaldehyde, glutaraldehyde, MRC-5 cellular protein, neomycin, polymyxin B sulfate, polysorbate 80, 2-phenoxyethanol
Menhibrix (Meningococcal, Hib)	Lyophilization (IM)	2-8	No	Tris, sucrose, formaldehyde
Vaxelis (Diphtheria, Tetanus, Pertussis, Inactivated Poliovirus, Haemophilus b Conjugate, Hepatitis B)	Liquid (IM)	2-8	Yes	polysorbate 80, formaldehyde, glutaraldehyde, bovine serum albumin, neomycin, streptomycin sulfate, polymyxin B sulfate, ammonium thiocyanate, yeast protein

Abbreviations: IM: Intramuscular, IN: Intranasal, ID: Intradermal, SC: Subcutaneous, PC: Percutaneous

References

1. Food and Drug Administration. Vaccines Licensed for Use in the United States. (2020).
2. *Excipients Included in U.S. Vaccines, by Vaccine* (2019).
3. O. S. Kumru *et al.*, Vaccine instability in the cold chain: Mechanisms, analysis and formulation strategies. *Biologicals* **42**, 237-259 (2014).

Appendix Table 2: Viral Based Vaccines.

Information and data was adapted from ref (1-3).

Product (Antigen)	Formulation (route)	Storage Temp (°C)	Shelf life	Formulation ingredients
Live Attenuated Virus				
Varivax (Varicella)	Lyophilization (SC)	-50 to -15	No	Dibasic sodium phosphate, ethylenediamine tetra acetic acid, sodium (EDTA), fetal bovine serum, gelatin, glutamate, monobasic potassium phosphate, monobasic sodium phosphate, monosodium L-glutamate, MRC-5 DNA and cellular protein, neomycin, phosphate, potassium chloride, sucrose
Zostavax (Zoster)	Lyophilization (SC)	-50 to -15	No	Bovine calf serum, dibasic sodium phosphate, hydrolyzed porcine gelatin, monosodium L-glutamate, MRC-5 DNA and cellular protein, monobasic potassium phosphate, neomycin, potassium chloride, sucrose
Ervebo (Ebola Zaire)	Liquid (IM)	-80 to -60	No	Tris, rice-derived recombinant, human serum albumin, vero cell DNA, benzonase
Jynneos (Smallpox, Monkeypox)	Liquid (SC)	-25 to -15	No	Tris (tromethamine), sodium chloride, host-cell DNA/protein, benzonase, gentamicin
Rotarix (Rotavirus)	Lyophilization (Oral)	2-8	No	Amino acids, calcium carbonate, dextran, sorbitol, sucrose, vitamins, xanthan

RotaTeq (Rotavirus)	Liquid (Oral)	2-8	N/A	fetal bovine serum, sodium citrate, sodium phosphate monobasic monohydrate, sodium hydroxide, sucrose, polysorbate 80
Flumist (Influenza)	Liquid (IN)	2-8	Yes	Arginine, dibasic potassium phosphate, egg protein, ethylenediaminetetraacetic acid, gentamicin sulfate, hydrolyzed porcine gelatin, monobasic potassium phosphate, monosodium glutamate, sucrose
Flumist Quadrivalent (Influenza)	Liquid (IN)	2-8	Yes	Arginine, dibasic potassium phosphate, egg protein, ethylenediaminetetraacetic acid, gentamicin sulfate, hydrolyzed porcine gelatin, monobasic potassium phosphate, monosodium glutamate, sucrose
Adenovirus (4, 7)	Tablet (Oral)	2-8	Yes	Acetone, alcohol, anhydrous lactose, castor oil, cellulose acetate phthalate, dextrose, D-fructose, D-mannose, FD&C Yellow #6 aluminum lake dye, fetal bovine serum, human serum albumin, magnesium stearate, micro crystalline cellulose, plasdone C, Polacrilin potassium, potassium phosphate, sodium bicarbonate, sucrose
ACAM2000 (Smallpox)	Lyophilization (PC)	Frozen	No	Glycerin, human serum albumin, mannitol, neomycin, phenol, polymyxin B
YF-Vax (Yellow Fever)	Lyophilization (SC)	2-8	Yes	Egg protein, gelatin, sorbitol
Inactivated Virus				
Vaqta (Hepatitis A)	Liquid (IM)	2-8	Yes	Amorphous aluminum hydroxyphosphate sulfate, bovine albumin or serum, formaldehyde, MRC-5 cellular protein, sodium borate

Havrix (Hepatitis A)	Liquid (IM)	2-8	Yes	Aluminum hydroxide, amino acid supplement, formalin, MRC-5 cellular protein, neomycin sulfate, phosphate buffers, polysorbate 20
Fluad (Influenza)	Liquid (IM)	2-8	Yes	Squalene, polysorbate 80, sorbitan trioleate, sodium citrate dehydrate, citric acid monohydrate, neomycin, kanamycin, barium, ovalbumin, CTAB(cetyltrimethylammonium bromide), formaldehyde
Fluad Quadrivalent (Influenza)	Liquid (IM)	2-8	Yes	Squalene, polysorbate 80, sorbitan trioleate, sodium citrate dehydrate, citric acid monohydrate, neomycin, kanamycin, ovalbumin, CTAB, formaldehyde
Fluarix (Influenza)	Liquid (IM)	2-8	Yes	Formaldehyde, octoxynol-10 (Triton X-100), α-tocopheryl hydrogen succinate, polysorbate 80 (Tween 80), hydrocortisone, gentamicin sulfate, ovalbumin, sodium deoxycholate, sucrose, phosphate buffer
Fluarix Quadrivalent (Influenza)	Liquid (IM)	2-8	Yes	Formaldehyde, octoxynol-10 (Triton X-100), α-tocopheryl hydrogen succinate, polysorbate 80 (Tween 80), hydrocortisone, gentamicin sulfate, ovalbumin, sodium deoxycholate, sucrose, phosphate buffer
Flulaval (Influenza)	Liquid (IM)	2-8	Yes	Formaldehyde, á-tocopheryl hydrogen succinate, polysorbate 80, sodium deoxycholate, thimerosal, ovalbumin
Flulaval Quadrivalent (Influenza)	Liquid (IM)	2-8	Yes	Formaldehyde, á-tocopheryl hydrogen succinate, polysorbate 80, sodium deoxycholate, thimerosal, ovalbumin

Agriflu (Influenza)	Liquid (IM)	2-8	Yes	Egg proteins, formaldehyde, polysorbate 80, cetyltrimethylammonium bromide, neomycin sulfate, kanamycin
Fluvirin (Influenza)	Liquid (IM)	2-8	Yes	Beta-propiolactone, egg protein, neomycin, nonylphenol ethoxylate, polymyxin, thimerosal (multi-dose containers), thimerosal[2] (single-dose syringes)
Fluzone (Influenza)	Liquid (IM)	2-8	Yes	Egg protein, formaldehyde, gelatin (standard formulation only), octylphenol ethoxylate (Triton X-100), sodium phosphate, thimerosal (multi-dose containers only)
Fluzone Quadrivalent (Influenza)	Liquid (IM)	2-8	Yes	Egg protein, formaldehyde, gelatin (standard formulation only), octylphenol ethoxylate (Triton X-100), sodium phosphate, thimerosal (multi-dose containers only)
Flucelvax (Influenza)	Liquid (IM)	2-8	Yes	Madin Darby Canine Kidney (MDCK) cell protein, MDCK cell DNA, polysorbate 80, cetyltrimethlyammonium bromide, β-propiolactone, phosphate buffer
Flucelvax Quadravlent (Influenza)	Liquid (IM)	2-8	Yes	Madin Darby Canine Kidney (MDCK) cell protein, MDCK cell DNA, polysorbate 80, cetyltrimethlyammonium bromide, β-propiolactone, phosphate buffer
Afluria (Influenza)	Liquid (IM)	2-8	Yes	Beta-propiolactone, calcium chloride, dibasic sodium phosphate, egg protein, monobasic potassium phosphate, monobasic sodium phosphate, neomycin sulfate, polymyxin B, potassium chloride, sodium

				taurodeoxychoalate, thimerosal (multi-dose vials only)
Afluria Quadrivalent (Influenza)	Liquid (IM)	2-8	Yes	sodium chloride, monobasic sodium phosphate, dibasic sodium phosphate, monobasic potassium phosphate, potassium chloride, calcium chloride, sodium taurodeoxycholate, ovalbumin, sucrose, neomycin sulfate 411, polymyxin B, beta-propiolactone, hydrocortisone
H5N1 Sanofi (Influenza)	Liquid (IM)	2-8	Yes	Porcine gelatin, thimerosal, formaldehyde, polyethylene glycol p-Isooctylphenyl Ether, sucrose
H5N1 Id Biomed (Influenza)	Liquid (IM)	2-8	Yes	Thimersol, AS03, ovalbumin, formaldehyde, sodium deoxycholate
Audenz H5N1 (Influenza)	Liquid (IM)	2-8	Yes	MDCK cell protein/DNA, polysorbate 80, cetyltrimethylammonium bromide, ß-propiolactone, squalene, sorbiton trioleate, sodium citrate dihydrate, citric acid monohydrate
2009 H1N1 – CSL Limited (Influenza)	Liquid (IM)	2-8	Yes	Sodium chloride, monobasic sodium phosphate, dibasic sodium phosphate, monobasic potassium phosphate, potassium chloride, calcium chloride
2009 H1N1 - MedImmune (Influenza)	Liquid (IN)	2-8	Yes	monosodium glutamate, hydrolyzed porcine gelatin, arginine, sucrose, dibasic potassium phosphate, monobasic potassium phosphate, gentamicin sulfate
2009 H1N1 – ID Biomed (Influenza)	Liquid (IM)	2-8	Yes	Thimerosal, ovalbumin, formaldehyde, sodium deoxycholate

2009 H1N1 – Novartis (Influenza)	Liquid (IM)	2-8	Yes	N/A
2009 H1N1 – Sanofi Pasteur (Influenza)	Liquid (IM)	2-8	Yes	Formaldehyde, polyethylene glycol p-isooctylphenyl ether, and sucrose
RabAvert (Rabies)	Lyophilization (IM)	2-8	No	Amphotericin B, beta-propiolactone, chicken protein, chlortetracycline, human serum albumin, neomycin, ovalbumin, polygeline (processed bovine 14 gelatin), potassium glutamate
Imovax (Rabies)	Lyophilization (IM)	2-8	Yes	Albumin, MRC-5 cells, neomycin sulfate, phenol
IPOL (Polio)	Liquid (IM, SC)	2-8	Yes	Calf serum protein, formaldehyde, neomycin, 2-phenoxyethanol, polymyxin B, streptomycin
Ixiaro (Japanese Encephalitis)	Liquid (IM)	2-8	Yes	Aluminum hydroxide, bovine serum albumin, formaldehyde, protamine sulfate, sodium metabisulphite
JE-Vax (Japanese Encephalitis)	Lyophilization (SC)	2-8	Yes	Formaldehyde or formalin, gelatin, mouse serum protein, polysorbate 80, thimerosal
Recombinant				
HEPLISAV-B (Hepatitis B-HBsAg)	Liquid (IM)	2-8	Yes	CpG 1018, sodium phosphate, dibasic dodecahydrate, sodium phosphate, monobasic dihydrate, polysorbate 80
Engerix B (Hepatitis B-HBsAg)	Liquid (IM)	2-8	Yes	Aluminum hydroxide, phosphate buffers, yeast protein

Recombivax HB (Hepatitis B-HBsAg)	Liquid (IM)	2-8	Yes	Amorphous aluminum hydroxyphosphate sulfate, amino acids, dextrose, formaldehyde, mineral salts, potassium aluminum sulfate, soy peptone, yeast protein
Gardasil (Human Papilloma Virus-L1)	Liquid (IM)	2-8	Yes	Amino acids, amorphous aluminum hydroxyphosphate sulfate, carbohydrates, L-histidine, mineral salts, polysorbate 80, sodium borate, vitamins, yeast protein
Gardasil 9 (Human Papilloma virus-L1)	Liquid (IM)	2-8	Yes	Aluminum, sodium chloride, L-histidine, polysorbate 80, sodium borate, yeast protein
Cervarix (Human Papilloma Virus-L1)	Liquid (IM)	2-8	Yes	Aluminum hydroxide, amino acids, lipids, mineral salts, sodium dihydrogen phosphate dehydrate, type 16 viral protein L1, type 18 viral protein L1, vitamins
FluBlok (Influenza-HA)	Liquid (IM)	2-8	Yes	Monobasic sodium phosphate, dibasic sodium phosphate, polysorbate 20, baculovirus and host cell proteins, baculovirus and cellular DNA, Triton X-100, lipids, vitamins, amino acids, mineral salts
FluBlok Quadrivalent (Influenza-HA)	Liquid (IM)	2-8	Yes	Monobasic sodium phosphate, dibasic sodium phosphate, polysorbate 20, baculovirus and host cell proteins, baculovirus and cellular DNA, Triton X-100, lipids, vitamins, amino acids, mineral salts
Shingrix (Zoster-gE)	Lyophilization (IM)	2-8	Yes	sucrose, sodium chloride, DOPC, potassium dihydrogen phosphate, cholesterol, sodium dihydrogen phosphate dihydrate, disodium phosphate anhydrous, dipotassium phosphate, polysorbate 80
Combination Vaccines				

MMRII (Measles, Mumps, Rubella)	Lyophilization (SC)	-50 to +8	No	Amino acids, fetal bovine serum, glutamate, hydrolyzed gelatin, neomycin, recombinant human serum albumin, sodium phosphate, sorbitol, sucrose, vitamins
Pediarix (Diphtheria, Tetanus, Pertussis w/ Hepatitis B)	Liquid (IM)	2-8	Yes	Aluminum hydroxide, aluminum phosphate, calf serum, lactalbumin hydrolysate, formaldehyde, glutaraldhyde, neomycin sulfate, polymyxin B, polysorbate 80, yeast protein
Kinrix (Diphtheria, Tetanus, Pertussis, w/ inactivated Polio)	Liquid (IM)	2-8	Yes	Aluminum hydroxide, calf serum, formaldehyde, glutaraldehyde, lactalbumin hydrolysate, neomycin sulfate, polymyxin B, polysorbate 80
Quadracel (Diphtheria, Tetanus, Pertussis, w/ inactivated Polio)	Liquid (IM)	2-8	Yes	aluminum phosphate, polysorbate 80, formaldehyde, glutaraldehyde, bovine serum albumin, 2-phenoxyethanol, neomycin, polymyxin B sulfate
Twinrix (Hepatitis A&B)	Liquid (IM)	2-8	Yes	Aluminum hydroxide, aluminum phosphate, amino acids, formalin, MRC-5 cells, neomycin sulfate, phosphate buffers, polysorbate 20, yeast protein
ProQuad (Measles, Mumps, Rubella w/ Varicella)	Lyophilization (SC)	-50	No	Bovine calf serum, dibasic potassium phosphate, dibasic sodium phosphate, human albumin, human serum albumin, hydrolyzed gelatin, monobasic potassium phosphate, monosodium L-glutamate, MRC-5 cellular protein, neomycin, sodium bicarbonate, sorbitol, sucrose, potassium chloride

Vaxelis (Diphtheria, Tetanus, Pertussis Inactivated Poliovirus, Haemophilus b Conjugate, Hepatitis B)	Liquid (IM)	2-8	Yes	polysorbate 80, formaldehyde, glutaraldehyde, bovine serum albumin, neomycin, streptomycin sulfate, polymyxin B sulfate, ammonium thiocyanate, yeast protein
Pentacel (Diphtheria and Tetanus, Acellular Pertussis, Inactivated Polio, Haemophilus b)	Liquid (IM)	2-8	Yes	Aluminum phosphate, bovine serum albumin, formaldehyde, glutaraldehyde, MRC-5 cellular protein, neomycin, polymyxin B sulfate, polysorbate 80, 2-phenoxyethanol

Abbreviations: IM: Intramuscular, IN: Intranasal, ID: Intradermal, SC: Subcutaneous, PC: Percutaneous

References

1. Food and Drug Administration. Vaccines Licensed for Use in the United States. (2020).
2. *Excipients Included in U.S. Vaccines, by Vaccine* (2019).
3. O. S. Kumru *et al.*, Vaccine instability in the cold chain: Mechanisms, analysis and formulation strategies. *Biologicals* **42**, 237-259 (2014).

Complete List of References

Chapter 1

1. J. Louten, in *Essential Human Virology*. (Elsevier Inc, Kennesaw, GA, 2016), chap. 8, pp. 133-134.
2. F. Fenner *et al.*, in *Smallpox and Its Eradication*. (World Health Organization, Geneva, 1988), pp. 1371-1409.
3. G. S. Marshall, Vaccine Hesitancy, History, and Human Nature: The 2018 Stanley A. Plotkin Lecture. *Journal of the Pediatric Infectious Diseases Society* **8**, 1-8 (2018).
4. P. D. Minor, Live attenuated vaccines: Historical successes and current challenges. *Virology* **479-480**, 379-392 (2015).
5. J. F. Mosley, 2nd, L. L. Smith, P. Brantley, D. Locke, M. Como, Vaxchora: The First FDA-Approved Cholera Vaccination in the United States. *P T* **42**, 638-640 (2017).
6. O. S. Kumru *et al.*, Vaccine instability in the cold chain: Mechanisms, analysis and formulation strategies. *Biologicals* **42**, 237-259 (2014).
7. A. S. Lauring, J. O. Jones, R. Andino, Rationalizing the development of live attenuated virus vaccines. *Nat Biotechnol* **28**, 573-579 (2010).
8. A. J. Cann *et al.*, Reversion to neurovirulence of the live-attenuated Sabin type 3 oral pollovirus vaccine. *Nucleic Acids Research* **12**, 7787-7792 (1984).
9. L. Pöyhönen, J. Bustamante, J.-L. Casanova, E. Jouanguy, Q. Zhang, Life-Threatening Infections Due to Live-Attenuated Vaccines: Early Manifestations of Inborn Errors of Immunity. *Journal of Clinical Immunology* **39**, 376-390 (2019).
10. World Health Organization, Introduction of inactivated poliovirus vaccine into oral poliovirus vaccine-using countries. *Weekly Epidemiological Record* **78**, 241-252 (2020).
11. World Health Organization, BCG vaccine: WHO position paper. *Weekly Epidemiological Record* **79**, 25-40 (2004).
12. World Health Organization, Measels vaccines: WHO position paper. *Weekly Epidemiological Record* **84**, 349-360 (2009).
13. World Health Organization, Rotavirus vaccines: an update. *Weekly Epidemiological Record* **84**, 533-538 (2009).
14. World Health Organization, Yellow fever vaccine: WHO position paper. *Weekly Epidemiological Record* **78**, 349-360 (2003).
15. L. Varghese *et al.*, Contraindication of live vaccines in immunocompromised patients: an estimate of the number of affected people in the USA and the UK. *Public Health* **142**, 46-49 (2017).
16. J. A. Whitaker, K. Valles, P. K. Tosh, G. A. Poland, in *Vaccinations*, Gregory A. Poland, Ed. (Elsevier, 2019), pp. 139-162.
17. A. Sabbaghi, S. M. Miri, M. Keshavarz, M. Zargar, A. Ghaemi, Inactivation methods for whole influenza vaccine production. *Reviews in Medical Virology* **29**, e2074 (2019).
18. B. Sanders, M. Koldijk, H. Schuitemaker, Inactivated Viral Vaccines. *Vaccine Analysis: Strategies, Principles, and Control*, 45-80 (2014).
19. J. Hawken, S. B. Troy, Adjuvants and inactivated polio vaccine: A systematic review. *Vaccine* **30**, 6971-6979 (2012).
20. S. I. Samson *et al.*, Immunogenicity of high-dose trivalent inactivated influenza vaccine: a systematic review and meta-analysis. *Expert Rev Vaccines* **18**, 295-308 (2019).

21. M. Paulke-Korinek *et al.*, Persistence of antibodies six years after booster vaccination with inactivated vaccine against Japanese encephalitis. *Vaccine* **33**, 3600-3604 (2015).
22. B. L. Innis *et al.*, Protection Against Hepatitis A by an Inactivated Vaccine. *JAMA* **271**, 1328-1334 (1994).
23. D. J. Hicks, A. R. Fooks, N. Johnson, Developments in rabies vaccines. *Clinical & Experimental Immunology* **169**, 199-204 (2012).
24. P. E. Kilgore, A. M. Salim, M. J. Zervos, H.-J. Schmitt, Pertussis: Microbiology, Disease, Treatment, and Prevention. *Clinical Microbiology Reviews* **29**, 449 (2016).
25. A. L. Lopez *et al.*, Immunogenicity and Protection From a Single Dose of Internationally Available Killed Oral Cholera Vaccine: A Systematic Review and Metaanalysis. *Clinical Infectious Diseases* **66**, 1960-1971 (2017).
26. D. R. Howlader *et al.*, A brief review on the immunological scenario and recent developmental status of vaccines against enteric fever. *Vaccine* **35**, 6359-6366 (2017).
27. C. E. Demeure *et al.*, Yersinia pestis and plague: an updated view on evolution, virulence determinants, immune subversion, vaccination, and diagnostics. *Genes & Immunity* **20**, 357-370 (2019).
28. K. Kardani, A. Bolhassani, S. Shahbazi, Prime-boost vaccine strategy against viral infections: Mechanisms and benefits. *Vaccine* **34**, 413-423 (2016).
29. A. Vartak, S. J. Sucheck, Recent Advances in Subunit Vaccine Carriers. *Vaccines* **4**, (2016).
30. I. P. Nascimento, L. C. C. Leite, Recombinant vaccines and the development of new vaccine strategies. *Braz J Med Biol Res* **45**, 1102-1111 (2012).
31. J. Beláková, M. Horynová, M. Krupka, E. Weigl, M. Raska, DNA vaccines: are they still just a powerful tool for the future? *Archivum immunologiae et therapiae experimentalis* **55**, 387-398 (2007).
32. R. Bastola *et al.*, Vaccine adjuvants: smart components to boost the immune system. *Archives of Pharmacal Research* **40**, 1238-1248 (2017).
33. D. Baxter, Active and passive immunity, vaccine types, excipients and licensing. *Occupational Medicine* **57**, 552-556 (2007).
34. R. Rappuoli, E. De Gregorio, A sweet T cell response. *Nature Medicine* **17**, 1551-1552 (2011).
35. R. Rappuoli, Glycoconjugate vaccines: Principles and mechanisms. *Science Translational Medicine* **10**, eaat4615 (2018).
36. S. Davis, D. Feikin, H. L. Johnson, The effect of Haemophilus influenzaetype B and pneumococcal conjugate vaccines on childhood meningitis mortality: a systematic review. *BMC Public Health* **13**, S21 (2013).
37. H. Ewald *et al.*, The Clinical Effectiveness of Pneumococcal Conjugate Vaccines: A Systematic Review and Meta-analysis of Randomized Controlled Trials. *Dtsch Arztebl Int* **113**, 139-146 (2016).
38. C. A. Robertson, J. Hedrick, E. Bassily, D. P. Greenberg, Persistence of bactericidal antibodies 4 years after a booster dose of quadrivalent meningococcal diphtheria toxoid conjugate vaccine (MenACWY-D). *Vaccine* **37**, 1016-1020 (2019).
39. F. Berti, F. Micoli, Improving efficacy of glycoconjugate vaccines: from chemical conjugates to next generation constructs. *Current opinion in immunology* **65**, 42-49 (2020).

40. P. M. Moyle, I. Toth, Modern subunit vaccines: development, components, and research opportunities. *ChemMedChem* **8**, 360-376 (2013).
41. Food and Drug Administration. (2020).
42. R. H. Griesenauer, M. S. Kinch, An overview of FDA-approved vaccines & their innovators. *Expert Rev Vaccines* **16**, 1253-1266 (2017).
43. B. Afrough, S. Dowall, R. Hewson, Emerging viruses and current strategies for vaccine intervention. *Clin Exp Immunol* **196**, 157-166 (2019).
44. E. Prompetchara, C. Ketloy, T. Palaga, Immune responses in COVID-19 and potential vaccines: Lessons learned from SARS and MERS epidemic. *Asian Pacific journal of allergy and immunology* **38**, 1-9 (2020).
45. P. Lostroh, in *Molecular and Cellular Biology of Viruses* CRC Press, Ed. (Boca Raton, FL, 2019), pp. 1-18.
46. A. N. Clements, R. E. Harbach, History of the discovery of the mode of transmission of yellow fever virus. *Journal of vector ecology : journal of the Society for Vector Ecology* **42**, 208-222 (2017).
47. D. R. Wessner, The Origins of Viruses. *Nature Education* **3**, 37 (2010).
48. R. W. Horne, J. M. Hobart, I. P. Ronchetti, Application of the negative staining-carbon technique to the study of virus particles and their components by electron microscopy. *Micron (1969)* **5**, 233-261 (1974).
49. J. D. Almeida, A CLASSIFICATION OF VIRUS PARTICLES BASED ON MORPHOLOGY. *Can Med Assoc J* **89**, 787-798 (1963).
50. P. Lenihan, H. F. Bassett, E. D. Weavers, Demonstration by electron microscopy of parvovirus-like particles in canine parvovirus myocarditis. *The Veterinary record* **107**, 201-202 (1980).
51. A. Augustyn *et al.*, in *Encyclopaedia Britannica*. (Encyclopaedia Britannica, 2019).
52. J. Wellehan, G. Cortes-Hinojosa, in *Fowler's Zoo and Wild Animal Medicine Current Therapy, Volume 9*, R. Eric Miller, Nadine Lamberski, Paul P. Calle, Eds. (W.B. Saunders, 2019), pp. 597-602.
53. C. J. Burrell, C. R. Howard, F. A. Murphy, in *Fenner and White's Medical Virology (Fifth Edition)*, Christopher J. Burrell, Colin R. Howard, Frederick A. Murphy, Eds. (Academic Press, London, 2017), pp. 383-394.
54. K. Saunders, G. P. Lomonossoff, In Planta Synthesis of Designer-Length Tobacco Mosaic Virus-Based Nano-Rods That Can Be Used to Fabricate Nano-Wires. *Front Plant Sci* **8**, 1335-1335 (2017).
55. G. W. Long, J. Nobel, Jr., F. A. Murphy, K. L. Herrmann, B. Lourie, Experience with electron microscopy in the differential diagnosis of smallpox. *Appl Microbiol* **20**, 497-504 (1970).
56. D. Raoult *et al.*, The 1.2-megabase genome sequence of Mimivirus. *Science (New York, N.Y.)* **306**, 1344-1350 (2004).
57. C. Xiao *et al.*, Structural Studies of the Giant Mimivirus. *PLOS Biology* **7**, e1000092 (2009).
58. H. Sobhy, A comparative review of viral entry and attachment during large and giant dsDNA virus infections. *Archives of Virology* **162**, 3567-3585 (2017).
59. D. Kazlauskas, M. Krupovic, Č. Venclovas, The logic of DNA replication in double-stranded DNA viruses: insights from global analysis of viral genomes. *Nucleic acids research* **44**, 4551-4564 (2016).

60. K. A. White, L. Enjuanes, B. Berkhout, RNA virus replication, transcription and recombination. *RNA Biol* **8**, 182-183 (2011).
61. M. Comas-Garcia, Packaging of Genomic RNA in Positive-Sense Single-Stranded RNA Viruses: A Complex Story. *Viruses* **11**, 253 (2019).
62. Y. J. Tao, Q. Ye, RNA Virus Replication Complexes. *PLOS Pathogens* **6**, e1000943 (2010).
63. N. Arnberg *et al.*, Adenovirus Type 37 Binds to Cell Surface Sialic Acid Through a Charge-Dependent Interaction. *Virology* **302**, 33-43 (2002).
64. G. R. Nemerow, P. L. Stewart, Role of αv Integrins in Adenovirus Cell Entry and Gene Delivery. *Microbiology and Molecular Biology Reviews* **63**, 725-734 (1999).
65. E. De Clercq, Antiviral agents active against influenza A viruses. *Nature reviews. Drug discovery* **5**, 1015-1025 (2006).
66. J. L. Shirley, Y. P. de Jong, C. Terhorst, R. W. Herzog, Immune Responses to Viral Gene Therapy Vectors. *Molecular Therapy* **28**, 709-722 (2020).
67. Y. Kobayashi, Y. Suzuki, Compensatory Evolution of Net-Charge in Influenza A Virus Hemagglutinin. *PLoS One* **7**, e40422 (2012).
68. C. P. Gerba, W. Q. Betancourt, Viral Aggregation: Impact on Virus Behavior in the Environment. *Environmental Science & Technology* **51**, 7318-7325 (2017).
69. M. A. Croyle, K. Gerding, K. S. Quick, Role of Container/Closure System and Formulation on Agitation-Induced Aggregation Phenomena in Recombinant Adenoviral Products. *BioProcessing* **2**, 35-41 (2003).
70. E. K. Jeong, J. E. Bae, I. S. Kim, Inactivation of influenza A virus H1N1 by disinfection process. *American Journal of Infection Control* **38**, 354-360 (2010).
71. G. Maheshwari, R. Jannat, L. McCormick, D. Hsu, Thermal inactivation of adenovirus type 5. *Journal of Virological Methods* **118**, 141-146 (2004).
72. J. Bernaud *et al.*, Characterization of AAV vector particle stability at the single-capsid level. *J Biol Phys* **44**, 181-194 (2018).
73. R. K. Evans *et al.*, Development of stable liquid formulations for adenovirus-based vaccines. *Journal of Pharmaceutical Sciences* **93**, 2458-2475 (2004).
74. D. Loewe *et al.*, Forced Degradation Studies to Identify Critical Process Parameters for the Purification of Infectious Measles Virus. *Viruses* **11**, 725 (2019).
75. J. E. Benbough, Some Factors Affecting the Survival of Airborne Viruses. *Journal of General Virology* **10**, 209-220 (1971).
76. A. C. Lowen, J. Steel, Roles of Humidity and Temperature in Shaping Influenza Seasonality. *Journal of Virology* **88**, 7692 (2014).
77. Y. Ma *et al.*, Effects of temperature variation and humidity on the death of COVID-19 in Wuhan, China. *Science of The Total Environment* **724**, 138226 (2020).
78. S. Wanning, R. Süverkrüp, A. Lamprecht, Pharmaceutical spray freeze drying. *International Journal of Pharmaceutics* **488**, 136-153 (2015).
79. C. D. Lytle, J.-L. Sagripanti, Predicted Inactivation of Viruses of Relevance to Biodefense by Solar Radiation. *Journal of Virology* **79**, 14244 (2005).
80. B. K. Mayer, Y. Yang, D. W. Gerrity, M. Abbaszadegan, The Impact of Capsid Proteins on Virus Removal and Inactivation During Water Treatment Processes. *Microbiol Insights* **8**, 15-28 (2015).
81. C.-C. Tseng, C.-S. Li, Inactivation of viruses on surfaces by ultraviolet germicidal irradiation. *J Occup Environ Hyg* **4**, 400-405 (2007).

82. K. J. Card *et al.*, UV Sterilization of Personal Protective Equipment with Idle Laboratory Biosafety Cabinets During the Covid-19 Pandemic. *medRxiv*, 2020.2003.2025.20043489 (2020).
83. I. H. Hamzavi *et al.*, Ultraviolet germicidal irradiation: Possible method for respirator disinfection to facilitate reuse during the COVID-19 pandemic. *Journal of the American Academy of Dermatology* **82**, 1511-1512 (2020).
84. G. Kampf, Efficacy of ethanol against viruses in hand disinfection. *Journal of Hospital Infection* **98**, 331-338 (2018).
85. J. S. Oxford, C. W. Potter, C. McLaren, W. Hardy, Inactivation of influenza and other viruses by a mixture of virucidal compounds. *Appl Microbiol* **21**, 606-610 (1971).
86. R. W. Doms, in *Viral Pathogenesis (Third Edition)*, Michael G. Katze, Marcus J. Korth, G. Lynn Law, Neal Nathanson, Eds. (Academic Press, Boston, 2016), pp. 29-40.
87. J. Rexroad, R. K. Evans, C. R. Middaugh, Effect of pH and ionic strength on the physical stability of adenovirus type 5. *Journal of Pharmaceutical Sciences* **95**, 237-247 (2006).
88. M. A. Croyle, X. Cheng, J. M. Wilson, Development of formulations that enhance physical stability of viral vectors for gene therapy. *Gene Therapy* **8**, 1281-1290 (2001).
89. R. L. Poulson, S. M. Tompkins, R. D. Berghaus, J. D. Brown, D. E. Stallknecht, Environmental Stability of Swine and Human Pandemic Influenza Viruses in Water under Variable Conditions of Temperature, Salinity, and pH. *Appl Environ Microbiol* **82**, 3721 (2016).
90. P. R. Junankar, R. J. Cherry, Temperature and pH dependence of the haemolytic activity of influenza virus and of the rotational mobility of the spike glycoproteins. *Biochimica et biophysica acta* **854**, 198-206 (1986).
91. B. Bobály, E. Sipkó, J. Fekete, Challenges in liquid chromatographic characterization of proteins. *Journal of Chromatography B* **1032**, 3-22 (2016).
92. K. A. Dill, J. L. MacCallum, The Protein-Folding Problem, 50 Years On. *Science (New York, N.Y.)* **338**, 1042 (2012).
93. T. N. Shamsi, T. Athar, R. Parveen, S. Fatima, A review on protein misfolding, aggregation and strategies to prevent related ailments. *International Journal of Biological Macromolecules* **105**, 993-1000 (2017).
94. M. J. Davies, The oxidative environment and protein damage. *Biochimica et Biophysica Acta (BBA) - Proteins and Proteomics* **1703**, 93-109 (2005).
95. S. W. Hovorka, C. Schöneich, Oxidative degradation of pharmaceuticals: Theory, mechanisms and inhibition. *Journal of Pharmaceutical Sciences* **90**, 253-269 (2001).
96. A. B. Robinson, C. J. Rudd, in *Current Topics in Cellular Regulation*, Bernard L. Horecker, Earl R. Stadtman, Eds. (Academic Press, 1974), vol. 8, pp. 247-295.
97. R. Bischoff, H. V. J. Kolbe, Deamidation of asparagine and glutamine residues in proteins and peptides: structural determinants and analytical methodology. *Journal of Chromatography B: Biomedical Sciences and Applications* **662**, 261-278 (1994).
98. L. J. J. Hansen, R. Daoussi, C. Vervaet, J. P. Remon, T. R. M. De Beer, Freeze-drying of live virus vaccines: A review. *Vaccine* **33**, 5507-5519 (2015).
99. W. Wang, S. Ohtake, Science and art of protein formulation development. *International Journal of Pharmaceutics* **568**, 118505 (2019).
100. N.-Y. Fang *et al.*, Effects of osmolytes on arginine kinase from Euphausia superba: A study on thermal denaturation and aggregation. *Process Biochemistry* **49**, 936-947 (2014).

101. A. Arsiccio, R. Pisano, Stability of Proteins in Carbohydrates and Other Additives during Freezing: The Human Growth Hormone as a Case Study. *The Journal of Physical Chemistry B* **121**, 8652-8660 (2017).
102. S. Ajito, H. Iwase, S.-i. Takata, M. Hirai, Sugar-Mediated Stabilization of Protein against Chemical or Thermal Denaturation. *The Journal of Physical Chemistry B* **122**, 8685-8697 (2018).
103. M. Kudou, K. Shiraki, S. Fujiwara, T. Imanaka, M. Takagi, Prevention of thermal inactivation and aggregation of lysozyme by polyamines. *European Journal of Biochemistry* **270**, 4547-4554 (2003).
104. N. K. Budhavaram, J. A. Miller, Y. Shen, J. R. Barone, Protein Substitution Affects Glass Transition Temperature and Thermal Stability. *Journal of Agricultural and Food Chemistry* **58**, 9549-9555 (2010).
105. M. F. Sabar *et al.*, Synthesis and Bioactivity Study of 30KDa Linear PEG-Interferon and its Comparison with Tri-Branched PEG-Interferon. *Journal- Chemical Society of Pakistan* **35**, (2012).
106. D. Prashar, D. Cui, D. Bandyopadhyay, Y.-Y. Luk, Modification of Proteins with Cyclodextrins Prevents Aggregation and Surface Adsorption and Increases Thermal Stability. *Langmuir* **27**, 13091-13096 (2011).
107. R. Liebner, M. Meyer, T. Hey, G. Winter, A. Besheer, Head to Head Comparison of the Formulation and Stability of Concentrated Solutions of HESylated versus PEGylated Anakinra. *Journal of Pharmaceutical Sciences* **104**, 515-526 (2015).
108. S. V. Thakkar *et al.*, Excipients Differentially Influence the Conformational Stability and Pretransition Dynamics of Two IgG1 Monoclonal Antibodies. *Journal of Pharmaceutical Sciences* **101**, 3062-3077 (2012).
109. S. P. Choudhari, K. P. Pendleton, J. D. Ramsey, T. G. Blanchard, W. D. Picking, A Systematic Approach Toward Stabilization of CagL, a Protein Antigen from Helicobacter Pylori That is a Candidate Subunit Vaccine. *Journal of Pharmaceutical Sciences* **102**, 2508-2519 (2013).
110. S. Shi *et al.*, Biophysical Characterization and Stabilization of the Recombinant Albumin Fusion Protein sEphB4–HSA. *Journal of Pharmaceutical Sciences* **101**, 1969-1984 (2012).
111. N. A. Kim, S. Hada, R. Thapa, S. H. Jeong, Arginine as a protein stabilizer and destabilizer in liquid formulations. *International Journal of Pharmaceutics* **513**, 26-37 (2016).
112. J. J. Hung *et al.*, Improving Viscosity and Stability of a Highly Concentrated Monoclonal Antibody Solution with Concentrated Proline. *Pharmaceutical research* **35**, 133 (2018).
113. W. Wang *et al.*, Effects of osmolytes on Pelodiscus sinensis creatine kinase: A study on thermal denaturation and aggregation. *International Journal of Biological Macromolecules* **60**, 277-287 (2013).
114. H. Yuan *et al.*, The pH stability of foot-and-mouth disease virus. *Virology Journal* **14**, 233 (2017).
115. J.-M. Mayotte, T. Grabs, S. Sutliff-Johansson, K. Bishop, The effects of ionic strength and organic matter on virus inactivation at low temperatures: general likelihood uncertainty estimation (GLUE) as an alternative to least-squares parameter optimization for the fitting of virus inactivation models. *Hydrogeology Journal* **25**, 1063 (2017).

116. T. Hasan *et al.*, Osmolytes in vaccine production, flocculation and storage: a critical review. *Human vaccines & immunotherapeutics* **15**, 514-525 (2019).
117. T. Perevozchikova, H. Nanda, D. P. Nesta, C. J. Roberts, Protein Adsorption, Desorption, and Aggregation Mediated by Solid-Liquid Interfaces. *Journal of Pharmaceutical Sciences* **104**, 1946-1959 (2015).
118. M. M. Castellanos, J. A. Pathak, R. H. Colby, Both protein adsorption and aggregation contribute to shear yielding and viscosity increase in protein solutions. *Soft matter* **10**, 122-131 (2014).
119. K. Talley, E. Alexov, On the pH-optimum of activity and stability of proteins. *Proteins* **78**, 2699-2706 (2010).
120. S. Ohtake, Y. Kita, T. Arakawa, Interactions of formulation excipients with proteins in solution and in the dried state. *Advanced drug delivery reviews* **63**, 1053-1073 (2011).
121. T. A. Khan, H. C. Mahler, R. S. Kishore, Key interactions of surfactants in therapeutic protein formulations: A review. *European journal of pharmaceutics and biopharmaceutics : official journal of Arbeitsgemeinschaft fur Pharmazeutische Verfahrenstechnik e.V* **97**, 60-67 (2015).
122. T. W. Randolph, L. S. Jones, in *Rational Design of Stable Protein Formulations: Theory and Practice*, John F. Carpenter, Mark C. Manning, Eds. (Springer US, Boston, MA, 2002), pp. 159-175.
123. J. S. Bee, T. W. Randolph, J. F. Carpenter, S. M. Bishop, M. N. Dimitrova, Effects of Surfaces and Leachables on the Stability of Biopharmaceuticals. *Journal of Pharmaceutical Sciences* **100**, 4158-4170 (2011).
124. P. A. Gunning *et al.*, Effect of surfactant type on surfactant--protein interactions at the air-water interface. *Biomacromolecules* **5**, 984-991 (2004).
125. F. Poncin-Epaillard *et al.*, Surface treatment of polymeric materials controlling the adhesion of biomolecules. *J Funct Biomater* **3**, 528-543 (2012).
126. *Excipients Included in U.S. Vaccines, by Vaccine* (2019).
127. P. Maffre *et al.*, Effects of surface functionalization on the adsorption of human serum albumin onto nanoparticles – a fluorescence correlation spectroscopy study. *Beilstein Journal of Nanotechnology* **5**, 2036-2047 (2014).
128. J. Gilbert, O. Campanella, O. G. Jones, Electrostatic Stabilization of β-lactoglobulin Fibrils at Increased pH with Cationic Polymers. *Biomacromolecules* **15**, 3119-3127 (2014).
129. A. A. Yaroslavov, A. V. Sybachin, A. A. Efimova, Stabilization of electrostatic polymer-colloid complexes. *Colloids and Surfaces A: Physicochemical and Engineering Aspects* **558**, 1-7 (2018).
130. R. Imamura, H. Mori, Protein-Stabilizing Effect of Amphiphilic Block Copolymers with a Tertiary Sulfonium-Containing Zwitterionic Segment. *ACS Omega* **4**, 18234-18247 (2019).
131. A. M. Azevedo, J. M. S. Cabral, D. M. F. Prazeres, T. D. Gibson, L. P. Fonseca, Thermal and operational stabilities of Hansenula polymorpha alcohol oxidase. *Journal of Molecular Catalysis B: Enzymatic* **27**, 37-45 (2004).
132. H. Zhang *et al.*, PPARβ/δ activation inhibits angiotensin II-induced collagen type I expression in rat cardiac fibroblasts. *Archives of Biochemistry and Biophysics* **460**, 25-32 (2007).

133. J. Mondal *et al.*, How osmolytes influence hydrophobic polymer conformations: A unified view from experiment and theory. *Proceedings of the National Academy of Sciences* **112**, 9270 (2015).
134. V. Kadajji, G. Betageri, Water Soluble Polymers for Pharmaceutical Applications. *Polymers* **3**, (2011).
135. J. C. Lee, S. N. Timasheff, The stabilization of proteins by sucrose. *The Journal of biological chemistry* **256**, 7193-7201 (1981).
136. T. Arakawa, Y. Kita, J. F. Carpenter, Protein–Solvent Interactions in Pharmaceutical Formulations. *Pharmaceutical research* **8**, 285-291 (1991).
137. L. Chang, M. J. Pikal, Mechanisms of protein stabilization in the solid state. *Journal of pharmaceutical sciences* **98 9**, 2886-2908 (2009).
138. B. M. Baynes, D. I. Wang, B. L. Trout, Role of arginine in the stabilization of proteins against aggregation. *Biochemistry* **44**, 4919-4925 (2005).
139. D. M. Matthias, J. Robertson, M. M. Garrison, S. Newland, C. Nelson, Freezing temperatures in the vaccine cold chain: a systematic literature review. *Vaccine* **25**, 3980-3986 (2007).
140. B. Adhikari *et al.*, Earthquakes, Fuel Crisis, Power Outages, and Health Care in Nepal: Implications for the Future. *Disaster medicine and public health preparedness* **11**, 625-632 (2017).
141. M. N. Yakum, J. Ateudjieu, F. R. Pélagie, E. A. Walter, P. Watcho, Factors associated with the exposure of vaccines to adverse temperature conditions: the case of North West region, Cameroon. *BMC Research Notes* **8**, 277 (2015).
142. T. Kitamura *et al.*, Assessment of temperatures in the vaccine cold chain in two provinces in Lao People's Democratic Republic: a cross-sectional pilot study. *BMC Research Notes* **11**, 261 (2018).
143. A. Ashok, M. Brison, Y. LeTallec, Improving cold chain systems: Challenges and solutions. *Vaccine* **35**, 2217-2223 (2017).
144. I. P. Garber Cohen, P. R. Castello, F. L. G. Flecha, Ice-induced partial unfolding and aggregation of an integral membrane protein. *Biochimica et Biophysica Acta (BBA) - Biomembranes* **1798**, 2040-2047 (2010).
145. U. Kartoglu, N. K. Ozguler, L. J. Wolfson, W. Kurzatkowski, Validation of the shake test for detecting freeze damage to adsorbed vaccines. *Bulletin of the World Health Organization* **88**, 624-631 (2010).
146. J. F. Carpenter, J. H. Crowe, The mechanism of cryoprotection of proteins by solutes. *Cryobiology* **25**, 244-255 (1988).
147. R. Surís-Valls, I. K. Voets, The Impact of Salts on the Ice Recrystallization Inhibition Activity of Antifreeze (Glyco)Proteins. *Biomolecules* **9**, 347 (2019).
148. A. E. Rydeen, E. M. Brustad, G. J. Pielak, Osmolytes and Protein–Protein Interactions. *Journal of the American Chemical Society* **140**, 7441-7444 (2018).
149. D. A. J. Tyrrell, B. Ridgwell, Freeze-drying of Certain Viruses. *Nature* **206**, 115-116 (1965).
150. M. Hollings, R. A. Lelliott, Preservation of some plant viruses by freeze-drying. *Plant Pathology* **9**, 63-66 pp. (1960).
151. L. M. Kraft, E. C. Pollard, Lyophilization of Poliomyelitis Virus. Heat Inactivation of Dry MEF1 Virus. *Proceedings of the Society for Experimental Biology and Medicine* **86**, 306-309 (1954).

152. S. D. Allison, T. J. Anchordoquy, in *Nonviral Vectors for Gene Therapy: Methods and Protocols*, Mark A. Findeis, Ed. (Humana Press, Totowa, NJ, 2001), pp. 225-252.
153. W. Wang, Lyophilization and development of solid protein pharmaceuticals. *International Journal of Pharmaceutics* **203**, 1-60 (2000).
154. W. Abdelwahed, G. Degobert, S. Stainmesse, H. Fessi, Freeze-drying of nanoparticles: Formulation, process and storage considerations. *Advanced drug delivery reviews* **58**, 1688-1713 (2006).
155. J. C. Kasper, G. Winter, W. Friess, Recent advances and further challenges in lyophilization. *European Journal of Pharmaceutics and Biopharmaceutics* **85**, 162-169 (2013).
156. A. Wasserman, R. Sarpal, B. Phillips, in *Vaccine Development and Manufacturing*. (2014), pp. 263-285.
157. W. R. Liu, R. Langer, A. M. Klibanov, Moisture-induced aggregation of lyophilized proteins in the solid state. *Biotechnology and bioengineering* **37**, 177-184 (1991).
158. M. E. Brewster, M. S. Hora, J. W. Simpkins, N. Bodor, Use of 2-Hydroxypropyl-β-cyclodextrin as a Solubilizing and Stabilizing Excipient for Protein Drugs. *Pharmaceutical research* **8**, 792-795 (1991).
159. B. S. Chang, C. S. Randall, Y. S. Lee, Stabilization of Lyophilized Porcine Pancreatic Elastase. *Pharmaceutical research* **10**, 1478-1483 (1993).
160. L. L. Chang, M. J. Pikal, Mechanisms of protein stabilization in the solid state. *J Pharm Sci* **98**, 2886-2908 (2009).
161. J. L. Cleland, T. W. Randolph, Mechanism of polyethylene glycol interaction with the molten globule folding intermediate of bovine carbonic anhydrase B. *The Journal of biological chemistry* **267**, 3147-3153 (1992).
162. L. Kreilgaard *et al.*, Effect of Tween 20 on freeze-thawing- and agitation-induced aggregation of recombinant human factor XIII. *J Pharm Sci* **87**, 1597-1603 (1998).
163. M. Mattern, G. Winter, U. Kohnert, G. Lee, Formulation of proteins in vacuum-dried glasses. II. Process and storage stability in sugar-free amino acid systems. *Pharm Dev Technol* **4**, 199-208 (1999).
164. F. Tian *et al.*, Spectroscopic evaluation of the stabilization of humanized monoclonal antibodies in amino acid formulations. *International Journal of Pharmaceutics* **335**, 20-31 (2007).
165. B. Chen *et al.*, Influence of Histidine on the Stability and Physical Properties of a Fully Human Antibody in Aqueous and Solid Forms. *Pharmaceutical research* **20**, 1952-1960 (2003).
166. T. T. Wyatt, H. A. B. Wösten, J. Dijksterhuis, in *Advances in Applied Microbiology*, Sima Sariaslani, Geoffrey M. Gadd, Eds. (Academic Press, 2013), vol. 85, pp. 43-91.
167. X. Tang, M. J. Pikal, Design of Freeze-Drying Processes for Pharmaceuticals: Practical Advice. *Pharmaceutical research* **21**, 191-200 (2004).
168. P. M. J. Costantino Henry R, *Lyophilization of biopharmaceuticals* Biotechnology: Pharmaceutical Aspects (American Association of Pharmaceutical Sciences, Arlington, VA, 2004).
169. S. M. Patel, T. Doen, M. J. Pikal, Determination of end point of primary drying in freeze-drying process control. *AAPS PharmSciTech* **11**, 73-84 (2010).

170. S. C. Schneid, H. Gieseler, W. J. Kessler, S. A. Luthra, M. J. Pikal, Optimization of the secondary drying step in freeze drying using TDLAS technology. *AAPS PharmSciTech* **12**, 379-387 (2011).
171. S. Khairnar, R. Kini, M. Harwalkar, K. Salunkhe, S. Chaudhari, A Review on Freeze Drying Process of Pharmaceuticals. *International Journal of Research in Pharmacy and science* **IJRPS 2013**, 76-94 (2012).
172. R. Lang *et al.*, Rational Design of a Stable, Freeze-Dried Virus-Like Particle-Based Vaccine Formulation. *Drug Development and Industrial Pharmacy* **35**, 83-97 (2009).
173. J. C. May, E. Grim, R. M. Wheeler, J. West, Determination of residual moisture in freeze-dried viral vaccines: Karl Fischer, gravimetric and thermogravimetric methodologies. *Journal of Biological Standardization* **10**, 249-259 (1982).
174. World Health Organization, "The Proper Handling and Use of Vaccine Diluents," *Vaccine Diluents* (World Health Organization, Geneva, Switzerland, 2015).
175. Immunization Action Coalition, "Vaccines with Diluents: How to Use Them," (Immunization Action Coalition, Saint Paul, Minnesota, 2017).
176. C. Czerkinsky *et al.*, Mucosal immunity and tolerance: relevance to vaccine development. *Immunological reviews* **170**, 197-222 (1999).
177. A. Flood, M. Estrada, D. McAdams, Y. Ji, D. Chen, Development of a Freeze-Dried, Heat-Stable Influenza Subunit Vaccine Formulation. *PLoS One* **11**, e0164692-e0164692 (2016).
178. G. Kanojia *et al.*, Developments in the formulation and delivery of spray dried vaccines. *Human vaccines & immunotherapeutics* **13**, 2364-2378 (2017).
179. A. Ziaee *et al.*, Spray drying of pharmaceuticals and biopharmaceuticals: Critical parameters and experimental process optimization approaches. *European Journal of Pharmaceutical Sciences* **127**, 300-318 (2019).
180. I. Roy, M. N. Gupta, Freeze-drying of proteins: some emerging concerns. *Biotechnology and applied biochemistry* **39**, 165-177 (2004).
181. S. H. Wang, S. M. Kirwan, S. N. Abraham, H. F. Staats, A. J. Hickey, Stable Dry Powder Formulation for Nasal Delivery of Anthrax Vaccine. *Journal of Pharmaceutical Sciences* **101**, 31-47 (2012).
182. M. Ameri, Y.-F. Maa, Spray Drying of Biopharmaceuticals: Stability and Process Considerations. *Drying Technology* **24**, 763-768 (2006).
183. G. Kanojia *et al.*, A Design of Experiment approach to predict product and process parameters for a spray dried influenza vaccine. *International Journal of Pharmaceutics* **511**, 1098-1111 (2016).
184. S. Ohtake *et al.*, Heat-stable measles vaccine produced by spray drying. *Vaccine* **28**, 1275-1284 (2010).
185. D. A. LeClair, E. D. Cranston, Z. Xing, M. R. Thompson, Optimization of Spray Drying Conditions for Yield, Particle Size and Biological Activity of Thermally Stable Viral Vectors. *Pharmaceutical research* **33**, 2763-2776 (2016).
186. V. Saluja *et al.*, A comparison between spray drying and spray freeze drying to produce an influenza subunit vaccine powder for inhalation. *Journal of Controlled Release* **144**, 127-133 (2010).
187. Y.-F. Maa, L. Zhao, L. G. Payne, D. Chen, Stabilization of alum-adjuvanted vaccine dry powder formulations: Mechanism and application. *Journal of Pharmaceutical Sciences* **92**, 319-332 (2003).

188. W. F. Tonnis *et al.*, Improved storage stability and immunogenicity of hepatitis B vaccine after spray-freeze drying in presence of sugars. *European Journal of Pharmaceutical Sciences* **55**, 36-45 (2014).
189. J. Huang *et al.*, Protective Immunity in Mice Achieved with Dry Powder Formulation and Alternative Delivery of Plague F1-V Vaccine. *Clinical and Vaccine Immunology* **16**, 719 (2009).
190. S. P. Sellers, G. S. Clark, R. E. Sievers, J. F. Carpenter, Dry powders of stable protein formulations from aqueous solutions prepared using supercritical CO(2)-assisted aerosolization. *J Pharm Sci* **90**, 785-797 (2001).
191. J. Kissmann *et al.*, Stabilization of measles virus for vaccine formulation. *Human vaccines* **4**, 350-359 (2008).
192. J. Burger *et al.*, Stabilizing Formulations for Inhalable Powders of Live-Attenuated Measles Virus Vaccine. *Journal of aerosol medicine and pulmonary drug delivery* **21**, 25-34 (2008).
193. S. P. Cape *et al.*, Preparation of active proteins, vaccines and pharmaceuticals as fine powders using supercritical or near-critical fluids. *Pharmaceutical research* **25**, 1967-1990 (2008).
194. United States Pharmacopeial Convention, in *USP35 NF30, 2012: U. S. Pharmacopoeia National Formulary*. (USP35 NF30, 2012), vol. 35, pp. 765-783.
195. M. Preis, C. Woertz, P. Kleinebudde, J. Breitkreutz, Oromucosal film preparations: classification and characterization methods. *Expert opinion on drug delivery* **10**, 1303-1317 (2013).
196. M. Montenegro-Nicolini, J. O. Morales, Overview and Future Potential of Buccal Mucoadhesive Films as Drug Delivery Systems for Biologics. *AAPS PharmSciTech* **18**, 3-14 (2017).
197. B. M. A. Silva, A. F. Borges, C. Silva, J. F. J. Coelho, S. Simões, Mucoadhesive oral films: The potential for unmet needs. *International Journal of Pharmaceutics* **494**, 537-551 (2015).
198. K. K. Peh, C. F. Wong, Polymeric films as vehicle for buccal delivery: swelling, mechanical, and bioadhesive properties. *Journal of pharmacy & pharmaceutical sciences : a publication of the Canadian Society for Pharmaceutical Sciences, Societe canadienne des sciences pharmaceutiques* **2**, 53-61 (1999).
199. E. Y. Chi, S. Krishnan, T. W. Randolph, J. F. Carpenter, Physical Stability of Proteins in Aqueous Solution: Mechanism and Driving Forces in Nonnative Protein Aggregation. *Pharmaceutical research* **20**, 1325-1336 (2003).
200. T. J. Kamerzell, R. Esfandiary, S. B. Joshi, C. R. Middaugh, D. B. Volkin, Protein-excipient interactions: mechanisms and biophysical characterization applied to protein formulation development. *Advanced drug delivery reviews* **63**, 1118-1159 (2011).
201. J. O. Morales, J. T. McConville, Manufacture and characterization of mucoadhesive buccal films. *European journal of pharmaceutics and biopharmaceutics : official journal of Arbeitsgemeinschaft fur Pharmazeutische Verfahrenstechnik e.V* **77**, 187-199 (2011).
202. J. O. Morales, J. T. McConville, Novel strategies for the buccal delivery of macromolecules. *Drug Development and Industrial Pharmacy* **40**, 579-590 (2014).
203. L. A. Felton, Mechanisms of polymeric film formation. *International Journal of Pharmaceutics* **457**, 423-427 (2013).

204. K. Huntrakul, N. Harnkarnsujarit, Effects of plasticizers on water sorption and aging stability of whey protein/carboxy methyl cellulose films. *Journal of Food Engineering* **272**, 109809 (2020).
205. F. Carvalho, M. Bruschi, R. Evangelista, M. Gremiao, Mucoadhesive drug delivery systems. *Brazilian Journal of Pharmaceutical Sciences* **46**, 1-17 (2010).
206. Y. Lu, E. Zhang, J. Yang, Z. Cao, Strategies to improve micelle stability for drug delivery. *Nano Res* **11**, 4985-4998 (2018).
207. I. Bajrovic, S. C. Schafer, D. K. Romanovicz, M. A. Croyle, Novel technology for storage and distribution of live vaccines and other biological medicines at ambient temperature. *Science Advances* **6**, eaau4819 (2020).
208. H. Sohi, A. Ahuja, F. J. Ahmad, R. K. Khar, Critical evaluation of permeation enhancers for oral mucosal drug delivery. *Drug Development and Industrial Pharmacy* **36**, 254-282 (2010).
209. E. Moghimipour, A. Ameri, S. Handali, Absorption-Enhancing Effects of Bile Salts. *Molecules* **20**, 14451-14473 (2015).
210. K. Kesarwani, R. Gupta, A. Mukerjee, Bioavailability enhancers of herbal origin: an overview. *Asian Pac J Trop Biomed* **3**, 253-266 (2013).
211. S. Kobayashi, S. Kondo, K. Juni, Permeability enhancing effect of oleic acid and its mechanism in human alveolar A549 cells. *European Journal of Pharmaceutical Sciences* **4**, 267-272 (1996).
212. V. Kumar, R. Chari, V. K. Sharma, D. S. Kalonia, Modulation of the thermodynamic stability of proteins by polyols: significance of polyol hydrophobicity and impact on the chemical potential of water. *Int J Pharm* **413**, 19-28 (2011).
213. S. Sharma, A. A. Singh, A. Majumdar, B. S. Butola, Tailoring the mechanical and thermal properties of polylactic acid-based bionanocomposite films using halloysite nanotubes and polyethylene glycol by solvent casting process. *Journal of Materials Science* **54**, 8971-8983 (2019).
214. P. Kanaujia, P. Poovizhi, W. K. Ng, R. B. H. Tan, Preparation, Characterization and Prevention of Auto-oxidation of Amorphous Sirolimus by Encapsulation in Polymeric Films Using Hot Melt Extrusion. *Current Drug Delivery* **16**, 663-671 (2019).
215. B. S. Yadav, S. Koppoju, S. R. Dey, S. R. Dhage, Microstructural investigation of inkjet printed Cu(In,Ga)Se2 thin film solar cell with improved efficiency. *Journal of Alloys and Compounds* **827**, 154295 (2020).
216. V. Leung *et al.*, Thermal Stabilization of Viral Vaccines in Low-Cost Sugar Films. *Scientific Reports* **9**, 7631 (2019).
217. J. A. Stinson *et al.*, Thin silk fibroin films as a dried format for temperature stabilization of inactivated polio vaccine. *Vaccine* **38**, 1652-1660 (2020).
218. M. J. Mistilis *et al.*, Long-term stability of influenza vaccine in a dissolving microneedle patch. *Drug Delivery and Translational Research* **7**, 195-205 (2017).
219. Y.-C. Kim, F.-S. Quan, R. W. Compans, S.-M. Kang, M. R. Prausnitz, Formulation and coating of microneedles with inactivated influenza virus to improve vaccine stability and immunogenicity. *Journal of Controlled Release* **142**, 187-195 (2010).
220. C. Hervé, B. Laupèze, G. Del Giudice, A. M. Didierlaurent, F. Tavares Da Silva, The how's and what's of vaccine reactogenicity. *npj Vaccines* **4**, 39 (2019).
221. I. F. Cook, Sex differences in injection site reactions with human vaccines. *Human vaccines* **5**, 441-449 (2009).

222. E. De Gregorio, E. Caproni, J. B. Ulmer, Vaccine adjuvants: mode of action. *Frontiers in immunology* **4**, 214 (2013).
223. J.-M. Zhang, J. An, Cytokines, inflammation, and pain. *Int Anesthesiol Clin* **45**, 27-37 (2007).
224. K. L. Rock, E. Reits, J. Neefjes, Present Yourself! By MHC Class I and MHC Class II Molecules. *Trends in immunology* **37**, 724-737 (2016).
225. S. C. Gilbert, T-cell-inducing vaccines - what's the future. *Immunology* **135**, 19-26 (2012).
226. G. Mutua *et al.*, Safety and Immunogenicity of a 2-Dose Heterologous Vaccine Regimen With Ad26.ZEBOV and MVA-BN-Filo Ebola Vaccines: 12-Month Data From a Phase 1 Randomized Clinical Trial in Nairobi, Kenya. *The Journal of infectious diseases* **220**, 57-67 (2019).
227. J. Zhu, H. Yamane, W. E. Paul, Differentiation of effector CD4 T cell populations (*). *Annual review of immunology* **28**, 445-489 (2010).
228. C. Kim, F. Fang, C. M. Weyand, J. J. Goronzy, The life cycle of a T cell after vaccination - where does immune ageing strike? *Clin Exp Immunol* **187**, 71-81 (2017).
229. C.-A. Siegrist, P.-H. Lambert, in *The Vaccine Book (Second Edition)*, Barry R. Bloom, Paul-Henri Lambert, Eds. (Academic Press, 2016), pp. 33-42.
230. J. O. Josefsberg, B. Buckland, Vaccine process technology. *Biotechnology and bioengineering* **109**, 1443-1460 (2012).
231. N. K. Jain *et al.*, Formulation and stabilization of recombinant protein based virus-like particle vaccines. *Advanced drug delivery reviews* **93**, 42-55 (2015).
232. J. Mohr, Y. P. Chuan, Y. Wu, L. H. Lua, A. P. Middelberg, Virus-like particle formulation optimization by miniaturized high-throughput screening. *Methods (San Diego, Calif.)* **60**, 248-256 (2013).
233. R. Khandia *et al.*, Modulation of Dengue/Zika Virus Pathogenicity by Antibody-Dependent Enhancement and Strategies to Protect Against Enhancement in Zika Virus Infection. *Frontiers in immunology* **9**, 597-597 (2018).
234. G. R. Doyle, J. A. McCutcheon, *Clinical Procedures for Safer Patient Care* (British Columbia Institute of Technology 2012).
235. J. N. Zuckerman, The importance of injecting vaccines into muscle. Different patients need different needle sizes. *BMJ* **321**, 1237-1238 (2000).
236. P. He, Y. Zou, Z. Hu, Advances in aluminum hydroxide-based adjuvant research and its mechanism. *Hum Vaccin Immunother* **11**, 477-488 (2015).
237. C. A. Shaw *et al.*, Aluminum-induced entropy in biological systems: implications for neurological disease. *Journal of toxicology* **2014**, 491316 (2014).
238. F. E. Shaw, Jr. *et al.*, Effect of anatomic injection site, age and smoking on the immune response to hepatitis B vaccination. *Vaccine* **7**, 425-430 (1989).
239. F. de Lalla, E. Rinaldi, D. Santoro, G. Pravettoni, Immune response to hepatitis B vaccine given at different injection sites and by different routes: a controlled randomized study. *European journal of epidemiology* **4**, 256-258 (1988).
240. T. Tapiainen, J. D. Cherry, U. Heininger, Effect of injection site on reactogenicity and immunogenicity of acellular and whole-cell pertussis component diphtheria-tetanus-pertussis vaccines in infants. *Vaccine* **23**, 5106-5112 (2005).
241. L. Zhang, W. Wang, S. Wang, Effect of vaccine administration modality on immunogenicity and efficacy. *Expert Rev Vaccines* **14**, 1509-1523 (2015).

242. Y. Gillet, P. Habermehl, S. Thomas, C. Eymin, A. Fiquet, Immunogenicity and safety of concomitant administration of a measles, mumps and rubella vaccine (M-M-RvaxPro) and a varicella vaccine (VARIVAX) by intramuscular or subcutaneous routes at separate injection sites: a randomised clinical trial. *BMC medicine* **7**, 16 (2009).
243. F. L. Ruben *et al.*, Choosing a Route of Administration for Quadrivalent Meningococcal Polysaccharide Vaccine: Intramuscular versus Subcutaneous. *Clinical Infectious Diseases* **32**, 170-172 (2001).
244. A. Fisch *et al.*, Immunogenicity and safety of a new inactivated hepatitis A vaccine: a clinical trial with comparison of administration route. *Vaccine* **14**, 1132-1136 (1996).
245. B. Malik, G. Rath, A. K. Goyal, Are the anatomical sites for vaccine administration selected judiciously? *International Immunopharmacology* **19**, 17-26 (2014).
246. M. T. Ochoa, A. Loncaric, S. R. Krutzik, T. C. Becker, R. L. Modlin, "Dermal dendritic cells" comprise two distinct populations: CD1+ dendritic cells and CD209+ macrophages. *J Invest Dermatol* **128**, 2225-2231 (2008).
247. A. K. Shakya, M. Y. E. Chowdhury, W. Tao, H. S. Gill, Mucosal vaccine delivery: Current state and a pediatric perspective. *J Control Release* **240**, 394-413 (2016).
248. J. K. Salmon, C. A. Armstrong, J. C. Ansel, The skin as an immune organ. *West J Med* **160**, 146-152 (1994).
249. W. T. Godbey, in *An Introduction to Biotechnology*, W. T. Godbey, Ed. (Woodhead Publishing, 2014), pp. 275-312.
250. S. H. T. Jorritsma, E. J. Gowans, B. Grubor-Bauk, D. K. Wijesundara, Delivery methods to increase cellular uptake and immunogenicity of DNA vaccines. *Vaccine* **34**, 5488-5494 (2016).
251. A. Tanghe *et al.*, Tuberculosis DNA vaccine encoding Ag85A is immunogenic and protective when administered by intramuscular needle injection but not by epidermal gene gun bombardment. *Infect Immun* **68**, 3854-3860 (2000).
252. R. Weiss *et al.*, Gene gun bombardment with gold particles displays a particular Th2-promoting signal that over-rules the Th1-inducing effect of immunostimulatory CpG motifs in DNA vaccines. *Vaccine* **20**, 3148-3154 (2002).
253. X. Zhou, L. Zheng, L. Liu, L. Xiang, Z. Yuan, T helper 2 immunity to hepatitis B surface antigen primed by gene-gun-mediated DNA vaccination can be shifted towards T helper 1 immunity by codelivery of CpG motif-containing oligodeoxynucleotides. *Scandinavian journal of immunology* **58**, 350-357 (2003).
254. D. J. Irvine, A. Aung, M. Silva, Controlling timing and location in vaccines. *Advanced drug delivery reviews*, S0169-0409X(0120)30065-X (2020).
255. M. C. Diehl *et al.*, Tolerability of intramuscular and intradermal delivery by CELLECTRA(®) adaptive constant current electroporation device in healthy volunteers. *Human vaccines & immunotherapeutics* **9**, 2246-2252 (2013).
256. L. Lambricht *et al.*, Clinical potential of electroporation for gene therapy and DNA vaccine delivery. *Expert opinion on drug delivery* **13**, 295-310 (2016).
257. A. Z. Alkilani, M. T. C. McCrudden, R. F. Donnelly, Transdermal Drug Delivery: Innovative Pharmaceutical Developments Based on Disruption of the Barrier Properties of the stratum corneum. *Pharmaceutics* **7**, 438-470 (2015).
258. C. I. Shin, S. D. Jeong, N. S. Rejinold, Y. C. Kim, Microneedles for vaccine delivery: challenges and future perspectives. *Ther Deliv* **8**, 447-460 (2017).

259. A. Pattani *et al.*, Microneedle mediated intradermal delivery of adjuvanted recombinant HIV-1 CN54gp140 effectively primes mucosal boost inoculations. *J Control Release* **162**, 529-537 (2012).
260. W. C. Weldon *et al.*, Microneedle vaccination with stabilized recombinant influenza virus hemagglutinin induces improved protective immunity. *Clin Vaccine Immunol* **18**, 647-654 (2011).
261. L. Y. Chu *et al.*, Enhanced Stability of Inactivated Influenza Vaccine Encapsulated in Dissolving Microneedle Patches. *Pharmaceutical research* **33**, 868-878 (2016).
262. E. V. Vassilieva *et al.*, Improved immunogenicity of individual influenza vaccine components delivered with a novel dissolving microneedle patch stable at room temperature. *Drug Deliv Transl Res* **5**, 360-371 (2015).
263. A. Vrdoljak *et al.*, Induction of broad immunity by thermostabilised vaccines incorporated in dissolvable microneedles using novel fabrication methods. *Journal of Controlled Release* **225**, 192-204 (2016).
264. X. Chen *et al.*, Improving the reach of vaccines to low-resource regions, with a needle-free vaccine delivery device and long-term thermostabilization. *J Control Release* **152**, 349-355 (2011).
265. G. Ma, C. Wu, Microneedle, bio-microneedle and bio-inspired microneedle: A review. *Journal of Controlled Release* **251**, 11-23 (2017).
266. C. F. Kuper *et al.*, The role of nasopharyngeal lymphoid tissue. *Immunology today* **13**, 219-224 (1992).
267. H. Yusuf, V. Kett, Current prospects and future challenges for nasal vaccine delivery. *Human Vaccines & Immunotherapeutics* **13**, 34-45 (2017).
268. M. A. Clark, M. A. Jepson, B. H. Hirst, Exploiting M cells for drug and vaccine delivery. *Advanced drug delivery reviews* **50**, 81-106 (2001).
269. I. Shannon, C. L. White, J. L. Nayak, Understanding Immunity in Children Vaccinated With Live Attenuated Influenza Vaccine. *J Pediatric Infect Dis Soc* **9**, S10-s14 (2020).
270. R. Dhere *et al.*, A pandemic influenza vaccine in India: from strain to sale within 12 months. *Vaccine* **29 Suppl 1**, A16-21 (2011).
271. C. Calzas, C. Chevalier, Innovative Mucosal Vaccine Formulations Against Influenza A Virus Infections. *Frontiers in immunology* **10**, (2019).
272. D. Albrecht, M. Iwashima, D. Dillon, S. Harris, J. Levy, A Phase 1, Randomized, Open-Label, Safety, Tolerability, and Comparative Bioavailability Study of Intranasal Dihydroergotamine Powder (STS101), Intramuscular Dihydroergotamine Mesylate, and Intranasal DHE Mesylate Spray in Healthy Adult Subjects. *Headache* **60**, 701-712 (2020).
273. J. H. Ryu *et al.*, Chitosan oral patches inspired by mussel adhesion. *J Control Release* **317**, 57-66 (2020).
274. P. Watts, A. Smith, M. Hinchcliffe, in *Mucosal Delivery of Biopharmaceuticals,* Bruno Sarmento, José das Neves, Eds. (Springer, Boston, MA, 2014), pp. 499-516
275. L. Casettari, L. Illum, Chitosan in nasal delivery systems for therapeutic drugs. *J Control Release* **190**, 189-200 (2014).
276. M. A. Gill, E. P. Schlaudecker, Perspectives from the Society for Pediatric Research: Decreased Effectiveness of the Live Attenuated Influenza Vaccine. *Pediatric research* **83**, 31-40 (2018).

277. H. Jang, T. M. Ross, Preexisting influenza specific immunity and vaccine effectiveness. *Expert Rev Vaccines* **18**, 1043-1051 (2019).
278. K. Edwards, P. H. Lambert, S. Black, Narcolepsy and Pandemic Influenza Vaccination: What We Need to Know to be Ready for the Next Pandemic. *The Pediatric infectious disease journal* **38**, 873-876 (2019).
279. D. J. Lewis *et al.*, Transient facial nerve paralysis (Bell's palsy) following intranasal delivery of a genetically detoxified mutant of Escherichia coli heat labile toxin. *PLoS One* **4**, e6999 (2009).
280. Z.-B. Wang, J. Xu, Better Adjuvants for Better Vaccines: Progress in Adjuvant Delivery Systems, Modifications, and Adjuvant-Antigen Codelivery. *Vaccines* **8**, 128 (2020).
281. H. B. Lee *et al.*, Oral Immunization of FMDV Vaccine Using pH-Sensitive and Mucoadhesive Thiolated Cellulose Acetate Phthalate Microparticles. *Tissue engineering and regenerative medicine* **15**, 1-11 (2018).
282. G. Azzali, Structure, lymphatic vascularization and lymphocyte migration in mucosa-associated lymphoid tissue. *Immunological reviews* **195**, 178-189 (2003).
283. M. F. Cesta, Normal Structure, Function, and Histology of Mucosa-Associated Lymphoid Tissue. *Toxicologic Pathology* **34**, 599-608 (2006).
284. B. Homayun, X. Lin, H.-J. Choi, Challenges and Recent Progress in Oral Drug Delivery Systems for Biopharmaceuticals. *Pharmaceutics* **11**, 129 (2019).
285. H. Cheroutre, F. Lambolez, D. Mucida, The light and dark sides of intestinal intraepithelial lymphocytes. *Nature Reviews Immunology* **11**, 445-456 (2011).
286. T. Magrone, E. Jirillo, Development and Organization of the Secondary and Tertiary Lymphoid Organs: Influence of Microbial and Food Antigens. *Endocrine, metabolic & immune disorders drug targets* **19**, 128-135 (2019).
287. T. Sun, A. Nguyen, J. L. Gommerman, Dendritic Cell Subsets in Intestinal Immunity and Inflammation. *Journal of immunology (Baltimore, Md. : 1950)* **204**, 1075-1083 (2020).
288. A. N. Vlasova, S. Takanashi, A. Miyazaki, G. Rajashekara, L. J. Saif, How the gut microbiome regulates host immune responses to viral vaccines. *Curr Opin Virol* **37**, 16-25 (2019).
289. R. A. Kuschner *et al.*, A phase 3, randomized, double-blind, placebo-controlled study of the safety and efficacy of the live, oral adenovirus type 4 and type 7 vaccine, in U.S. military recruits. *Vaccine* **31**, 2963-2971 (2013).
290. D. Amicizia, L. Arata, F. Zangrillo, D. Panatto, R. Gasparini, Overview of the impact of Typhoid and Paratyphoid fever. Utility of Ty21a vaccine (Vivotif®). *Journal of preventive medicine and hygiene* **58**, E1-e8 (2017).
291. Advisory Committee on Immunization Practices, "Typhoid Immunization Recommendations of the Advisory Committee on Immunization Practices (ACIP)," (1994).
292. S.-H. Kim, Y.-S. Jang, The development of mucosal vaccines for both mucosal and systemic immune induction and the roles played by adjuvants. *Clin Exp Vaccine Res* **6**, 15-21 (2017).
293. P. Pereira, V. Vetter, B. Standaert, B. Benninghoff, Fifteen years of experience with the oral live-attenuated human rotavirus vaccine: reflections on lessons learned. *Expert Rev Vaccines*, 1-15 (2020).
294. O. S. Folorunso, O. M. Sebolai, Overview of the Development, Impacts, and Challenges of Live-Attenuated Oral Rotavirus Vaccines. *Vaccines (Basel)* **8**, (2020).

295. T. Nakagomi, O. Nakagomi, A critical review on a globally-licensed, live, orally-administrable, monovalent human rotavirus vaccine: Rotarix. *Expert opinion on biological therapy* **9**, 1073-1086 (2009).
296. J. J. Liau, S. Hook, C. A. Prestidge, T. J. Barnes, A lipid based multi-compartmental system: Liposomes-in-double emulsion for oral vaccine delivery. *European journal of pharmaceutics and biopharmaceutics : official journal of Arbeitsgemeinschaft fur Pharmazeutische Verfahrenstechnik e.V* **97**, 15-21 (2015).
297. S.-J. Cao *et al.*, Nanoparticles: Oral Delivery for Protein and Peptide Drugs. *AAPS PharmSciTech* **20**, 190-190 (2019).
298. E. M. Pridgen, F. Alexis, O. C. Farokhzad, Polymeric nanoparticle technologies for oral drug delivery. *Clin Gastroenterol Hepatol* **12**, 1605-1610 (2014).
299. V. M. Kurup, J. Thomas, Edible Vaccines: Promises and Challenges. *Mol Biotechnol* **62**, 79-90 (2020).
300. M. S. Khan, F. A. Joyia, G. Mustafa, Seeds as Economical Production Platform for Recombinant Proteins. *Protein and peptide letters* **27**, 89-104 (2020).
301. S. Pillet *et al.*, Immunogenicity and safety of a quadrivalent plant-derived virus like particle influenza vaccine candidate-Two randomized Phase II clinical trials in 18 to 49 and ≥50 years old adults. *PLoS One* **14**, e0216533 (2019).
302. S. Rosales-Mendoza, V. A. Márquez-Escobar, O. González-Ortega, R. Nieto-Gómez, J. I. Arévalo-Villalobos, What Does Plant-Based Vaccine Technology Offer to the Fight against COVID-19? *Vaccines (Basel)* **8**, (2020).
303. M. N. Uddin, A. Allon, M. A. Roni, S. Kouzi, Overview and Future Potential of Fast Dissolving Buccal Films as Drug Delivery System for Vaccines. *Journal of pharmacy & pharmaceutical sciences : a publication of the Canadian Society for Pharmaceutical Sciences, Societe canadienne des sciences pharmaceutiques* **22**, 388-406 (2019).
304. H. Kraan *et al.*, Buccal and sublingual vaccine delivery. *Journal of Controlled Release* **190**, 580-592 (2014).
305. N. Narang, J. Sharma, Sublingual mucosa as a route for systemic drug delivery. *International Journal of Pharmacy and Pharmaceutical Sciences* **3**, 18-22 (2011).
306. S. Hua, Advances in Nanoparticulate Drug Delivery Approaches for Sublingual and Buccal Administration. *Frontiers in Pharmacology* **10**, (2019).
307. T. J. De Marco, I. Blomsnes, Effect of various conditions on the sublingual absorption of para-aminosalicylic acid. *Oral surgery, oral medicine, and oral pathology* **37**, 320-326 (1974).
308. J. Upadhyay, R. B. Upadhyay, P. Agrawal, S. Jaitley, R. Shekhar, Langerhans cells and their role in oral mucosal diseases. *N Am J Med Sci* **5**, 505-514 (2013).
309. J. H. Choi *et al.*, A single sublingual dose of an adenovirus-based vaccine protects against lethal Ebola challenge in mice and guinea pigs. *Molecular pharmaceutics* **9**, 156-167 (2012).
310. C. Czerkinsky, J. Holmgren, in *Mucosal Vaccines: Modern Concepts, Strategies, and Challenges*, Pamela A. Kozlowski, Ed. (Springer Berlin Heidelberg, Berlin, Heidelberg, 2012), pp. 1-18.
311. V. F. Patel, F. Liu, M. B. Brown, Advances in oral transmucosal drug delivery. *Journal of Controlled Release* **153**, 106-116 (2011).
312. D. J. Aframian, T. Davidowitz, R. Benoliel, The distribution of oral mucosal pH values in healthy saliva secretors. *Oral Diseases* **12**, 420-423 (2006).

313. P. W. Wertz, C. A. Squier, Cellular and molecular basis of barrier function in oral epithelium. *Critical reviews in therapeutic drug carrier systems* **8**, 237-269 (1991).
314. H. S. Oberoi, Y. M. Yorgensen, A. Morasse, J. T. Evans, D. J. Burkhart, PEG modified liposomes containing CRX-601 adjuvant in combination with methylglycol chitosan enhance the murine sublingual immune response to influenza vaccination. *Journal of Controlled Release* **223**, 64-74 (2016).
315. J. A. White *et al.*, Serum and mucosal antibody responses to inactivated polio vaccine after sublingual immunization using a thermoresponsive gel delivery system. *Human vaccines & immunotherapeutics* **10**, 3611-3621 (2014).
316. A. Borde, A. Ekman, J. Holmgren, A. Larsson, Effect of protein release rates from tablet formulations on the immune response after sublingual immunization. *European Journal of Pharmaceutical Sciences* **47**, 695-700 (2012).
317. J.-H. Song *et al.*, Sublingual vaccination with influenza virus protects mice against lethal viral infection. *Proc Natl Acad Sci U S A* **105**, 1644-1649 (2008).
318. J. Y. Kim, Y. Choi, H. H. Nguyen, M. K. Song, J. Chang, Mucosal immunization with recombinant adenovirus encoding soluble globular head of hemagglutinin protects mice against lethal influenza virus infection. *Immune Netw* **13**, 275-282 (2013).
319. P. N. Boyaka, Inducing Mucosal IgA: A Challenge for Vaccine Adjuvants and Delivery Systems. *The Journal of Immunology* **199**, 9 (2017).
320. L. B. Lawson, E. B. Norton, J. D. Clements, Defending the mucosa: adjuvant and carrier formulations for mucosal immunity. *Current opinion in immunology* **23**, 414-420 (2011).
321. C. Hervouet *et al.*, Sublingual immunization with an HIV subunit vaccine induces antibodies and cytotoxic T cells in the mouse female genital tract. *Vaccine* **28**, 5582-5590 (2010).
322. Vaccine Innovation Prioritisation Strategy, "Sublingual Dosage Forms," (Geneva, Switzerland, 2019).
323. ClinicalTrials.gov. (National Library of Medicine Bethesda, MD, 2016).
324. G. Passalacqua, D. Bagnasco, G. W. Canonica, 30 years of sublingual immunotherapy. *Allergy* **75**, 1107-1120 (2020).
325. P. Demoly, G. Passalacqua, M. A. Calderon, T. Yalaoui, Choosing the optimal dose in sublingual immunotherapy: Rationale for the 300 index of reactivity dose. *Clinical and Translational Allergy* **5**, 44 (2015).
326. K. Aran *et al.*, An oral microjet vaccination system elicits antibody production in rabbits. *Science Translational Medicine* **9**, eaaf6413 (2017).
327. C. L. McNeilly *et al.*, Microprojection arrays to immunise at mucosal surfaces. *J Control Release* **196**, 252-260 (2014).
328. Y. Zhen *et al.*, Multifunctional liposomes constituting microneedles induced robust systemic and mucosal immunoresponses against the loaded antigens via oral mucosal vaccination. *Vaccine* **33**, 4330-4340 (2015).
329. T. Wang *et al.*, Mannosylated and lipid A-incorporating cationic liposomes constituting microneedle arrays as an effective oral mucosal HBV vaccine applicable in the controlled temperature chain. *Colloids and Surfaces B: Biointerfaces* **126**, 520-530 (2015).
330. J. Mašek *et al.*, Multi-layered nanofibrous mucoadhesive films for buccal and sublingual administration of drug-delivery and vaccination nanoparticles - important step towards effective mucosal vaccines. *Journal of Controlled Release* **249**, 183-195 (2017).

331. J. H. Choi, S. C. Schafer, A. N. Freiberg, M. A. Croyle, Bolstering Components of the Immune Response Compromised by Prior Exposure to Adenovirus: Guided Formulation Development for a Nasal Ebola Vaccine. *Molecular Pharmaceutics* **12**, 2697-2711 (2015).
332. J. H. Choi *et al.*, A Single Dose Respiratory Recombinant Adenovirus-Based Vaccine Provides Long-Term Protection for Non-Human Primates from Lethal Ebola Infection. *Molecular Pharmaceutics* **12**, 2712-2731 (2015).

Chapter 2

1. B. Greenwood, The contribution of vaccination to global health: past, present and future. *Philos Trans R Soc Lond B Biol Sci* **369**, 20130433-20130433 (2014).
2. D. S. Jones, S. H. Podolsky, J. A. Greene, The Burden of Disease and the Changing Task of Medicine. *New England Journal of Medicine* **366**, 2333-2338 (2012).
3. World Health Organization. The top 10 causes of death: Leading causes of death by economy income group. (2018).
4. K. Hardt *et al.*, Vaccine strategies: Optimising outcomes. *Vaccine* **34**, 6691-6699 (2016).
5. A. B. Hill, C. Kilgore, M. McGlynn, C. H. Jones, Improving global vaccine accessibility. *Current Opinion in Biotechnology* **42**, 67-73 (2016).
6. R. J. Carter *et al.*, Implementing a Multisite Clinical Trial in the Midst of an Ebola Outbreak: Lessons Learned From the Sierra Leone Trial to Introduce a Vaccine Against Ebola. *J Infect Dis* **217**, S16-S23 (2018).
7. D. Schopper *et al.*, Research Ethics Governance in Times of Ebola. *Public Health Ethics* **10**, 49-61 (2017).
8. R. Shaker, D. Fayad, G. Dbaibo, Challenges and opportunities for meningococcal vaccination in the developing world. *Hum Vaccin Immunother* **14**, 1084-1097 (2018).
9. Jacqueline E. Tate, Anthony H. Burton, Cynthia Boschi-Pinto, U. D. Parashar, Global, Regional, and National Estimates of Rotavirus Mortality in Children <5 Years of Age, 2000–2013. *Clinical Infectious Disease* **62**, S96-S105 (2016).
10. S. Plotkin, J. M. Robinson, G. Cunningham, R. Iqbal, S. Larsen, The complexity and cost of vaccine manufacturing - An overview. *Vaccine* **35**, 4064-4071 (2017).
11. J. Lloyd, J. Cheyne, The origins of the vaccine cold chain and a glimpse of the future. *Vaccine* **35**, 2115-2120 (2017).
12. A. Portnoy *et al.*, Costs of vaccine programs across 94 low- and middle-income countries. *Vaccine* **33**, A99-A108 (2015).
13. D. R. Feikin, B. Flannery, M. J. Hamel, M. Stack, P. M. Hansen, in *Reproductive, Maternal, Newborn, and Child Health: Disease Control Priorities, Third Edition (Volume 2)*, R. E. Black, R. Laxminarayan, M. Temmerman, N. Walker, Eds. (The International Bank for Reconstruction and Development / The World Bank (c) 2016 International Bank for Reconstruction and Development / The World Bank., Washington (DC), 2016).
14. A. Ashok, M. Brison, Y. LeTallec, Improving cold chain systems: Challenges and solutions. *Vaccine* **35**, 2217-2223 (2017).

15. B. Adhikari *et al.*, Earthquakes, Fuel Crisis, Power Outages, and Health Care in Nepal: Implications for the Future. *Disaster Medicine and Public Health Preparedness* **11**, 625-632 (2017).
16. M. N. Yakum, J. Ateudjieu, F. R. Pélagie, E. A. Walter, P. Watcho, Factors associated with the exposure of vaccines to adverse temperature conditions: the case of North West region, Cameroon. *BMC Research Notes* **8**, 277 (2015).
17. T. Kitamura *et al.*, Assessment of temperatures in the vaccine cold chain in two provinces in Lao People's Democratic Republic: a cross-sectional pilot study. *BMC research notes* **11**, 261-261 (2018).
18. M. Y. Chan, T. S. Dutill, R. M. Kramer, Lyophilization of Adjuvanted Vaccines: Methods for Formulation of a Thermostable Freeze-Dried Product. *Vaccine Adjuvants: Methods and Protocols*, 215-226 (2017).
19. M. A. Croyle, X. Cheng, J. M. Wilson, Development of formulations that enhance physical stability of viral vectors for gene therapy. *Gene Therapy* **8**, 1281-1290 (2001).
20. F. M. C. Cardoso, D. Petrovajova, T. Hornakova, Viral vaccine stabilizers: status and trends. *Acta virologica* **61**, 231-239 (2017).
21. B. Y. Lee *et al.*, The impact of making vaccines thermostable in Niger's vaccine supply chain. *Vaccine* **30**, 5637-5643 (2012).
22. World Health Organization (WHO). (2018).
23. A. Shastay, Administering Just the Diluent or One of Two Vaccine Components Leaves Patients Unprotected. *Home Healthcare Now* **34**, 218-220 (2016).
24. C. Duttagupta, D. Bhattacharyya, P. Narayanan, S. M. Pattanshetty, Vaccine wastage at the level of service delivery: a cross-sectional study. *Public Health* **148**, 63-65 (2017).
25. A. K. Shakya, M. Y. E. Chowdhury, W. Tao, H. S. Gill, Mucosal vaccine delivery: Current state and a pediatric perspective. *J Control Release* **240**, 394-413 (2016).
26. R. W. Cross, C. E. Mire, H. Feldmann, T. W. Geisbert, Post-exposure treatments for Ebola and Marburg virus infections. *Nature Reviews Drug Discovery* **17**, 413-434 (2018).
27. K. Schulze *et al.*, in *How to Overcome the Antibiotic Crisis : Facts, Challenges, Technologies and Future Perspectives*, Marc Stadler, Petra Dersch, Eds. (Springer International Publishing, Cham, 2016), pp. 207-234.
28. World Health Organization, *International Travel and Health*. Chapter 6 Vaccine-Preventable Diseases and Vaccines (WHO Press, Geneva, Switzerland 2017).
29. J. H. Choi, S. C. Schafer, A. N. Freiberg, M. A. Croyle, Bolstering Components of the Immune Response Compromised by Prior Exposure to Adenovirus: Guided Formulation Development for a Nasal Ebola Vaccine. *Mol Pharm* **12**, 2697-2711 (2015).
30. J. H. Choi *et al.*, A Single Dose Respiratory Recombinant Adenovirus-Based Vaccine Provides Long-Term Protection for Non-Human Primates from Lethal Ebola Infection. *Mol Pharm* **12**, 2712-2731 (2015).
31. H. T. Le, Q.-C. Yu, J. M. Wilson, M. A. Croyle, Utility of PEGylated recombinant adeno-associated viruses for gene transfer. *Journal of Controlled Release* **108**, 161-177 (2005).
32. G. W. Radebaugh, J. L. Murtha, T. N. Julian, J. N. Bondi, Methods for evaluating the puncture and shear properties of pharmaceutical polymeric films. *International Journal of Pharmaceutics* **45**, 39-46 (1988).

33. J. C. Visser *et al.*, Quality by design approach for optimizing the formulation and physical properties of extemporaneously prepared orodispersible films. *International Journal of Pharmaceutics* **485**, 70-76 (2015).
34. M. Preis, K. Knop, J. Breitkreutz, Mechanical strength test for orodispersible and buccal films. *International Journal of Pharmaceutics* **461**, 22-29 (2014).
35. M. Pelliccia *et al.*, Additives for vaccine storage to improve thermal stability of adenoviruses from hours to months. *Nat Commun* **7**, 13520-13520 (2016).
36. M. A. Croyle, Q.-C. Yu, J. M. Wilson, Development of a Rapid Method for the PEGylation of Adenoviruses with Enhanced Transduction and Improved Stability under Harsh Storage Conditions. *Human Gene Therapy* **11**, 1713-1722 (2000).
37. S. Mercier, S. Villeneuve, M. Mondor, I. Uysal, Time–Temperature Management Along the Food Cold Chain: A Review of Recent Developments. *Comprehensive Reviews in Food Science and Food Safety* **16**, 647-667 (2017).
38. H. T. Rupniak *et al.*, Characteristics of four new human cell lines derived from squamous cell carcinomas of the head and neck. *Journal of the National Cancer Institute* **75**, 621-635 (1985).
39. D. D. Kristensen, K. Bartholomew, S. Villadiego, K. Lorenson, What vaccine product attributes do immunization program stakeholders value? Results from interviews in six low- and middle-income countries. *Vaccine* **34**, 6236-6242 (2016).
40. World Health Organization. (WHO Press, Geneva, Switzerland, 2017).
41. D. Liebowitz, J. D. Lindbloom, J. R. Brandl, S. J. Garg, S. N. Tucker, High titre neutralising antibodies to influenza after oral tablet immunisation: a phase 1, randomised, placebo-controlled trial. *The Lancet Infectious Diseases* **15**, 1041-1048 (2015).
42. G. Koopman *et al.*, Correlation between Virus Replication and Antibody Responses in Macaques following Infection with Pandemic Influenza A Virus. *Journal of virology* **90**, 1023-1033 (2016).
43. S. Pillet *et al.*, Cellular immune response in the presence of protective antibody levels correlates with protection against 1918 influenza in ferrets. *Vaccine* **29**, 6793-6801 (2011).
44. S. J. Samet, S. M. Tompkins, Influenza Pathogenesis in Genetically Defined Resistant and Susceptible Murine Strains. *Yale J Biol Med* **90**, 471-479 (2017).
45. T. Werk *et al.*, New Processes for Freeze-Drying in Dual-Chamber Systems. *PDA Journal of Pharmaceutical Science and Technology* **70**, 191 (2016).
46. L. Mirmoghtadaie, S. Shojaee Aliabadi, S. M. Hosseini, Recent approaches in physical modification of protein functionality. *Food Chemistry* **199**, 619-627 (2016).
47. J. O. Morales, D. J. Brayden, Buccal delivery of small molecules and biologics: of mucoadhesive polymers, films, and nanoparticles. *Current Opinion in Pharmacology* **36**, 22-28 (2017).
48. B. Fonseca-Santos, M. Chorilli, An overview of polymeric dosage forms in buccal drug delivery: State of art, design of formulations and their in vivo performance evaluation. *Materials Science and Engineering: C* **86**, 129-143 (2018).
49. C. M. Hanson, A. M. George, A. Sawadogo, B. Schreiber, Is freezing in the vaccine cold chain an ongoing issue? A literature review. *Vaccine* **35**, 2127-2133 (2017).
50. R. K. Evans *et al.*, Development of stable liquid formulations for adenovirus-based vaccines. *Journal of Pharmaceutical Sciences* **93**, 2458-2475 (2004).

51. S. S. Renteria, C. C. Clemens, M. A. Croyle, Development of a nasal adenovirus-based vaccine: Effect of concentration and formulation on adenovirus stability and infectious titer during actuation from two delivery devices. *Vaccine* **28**, 2137-2148 (2010).
52. R. H. M. Price, C. Graham, S. Ramalingam, Association between viral seasonality and meteorological factors. *Sci Rep* **9**, 929-929 (2019).
53. W. H. O. E. C. o. S. f. P. Preparations, "Fifty Second Report on Stability Testing of Active Pharmaceutical Ingredients and Finished Pharmaceutical Products.," *WHO Technical Report* (Geneva, Switzerland. , 2018).
54. J. L. Nguyen, D. W. Dockery, Daily indoor-to-outdoor temperature and humidity relationships: a sample across seasons and diverse climatic regions. *Int J Biometeorol* **60**, 221-229 (2016).
55. G. E. Walsberg, Small Mammals in Hot Deserts: Some Generalizations Revisited. *BioScience* **50**, 109-120 (2000).
56. J. Rexroad, T. T. Martin, D. McNeilly, S. Godwin, C. Russell Middaugh, Thermal Stability of Adenovirus type 2 as a Function of pH. *Journal of Pharmaceutical Sciences* **95**, 1469-1479 (2006).
57. G. Gomez, M. J. Pikal, N. Rodriguez-Hornedo, Effect of initial buffer composition on pH changes during far-from-equilibrium freezing of sodium phosphate buffer solutions. *Pharmaceutical research* **18**, 90-97 (2001).
58. V. G. Kadajji, G. V. Betageri, Water Soluble Polymers for Pharmaceutical Applications. *Polymers* **3**, (2011).
59. R. Gheribi *et al.*, Development of plasticized edible films from Opuntia ficus-indica mucilage: A comparative study of various polyol plasticizers. *Carbohydrate Polymers* **190**, 204-211 (2018).
60. Y. Lu, L. Jipeng, D. Lu, The mechanism for the complexation and dissociation between siRNA and PMAL: a molecular dynamics simulation study based on a coarse-grained model. *Molecular Simulation* **43**, 1-9 (2017).
61. S. Karlin, V. Brendel, Charge configurations in viral proteins. *Proceedings of the National Academy of Sciences* **85**, 9396 (1988).

Chapter 3

1. M. G. Mateu, Virus engineering: functionalization and stabilization. *Protein Engineering, Design and Selection* **24**, 53-63 (2010).
2. C. P. Gerba, W. Q. Betancourt, Viral Aggregation: Impact on Virus Behavior in the Environment. *Environmental Science & Technology* **51**, 7318-7325 (2017).
3. M. E. Krause, E. Sahin, Chemical and physical instabilities in manufacturing and storage of therapeutic proteins. *Current Opinion in Biotechnology* **60**, 159-167 (2019).
4. U. Kartoglu, *Monitoring Vaccine Wastage at a Country Level*. (World Health Organization Geneva, Switzerland, 2005).
5. Raymond W Nims, M. Plavsic, Intra-family and inter-family comparisons for viral susceptibility to heat inactivation. *Journal of Microbial and Biochemical Technology* **5**, 136-141 (2013).

6. J. Dijkstra, C. P. de Jager, in *Practical Plant Virology: Protocols and Exercises*, Jeanne Dijkstra, Cees P. de Jager, Eds. (Springer Berlin Heidelberg, Berlin, Heidelberg, 1998), pp. 102-104.
7. S. Gard, O. MaalØE, in *General Virology*, F. M. Burnet, W. M. Stanley, Eds. (Academic Press, 1959), pp. 359-427.
8. E. K. Jeong, J. E. Bae, I. S. Kim, Inactivation of influenza A virus H1N1 by disinfection process. *American journal of infection control* **38**, 354-360 (2010).
9. G. Maheshwari, R. Jannat, L. McCormick, D. Hsu, Thermal inactivation of adenovirus type 5. *Journal of Virological Methods* **118**, 141-146 (2004).
10. C. M. Hanson, A. M. George, A. Sawadogo, B. Schreiber, Is freezing in the vaccine cold chain an ongoing issue? A literature review. *Vaccine* **35**, 2127-2133 (2017).
11. Ümit Kartoglu, Nejat Kenan Özgüler, Lara J Wolfson, W. Kurzatkowski, Validation of the shake test for detecting freeze damage to adsorbed vaccines. *Bulletin of the World Health Organization*, 624-631 (2010).
12. J. Emmanuel, M. Ferrer, F. Ferrer, "Disposal of Mass Immunization Waste Without Incineration," (Department of Health, Manila, Philippines, 2004).
13. I. Bajrovic, S. C. Schafer, D. K. Romanovicz, M. A. Croyle, Novel technology for storage and distribution of live vaccines and other biological medicines at ambient temperature. *Science Advances* **6**, eaau4819 (2020).
14. S. Karlin, V. Brendel, Charge configurations in viral proteins. *Proceedings of the National Academy of Sciences* **85**, 9396 (1988).
15. N. A. Malik, Surfactant–Amino Acid and Surfactant–Surfactant Interactions in Aqueous Medium: a Review. *Applied Biochemistry and Biotechnology* **176**, 2077-2106 (2015).
16. M. A. Croyle, X. Cheng, J. M. Wilson, Development of formulations that enhance physical stability of viral vectors for gene therapy. *Gene Therapy* **8**, 1281-1290 (2001).
17. R. J. Carter *et al.*, Implementing a Multisite Clinical Trial in the Midst of an Ebola Outbreak: Lessons Learned From the Sierra Leone Trial to Introduce a Vaccine Against Ebola. *J Infect Dis* **217**, S16-S23 (2018).
18. W. Abdelwahed, G. Degobert, S. Stainmesse, H. Fessi, Freeze-drying of nanoparticles: Formulation, process and storage considerations. *Advanced Drug Delivery Reviews* **58**, 1688-1713 (2006).
19. J. Rexroad, T. T. Martin, D. McNeilly, S. Godwin, C. Russell Middaugh, Thermal Stability of Adenovirus type 2 as a Function of pH. *Journal of Pharmaceutical Sciences* **95**, 1469-1479 (2006).
20. R. J. C. Harris, *Biological applications of freezing and drying*. (New York: Academic Press Inc., 1954), pp. xii + 415 pp.
21. J. E. Boyd, in *Gene Therapy Technologies, Applications and Regulations*, John Wiley, Ed. (Chichester, 1999), pp. 383-400.
22. P. E. Cruz *et al.*, Screening of Novel Excipients for Improving the Stability of Retroviral and Adenoviral Vectors. *Biotechnology Progress* **22**, 568-576 (2006).
23. W. C. Russell, Adenoviruses: update on structure and function. *The Journal of general virology* **90**, 1-20 (2009).
24. Y. S. Ahi, S. K. Mittal, Components of Adenovirus Genome Packaging. *Front Microbiol* **7**, 1503-1503 (2016).
25. S. Bhattacharjee, DLS and zeta potential – What they are and what they are not? *Journal of Controlled Release* **235**, 337-351 (2016).

26. O. Kalyuzhniy *et al.*, Adenovirus serotype 5 hexon is critical for virus infection of hepatocytes in vivo. *Proceedings of the National Academy of Sciences* **105**, 5483 (2008).
27. B. Michen, T. Graule, Isoelectric points of viruses. *Journal of Applied Microbiology* **109**, 388-397 (2010).
28. M. A. Croyle, B. J. Roessler, B. L. Davidson, J. M. Hilfinger, G. L. Amidon, Factors that Influence Stability of Recombinant Adenoviral Preparations for Human Gene Therapy. *Pharmaceutical Development and Technology* **3**, 373-383 (1998).
29. J. Rexroad, R. K. Evans, C. R. Middaugh, Effect of pH and ionic strength on the physical stability of adenovirus type 5. *Journal of Pharmaceutical Sciences* **95**, 237-247 (2006).
30. S. M. Callahan, P. Wonganan, M. A. Croyle, Molecular and macromolecular alterations of recombinant adenoviral vectors do not resolve changes in hepatic drug metabolism during infection. *Virol J* **5**, 111-111 (2008).
31. A. B. Hill, C. Kilgore, M. McGlynn, C. H. Jones, Improving global vaccine accessibility. *Current Opinion in Biotechnology* **42**, 67-73 (2016).
32. R. W. Ruigrok, M. V. Nermut, P. J. Andree, The molecular mass of adenovirus type 5 as determined by means of scanning transmission electron microscopy (STEM). *J Virol Methods* **9**, 69-78 (1984).
33. J. Aguiar, P. Carpena, J. A. Molina-Bolívar, C. Carnero Ruiz, On the determination of the critical micelle concentration by the pyrene 1:3 ratio method. *Journal of Colloid and Interface Science* **258**, 116-122 (2003).
34. D. Al-Koofee, Effect of Temperature Changes on Critical Micelle Concentration for Tween Series Surfactant. *Global Journal of Science Frontier Research Chemistry* **13**, (2013).
35. A. B. Mandal, B. U. Nair, D. Ramaswamy, Determination of the critical micelle concentration of surfactants and the partition coefficient of an electrochemical probe by using cyclic voltammetry. *Langmuir* **4**, 736-739 (1988).
36. N. Saadatkhah *et al.*, Experimental methods in chemical engineering: Thermogravimetric analysis—TGA. *The Canadian Journal of Chemical Engineering* **98**, 34-43 (2020).
37. D. Greiff, Stabilities of suspensions of influenza virus dried by sublimation of ice in vacuo to different contents of residual moisture and sealed under different gases. *Appl Microbiol* **20**, 935-938 (1970).
38. D. Greiff, Protein structure and freeze-drying: The effects of residual moisture and gases. *Cryobiology* **8**, 145-152 (1971).
39. J. K. Towns, Moisture content in proteins: its effects and measurement. *Journal of Chromatography A* **705**, 115-127 (1995).
40. M. A. Kennedy, R. J. Parks, Adenovirus virion stability and the viral genome: size matters. *Mol Ther* **17**, 1664-1666 (2009).
41. E. D. Horowitz *et al.*, Biophysical and ultrastructural characterization of adeno-associated virus capsid uncoating and genome release. *Journal of virology* **87**, 2994-3002 (2013).
42. T. J. Utley *et al.*, Respiratory syncytial virus uses a Vps4-independent budding mechanism controlled by Rab11-FIP2. *Proceedings of the National Academy of Sciences* **105**, 10209 (2008).
43. R. F. Laine *et al.*, Structural analysis of herpes simplex virus by optical super-resolution imaging. *Nature Communications* **6**, 5980 (2015).

44. J. Vajda, D. Weber, D. Brekel, B. Hundt, E. Müller, Size distribution analysis of influenza virus particles using size exclusion chromatography. *Journal of Chromatography A* **1465**, 117-125 (2016).
45. H. T. Rupniak *et al.*, Characteristics of Four New Human Cell Lines Derived From Squamous Cell Carcinomas of the Head and Neck2. *JNCI: Journal of the National Cancer Institute* **75**, 621-635 (1985).
46. K. Patel, C. A. Pasternak, Permeability changes elicited by influenza and Sendai viruses: separation of fusion and leakage by pH-jump experiments. *The Journal of general virology* **66 (Pt 4)**, 767-775 (1985).
47. D. Rengstl, B. Kraus, M. Van Vorst, G. D. Elliott, W. Kunz, Effect of choline carboxylate ionic liquids on biological membranes. *Colloids Surf B Biointerfaces* **123**, 575-581 (2014).
48. M. J. Mistilis *et al.*, Long-term stability of influenza vaccine in a dissolving microneedle patch. *Drug Deliv Transl Res* **7**, 195-205 (2017).
49. W. Wang, S. Ohtake, Science and art of protein formulation development. *International Journal of Pharmaceutics* **568**, 118505 (2019).
50. G. Gomez, M. J. Pikal, N. Rodriguez-Hornedo, Effect of initial buffer composition on pH changes during far-from-equilibrium freezing of sodium phosphate buffer solutions. *Pharmaceutical research* **18**, 90-97 (2001).
51. V. G. Kadajji, G. V. Betageri, Water Soluble Polymers for Pharmaceutical Applications. *Polymers* **3**, (2011).
52. M. Picard *et al.*, Protective and Inhibitory Effects of Various Types of Amphipols on the Ca2+-ATPase from Sarcoplasmic Reticulum: A Comparative Study. *Biochemistry* **45**, 1861-1869 (2006).
53. K. W. Huynh *et al.*, CryoEM structure of the human SLC4A4 sodium-coupled acid-base transporter NBCe1. *Nat Commun* **9**, 900 (2018).
54. K. P. K. Lee, J. Chen, R. MacKinnon, Molecular structure of human KATP in complex with ATP and ADP. *eLife* **6**, (2017).
55. S. Schoebel *et al.*, Cryo-EM structure of the protein-conducting ERAD channel Hrd1 in complex with Hrd3. *Nature* **548**, 352-355 (2017).
56. C. E. Paulsen, J. P. Armache, Y. Gao, Y. Cheng, D. Julius, Structure of the TRPA1 ion channel suggests regulatory mechanisms. *Nature* **520**, 511-517 (2015).
57. D. Otzen, Protein-surfactant interactions: A tale of many states. *Biochimica et biophysica acta* **1814**, 562-591 (2011).
58. B. S. Gupta, C.-R. Shen, M.-J. Lee, Effect of biological buffers on the colloidal behavior of sodium dodecyl sulfate (SDS). *Colloids and Surfaces A: Physicochemical and Engineering Aspects* **529**, 64-72 (2017).
59. H. Zettl, Y. Portnoy, M. Gottlieb, G. Krausch, Investigation of Micelle Formation by Fluorescence Correlation Spectroscopy. *The Journal of Physical Chemistry B* **109**, 13397-13401 (2005).
60. M. Méndez-Pérez, B. Vaz, L. García-Río, M. Pérez-Lorenzo, Polymeric Premicelles as Efficient Lipophilic Nanocarriers: Extending Drug Uptake to the Submicellar Regime. *Langmuir* **29**, 11251-11259 (2013).
61. D. Lombardo, M. A. Kiselev, S. Magazù, P. Calandra, Amphiphiles Self-Assembly: Basic Concepts and Future Perspectives of Supramolecular Approaches. *Advances in Condensed Matter Physics* **2015**, 151683 (2015).

62. R. Hadgiivanova, H. Diamant, Premicellar aggregation of amphiphilic molecules: Aggregate lifetime and polydispersity. *The Journal of chemical physics* **130**, 114901 (2009).
63. T. Tadros, in *Encyclopedia of Colloid and Interface Science*, Tharwat Tadros, Ed. (Springer Berlin Heidelberg, Berlin, Heidelberg, 2013), pp. 209-210.
64. B. Brycki *et al.*, Effect of the alkyl chain length on micelle formation for bis(N-alkyl-N,N-dimethylethylammonium)ether dibromides. *Comptes Rendus Chimie* **22**, 386-392 (2019).
65. G. K. Bains, S. H. Kim, E. J. Sorin, V. Narayanaswami, The extent of pyrene excimer fluorescence emission is a reflector of distance and flexibility: analysis of the segment linking the LDL receptor-binding and tetramerization domains of apolipoprotein E3. *Biochemistry* **51**, 6207-6219 (2012).
66. M. Zoonens, J.-L. Popot, Amphipols for each season. *J Membr Biol* **247**, 759-796 (2014).
67. J. L. Popot *et al.*, Amphipols From A to Z. *Annual Review of Biophysics* **40**, 379-408 (2011).
68. J.-L. Popot, Amphipols, Nanodiscs, and Fluorinated Surfactants: Three Nonconventional Approaches to Studying Membrane Proteins in Aqueous Solutions. *Annual Review of Biochemistry* **79**, 737-775 (2010).
69. W. Wang, A. A. Ignatius, S. V. Thakkar, Impact of Residual Impurities and Contaminants on Protein Stability. *Journal of Pharmaceutical Sciences* **103**, 1315-1330 (2014).
70. Q. G. Li, K. Lindman, G. Wadell, Hydropathic characteristics of adenovirus hexons. *Arch Virol* **142**, 1307-1322 (1997).
71. S. Skoglund *et al.*, Difficulties and flaws in performing accurate determinations of zeta potentials of metal nanoparticles in complex solutions-Four case studies. *PloS one* **12**, e0181735-e0181735 (2017).
72. E. Drinkel, F. D. Souza, H. D. Fiedler, F. Nome, The chameleon effect in zwitterionic micelles: Binding of anions and cations and use as nanoparticle stabilizing agents. *Current Opinion in Colloid & Interface Science* **18**, 26-34 (2013).
73. ForteBio, "Dip and Read Amine Reactive Second-Generation (AR2G) Biosensors," (Menlo Park, CA).
74. K. E. Hevener *et al.*, in *Methods in Enzymology*, Charles A. Lesburg, Ed. (Academic Press, 2018), vol. 610, pp. 265-309.
75. D. J. Butcher, G. R. Moe, Role of hydrophobic interactions and desolvation in determining the structural properties of a model alpha beta peptide. *Proc Natl Acad Sci U S A* **93**, 1135-1140 (1996).
76. J. Wang *et al.*, Cryo-EM structures of PAC1 receptor reveal ligand binding mechanism. *Cell Research* **30**, 436-445 (2020).
77. C. J. Breen, M. Raverdeau, H. P. Voorheis, Development of a quantitative fluorescence-based ligand-binding assay. *Sci Rep* **6**, 25769-25769 (2016).
78. R. Sridharan, J. Zuber, S. M. Connelly, E. Mathew, M. E. Dumont, Fluorescent approaches for understanding interactions of ligands with G protein coupled receptors. *Biochimica et biophysica acta* **1838**, 15-33 (2014).
79. C. Lyle, F. McCormick, Integrin αvβ5 is a primary receptor for adenovirus in CAR-negative cells. *Virol J* **7**, 148 (2010).

80. V. Legrand *et al.*, Fiberless recombinant adenoviruses: virus maturation and infectivity in the absence of fiber. *Journal of virology* **73**, 907-919 (1999).
81. J. K. Towns, Moisture content in proteins: its effects and measurement. *Journal of chromatography. A* **705**, 115-127 (1995).
82. P. Bergo, I. Moraes, P. J. A. Sobral, Effects of plasticizer concentration and type on moisture content in gelatin films. *Food Hydrocolloids* **32**, 412–415 (2013).
83. M. L. Sanyang, S. M. Sapuan, M. Jawaid, M. R. Ishak, J. Sahari, Effect of plasticizer type and concentration on physical properties of biodegradable films based on sugar palm (arenga pinnata) starch for food packaging. *J Food Sci Technol* **53**, 326-336 (2016).
84. Y. Kobayashi, Y. Suzuki, Compensatory evolution of net-charge in influenza A virus hemagglutinin. *PLoS One* **7**, e40422 (2012).
85. M. Hoffmann, S. Pöhlmann, Cell Entry of Influenza A Viruses: Sweet Talk between HA and CaV1.2. *Cell Host & Microbe* **23**, 697-699 (2018).
86. R. L. Poulson, S. M. Tompkins, R. D. Berghaus, J. D. Brown, D. E. Stallknecht, Environmental Stability of Swine and Human Pandemic Influenza Viruses in Water under Variable Conditions of Temperature, Salinity, and pH. *Applied and environmental microbiology* **82**, 3721-3726 (2016).
87. P. R. Junankar, R. J. Cherry, Temperature and pH dependence of the haemolytic activity of influenza virus and of the rotational mobility of the spike glycoproteins. *Biochimica et biophysica acta* **854**, 198-206 (1986).

Chapter 4

1. D. A. Henderson, The eradication of smallpox – An overview of the past, present, and future. *Vaccine* **29**, D7-D9 (2011).
2. R. Rappuoli, H. I. Miller, S. Falkow, Medicine. The intangible value of vaccination. *Science (New York, N.Y.)* **297**, 937-939 (2002).
3. World Health Organization. The top 10 causes of death: Leading causes of death by economy income group. (2018).
4. C. Dye, After 2015: infectious diseases in a new era of health and development. *Philos Trans R Soc Lond B Biol Sci* **369**, 20130426-20130426 (2014).
5. Margaret E Kruk *et al.*, Mortality due to low-quality health systems in the universal health coverage era: a systematic analysis of amenable deaths in 137 countries. *The Lancet* **392**, 2203-2212 (2018).
6. C. Hansen, E. Paintsil, Infectious Diseases of Poverty in Children: A Tale of Two Worlds. *Pediatr Clin North Am* **63**, 37-66 (2016).
7. World Health Organization, in *World Health Statistics*. (2010), chap. Selected Infectious Diseases: Number of Reported Cases, pp. 73-84.
8. B. K. Giersing *et al.*, Challenges of vaccine presentation and delivery: How can we design vaccines to have optimal programmatic impact? *Vaccine* **35**, 6793-6797 (2017).
9. D. E. Phillips, J. L. Dieleman, S. S. Lim, J. Shearer, Determinants of effective vaccine coverage in low and middle-income countries: a systematic review and interpretive synthesis. *BMC Health Serv Res* **17**, 681-681 (2017).

10. S. Plotkin, J. M. Robinson, G. Cunningham, R. Iqbal, S. Larsen, The complexity and cost of vaccine manufacturing - An overview. *Vaccine* **35**, 4064-4071 (2017).
11. D. D. Kristensen, T. Lorenson, K. Bartholomew, S. Villadiego, Can thermostable vaccines help address cold-chain challenges? Results from stakeholder interviews in six low- and middle-income countries. *Vaccine* **34**, 899-904 (2016).
12. A. Portnoy *et al.*, Costs of vaccine programs across 94 low- and middle-income countries. *Vaccine* **33**, A99-A108 (2015).
13. H. Xu *et al.*, High expression of ACE2 receptor of 2019-nCoV on the epithelial cells of oral mucosa. *International Journal of Oral Science* **12**, 8 (2020).
14. B. Killingley, J. Nguyen-Van-Tam, Routes of influenza transmission. *Influenza and Other Respiratory Viruses* **7**, 42-51 (2013).
15. Y. J. Hou *et al.*, SARS-CoV-2 Reverse Genetics Reveals a Variable Infection Gradient in the Respiratory Tract. *Cell* **182**, 429-446.e414 (2020).
16. N. Lycke, M. Bemark, Mucosal adjuvants and long-term memory development with special focus on CTA1-DD and other ADP-ribosylating toxins. *Mucosal immunology* **3**, 556-566 (2010).
17. J. Wang *et al.*, Single mucosal, but not parenteral, immunization with recombinant adenoviral-based vaccine provides potent protection from pulmonary tuberculosis. *Journal of immunology (Baltimore, Md. : 1950)* **173**, 6357-6365 (2004).
18. A. Iwasaki, Exploiting Mucosal Immunity for Antiviral Vaccines. *Annual Review of Immunology* **34**, 575-608 (2016).
19. A. J. McDermott, G. B. Huffnagle, The microbiome and regulation of mucosal immunity. *Immunology* **142**, 24-31 (2014).
20. J. E. Vela Ramirez, L. A. Sharpe, N. A. Peppas, Current state and challenges in developing oral vaccines. *Adv Drug Deliv Rev* **114**, 116-131 (2017).
21. K. M. Van De Graaff, Anatomy and physiology of the gastrointestinal tract. *The Pediatric Infectious Disease Journal* **5**, (1986).
22. D. M. Mudie, G. L. Amidon, G. E. Amidon, Physiological parameters for oral delivery and in vitro testing. *Mol Pharm* **7**, 1388-1405 (2010).
23. H. Kraan *et al.*, Buccal and sublingual vaccine delivery. *Journal of Controlled Release* **190**, 580-592 (2014).
24. S. Hua, Advances in Nanoparticulate Drug Delivery Approaches for Sublingual and Buccal Administration. *Frontiers in Pharmacology* **10**, (2019).
25. M. Sattar, O. M. Sayed, M. E. Lane, Oral transmucosal drug delivery – Current status and future prospects. *International Journal of Pharmaceutics* **471**, 498-506 (2014).
26. S. P. Humphrey, R. T. Williamson, A review of saliva: normal composition, flow, and function. *The Journal of prosthetic dentistry* **85**, 162-169 (2001).
27. Vaccine Innovation Prioritisation Strategy, "Sublingual Dosage Forms," (Geneva, Switzerland, 2019).
28. ClinicalTrials.gov. Identifier: NCT02955030, Evaluation of the Safety and Immunogenicity of a Sublingual Influenza Vaccine NSV0001 in Healthy Male Volunteers. (National Library of Medicine Bethesda, MD, 2016).
29. L. Zeng, Mucosal adjuvants: Opportunities and challenges. *Hum Vaccin Immunother* **12**, 2456-2458 (2016).

30. C. Marques, C. Som, M. Schmutz, O. Borges, G. Borchard, How the Lack of Chitosan Characterization Precludes Implementation of the Safe-by-Design Concept. *Frontiers in Bioengineering and Biotechnology* **8**, (2020).
31. I. M. van der Lubben, J. C. Verhoef, G. Borchard, H. E. Junginger, Chitosan and its derivatives in mucosal drug and vaccine delivery. *European Journal of Pharmaceutical Sciences* **14**, 201-207 (2001).
32. P. Pellegrino, E. Clementi, S. Radice, On vaccine's adjuvants and autoimmunity: Current evidence and future perspectives. *Autoimmunity Reviews* **14**, 880-888 (2015).
33. J. Alijotas-Reig, Human adjuvant-related syndrome or autoimmune/inflammatory syndrome induced by adjuvants. Where have we come from? Where are we going? A proposal for new diagnostic criteria. *Lupus* **24**, 1012-1018 (2015).
34. B. Laupèze, C. Hervé, A. Di Pasquale, F. Tavares Da Silva, Adjuvant Systems for vaccines: 13 years of post-licensure experience in diverse populations have progressed the way adjuvanted vaccine safety is investigated and understood. *Vaccine* **37**, 5670-5680 (2019).
35. J. Vriens, B. Nilius, R. Vennekens, Herbal compounds and toxins modulating TRP channels. *Curr Neuropharmacol* **6**, 79-96 (2008).
36. R. A. Ross, Anandamide and vanilloid TRPV1 receptors. *British Journal of Pharmacology* **140**, 790-801 (2003).
37. S. Mihara, T. Shibamoto, The role of flavor and fragrance chemicals in TRPA1 (transient receptor potential cation channel, member A1) activity associated with allergies. *Allergy, Asthma & Clinical Immunology* **11**, 11 (2015).
38. A. M. Peier *et al.*, A TRP Channel that Senses Cold Stimuli and Menthol. *Cell* **108**, 705-715 (2002).
39. S. Basu, P. Srivastava, Immunological role of neuronal receptor vanilloid receptor 1 expressed on dendritic cells. *Proc Natl Acad Sci U S A* **102**, 5120-5125 (2005).
40. L. L. Nohara, S. R. Stanwood, K. D. Omilusik, W. A. Jefferies, Tweeters, Woofers and Horns: The Complex Orchestration of Calcium Currents in T Lymphocytes. *Frontiers in Immunology* **6**, (2015).
41. J. H. Choi *et al.*, A single sublingual dose of an adenovirus-based vaccine protects against lethal Ebola challenge in mice and guinea pigs. *Mol Pharm* **9**, 156-167 (2012).
42. I. Bajrovic, S. C. Schafer, D. K. Romanovicz, M. A. Croyle, Novel technology for storage and distribution of live vaccines and other biological medicines at ambient temperature. *Science Advances* **6**, eaau4819 (2020).
43. Y. Zhang *et al.*, Influenza Research Database: An integrated bioinformatics resource for influenza virus research. *Nucleic Acids Res* **45**, D466-D474 (2017).
44. J. H. Choi, S. C. Schafer, A. N. Freiberg, M. A. Croyle, Bolstering Components of the Immune Response Compromised by Prior Exposure to Adenovirus: Guided Formulation Development for a Nasal Ebola Vaccine. *Molecular Pharmaceutics* **12**, 2697-2711 (2015).
45. H. T. Rupniak *et al.*, Characteristics of four new human cell lines derived from squamous cell carcinomas of the head and neck. *Journal of the National Cancer Institute* **75**, 621-635 (1985).
46. N. P. Yadev, C. Murdoch, S. P. Saville, M. H. Thornhill, Evaluation of tissue engineered models of the oral mucosa to investigate oral candidiasis. *Microbial Pathogenesis* **50**, 278-285 (2011).

47. J. Kubilus *et al.*, "Characterization and testing of new buccal and gingival tissue models," (MatTek Corporation, Ashland, MA, 2006).
48. FluMist (influenza vaccine live) [package insert]. Gaithersburg, MD: MedImmune; 2019.
49. L. B. Schenkel *et al.*, Optimization of a Novel Quinazolinone-Based Series of Transient Receptor Potential A1 (TRPA1) Antagonists Demonstrating Potent in Vivo Activity. *Journal of medicinal chemistry* **59**, 2794-2809 (2016).
50. M. Cheung *et al.*, Discovery of GSK2193874: An Orally Active, Potent, and Selective Blocker of Transient Receptor Potential Vanilloid 4. *ACS medicinal chemistry letters* **8**, 549-554 (2017).
51. F. Roth-Walter *et al.*, Immune suppressive effect of cinnamaldehyde due to inhibition of proliferation and induction of apoptosis in immune cells: implications in cancer. *PloS one* **9**, e108402 (2014).
52. D. J. Lefeber *et al.*, Th1-Directing Adjuvants Increase the Immunogenicity of Oligosaccharide-Protein Conjugate Vaccines Related to Streptococcus pneumoniae Type 3. *Infection and Immunity* **71**, 6915 (2003).
53. M. L. Visciano, M. Tagliamonte, M. L. Tornesello, F. M. Buonaguro, L. Buonaguro, Effects of adjuvants on IgG subclasses elicited by virus-like Particles. *Journal of Translational Medicine* **10**, 4 (2012).
54. H. L. Weiner, Oral tolerance: immune mechanisms and the generation of Th3-type TGF-beta-secreting regulatory cells. *Microbes and infection* **3**, 947-954 (2001).
55. T. M. McIntyre *et al.*, Transforming growth factor beta 1 selectivity stimulates immunoglobulin G2b secretion by lipopolysaccharide-activated murine B cells. *The Journal of experimental medicine* **177**, 1031-1037 (1993).
56. P. N. Boyaka, Inducing Mucosal IgA: A Challenge for Vaccine Adjuvants and Delivery Systems. *J Immunol* **199**, 9-16 (2017).
57. E. A. Weaver, A. M. Rubrum, R. J. Webby, M. A. Barry, Protection against Divergent Influenza H1N1 Virus by a Centralized Influenza Hemagglutinin. *PloS one* **6**, e18314 (2011).
58. M. Couto, in *Vertebrate Embryogenesis: Embryological, Cellular, and Genetic Methods*, Francisco J. Pelegri, Ed. (Humana Press, Totowa, NJ, 2011), pp. 579-599.
59. J. R. Tisoncik *et al.*, Into the eye of the cytokine storm. *Microbiology and molecular biology reviews : MMBR* **76**, 16-32 (2012).
60. J. S. Peiris, K. P. Hui, H. L. Yen, Host response to influenza virus: protection versus immunopathology. *Current opinion in immunology* **22**, 475-481 (2010).
61. Q. Liu, Y.-h. Zhou, Z.-q. Yang, The cytokine storm of severe influenza and development of immunomodulatory therapy. *Cellular & Molecular Immunology* **13**, 3-10 (2016).
62. M. A. Gill, E. P. Schlaudecker, Perspectives from the Society for Pediatric Research: Decreased Effectiveness of the Live Attenuated Influenza Vaccine. *Pediatric Research* **83**, 31-40 (2018).
63. J. R. Chung *et al.*, Live Attenuated and Inactivated Influenza Vaccine Effectiveness. *Pediatrics* **143**, e20182094 (2019).
64. G. P. Kobinger *et al.*, Assessment of the Efficacy of Commercially Available and Candidate Vaccines against a Pandemic H1N1 2009 Virus. *The Journal of Infectious Diseases* **201**, 1000-1006 (2010).
65. L. A. Grohskopf *et al.*, Prevention and Control of Seasonal Influenza with Vaccines: Recommendations of the Advisory Committee on Immunization Practices-United States,

2018-19 Influenza Season. *MMWR. Recommendations and reports : Morbidity and mortality weekly report. Recommendations and reports* **67**, 1-20 (2018).
66. F. Krammer, J. P. Weir, O. Engelhardt, J. M. Katz, R. J. Cox, Meeting report and review: Immunological assays and correlates of protection for next-generation influenza vaccines. *Influenza Other Respir Viruses* **14**, 237-243 (2020).
67. T. T. Wang, S. Bournazos, J. V. Ravetch, Immunological responses to influenza vaccination: lessons for improving vaccine efficacy. *Current opinion in immunology* **53**, 124-129 (2018).
68. D. Liebowitz, J. D. Lindbloom, J. R. Brandl, S. J. Garg, S. N. Tucker, High titre neutralising antibodies to influenza after oral tablet immunisation: a phase 1, randomised, placebo-controlled trial. *The Lancet Infectious Diseases* **15**, 1041-1048 (2015).
69. G. Koopman *et al.*, Correlation between Virus Replication and Antibody Responses in Macaques following Infection with Pandemic Influenza A Virus. *Journal of virology* **90**, 1023-1033 (2016).
70. S. Pillet *et al.*, Cellular immune response in the presence of protective antibody levels correlates with protection against 1918 influenza in ferrets. *Vaccine* **29**, 6793-6801 (2011).
71. S. J. Samet, S. M. Tompkins, Influenza Pathogenesis in Genetically Defined Resistant and Susceptible Murine Strains. *Yale J Biol Med* **90**, 471-479 (2017).
72. J. O. Morales *et al.*, Challenges and Future Prospects for the Delivery of Biologics: Oral Mucosal, Pulmonary, and Transdermal Routes. *The AAPS journal* **19**, 652-668 (2017).
73. J. A. Bartlett, K. van der Voort Maarschalk, Understanding the oral mucosal absorption and resulting clinical pharmacokinetics of asenapine. *AAPS PharmSciTech* **13**, 1110-1115 (2012).
74. C. P. Jain, G. Joshi, U. Kataria, K. Patel, Enhanced Permeation of an Antiemetic Drug from Buccoadhesive Tablets by Using Bile Salts as Permeation Enhancers: Formulation Characterization, In Vitro, and Ex Vivo Studies. *Sci Pharm* **84**, 379-392 (2016).
75. J. O. Morales, D. J. Brayden, Buccal delivery of small molecules and biologics: of mucoadhesive polymers, films, and nanoparticles. *Current Opinion in Pharmacology* **36**, 22-28 (2017).
76. A. Miquel-Clopés, E. G. Bentley, J. P. Stewart, S. R. Carding, Mucosal vaccines and technology. *Clinical & Experimental Immunology* **196**, 205-214 (2019).
77. T. Caon, L. Jin, C. M. Simões, R. S. Norton, J. A. Nicolazzo, Enhancing the buccal mucosal delivery of peptide and protein therapeutics. *Pharmaceutical research* **32**, 1-21 (2015).
78. A. Shukla, V. Mishra, P. Kesharwani, Bilosomes in the context of oral immunization: development, challenges and opportunities. *Drug Discovery Today* **21**, 888-899 (2016).
79. L. Xing *et al.*, Chemical Modification of Chitosan for Efficient Vaccine Delivery. *Molecules (Basel, Switzerland)* **23**, (2018).
80. J. Boateng, O. Okeke, Evaluation of Clay-Functionalized Wafers and Films for Nicotine Replacement Therapy via Buccal Mucosa. *Pharmaceutics* **11**, (2019).
81. C. Padula, S. Pescina, S. Nicoli, P. Santi, New Insights on the Mechanism of Fatty Acids as Buccal Permeation Enhancers. *Pharmaceutics* **10**, (2018).
82. D. Kottke, H. Majid, J. Breitkreutz, B. B. Burckhardt, Development and evaluation of mucoadhesive buccal dosage forms of lidocaine hydrochloride by ex-vivo permeation studies. *International Journal of Pharmaceutics* **581**, 119293 (2020).

83. H. Abd El Azim, N. Nafee, A. Ramadan, N. Khalafallah, Liposomal buccal mucoadhesive film for improved delivery and permeation of water-soluble vitamins. *International Journal of Pharmaceutics* **488**, 78-85 (2015).
84. S. Awate, L. A. Babiuk, G. Mutwiri, Mechanisms of action of adjuvants. *Frontiers in immunology* **4**, 114-114 (2013).
85. K. Brewer *et al.*, Unique depot formed by an oil based vaccine facilitates active antigen uptake and provides effective tumour control. *Journal of Biomedical Science* **25**, (2018).
86. G. Ahlén *et al.*, In Vivo Electroporation Enhances the Immunogenicity of Hepatitis C Virus Nonstructural 3/4A DNA by Increased Local DNA Uptake, Protein Expression, Inflammation, and Infiltration of CD3+ T Cells. *J Immunol* **179**, 4741-4753 (2007).
87. G. Lopez-Castejon, D. Brough, Understanding the mechanism of IL-1β secretion. *Cytokine Growth Factor Rev* **22**, 189-195 (2011).
88. F. T. Crews *et al.*, Cytokines and Alcohol. *Alcoholism: Clinical and Experimental Research* **30**, 720-730 (2006).
89. C. J. M. Kane *et al.*, Effects of Ethanol on Immune Response in the Brain: Region-Specific Changes in Adolescent Versus Adult Mice. *Alcoholism: Clinical and Experimental Research* **38**, 384-391 (2014).
90. A. O. Hovden, R. J. Cox, L. R. Haaheim, Whole influenza virus vaccine is more immunogenic than split influenza virus vaccine and induces primarily an IgG2a response in BALB/c mice. *Scandinavian Journal of Immunology* **62**, 36-44 (2005).
91. J. F. S. Mann *et al.*, Lipid vesicle size of an oral influenza vaccine delivery vehicle influences the Th1/Th2 bias in the immune response and protection against infection. *Vaccine* **27**, 3643-3649 (2009).
92. J. Hinkula, S. Nyström, C. Devito, A. Bråve, S. E. Applequist, Long-Lasting Mucosal and Systemic Immunity against Influenza A Virus Is Significantly Prolonged and Protective by Nasal Whole Influenza Immunization with Mucosal Adjuvant N3 and DNA-Plasmid Expressing Flagellin in Aging In- and Outbred Mice. *Vaccines (Basel)* **7**, 64 (2019).
93. J. P. Amorij, A. Huckriede, J. Wilschut, H. W. Frijlink, W. L. Hinrichs, Development of stable influenza vaccine powder formulations: challenges and possibilities. *Pharmaceutical research* **25**, 1256-1273 (2008).
94. S. L. Swain *et al.*, CD4+ T-cell memory: generation and multi-faceted roles for CD4+ T cells in protective immunity to influenza. *Immunol Rev* **211**, 8-22 (2006).
95. A. Bot, S. Bot, C. A. Bona, Protective Role of Gamma Interferon during the Recall Response to Influenza Virus. *Journal of Virology* **72**, 6637 (1998).
96. P. Brandtzaeg *et al.*, The B-cell system of human mucosae and exocrine glands. *Immunol Rev* **171**, 45-87 (1999).
97. W.-D. Zhang, W.-H. Wang, S. Jia, The Distribution of SIgA and IgG Antibody-Secreting Cells in the Small Intestine of Bactrian Camels (Camelus bactrianus) of Different Ages. *PloS one* **11**, e0156635 (2016).
98. X. Chen *et al.*, Host Immune Response to Influenza A Virus Infection. *Frontiers in Immunology* **9**, (2018).
99. T. M. Moran, H. Park, A. Fernandez-Sesma, J. L. Schulman, Th2 Responses to Inactivated Influenza Virus Can Be Converted to Th1 Responses and Facilitate Recovery from Heterosubtypic Virus Infection. *The Journal of Infectious Diseases* **180**, 579-585 (1999).

100. A. S. El-Madhun, R. J. Cox, L. R. Haaheim, The Effect of Age and Natural Priming on the IgG and IgA Subclass Responses after Parenteral Influenza Vaccination. *The Journal of Infectious Diseases* **180**, 1356-1360 (1999).
101. M. S. Miller *et al.*, Neutralizing antibodies against previously encountered influenza virus strains increase over time: a longitudinal analysis. *Sci Transl Med* **5**, 198ra107-198ra107 (2013).
102. Y. Adachi *et al.*, Exposure of an occluded hemagglutinin epitope drives selection of a class of cross-protective influenza antibodies. *Nature Communications* **10**, 3883 (2019).
103. C. L. Maruyama, M. M. Monroe, J. P. Hunt, L. Buchmann, O. J. Baker, Comparing human and mouse salivary glands: A practice guide for salivary researchers. *Oral Diseases* **25**, 403-415 (2019).
104. Z. F. H. M. Boonman *et al.*, Intraocular Tumor Antigen Drains Specifically to Submandibular Lymph Nodes, Resulting in an Abortive Cytotoxic T Cell Reaction. *The Journal of Immunology* **172**, 1567 (2004).
105. C. Thirion-Delalande *et al.*, Comparative analysis of the oral mucosae from rodents and non-rodents: Application to the nonclinical evaluation of sublingual immunotherapy products. *PloS one* **12**, e0183398-e0183398 (2017).
106. P. Yang *et al.*, Response of BALB/c mice to a monovalent influenza A (H1N1) 2009 split vaccine. *Cellular & Molecular Immunology* **7**, 116-122 (2010).
107. N. Du *et al.*, Generation and evaluation of the trivalent inactivated reassortant vaccine using human, avian, and swine influenza A viruses. *Vaccine* **26**, 2912-2918 (2008).
108. H. T. Groves *et al.*, Mouse Models of Influenza Infection with Circulating Strains to Test Seasonal Vaccine Efficacy. *Frontiers in Immunology* **9**, (2018).
109. T. Burkholder, C. Foltz, E. Karlsson, C. G. Linton, J. M. Smith, Health Evaluation of Experimental Laboratory Mice. *Curr Protoc Mouse Biol* **2**, 145-165 (2012).
110. C. A. Dinarello, Interleukin-18, a proinflammatory cytokine. *European cytokine network* **11**, 483-486 (2000).
111. E. Hakimizadeh *et al.*, TRPV1 receptor-mediated expression of Toll-like receptors 2 and 4 following permanent middle cerebral artery occlusion in rats. *Iran J Basic Med Sci* **20**, 863-869 (2017).
112. M. Tauseef *et al.*, TLR4 activation of TRPC6-dependent calcium signaling mediates endotoxin-induced lung vascular permeability and inflammation. *The Journal of experimental medicine* **209**, 1953-1968 (2012).
113. C. Maisonneuve, S. Bertholet, D. J. Philpott, E. De Gregorio, Unleashing the potential of NOD- and Toll-like agonists as vaccine adjuvants. *Proceedings of the National Academy of Sciences* **111**, 12294 (2014).
114. R. S. Rudicell *et al.*, Comparison of adjuvants to optimize influenza neutralizing antibody responses. *Vaccine* **37**, 6208-6220 (2019).

Appendix Table 1 and 2

1. Food and Drug Administration. Vaccines Licensed for Use in the United States. (2020).
2. *Excipients Included in U.S. Vaccines, by Vaccine* (2019).

3. O. S. Kumru *et al.*, Vaccine instability in the cold chain: Mechanisms, analysis and formulation strategies. *Biologicals* **42**, 237-259 (2014).

Vita

Irnela Bajrovic was born the daughter of Džemal and Rahima Bajrovic in Sarajevo, Bosnia and Herzegovina. She graduated from The University of Texas at Austin in May 2015 with a Bachelor of Science in Biochemistry. She subsequently enrolled in the Ph.D. program of pharmaceutics at The University of Texas at Austin in August 2015. While earning her doctorate degree she served as a teaching assistant to pharmacy students and was also supported by a research assistantship from the National Institute of Health. Irnela was the recipient of the Graduate School Diversity Mentoring Recruitment Fellowship, Williams & McGinity Graduate Fellowship, Duane A. Boyle Fellowship in Pharmaceutics and Dr. Robert J. Wills Graduate Fellowship Endowment, Johnson and Johnson Graduate Fellowship and Dr. James W. McGinity Graduate Endowment, and the PhRMA Foundation's Pre-Doctoral Fellowship in Pharmaceutics. Her research interests include formulation science and vaccine development.

Permanent email address: i.bajrovic@gmail.com

This dissertation was typed by Irnela Bajrovic.